

Role of filamentation in the pathogenesis of Candidiasis

DISSERTATION

in Partial Fulfilment of the Requirements for the Degree of
“doctor rerum naturalium” (Dr. rer. nat.)

**Submitted to the Council of the Faculty of Biological Sciences
of Friedrich Schiller University Jena**



**FRIEDRICH-SCHILLER-
UNIVERSITÄT
JENA**

by Dipl. Biol. Christine Dunker

born on 03.06.1987 in Jena

Jena, August 2021

Reviewers:

Prof. Ilse D. Jacobsen, Hans Knoell Institute Jena

Prof. Berit Jungnickel, Friedrich Schiller University Jena

Prof. Sven Krappmann, Universitätsklinikum Erlangen

Date of defense: 22.04.2022

This thesis was prepared at the “Leibniz Institute for Natural Product Research and Infection Biology – Hans Knoell Institute (HKI)”, Jena in the Research Group Microbial Immunology (MI) under the supervision of Prof. Ilse D. Jacobsen. This work was financially supported by the Deutsche Forschungsgemeinschaft (DFG), the HKI, and the International Leibniz Research School for Microbial and Biomolecular Interactions (ILRS).



Leibniz Institute
for Natural Product Research
and Infection Biology
Hans Knöll Institute



Deutsche
Forschungsgemeinschaft



ILRS
JENA
MIBINTACT

Table of Contents

Summary	1
Zusammenfassung	3
1. Introduction	5
1.1 Human pathogenic fungi.....	5
1.2. <i>Candida albicans</i>	5
1.3. Infections caused by <i>C. albicans</i>	6
1.3.1. Mucosal infections	6
1.3.2. Invasive Candidiasis.....	7
1.4. Host defense against <i>C. albicans</i> infections.....	8
1.5. <i>C. albicans</i> virulence factors and fitness attributes	10
1.5.1. Adhesion, invasion and damage	10
1.5.2. Hydrolytic enzymes	11
1.5.3. Metabolic flexibility.....	11
1.5.4. Polymorphism	12
1.5.4.1. Regulation of the transition from yeast to hypha morphology	14
1.5.4.2. The <i>C. albicans</i> <i>EED1</i> gene	17
1.5.4.3 Role of morphology during commensalism and disease	18
2. Aim of this study	20
3. Manuscripts	21
3.1. Manuscript I: Gerwien <i>et al.</i> , mSphere, 2020	21
3.2. Manuscript II: Machata <i>et al.</i> , Front. Immunol., 2021.....	31
3.3. Manuscript III: Dunker <i>et al.</i> , Nat. Commun., 2021	54
4. Additional results related to Manuscript III	97
4.1. tet- <i>NRG1</i> - yeast are avirulent in a murine intraperitoneal infection model	97
4.2 The initial fungal load in kidney, liver and spleen is higher than in the brain	99
4.3. Kidney fungal loads are similar in moribund mice.....	99
4.4. Organ fungal burden in mice challenged with low infectious doses	103

4.5. Neutrophil activation in kidneys of systemically infected mice is comparable between WT+ and t-EED1+ yeast.....	103
5. Discussion	105
5.1. Yeast growth of <i>C. albicans</i> results in decreased damage and virulence in invasion-based infection models.....	105
5.2. In the absence of <i>EED1</i> expression, <i>C. albicans</i> yeast retain their virulence potential in a murine systemic infection model.....	106
5.3. The <i>eed1Δ/Δ</i> mutant rapidly proliferates <i>in vivo</i>	113
5.4. High numbers of <i>EED1</i> -repressing yeast damage kidneys to the same extent as the WT..	118
5.5. Contribution of immunopathology to virulence of the <i>eed1Δ/Δ</i> mutant	119
5.6. Conclusion	122
6. References	123
7. Appendix	I
7.1. Abbreviations.....	I
7.2. Additional methods.....	III
7.3 Curriculum vitae	IV
7.4. Candidate's contributions to original publications	V
7.5. Publications	VI
7.6. Talks and Posters	VII
7.6.1. Talks.....	VII
7.6.2. Posters.....	VII
7.7. Additional trainings and activities	VIII
7.8. Danksagung	IX
7.9. Selbstständigkeitserklärung	X

Summary

Opportunistic fungal pathogens, such as *Candida albicans*, are serious threats especially for the increasing number of immunocompromised patients susceptible to infection. *C. albicans*, which is an otherwise harmless commensal on mucosal surfaces, can under certain circumstances cause both relatively benign superficial as well as life-threatening systemic infections. Main risk factors associated with the development of candidiasis are immunosuppression, especially neutropenia, and use of long-term antibiotics. Systemic infections can arise endogenously from primary sites of colonization, mainly the gastrointestinal tract, from local infections or as consequence of the use of medical devices such as intravenous catheters. *Via* distribution of fungal cells through the blood stream, *C. albicans* infections can affect all inner organs. With a mortality rate of up to 50% despite antifungal therapy and the development of resistance against antifungal drugs, systemic candidiasis is of significant clinical importance.

The ability to undergo morphologic transition from yeast to hypha has been considered for a long time to be essential for pathogenesis and virulence of *C. albicans*. This view has been supported by findings that *C. albicans* strains locked in the yeast or filamentous morphology are less or even avirulent in murine systemic infection models. Nevertheless, both morphologies are found during colonization and infection in men and mice and are thought to contribute to pathogenesis: Whereas yeast are believed to promote dissemination, hyphae are likely required for the traversal from the gastrointestinal tract to the blood stream, mediate tissue invasion, damage, and escape from immune cells. In line with this, this thesis shows that *C. albicans* mutants lacking *EED1*, either due to deletion (*eed1Δ/Δ* mutant) or repressed expression (t-*EED1* strain in the presence of doxycycline), which are unable to maintain hyphal growth resulting in the switch back to yeast cell growth after germ tube formation, are attenuated in virulence in an invasion-based intraperitoneal infection model. Surprisingly though, these mutants retain their virulence in a murine infection model of systemic candidiasis leading to disease progression indistinguishable from the filamentous wild type. The results of this thesis challenge the central dogma that hyphal formation *per se* is required for virulence in candidiasis. The retained virulence of mutants lacking *EED1* or its expression was accompanied by rapid yeast replication within internal organs, especially in the kidney, the main target organ of systemic candidiasis. Whereas the renal pro-inflammatory cytokine response was delayed early after infection, increased cytokine production was observed at later time points, likely as the result of the increased immune cell infiltration, suggesting a contribution of immunopathology to pathogenesis. This work shows that rapid proliferation is likely the consequence of enhanced metabolic adaptation and increased fitness, as the *eed1Δ/Δ* mutant shows better growth in kidney homogenates and on certain physiologically relevant carbon sources

in vitro. High kidney yeast burden resulted in kidney damage and systemic inflammation comparable to wild type infections. Therefore, rapid proliferation by metabolic adaptation and increased fitness, resulting in high organ yeast burden, can compensate for the loss of filament formation in *C. albicans*.

Taken together, this thesis shows that hyphae are required for damage and virulence in invasion-based infection models but are dispensable for pathogenesis during systemic candidiasis. The data obtained in this study might have implications on the development of therapeutic strategies: Drugs preventing hyphal formation might be advantageous to treat candidiasis to a certain extent, but it has to be kept in mind that *C. albicans* can vigorously adapt and can compensate for the loss of hyphae by using other virulence properties.

Zusammenfassung

Opportunistische Krankheitserreger wie z.B. *Candida albicans* stellen ernstzunehmende Bedrohungen vor allem für die zunehmende Anzahl an immunsupprimierten Patienten dar. Der Pilz *C. albicans*, der als harmloser Kommensale auf Schleimhäuten gesunder Menschen zu finden ist, kann unter bestimmten Voraussetzungen sowohl oberflächliche Schleimhautinfektionen als auch lebensbedrohliche systemische Infektionen verursachen. Die Hauptrisikofaktoren, die zur Entwicklung einer Candidose beitragen können, sind Immunsuppression und die Verwendung von Antibiotika über einen längeren Zeitraum. Die meisten systemischen Candidosen haben einen endogenen Ursprung und können durch Translokation aus dem kolonisierten Magen-Darm-Trakt, Disseminierung lokaler Infektionen, oder auch über die Bildung von Biofilmen auf Medizinprodukten wie z.B. intravenösen Kathetern, in die Blutbahn gelangen. Über den Blutstrom kann der Pilz alle inneren Organe befallen. Mit einer Mortalitätsrate, die trotz der Verwendung von Antimykotika bei bis zu 50% liegt, sowie der Entwicklung behandlungsresistenter *C. albicans* Stämme ist die systemische Candidose von großer klinischer Bedeutung.

Der Fähigkeit von *C. albicans*, vom Hefewachstum in ein filamentöses Wachstum übergehen zu können, wird seit jeher als essentieller Virulenzfaktor angesehen. Diese Ansicht beruht unter anderem auf Beobachtungen, dass Mutanten, die ausschließlich in der Hefeform oder als Filamente wachsen können, in murinen systemischen Infektionsmodellen eine reduzierte Virulenz aufweisen oder gar avirulent sind. Nichtsdestotrotz sind beide Morphologien während der Kolonisierung und der Infektion in Mäusen und Menschen zu finden und tragen mutmaßlich zur Pathogenese bei. Während der Hefeform eine Rolle bei der Disseminierung zugeschrieben wird, tragen Filamente wahrscheinlich zur Translokation vom Magen-Darm-Trakt, zum invasiven Wachstum im Gewebe, zur Gewebsschädigung, und dem Entkommen aus Phagozyten bei. Im Einklang damit konnte innerhalb dieser Arbeit gezeigt werden, dass *C. albicans* Mutanten, die Aufgrund der Deletion (*eed1Δ/Δ* Mutante) oder Repression von *EED1* (t-EED1 Stamm in Gegenwart von Doxycyclin) das Hyphenwachstum nicht aufrechterhalten können, eine attenuierte Virulenz in einem invasionsbasierten intraperitonealen Infektionsmodell aufweisen. Überraschenderweise waren diese Mutanten, die zwar noch Keimschläuche ausbilden können, danach aber wieder ins Hefewachstum zurückwechseln, in einem systemischen Infektionsmodell genauso virulent und wiesen einen vergleichbaren Infektionsverlauf wie der filamentöse Wildtyp auf. Die Ergebnisse der hier vorliegenden Arbeit stellen daher das zentrale Dogma in Frage, dass die Hyphenbildung essentiell für die Virulenz von *C. albicans* ist. Die Virulenz der Mutanten, die kein *EED1* besitzen/exprimieren, ging mit einer erhöhten Replikation in der Hefeform in den Organen einher. Im Besonderen waren die Nieren betroffen, die das Hauptzielorgan der systemischen Candidose

darstellen. Während die anfängliche proinflammatorische Zytokinfreisetzung innerhalb der Nieren verzögert war, kam es zu späteren Zeitpunkten zu einer erhöhten Produktion, mutmaßlich begründet durch den vermehrten Einstrom von Immunzellen, was auf einen Beitrag der Immunpathologie zur Pathogenese in der Abwesenheit von *EED1* schließen lässt. Diese Arbeit zeigt, dass die schnelle Vermehrung wahrscheinlich die Folge einer verbesserten metabolischen Anpassung und einer erhöhten Fitness ist, da die *eed1Δ/Δ* Mutante ein besseres Wachstum *in vitro* in Medien zeigt, die Nierenhomogenisat oder andere physiologisch relevante Kohlenstoffquellen enthalten. Die hohe Nierenbelastung durch die Hefezellen führte zu einer Nierenschädigung und systemischen Entzündung, vergleichbar mit Infektionen, die durch den *C. albicans* Wildtyp ausgelöst wurden. Daher kann durch rapide Vermehrung des Pilzes, gewährleistet durch metabolische Anpassung und gesteigerter Fitness die fehlende Hyphenbildung kompensiert werden.

Zusammengefasst konnte in dieser Arbeit gezeigt werden, dass Hyphen zwar für Schädigung und Virulenz innerhalb invasionsbasierter Infektionsmodelle, jedoch nicht für die Pathogenese systemischer Infektionen benötigt werden. Die Ergebnisse dieser Arbeit sind für die Entwicklung therapeutischer Strategien relevant: Therapeutika, welche die Filamentierung unterdrücken, können zu einem gewissen Grad für die Behandlung von Vorteil sein, da sie invasives Wachstum verhindern. Jedoch ist dabei zu bedenken, dass *C. albicans* in der Lage ist, sich rasch anzupassen und der Verlust der Hyphenbildung eventuell durch andere Virulenzfaktoren und Fitnessattribute kompensiert werden kann.

1. Introduction

1.1 Human pathogenic fungi

The fungal kingdom is estimated to include 3.5-5.1 million species (Brien et al. 2005). Of the 120,000 fungal species described so far, around 600 are known to cause disease in humans (Hoog 2000). Healthy individuals are armed with effective mechanisms provided by the immune system to prevent fungal infections and battle disease progression successfully in most cases (Köhler et al. 2017, Brown et al. 2012). Nevertheless, some fungi like e.g. *Histoplasma capsulatum*, *Paracoccidioides brasiliensis* and *Cryptococcus gattii* are true pathogens that are able to infect humans independent of their immune status (Hall and Noverr 2017, Klein and Tebbets 2007, Sil and Andrianopoulos 2014, Kronstad et al. 2011, Byrnes et al. 2011). However, the majority of the pathogenic fungi are considered opportunistic pathogens that primarily cause infections in individuals with a weakened or dysfunctional immune system (Hall and Noverr 2017, Gostinčar et al. 2018). Fungal opportunistic pathogens are distributed all over the fungal tree (Gostinčar et al. 2018) and include amongst others *Aspergillus spp.*, *Candida spp.*, *Cryptococcus neoformans*, and *Taleromyces marneffeii* (Pasricha et al. 2017, Kronstad et al. 2011, Pfaller and Diekema 2004). Most of the fungal infections present as benign superficial infections of the skin or mucosa that can even be asymptomatic. Dermatophytes like *Epidermophyllum spp.*, *Microsporum spp.* and *Trichophyton spp.* as well as *Malassezia spp.* are able to infect keratinized tissue like skin, hair, and nails superficially and together account for the majority of fungal infections worldwide (White et al. 2014, Weitzman and Summerbell 1995). However, fungi can potentially cause life-threatening systemic infections associated with high morbidity and mortality despite antifungal treatment (Horn et al. 2009, Perloth, Choi, and Spellberg 2007). In fact, every year around 1.6 million people die worldwide due to fungal infections but still, in comparison to pathogenic bacteria, fungal pathogens remain underestimated and understudied (Almeida, Rodrigues, and Coelho 2019, Casadevall 2017, Brown et al. 2012).

1.2. *Candida albicans*

Within the phylum Ascomycota the genus *Candida* comprises approximately 150 very heterogeneous species (Moran, Coleman, and Sullivan 2012). Most of these mainly grow as yeast but some have the ability to grow in filamentous forms as pseudo- or true hypha. More than 20 *Candida* species can cause infections in humans (Calderone and Clancy 2012, Pfaller et al. 2010). The medically most important ones are *C. albicans*, *C. glabrata*, *C. parapsilosis*, *C. tropicalis*, *C. krusei* (Yapar 2014, Das et al. 2011), and the recently emerging *C. auris* (Pfaller et al. 2010, Meis

and Chowdhary 2018). In fact, *C. albicans* is the species most commonly isolated from infection sites (Pfaller et al. 2010). Most of the time *C. albicans* infections are of intrinsic origin; in fact in up to 70-80 % of the human population, *C. albicans* resides as a harmless commensal, thereby colonizing the mucosal surfaces of the gastrointestinal (GI) and/or genitourinary tract as part of the normal microbiota (Hall and Noverr 2017). *C. albicans* has coevolved with its mammalian host (Kadosh and Lopez-Ribot 2013) and is considered an obligate commensal (Odds 1988). Although some environmental isolates have been found (Bensasson et al. 2019), a natural environmental reservoir has not been identified, yet (Hall and Noverr 2017).

1.3. Infections caused by *C. albicans*

As with other diseases caused by opportunistic fungal pathogens, immunosuppression or a dysfunctional immune system, the use of long-term and/or broad-spectrum antibiotics, and uncontrolled diabetes are amongst others the main risk factor for the development of candidiasis (Brusselsaers, Blot, and Vogelaers 2011, Delaloye and Calandra 2014, Greenfield 1992). The spectrum of diseases ranges from mild superficial mucosal to severe and life-threatening systemic candidiasis.

1.3.1. Mucosal infections

The most common and relatively benign infections are superficial infections affecting the vulvovaginal, oropharyngeal and/or esophageal mucosa (Fidel 2002, Delaloye and Calandra 2014). Although in most of the cases non-lethal, symptomatic infections reduce the quality of life and are globally associated with high medical costs (Willems et al. 2020). Oropharyngeal candidiasis (OPC) is most prevalent in human immunodeficiency virus (HIV)-infected individuals (Pankhurst 2009) and is frequently one of the first clinical indications of an HIV infection (Berberi, Noujeim, and Aoun 2015). More than 90% of HIV⁺/acquired immunodeficiency syndrome (AIDS) patients will experience OPC at some time during the disease progression (Samaranayake 1992, Samaranayake and Holmstrup 1989). In addition, risk factors for OPC include e.g. local or systemic immunosuppression, wearing of dentures, and chemotherapeutic therapy (Swidergall and Filler 2017, Akpan and Morgan 2002). In some cases *C. albicans* can spread from the oropharynx to the esophagus causing esophageal candidiasis. This illness is commonly observed in patients with advanced AIDS, leads to difficulties in swallowing and is often associated with pain (Vazquez 2000). The most prevalent *C. albicans* infection, however, is represented by vulvovaginal candidiasis (VVC), with three out of four women experiencing VVC at least once in their lifetime (Willems et al. 2020). Eight percent of women suffer from recurrent VVC, defined as more than 3 episodes per year

(Denning et al. 2018). In contrast to other mucosal infections caused by *C. albicans* VVC is often affecting otherwise immunocompetent women that are predominantly in child-bearing age (Willems et al. 2020). Further factors that predispose for VVC are hormone therapy, high-estrogen containing oral contraceptives, pregnancy, and sexual activity (Sobel et al. 1998, Fidel 2004).

1.3.2. Invasive Candidiasis

C. albicans is able to cause life-threatening infections that are often health-care-associated and primarily affect critically ill immunocompetent or severely immunocompromised patients (Pfaller 1996, Perlroth, Choi, and Spellberg 2007) resulting in high mortality rates of up to 50% despite antifungal therapy (Horn et al. 2009, Perlroth, Choi, and Spellberg 2007, Delaloye and Calandra 2014). With the advances of modern medicine, the incidence of candidiasis increased together with the number of immunosuppressed patients susceptible to opportunistic pathogens (Yapar 2014, Delaloye and Calandra 2014, MacCallum 2012). Invasive or systemic candidiasis (terms are often interchangeably used) can be divided in bloodstream infections, defined as the presence of *Candida* in the blood (candidemia), and deep-seated candidiasis (Pappas et al. 2018, Clancy and Nguyen 2013). Candidemia is considered the third or fourth most common cause of bloodstream infections in the intensive care unit (ICU) in the USA and therefore represents a significant clinical problem (Kullberg and Arendrup 2015, Delaloye and Calandra 2014). Risk factors for the development of systemic infections are multi-factorial and include: I) Intrinsic factors such as *C. albicans* colonization, increased age, gastrointestinal perforation (Pappas et al. 2018); II) iatrogenic factors such as prolonged stays in the hospital or ICU, hematological and solid malignancies, chemotherapeutic/immunosuppressive therapy, organ transplantation, major surgery (especially gastrointestinal surgery), and the presence of a central venous catheter (Pappas et al. 2018, Yapar 2014, Das et al. 2011). Further factors associated with an increased risk to develop systemic candidiasis are profound neutropenia and graft-versus-host disease (Pappas et al. 2018). Additionally, congenital immune deficiencies and genetic alterations such as single-nucleotide polymorphisms (SNPs) can predispose for systemic *C. albicans* infections. For example SNPs in genes coding for Toll-like receptors (TLR1-4) mediating pathogen recognition or in the interleukins IL-12b and IL-10 (Johnson et al. 2012) are associated with an increased risk for systemic and persistent candidemia, respectively (Kumar et al. 2014, Johnson et al. 2012).

Different scenarios exist how *C. albicans* is able to reach the bloodstream: I) endogenously from the gut, either directly due to fungal overgrowth as a consequence of microbial dysbiosis, leading to fungal invasion, damage and breaching of the intestinal barrier or indirectly by leakage of the gut during abdominal surgery or due to secondary effects of medications such as e.g. cyclophosphamide, having a negative impact on the intestinal barrier function (Owari et al. 2012,

Koh et al. 2008); **II**) from deep-seated local infections, as consequence of e.g. a progressing peritonitis or mucocutaneous infection (Kullberg and Arendrup 2015); **III**) *C. albicans* is introduced directly *via* intravenous catheters in the nosocomial setting, directly circumventing the hosts physical barrier functions (Kullberg and Arendrup 2015, Delaloye and Calandra 2014). Once in the bloodstream *C. albicans* is able to disseminate systemically and to infect and invade into almost all internal organs (referred to as systemic candidiasis) (Lionakis et al. 2011) resulting in different clinical manifestations. Depending on the host immune status and the route of infection, the kidneys, liver, spleen but also the brain and the heart are the organs most often affected by systemic candidiasis (Moore, Leef, and Pang 2003, Cornely, Bangard, and Jaspers 2015, Walsh and Dixon 1996). Deep-seated candidiasis is defined as the fungal invasion and growth in otherwise sterile tissues that is arising often preceding candidemia (Kullberg and Arendrup 2015, Pappas et al. 2018). Severe *Candida* infections can progress to sepsis (Delaloye and Calandra 2014, Spellberg et al. 2005), defined as “life-threatening organ dysfunction caused by a dysregulated host response to infection” (Singer et al. 2016). Accurate early diagnosis is key to a successful treatment (Pappas et al. 2018, MacCallum and Odds 2004, Garey et al. 2006), however, clinical presentations of invasive candidiasis are rather unspecific and mimic those of viral and bacterial infections (Delaloye and Calandra 2014, Dolin et al. 2019) and therefore present a diagnostic challenge.

1.4. Host defense against *C. albicans* infections

In the healthy host a balanced interplay between *C. albicans* and the host immune system is required to keep *C. albicans* in a commensal state (Richardson and Moyes 2015). The innate immune system constituting of epithelial and endothelial cells, providing a passive physical barrier, together with the complement system and phagocytic cells present the first line of defense against potential pathogens (Gilbert, Wheeler, and May 2014, Yan, Yang, and Tang 2013, Chowdhury, Sacks, and Sheerin 2004). Professional phagocytes such as neutrophils, monocytes/macrophages and dendritic cells (DCs) are key players in the antifungal host response as they are able to engulf and kill pathogens (Miramón et al. 2012, Brown 2011). The importance of neutrophils but also macrophages for controlling fungal infections was shown in infection models in mice depleted of these cells rendering the mice susceptible to systemic *C. albicans* infections (Fulurija, Ashman, and Papadimitriou 1996, Qian et al. 1994). The requirement of neutrophils to combat fungal infection is consistent with neutropenia being a predisposing factor for the development of candidemia in humans (Pappas et al. 2018). The first point of interaction between host cells and pathogen is the cell wall of *C. albicans* (Chaffin 2008). The cell wall constitutes of two layers built of the polysaccharides mannans (*O*-linked and *N*-linked), glucans and chitin. The outer most exposed layer

consists of mannosylated proteins. They shield the inner layer consisting of carbohydrate polymers β -1,3 glucan covalently linked to β -1,6 glucan and chitin (Gow and Hube 2012). Phagocytes as well as epithelial and endothelial cells are able to sense pathogens through the action of pattern recognition receptors (PRRs) recognizing various conserved pathogen-associated molecular patterns (PAMPs) that in part are present on the fungal cell wall (Brown 2011). PRRs such as the Toll-like receptors TLR2 and TLR4 and the C-type lectin receptors Dectin-1 and mannose receptor (MR) recognize phospholipomannan, *O*-mannan, β -glucan and *N*-mannan, respectively (Cheng et al. 2012). Receptor binding triggers a signaling cascade that results in the release of pro-inflammatory cytokines and activation of the innate immune response (Netea et al. 2006). In addition to the immediate but rather unspecific innate immune response, phagocytosis of pathogens by antigen-presenting cells such as DCs is crucial for the initiation of the specific adaptive immune response (Richardson and Moyes 2015). DCs are able to degrade phagocytosed fungal cells and present antigenic peptides using major histocompatibility complex class II molecules (MHC II) and present them to antigen-reactive T cells after migration to the lymphoid tissue (Clement et al. 2016, Steinman 2006). After activation these T cells can, depending on e.g. the external cytokine environment, differentiate into different subsets of T-helper effector cells such as Th1, Th2, Th17 and Treg cells (Dong and Flavell 2000, Richardson and Moyes 2015, Alberts et al. 2002). These subsets differ in their cytokine expression pattern as well as in their effect on the immune function. Th1 cells, characterized amongst others by the release of pro-inflammatory cytokines such as interferon- γ (IFN- γ) (van de Veerdonk and Netea 2010), mediate protective effects against *C. albicans* mucosal and systemic infections (Balish et al. 1998, Cenci et al. 1998). Activation of Th1 cells results in macrophage and neutrophil activation, enhanced phagocytic function and killing (van de Veerdonk and Netea 2010, Alberts et al. 2002). In contrast Th2 cells, characterized by producing interleukins IL-4 and IL-10, have a dampening effect on inflammation. Although they are helpful in fighting parasitic pathogens (van de Veerdonk and Netea 2010), if activated in the context of candidiasis, they rather mediate fungal growth and dissemination and are therefore considered non-protective (Richardson and Moyes 2015, Alberts et al. 2002). Differentiation of naïve T cells into IL-17 producing Th17 cells is crucial for the recruitment and activation of neutrophils to the site of infection. While a Th17 response is needed to fight systemic candidiasis in mice (Huang et al. 2004), in humans it is mainly needed for protection against mucocutaneous *C. albicans* infections (Eyerich et al. 2008).

1.5. *C. albicans* virulence factors and fitness attributes

In microbiology virulence is defined as the capacity of an organism to cause damage and/or disease in a host (Shapiro-Ilan et al. 2005, Casadevall and Pirofski 1999). In order to do so, *C. albicans* must be able to evade or counter the host immune system, survive, replicate and adapt quickly to ever-changing conditions *in vivo* (Köhler et al. 2017, Gauthier 2017). Many virulence factors and fitness attributes have been described to contribute to the pathogenic potential of *C. albicans*. The fungal polymorphism, the ability to adhere to, invade, and damage host cells, and the production of extracellular hydrolytic enzymes like secreted aspartyl proteases (Saps), lipases and phospholipases are amongst the most important virulence factors (Mayer, Wilson, and Hube 2013).

1.5.1. Adhesion, invasion and damage

The prerequisite for successful colonization and the establishment of an infection is the ability of *C. albicans* to adhere to cells, tissues and inert abiotic surfaces, e.g. medical devices such as intravascular catheters or prostheses (de Groot et al. 2013, Verstrepen and Klis 2006). Furthermore, adhesion is required for biofilm formation and for cell-cell interaction of *C. albicans* (flocculation) or interaction with other microbes termed coaggregation (Chaffin 2008). *C. albicans* possesses plenty of specialized cell-surface proteins, mainly glycoproteins that promote adhesion (Verstrepen and Klis 2006, Essen, Vogt, and Mösch 2020). These adhesins commonly share a three-domain structure and are linked to the glucan layer of the cell wall *via* a glycosyl-phosphatidyl-inositol (GPI)-anchor (Verstrepen and Klis 2006, de Groot et al. 2013). The N-terminal domain, exposed at the cell surface is required for ligand recognition and binding (Essen, Vogt, and Mösch 2020). Although yeast have the capacity to adhere, the morphological transition to hyphae is coinciding with enhanced adhesive properties as a result of varying expression and surface exposure of adhesins during different morphological stages (Chaffin 2008). The most thoroughly studied adhesins are the hyphal wall protein Hwp1 and the members of the agglutinin-like sequence (ALS)-family, consisting of Als1-7 and Als9 (Hoyer 2001). Hwp1 is hypha-associated and the N-terminus that mimics transglutaminase substrate is covalently cross-linked to yet unknown host proteins *via* the activity of mammalian transglutaminase (Nobile et al. 2006, Staab et al. 1999). Although not required for systemic infection, Hwp1 is needed for colonization of the oral cavity (Staab, Datta, and Rhee 2013). Among the eight Als proteins Als3 is the most prominent adhesin, only expressed during hyphal development (Hoyer et al. 1998). Als3 promotes adhesion to host cells through interaction with N-cadherin on endothelial and E-cadherin on epithelial cells (Phan et al. 2007). In addition, Als3 but also Ssa1 serve as fungal invasins required for *C. albicans* to promote induced endocytosis by endothelial and epithelial cells (Phan et al. 2007, Yang et al. 2014, Sun et al. 2010). Besides induced endocytosis which is a passive process, *C. albicans* is able to invade *via* active fungal-driven

penetration (Phan et al. 2007, Dalle et al. 2010, Zakikhany et al. 2007). Both mechanisms can result in epithelial cell damage but require proper hyphal formation (Filler et al. 1995, Phan et al. 2007, Zhu and Filler 2010). Fungal driven penetration requires hyphal elongation, physical forces and the secretion of hydrolytic enzymes (Yang et al. 2014). However, damage of epithelial cells is not directly coupled to hyphae formation or fungal invasion, as it requires the hypha-associated secreted peptide toxin Candidalysin (Moyes et al. 2016). A mutant unable to produce Candidalysin encoded by *ECE1* is still able to invade and penetrate through epithelial cells but lost its damage potential resulting in avirulence or reduced virulence in a murine OPC model (Moyes et al. 2016) and a systemic infection model (Swidergall et al. 2019), respectively, despite proper hyphal formation.

1.5.2. Hydrolytic enzymes

Hydrolytic enzymes contribute directly to the virulence potential of *C. albicans*. Secreted enzymes like the secreted aspartyl proteases (Saps), lipases and phospholipases facilitate nutrient acquisition by degradation of extracellular complex substrates allowing the fungus to transport the breakdown products into the cell (Chaffin 2008). However, in addition to their role in nutrient acquisition, proteinases can directly damage host cells and can be involved in immune evasion by degradation of host molecules of the immune system (Naglik, Challacombe, and Hube 2003). The Sap family comprises ten members that have different pH optima for activity and differ in their substrate specificity (Schild et al. 2011, Naglik et al. 2004). Whereas Sap1-3 are mainly associated with yeast cells, Sap 4-6 are hyphae-associated (Naglik et al. 2004).

1.5.3. Metabolic flexibility

During colonization of different niches as well as during infection *C. albicans* faces a great variety of different nutrient compositions (Brock 2009). Metabolic flexibility is the ability to quickly respond and adapt to changing conditions and different nutrients to generate energy depending on the energy demand (Smith et al. 2018). Metabolic flexibility is considered a fitness attribute of *C. albicans* (Mayer, Wilson, and Hube 2013) and is key for the success of *C. albicans* as a commensal but also provides advantages during infection. In addition, it is known to increase fungal colonization, resistance to phagocytic recognition and killing (Ballou et al. 2016), and enhances pathogenicity (Childers et al. 2016, Ene et al. 2014). In an effort to restrict fungal growth, especially during infection, the host actively withholds nutrients, a measure known as 'nutritional immunity' (Crawford and Wilson 2015). Like every other living cell, *C. albicans* requires macronutrients (e.g. carbon and nitrogen; needed in higher quantities) and micronutrients (e.g. vitamins, trace metals such as zinc and iron; needed in smaller quantities) for survival and growth (Ene et al. 2014, Crawford and Wilson 2015). Especially in niches in which nutrients are limited, e.g. within

phagocytic cells or in the GI tract, where *C. albicans* has to compete with other microorganisms for nutrients (Brock 2009), metabolic flexibility allows *C. albicans* to assimilate the available carbon sources (Huang et al. 2017). *C. albicans* is a Crabtree-negative yeast that, in contrast to e.g. *Saccharomyces cerevisiae*, is able to assimilate glucose and alternative carbon sources such as amino acids, fatty acids, and carboxylic acids at the same time (Sandai et al. 2012, Childers et al. 2016). Physiological concentrations of preferred fermentable carbon sources such as glucose and fructose vary greatly in the GI tract depending on food intake (Van Ende, Wijnants, and Van Dijck 2019), are low in blood (Brown et al. 2014, Laughlin 2014), and are rather scarce in tissues or even absent in micro-environments and in phagocytes (Barelle et al. 2006, Lorenz, Bender, and Fink 2004). Therefore, *C. albicans* has to additionally rely on the assimilation of non-fermentable carbon sources *via* the glyoxylate cycle, β -oxidation and gluconeogenesis (Ramírez and Lorenz 2007) to feed its demand for energy and to generate macromolecules from C_2 compounds such as acetate, ethanol and citrate (Lorenz and Fink 2002) in order to survive and replicate *in vivo*. *C. albicans* deletion mutants lacking genes coding for key enzymes of alternative carbon metabolic pathways like the glyoxylate cycle (*ICL1*) and gluconeogenesis (*PCK1*) appeared less virulent in murine systemic infection models (Lorenz and Fink 2001, Barelle et al. 2006). However, a mutant lacking the gene coding for the glycolytic enzyme pyruvate kinase *PYK1* was avirulent as well indicating that glycolysis is needed for growth inside the host (Barelle et al. 2006). Interestingly, Barelle *et al.* showed that within an organ, or even within close proximity, fungal cells are able to activate different pathways indicating that fungal cells are exposed to micro-environments with varying carbon sources and are therefore highly heterogeneous with respect to assimilation (Barelle et al. 2006).

1.5.4. Polymorphism

C. albicans is a polymorphic fungus that can grow in three major vegetative growth forms: as unicellular yeast or filamentous as pseudohypha or hypha (Fig.1) (Sudbery, Gow, and Berman 2004). Oval-shaped yeast are around 6-7 μm in diameter (Mukaremera et al. 2017) and propagate by asymmetric budding (Berman 2006). Both filamentous forms are able to grow in a highly polarized fashion (Thompson, Carlisle, and Kadosh 2011). However, whereas pseudohyphae are ellipsoid with a minimum width of 2.8 μm in the middle, have constrictions at the septal side and are highly branched (Sudbery, Gow, and Berman 2004), true hyphae appear parallel-walled with segments that are constant in width (approximately 2 μm) (Desai 2018, Thompson, Carlisle, and Kadosh 2011, Chen et al. 2020, Carlisle et al. 2009). It is still a matter of debate whether pseudohypha, that appear like elongated yeast cells attached end-to-end can be considered an independent morphotype or whether they are resembling an intermediate form between yeast and hyphae as they show some

similarities with both cell types (Noble, Gianetti, and Witchley 2017, Sudbery, Gow, and Berman 2004).

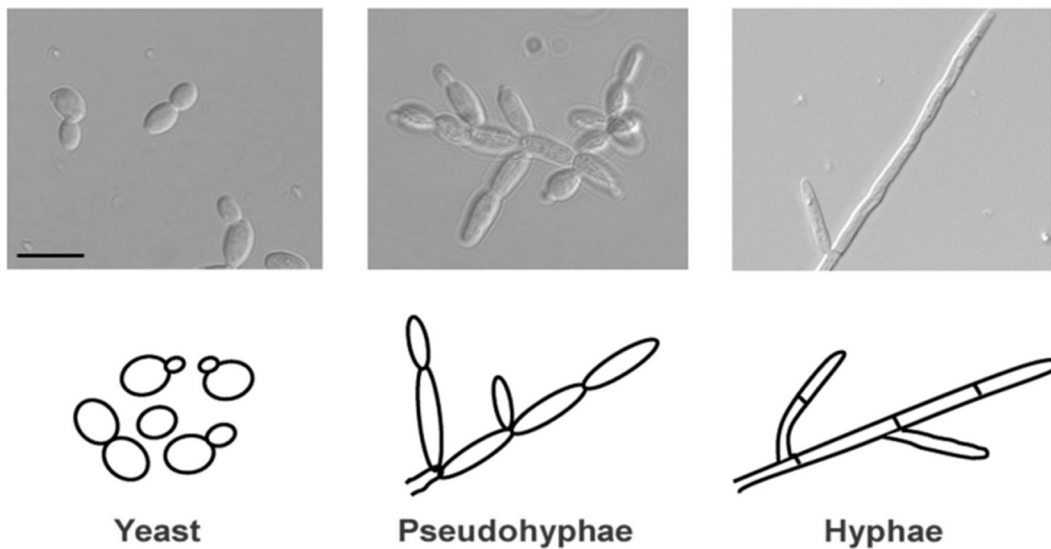


Fig. 1: *C. albicans* can exist in three main morphologies: Yeast, pseudohyphae and hyphae. The figure was adapted from Thompson *et al.* (Thompson, Carlisle, and Kadosh 2011). The scale bar represents 10 μm .

C. albicans is able to rapidly and reversibly transit between these morphologies, also known as phenotypic plasticity (Whiteway and Bachewich 2007), which can have an impact on both commensalism and pathogenicity (Xie *et al.* 2013). Phenotypic plasticity is the consequence of the response to different environmental conditions and stimuli *via* expression of different gene sets (Rai *et al.* 2018, Tao *et al.* 2014). In addition to the three main morphologies described above *C. albicans* is capable of forming chlamyospores, which are large 10-20 μm in diameter, thick-walled cells that can be formed by filaments at the hyphal tip (the so-called suspensor cell) under certain nutrient starvation conditions (Staib and Morschhäuser 2007, Böttcher *et al.* 2016). Until now it is unknown whether chlamyospores have a biological function (Staib and Morschhäuser 2007, Böttcher *et al.* 2016). Furthermore, yeast-like morphotypes have been described such as opaque cells that play a role in mating (Soll 2004), gastrointestinal-induced transition (GUT) and gray cells (Noble, Gianetti, and Witchley 2017, Tao *et al.* 2014). *C. albicans* is, in addition, able to form (single species or mixed species) biofilms composed of yeast, pseudohyphae and hyphae that form a three-dimensional structure surrounded by an extracellular matrix (Blankenship and Mitchell 2006). Biofilms are established primarily by planktonic yeast cells that adhere to a suitable biotic or abiotic surface (Chin *et al.* 2016). In the clinical setting *C. albicans* biofilms formation on

implanted devices e.g. on catheters, pacemakers or prosthetic joints are a serious concern as they can directly and perpetually seed systemic infections (Nobile and Johnson 2015, Chin et al. 2016). Following adhesion, yeast start to proliferate and to form hypha in the initiation stage of biofilm formation (Gulati and Nobile 2016). Afterwards, the biofilm starts to mature coinciding with repression of yeast and enhancement of filamentous growth (Nobile and Johnson 2015). At this stage the three-dimensional structure is developing and the extracellular matrix is built that protects the biofilm by maintaining its integrity, preventing the diffusion of administered antibiotics/antifungals or other toxic substances from diffusion into the biofilm and/or ultimately defends the biofilm against phagocytic activity in the *in vivo* setting (Blankenship and Mitchell 2006, Wall et al. 2019, Chandra et al. 2001). As a consequence, biofilms present a therapeutic challenge as they exhibit a high resistance to antifungal drugs and the defense measures of the host immune system (Nobile and Johnson 2015). The depletion of nutrients and accumulation of quorum sensing molecules inside the biofilm is initiating the dispersal stage that closes the life-cycle of biofilms (Blankenship and Mitchell 2006). In the dispersal stage yeast can be released by budding off from the top-most hyphal layer from biofilms creating the opportunity to access and colonize new host niches (Uppuluri et al. 2010, Gulati and Nobile 2016).

1.5.4.1. Regulation of the transition from yeast to hypha morphology

The transition from yeast to hypha has been extensively studied in *C. albicans*. Hypha formation is a two-step process that requires the initiation of filamentation and the maintenance of hyphal growth (Martin et al. 2011, Lu, Su, and Liu 2014) and is regulated in a complex signaling network (Chen et al. 2020, Noble, Gianetti, and Witchley 2017). Several environmental and nutritional cues present in the mammalian host such as physiological temperature (37 °C), serum, neutral/alkaline pH, N-acetyl-glucosamine (GlcNAc), elevated CO₂ and low O₂ concentration alone or in combination have the potential to trigger the yeast-to-hypha transition (Fig. 2) (Sudbery 2011, Ernst 2000, Noble, Gianetti, and Witchley 2017, Kornitzer 2019, Desai 2018, Taschdjian, Burchall, and Kozinn 1960, Biswas, Van Dijck, and Datta 2007). Depending on the signals sensed, different signaling cascades, which are partly interconnected, are activated and transduce the signal into the cell resulting in the underlying cellular response (Kornitzer 2019, Sudbery 2011). This response can have an extensive impact not only on morphology but also on the structure of the cell wall, the gene expression profile and the expression of virulence characteristics (Jacobsen et al. 2012, Biswas, Van Dijck, and Datta 2007). One central signaling pathway involved in the initiation of filamentation is the Ras1-cAMP-protein kinase A (PKA) pathway (Shapiro, Robbins, and Cowen 2011). Sensing of a broad range of environmental stimuli (GlcNAc, CO₂, physiological temperature, hypoxia, nutrient limitation and serum amongst others) result in the activation of the small GTPase Ras1 (Inglis and Sherlock 2013,

Huang et al. 2019, Hogan and Muhlschlegel 2011). By physical interaction, the activated Ras1 stimulates the enzymatic activity of the downstream located adenylyl cyclase Cyr1, resulting in increasing intracellular cAMP level. The cAMP level can be influenced by the phosphodiesterases Pde1 and Pde2 that can degrade cAMP (Inglis and Sherlock 2013). However, the Ras1-cAMP-protein kinase A (PKA) pathway can also be activated independently of Ras1 through sensing of hyphal inducing conditions directly by Cyr1 (Hogan and Muhlschlegel 2011). The cAMP-dependent PKA is consisting of the catalytic subunits Tpk1 and Tpk2 and the regulatory subunit Bcy1 (Huang et al. 2019). Bcy1 is able to bind cAMP, leading to its dissociation from PKA and the release of the catalytic subunit (Huang et al. 2019), resulting in the regulation of transcription factors (TFs). The master transcriptional regulator downstream of the cAMP-PKA pathway is represented by Efg1 (Bockmühl and Ernst 2001) (Biswas, Van Dijck, and Datta 2007). In addition, Ras signaling can activate a conserved mitogen-activated protein kinase (MAPK) pathway with the downstream major TF Cph1 (Inglis and Sherlock 2013, Biswas, Van Dijck, and Datta 2007). Both, Efg1 and Cph1 promote the transcription of hypha-associated genes (HAGs). One of the key targets of these TFs is the *UME6* gene coding for a transcriptional regulator that is required for the induction of the hyphal-specific G1 cyclin encoded by *HGC1* (Carlisle and Kadosh 2010, Zeidler et al. 2009). Besides Hgc1 and Ume6, Eed1 is essential for hyphal elongation (Martin et al. 2011, Zheng, Wang, and Wang 2004, Carlisle and Kadosh 2010).

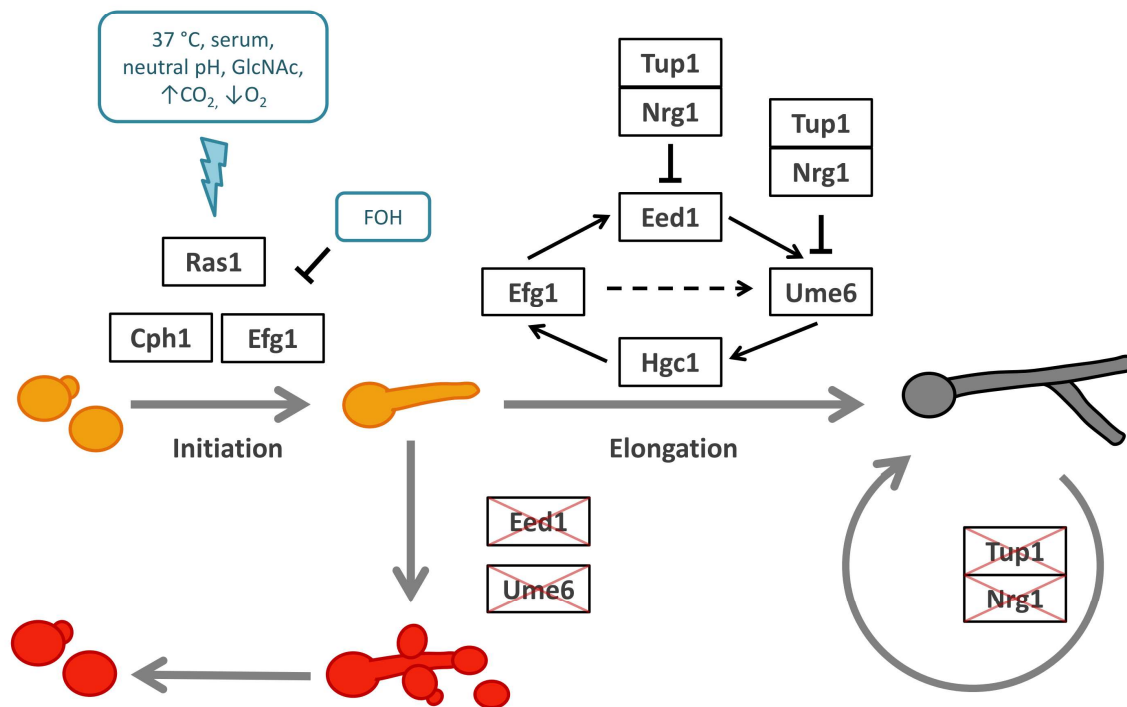


Fig. 2: Simplified regulatory network for hyphal initiation and elongation adapted from Martin et al. (Martin et al. 2011). Hyphal formation requires the initiation of germ tube formation of yeast cells (yellow) by sensing environmental signals such as 37 °C, serum components, neutral pH, GlcNAc, elevated CO₂ or low O₂ concentration. Via e.g. the Ras1-cAMP-PKA pathway the signals are transduced into the cell resulting in the activation of downstream TFs such as Cph1 and Efg1 promoting expression of hypha-associated genes. The quorum sensing molecule farnesol (FOH) is able to inhibit the yeast-to-hypha transition by binding to the Ras1-cAMP-PKA pathway component Cyr1 thereby interfering with cAMP production. The elongation of germ tubes into true hypha (grey) requires derepression of genes targeted by the transcriptional repressors Nrg1 and Tup1, and expression of *UME6* and *EED1*. In red: homozygous deletion of *UME6* or *EED1* results in the switch from hyphal to yeast cell growth as elongation of germ tubes into hypha could not be maintained. In contrast, deletion of *TUP1* or *NRG1* results in filamentous growth even under conditions that do not favor hyphal growth.

In addition to the positive regulations described above, pathways that are negatively regulating morphogenesis exist. Tup1, Nrg1 and Rfg1 represent repressor of filamentation that in the absence of hyphal inducing signals prevent hyphal formation (Cleary et al. 2012, Braun et al. 2000, Banerjee et al. 2008). Initiation of filamentation requires Nrg1 level to decrease (Braun, Kadosh, and Johnson 2001) and the subsequent dissociation of Nrg1 allows the GATA family TF Brg1 to recruit the histone

deacetylase 1 (Hda1) to the promotor regions of HAGs resulting in chromatin modifications. As a consequence, this prevents Nrg1 from binding promoting the elongation of germ tubes into hyphae (Lu, Su, and Liu 2012).

1.5.4.2. The *C. albicans* *EED1* gene

One of the genes strictly required for hyphal maintenance in *C. albicans* is *EED1* (alias *DEF1*, *EDT1*, *ORF19.7561*). *EED1* was identified as one of the genes up-regulated in samples from HIV⁺ patients with oropharyngeal candidiasis and in a reconstituted human oral epithelium (RHE) model by Zakikhany *et al.* (Zakikhany *et al.* 2007). A mutant lacking *EED1* (*eed1Δ/Δ*) is able to initiate hyphal growth under hypha-inducing conditions resulting in germ tube formation, but switches back to yeast cell growth by budding off yeast at the apical pole, the site of septation and from the mother cells after approximately 4 h of growth *in vitro* (Polke *et al.* 2017, Martin *et al.* 2011, Zakikhany *et al.* 2007). Within the time frame of hyphal initiation, the *eed1Δ/Δ* mutant is able to express HAGs such as *HGC1*, *ALS3*, *HWP1* and *UME6* at wild type (WT) levels (Zakikhany *et al.* 2007, Martin *et al.* 2011). With the switch back to yeast growth the expression of HAGs is abolished (Martin *et al.* 2011). The phenotype of the *eed1Δ/Δ* mutant closely resembles the phenotype of a mutant lacking *UME6*, a TF that is also required to maintain hyphal extension (Banerjee *et al.* 2008).

The defect in maintaining hyphal elongation, which was found under various hypha-inducing conditions (Zakikhany *et al.* 2007, Martin *et al.* 2011), resulted in a reduced capacity of the *eed1Δ/Δ* mutant to induce tissue damage in oral epithelial cells and enterocytes and in the RHE model *in vitro* (Wächtler *et al.* 2011, Zakikhany *et al.* 2007). Adhesion and invasion of *C. albicans* was not affected by the absence of *EED1* (Wächtler *et al.* 2011, Zakikhany *et al.* 2007). However, the *eed1Δ/Δ* mutant was unable to escape from epithelial cells but instead remained trapped and proliferated in the yeast form in the upper layer of the RHE, the reason why it was termed Epithelial Escape and Dissemination (Zakikhany *et al.* 2007). Martin *et al.* showed, that *EED1* can be integrated into the regulatory circuit of hyphal maintenance, as expression of *EED1* was regulated by Efg1, Nrg1 and Tup1 and that *UME6* expression depends on the expression level of *EED1* (Fig. 2)(Martin *et al.* 2011).

Recently it was shown that the *eed1Δ/Δ* mutant produces high amounts of the quorum sensing molecule farnesol (FOH) and, in addition, is hypersensitive to this compound (Polke *et al.* 2017). The presence of small amounts of FOH exert a negative impact on the length of germ tubes and the number of cells that are able to initiate filamentation, an effect that could also be observed when

cells were seeded in higher densities (Polke et al. 2017). Despite considerable efforts (Polke 2017), the molecular function of *EED1* remains unknown until today.

1.5.4.3 Role of morphology during commensalism and disease

It has been proposed that all morphologies of *C. albicans* play their own role during commensalism and pathogenicity (Jacobsen et al. 2012). This view is supported by the fact that all morphologies can be detected during infection in men and mice (Cleary et al. 2016, Di Carlo et al. 2013, Gupta 2001). As a harmless colonizer of mucosal surfaces of the GI tract and/or the vaginal mucosa, *C. albicans* is primarily found in the yeast form (Willems et al. 2020, Vautier et al. 2015). The yeast-to-hyphal transition has been linked with the shift from the commensal to the pathogenic state (Cleary et al. 2016, Desai 2018). Hyphal formation: I) enables the fungus to invade and II) damage epithelial layers and tissues *in vitro* (Wächtler et al. 2011, Dalle et al. 2010) and *in vivo* (Felk et al. 2002); III) represents a mechanism to evade phagocytes, e.g. macrophages after phagocytosis by piercing leading to the fungal outgrowth (Lorenz, Bender, and Fink 2004, Miramón, Kasper, and Hube 2013); and IV) is linked to the expression of genes coding for virulence factors such as Sap4-6, Hwp1 and Als3, Ece1 and Hgc1 (Mayer, Wilson, and Hube 2013, Jacobsen et al. 2012). Therefore, it is not very surprising that hyphal formation is thought to be closely linked to virulence. During the course of infection, the yeast form is believed to promote dissemination through the bloodstream, adherence to endothelial cells and to play a role in the establishment of biofilms (Thompson, Carlisle, and Kadosh 2011, Jacobsen et al. 2012, Gulati and Nobile 2016). Further insights into the role of morphology during infection was obtained by the generation of *C. albicans* strains locked in the yeast or filamentous form, which were tested in different *in vitro* and *in vivo* infection models. In colonization experiments, yeast-locked strains showed higher and more stable colonization levels compared to strains locked in the filamentous form in the GI tract (Vautier et al. 2015) as well as in the vagina (Peters et al. 2014). Mucosal infection models *in vitro* (Wächtler et al. 2011, Zakikhany et al. 2007) as well as *in vivo* models such as OPC (Swidergall et al. 2019, Park et al. 2005) and vaginitis models (Peters et al. 2014) revealed that hypha (together with *ECE1* expression) are essential for pathogenesis whereas yeast appeared to be avirulent. Similar results have been obtained for systemic infection models mimicking disseminated *C. albicans* infections in humans (Spellberg et al. 2005): Strains locked in the yeast form such as *efg1Δ/Δcph1Δ/Δ* (Lo et al. 1997), *hgc1Δ/Δ* (Zheng, Wang, and Wang 2004) and a strain constitutively expressing the hyphal repressor *NRG1* (*tet-NRG1* in the absence of doxycycline (Saville et al. 2003, Saville et al. 2008)) have been shown to be avirulent or attenuated in virulence. Although it seems that hyphae are fundamental for virulence, hyphal formation alone is not sufficient to drive pathogenesis during systemic

candidiasis as mutants locked in a filamentous state such as the *tup1Δ/Δ* mutant (Cleary et al. 2016, Braun et al. 2000), the *nrg1Δ/Δ* mutant (Murad et al. 2001, Braun, Kadosh, and Johnson 2001) and the *rfx2Δ/Δ* Mutant (Hao et al. 2009) are attenuated in virulence in comparison to the wild type in systemic infections as well. Hence, it was therefore concluded that morphological plasticity is required for pathogenicity in systemic candidiasis (Kadosh and Lopez-Ribot 2013).

2. Aim of this study

The ability of *C. albicans* to form hyphae is considered one of its most important virulence factors. Hyphae are important for invasive growth and tissue damage (Dalle et al. 2010, Wächtler et al. 2011, Felk et al. 2002). In addition, upon phagocytosis by professional phagocytes such as macrophages, *C. albicans* is able to initiate the yeast-to-hypha transition within the phagosomes. This eventually can lead to fungal outgrowth and damage of the immune cells and therefore represents one mechanism of *C. albicans* to evade the immune system (Lorenz, Bender, and Fink 2004, Miramón, Kasper, and Hube 2013). **Manuscript I** (Gerwien et al. 2020) shows that clinical vaginal isolates of *C. albicans* with certain defects in filamentation are less able to damage macrophages. In addition, *C. albicans* mutants unable to form proper hyphae and mutants locked in the yeast form are attenuated or even avirulent in murine systemic infection models (Lo et al. 1997, Zheng, Wang, and Wang 2004, Saville et al. 2008, Saville et al. 2003). On the other hand, *C. albicans* strains locked in the hyphal form are attenuated in virulence as well (Cleary et al. 2016, Braun et al. 2000, Murad et al. 2001, Braun, Kadosh, and Johnson 2001, Hao et al. 2009), indicating that the reversible transition and the presence of different morphologies *in vivo* are required for proper virulence during systemic candidiasis. The first host cells *C. albicans* encounters during experimentally induced systemic candidiasis are cells of the blood. **Manuscript II** (Machata et al. 2021) deals with the establishment of an *ex vivo* murine whole-blood model to investigate the host-pathogen interplay early after systemic infection. Interestingly, in contrast to human blood, murine blood was not able to kill fungal cells and to prevent hyphal formation. However, hyphal formation was not the reason for reduced killing in murine blood, as a filament-deficient strain likewise survived. While *ex vitro* and *in vitro* experiments are helpful to investigate certain aspects of the interaction between a pathogen and the host, they can only in part reflect the complex *in vivo* situation: An *eed1Δ/Δ* mutant, unable to maintain hyphal growth, shows reduced invasion and damage capacities *in vitro* (Wächtler et al. 2011), surprisingly however, although slightly delayed in comparison to the WT, the mutant was causing 100% mortality in a systemic infection model (Martin *et al.*, unpublished). These results challenge the long-standing hypothesis of the requirement of hyphal formation for virulence during systemic candidiasis. The major aim of this study was to characterize the virulence phenotype of strains lacking *EED1* or repressing its expression in different *in vitro* and *in vivo* infection models, and to discover mechanisms leading to virulence in the absence of hyphal formation. The results are summarized in **manuscript III** (Dunker et al. 2021). The insights gained from this thesis shed new light on the role of filamentation in systemic *C. albicans* infections.

3. Manuscripts

3.1. Manuscript I: Gerwien *et al.*, mSphere, 2020

Clinical *Candida albicans* Vaginal Isolates and a Laboratory Strain Show Divergent Behaviors during Macrophage Interactions

Franziska Gerwien, **Christine Dunker**, Philipp Brandt, Enrico Garbe, Ilse D. Jacobsen, Slavena Vylkova

mSphere. 2020 Aug 19. 5(4):e00393-20. doi: 10.1128/mSphere.00393-20.

Summary

The opportunistic fungal pathogen *C. albicans* is the most common cause of vulvovaginal candidiasis, affecting 75% of women at least once in their lifetime. Although non-lethal, infections can affect quality of life and are globally associated with high medical costs. In this study, *C. albicans* isolates from three different patient groups: I) asymptomatic *C. albicans* colonization, II) symptomatic vulvovaginal candidiasis and III) recurrent vulvovaginal candidiasis were compared with the commonly used *C. albicans* laboratory strain SC5314 regarding their interaction with macrophages as key players of the innate immune system. The ability to form hyphae shaped the interaction with macrophages in a group-independent manner: Strains capable of proper hyphal formation damaged macrophages more efficiently than strains with certain defects in filamentation. However, strains that caused symptomatic infections showed a higher β -glucan exposure on their surface, indicating that they are potentially more immunoreactive. The results show, that although heterogenic with respect to filamentation and macrophage interaction, all these strains are highly adapted to their local environment.

The candidate is:

First author, Co-first author, Corresponding author, Coauthor.

Estimated authors' contributions in %:

Author	Conception	Data analysis	Experimental	Writing	Provision of the material
Franziska Gerwien	80	53	53	90	55
Christine Dunker		45	45	5	45
Philipp Brandt		1	1		
Enrico Garbe		1	1		
Ilse D. Jacobsen					
Slavena Vylkova	20			5	



Clinical *Candida albicans* Vaginal Isolates and a Laboratory Strain Show Divergent Behaviors during Macrophage Interactions

Franziska Gerwien,^a Christine Dunker,^b Philipp Brandt,^a Enrico Garbe,^a Ilse D. Jacobsen,^b  Slavena Vylkova^a

^aSeptomics Research Center, Friedrich Schiller University and Leibniz Institute for Natural Product Research and Infection Biology–Hans Knoell Institute, Jena, Germany

^bResearch Group Microbial Immunology, Leibniz Institute for Natural Product Research and Infection Biology–Hans Knoell Institute, Jena, Germany

ABSTRACT Typically, established lab strains are widely used to study host-pathogen interactions. However, to better reflect the infection process, the experimental use of clinical isolates has come more into focus. Here, we analyzed the interaction of multiple vaginal isolates of the opportunistic fungal pathogen *Candida albicans*, the most common cause of vulvovaginal candidiasis in women, with key players of the host immune system: macrophages. We tested several strains isolated from asymptomatic or symptomatic women with acute and recurrent infections. While all clinical strains showed a response similar to the commonly used lab strain SC5314 in various *in vitro* assays, they displayed remarkable differences during interaction with macrophages. This coincided with significantly reduced β -glucan exposure on the cell surface, which appeared to be a shared property among the tested vaginal strains for yeast extract/peptone/dextrose-grown cells, which is partly lost when the isolates faced vaginal niche-like nutrient conditions. However, macrophage damage, survival of phagocytosis, and filamentation capacities were highly strain-specific. These results highlight the high heterogeneity of *C. albicans* strains in host-pathogen interactions, which have to be taken into account to bridge the gap between laboratory-gained data and disease-related outcomes in an actual patient.

IMPORTANCE Vulvovaginal candidiasis is one of the most common fungal infections in humans with *Candida albicans* as the major causative agent. This study is the first to compare clinical vaginal isolates of defined patient groups in their interaction with macrophages, highlighting the vastly different outcomes in comparison to a laboratory strain using commonly applied virulence-determining assays.

KEYWORDS *Candida albicans*, vulvovaginal candidiasis, macrophages, cell wall

Candida albicans is an opportunistic fungal pathogen and a normal colonizer of mucosa of the gut, the oral cavity, and the vulvovaginal tract. When the balance of the microbial flora is disrupted or the immune defenses are compromised, it can become pathogenic, often causing recurrent disease in susceptible individuals (1). Symptomatic infections in the female reproductive tract, termed vulvovaginal candidiasis (VVC), typically occur in otherwise healthy women. Fungal overgrowth, subsequent epithelial invasion, and immune cell infiltration lead to inflammatory symptoms like vaginal itching, burning, and pain (2). Albeit nonlethal, this disease affects 75% of all women at least once in their lifetime (3), while recurrent VVC (RVVC; defined as >3 episodes per year) affects about 8% of all women (4). These clinical representations diminish life quality and cause high costs in the global health system (5).

VVC is a multifactorial hyperinflammatory disorder with several known risk factors from the host side (antibiotic treatment, imbalance in vaginal microbiome, sexual activity, high estrogen levels, pregnancy, and low lactate levels), whereas the reasons

Citation Gerwien F, Dunker C, Brandt P, Garbe E, Jacobsen ID, Vylkova S. 2020. Clinical *Candida albicans* vaginal isolates and a laboratory strain show divergent behaviors during macrophage interactions. *mSphere* 5:e00393-20. <https://doi.org/10.1128/mSphere.00393-20>.

Editor Aaron P. Mitchell, University of Georgia

Copyright © 2020 Gerwien et al. This is an open-access article distributed under the terms of the [Creative Commons Attribution 4.0 International license](https://creativecommons.org/licenses/by/4.0/).

Address correspondence to Slavena Vylkova, Slavena.Vylkova@leibniz-hki.de.

Received 29 April 2020

Accepted 28 July 2020

Published 19 August 2020

for RVVC remain largely unknown (6). In the course of infection, *C. albicans* exploits one of its key virulence attributes: the ability to form hyphae. The filamenting fungus breaches epithelial barriers, and as a first line of defense phagocytic immune cells are recruited in vast numbers to mediate clearance. Elevated Th17-mediated cytokine secretion (interleukin-22 [IL-22], IL-17A, and IL-17F) and inflammasome activation, followed by IL-1 β cleavage, also accompanies this process of hyperinflammatory immune cell infiltration into the vaginal tissues, which is largely responsible for the observed clinical symptoms (7). In this context, nutritional prerequisites have been shown to play an important role in modeling the fungal cell wall architecture and subsequent immune cell recognition (8, 9). In particular, lactate, a predominant carbon source in the vaginal tract (10) has been shown to influence host pathogen interaction and infection outcomes (11–13). Hence, we were particularly interested in studying host-pathogen interactions with strains that have not been extensively propagated in laboratories and come directly from a host niche, using a macrophage cell line as a feasible tool. For this purpose, we compared the commonly used laboratory *C. albicans* strain SC5314 to multiple clinical vaginal isolates from three defined patient groups: (i) asymptomatic *C. albicans* colonization, (ii) VVC, or (iii) RVVC. We observed that during macrophage encounter the isolates behave group-independently different than SC5314, which might be associated with their various capabilities to filament. However, fungal cell wall architecture, while vastly uniform for all tested vaginal isolates, is remarkably different from SC5314 for YPD (yeast extract, peptone, dextrose)-grown cells. Growth in the lactate containing vaginal simulating media unveiled partly group-specific differences in cell wall composition between the isolates, specifically in chitin and β -glucan exposure. Thus, the differences in cell surface architecture might lead to altered initiation of an immune response in the corresponding host niche.

Vaginal isolates show great variability in macrophage interaction. Macrophages, similarly to polymorphonuclear leukocytes, recognize, phagocytose, and subsequently kill invading pathogens as part of their role in the innate immune response. *C. albicans* has been shown to be able to escape phagocytosis via hyphae formation (14). Therefore, we tested the ability of the clinical isolates to filament in various hyphae-inducing *in vitro* conditions (see Fig. S1 in the supplemental material) and observed great variability between the isolates with no clear pattern within a specific patient group. Likewise, various degrees of filamentation were noted when the vaginal strains were cocultured with macrophages in Dulbecco's modified Eagle's medium (DMEM), with the majority of the isolates showing prominent defects in hyphal growth compared to the SC5314 control (Fig. 1A; see also Fig. S2). Overall, a clear association between filamentation and macrophage damage was observed: strains with robust hyphal growth were more likely to cause immune cell damage similar to the SC5314 strain, whereas less filamenting strains failed to induce a SC5314-like LDH release (Fig. 1A). Consequently, the capacity to form filaments appeared to be tightly connected with fungal survival following confrontation with macrophages, with the exception of isolates JS7 and JS20 (Fig. 1B). Of particular interest were strains JS14 and JS16, both isolated from VVC patients, due to their opposing characteristics: while JS14 was able to filament, damage macrophages, and survive phagocytosis, JS16 was impaired in all of these aspects. Importantly, these two strains appeared to be nearly indistinguishable in the *in vitro* filamentation assays. Since both fungal recognition by the immune cells and the ability to filament within the phagosome can influence the outcome of infection, we chose these particular strains to test in detail their interaction with J774.1 cells. JS16 showed a slightly diminished intracellular hyphal length compared to the SC5314 laboratory strain (Fig. 1C), whereas JS14 was not as well recognized by macrophages (Fig. 1D). These mild phenotypes were rather surprising since they could not explain the gross differences in infection outcomes. In summary, the vaginal isolates react to macrophages in a patient group-independent manner, showing various filamentation defects that affect macrophage interaction. Infection outcome

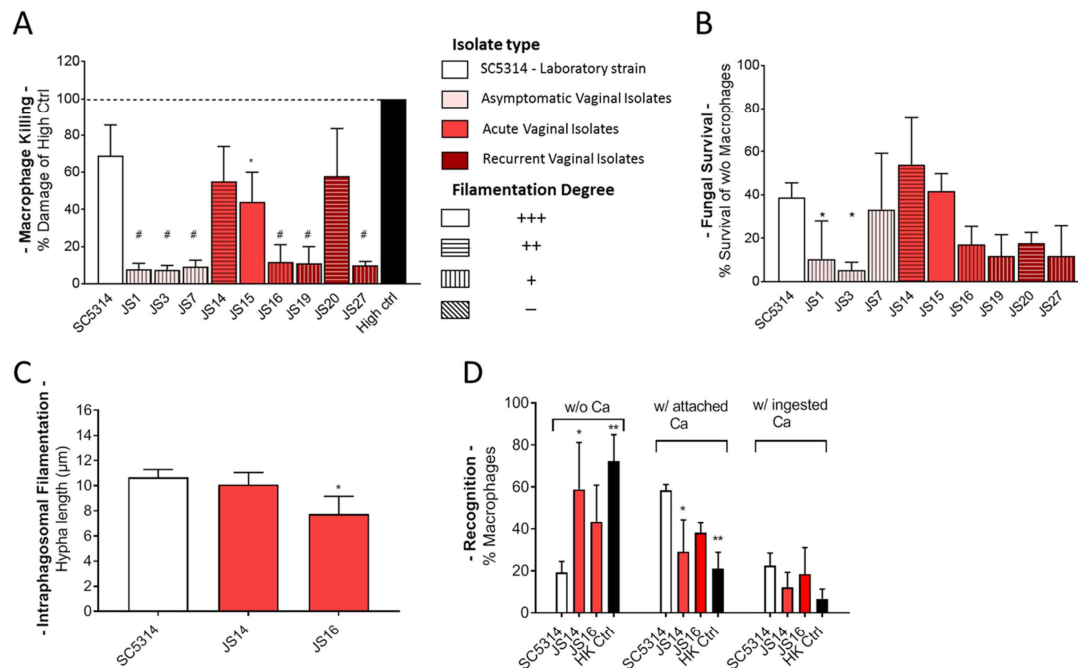


FIG 1 J774.1 macrophage interaction with *C. albicans* vaginal isolates. Color coding indicates Isolate type. (A) Macrophage killing (measured via LDH release) following infection with the selected strains. Damage is displayed as the percentage of Triton-X-treated high control (100% macrophage lysis) at 24 h postinfection. Uninfected macrophage control results were subtracted beforehand. Five biological replicates in technical triplicates were conducted. The degree of hyphal formation (DMEM with macrophages, 24 h, 37°C) is indicated by the pattern of the bar: +++, SC5314-like hypha length with branching; ++, moderate hyphae length with marginal branching; +, short hyphae; -, no hyphae or sporadic germ tubes. (B) Fungal killing was assessed for SC5314 and all tested isolates after 24 h by calculating the ratio of *Candida* microcolonies using the following formula: (colonies in the presence of macrophages/colonies in DMEM) × 100. Three biological replicates were conducted. The degree of hyphal formation (DMEM with macrophages, 24 h, 37°C) is indicated by pattern of the bar: +++, SC5314-like hypha length with branching; ++, moderate hyphae length with marginal branching; +, short hyphae; -, no hyphae or sporadic germ tubes. (C) Intraphagosomal filamentation was assessed for SC5314, JS14, and JS16 by measuring the hyphal lengths of 100 phagocytosed yeasts at 1 h postinfection by fluorescence microscopy and differential staining (phagocytosed *Candida* cells: ConA negative and CFW positive). The presented data are from three biological replicates. (D) Recognition by macrophages was assessed 30 min postinfection for SC5314, JS14, or JS16 strains and presented as the percentage of macrophages nonassociated with fungal cells (w/o Ca), with attached fungal cells (w/attached Ca), or with ingested fungal cells (w/ingested Ca). Heat-killed *Candida* cells (HK Ctrl) were included as control with known diminished recognition due to induced cell wall aberrations. Three biological replicates were conducted. For statistical analysis, a one-way analysis of variance (ANOVA) was performed, followed by Dunnett's multiple-comparison test (*, $P < 0.05$; **, $P < 0.01$; #, $P < 0.0001$ [compared to SC5314]).

is highly strain specific and does not reflect pathogenicity-related grouping in a clinical setting.

Vaginal isolates have different cell wall architecture in rich medium compared to SC5314. The fungal cell wall composition plays an essential role in initial recognition by the immune cells with chitin, mannan, and β -glucan being the main components (15). It is known that fungal β -glucan is highly immuno-reactive (16) and β -glucan masking by mannan can inhibit fungal recognition and killing by macrophages (17, 18). Nutritional factors, such as lactate, can induce β -glucan masking mediated by the exoglucanase Xog1 presumably as a strategy to reduce the visibility of the commensal fungus to the immune system (19). Here, we compared surface exposure of the cell wall components of the vaginal isolates when grown either in commonly used laboratory rich medium (YPD) or in niche-specific vaginal simulating medium (VSM). Surprisingly, all vaginal isolates displayed significantly less β -glucan exposure (25 to 50% of the laboratory strain SC5314) and elevated mannan and chitin exposure when grown in YPD (Fig. 2A). However, when grown in VSM the total β -glucan MFI values were decreased for SC5314, compared to YPD, with similar intensities in strains of the

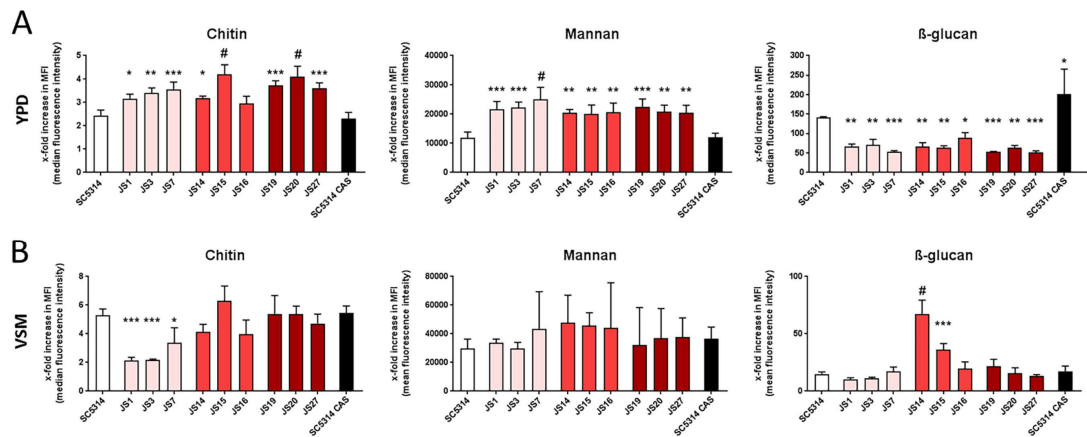


FIG 2 Cell wall architecture of SC5314 and *C. albicans* vaginal isolates. The levels of chitin, mannan, and β -glucan were measured as the x-fold increase of median fluorescence intensity (MFI) over an unstained control via differential staining and flow cytometry. Values are shown as means \pm the standard deviations ($n = 3$). For statistical analysis, a one-way ANOVA was performed, followed by Dunnett's multiple-comparison test (*, $P < 0.05$; **, $P < 0.01$; ***, $P < 0.001$; #, $P < 0.0001$ [compared to SC5314]). (A) Fungal cells were grown as an ON culture in YPD. A sublethal concentration of caspofungin (CAS; $0.625 \text{ ng/ml} = 1/4 \text{ MIC}_{50}$) was added to SC5314 as a positive control for β -glucan exposure. (B) Fungal cells were grown for 2 days in VSM.

asymptomatic and recurrent group (Fig. 2B). In VSM, there also appeared to be group-specific effects for asymptomatic strains (less chitin) and acute strains (more β -glucan) compared to SC5314 and the other tested strains. Since β -glucan masking in lactate containing media such as VSM has been reported to reduce immune visibility (19), our results imply specifically that the acute strains might be more immunoreactive. This would fit to the common view that clinical symptoms during acute vaginal infections are mostly accounted for host-driven hyperinflammatory response toward *Candida* colonization (7). The vaginal isolates might have lost their typical response pattern to the rich medium YPD (in contrast to SC5314), keeping their lactate-primed β -glucan masking constitutively active. However, upon exposure to environmental conditions representing the host niche, we noted group-specific patterns in β -glucan and chitin exposure, which might explain the differences in pathogenicity.

Conclusion. Altogether, these results suggest that vaginal clinical isolates are highly specialized to their host niche and likely even to the immunological and nutritional status of the individual they have been isolated from. In this form they might lose adaption capacity to environmental changes, as was seen with the filamentation defects during lab cultivation conditions and the altered cell wall arrangements, when exposed to the laboratory rich medium YPD. Tight adaption to the originating host niche might render clinical strains less flexible to the conditions used in typical laboratory tests but still highly specialized to persist in their host niche. Caution has to be applied since these strains might appear defective in commonly applied laboratory tests, and yet they are likely highly competent in the niche where they originate, as shown by their ability to persist and even cause disease. These observations highlight the importance of studying more niche-specific nutritional, immunological, and microbiome conditions.

Macrophage infection assays. For all macrophage experiments J774A.1 cells were cultivated in DMEM plus 10% fetal bovine serum at 37°C and $5\% \text{ CO}_2$. Macrophages were seeded in a 96-well plate (4×10^4 cells/well for the macrophage killing assay or 1×10^4 cells/well for the fungal survival assay) or in a 24-well plate (1×10^5 cells/well, 24-well plate for the recognition and filamentation assay) and incubated overnight (ON). The medium was replaced with fresh DMEM, and the cells were infected with YPD-grown (30°C , 180 rpm) and washed *Candida* strains at a defined multiplicity of infection (MOI).

(i) Macrophage killing assay. For the macrophage killing assay, the macrophages were infected with 8×10^4 *Candida* cells/well (MOI of 2), followed by incubation for 24 h. Then, 10 μ l of 5% Triton X-100 was added (10 min, 37°C) to the noninfected high control to obtain full lysis. The plate was then centrifuged, and the supernatant was diluted 1:10 in phosphate-buffered saline (PBS). For lactate dehydrogenase (LDH) measurement, a cytotoxicity detection kit (Roche) was used according to the manufacturer's protocol in technical triplicates. Emission at 542 nm was measured with a TECAN ElisaReader M200 (Software iControl). Noninfected macrophages were used as a negative control, and optical density values were subtracted from sample values.

(ii) Fungal survival assay. The fungal survival assay was performed in DMEM as described previously (20), with slight variations. A total of 2.5×10^4 fungal cells/well (MOI of 2.5) were added to wells with or without macrophages, followed by five serial 1:5 dilutions. After 24 h of incubation, the cells were fixed, and microcolonies were counted using an inverse microscope in wells of the same dilution where a clear discrimination of the microcolonies was possible. Fungal survival was calculated as follows: (number of colonies in the presence of macrophages/number of colonies without macrophages) \times 100.

(iii) Recognition and filamentation assay. For the recognition and filamentation assay, macrophages were infected with 5×10^5 *Candida* cells (MOI of 5) and heat-killed (80°C, 20 min) SC5314 cells were added as the control, since heat treatment leads to poor recognition by the host cells due to disturbances in the cell wall architecture. The assay plate was incubated on ice for 30 min for synchronization of phagocytosis. Nonadhered *C. albicans* cells were washed away with DMEM. After incubation in DMEM for 30 min or 1 h, washing, and fixation (4% Histofix, 15 min, 37°C), nonphagocytosed fungal cells were stained with ConA-647 (concanavalin A conjugated to Alexa Fluor 647; 50 μ g/ml in PBS, 30 min). After washing, cells were permeabilized with 0.5% Triton (5 min), and then counterstained with Calcofluor White (CFW; 35 μ g/ml in 0.1 M Tris-HCl [pH 9], 20 min). Cells were washed with ddH₂O (three times, 10 min), and samples were analyzed with a Zeiss Axio observer fluorescence microscope. The hyphal lengths of 100 phagocytosed cells (ConA negative, CFW positive) were measured. Recognition was determined by assessing the phagocytosis state of 200 macrophages via differential staining for having no association, attached (ConA positive, CFW positive), or ingested *Candida* cells (ConA negative, CFW positive).

Staining of cell wall components. Fungal cells were cultivated in either YPD (1 liter: 20 g peptone, 10 g yeast extract, 20 g glucose) or vaginal simulating media (1 liter: 2 g glucose, 0.16 g glycerol, 2 g lactic acid, 1 g acetic acid, 0.018 g bovine serum albumin [BSA], 0.4 g urea, 1.4 g KOH, 0.222 g CaCl₂, 3.51 g NaCl [pH 4.2]), adapted from Vylkova and Lorenz (20). As previously described, a sublethal concentration of caspofungin (0.625 ng/ml = 1/4 MIC₅₀) was added to SC5314 to obtain elevated β -glucan levels (21). Next, 1×10^6 *Candida* cells were harvested, washed once in PBS, and fixed in 2% Histofix for 20 min and 600 rpm at room temperature. After an additional PBS washing step, the pellet was dissolved in 2% BSA/PBS and incubated for at least 10 min at 37°C to block unspecific binding. Simultaneous staining was performed for 1 h at 37°C and 100 rpm by the addition of 0.5 μ l of primary anti- β -1,3-glucan antibody (Biosupplies, 1 mg/ml, stains β -1,3-glucan), 0.3 μ l of ConA647 (Sigma, 5 mg/ml, stains mannan), and 7 μ l of WGA-FITC (Sigma, 2 mg/ml, stains chitin) in 100 μ l of 2% BSA/PBS per sample. After two washing steps with 2% BSA/PBS, 2 μ l of secondary goat anti-mouse PE-Cy7 antibody (BioLegend, 0.2 mg/ml) was added in 100 μ l of 2% BSA/PBS per sample for 30 min at 37°C and 100 rpm. After washing, the cells were resuspended in 2% BSA/PBS and analyzed with a FACVerse (BD Biosciences) counting 10,000 events. Data analysis was performed using FlowJo 10.6.2 software.

SUPPLEMENTAL MATERIAL

Supplemental material is available online only.

FIG S1, TIF file, 0.2 MB.

FIG S2, TIF file, 0.7 MB.

FIG S3, TIF file, 0.3 MB.

ACKNOWLEDGMENTS

The clinical vaginal isolate strains used in this study were a generous gift from Brian Peters. These strains were collected by Jack Sobel from women attending a vaginitis clinic at the Detroit Medical Center. We especially thank Therese-Christin Voges for gathering some preliminary data and the Septomics Host Fungal Interfaces team for fruitful discussions.

This study was supported by the German Ministry for Education and Science in the program Unternehmen Region (BMBF 03Z22JN11) and by the German Research Foundation (DFG) through the TRR 124 FungiNet, "Pathogenic fungi and their human host: networks of interaction," DFG project number 210879364, project C2 to S.V. and project C5 to I.D.J.

REFERENCES

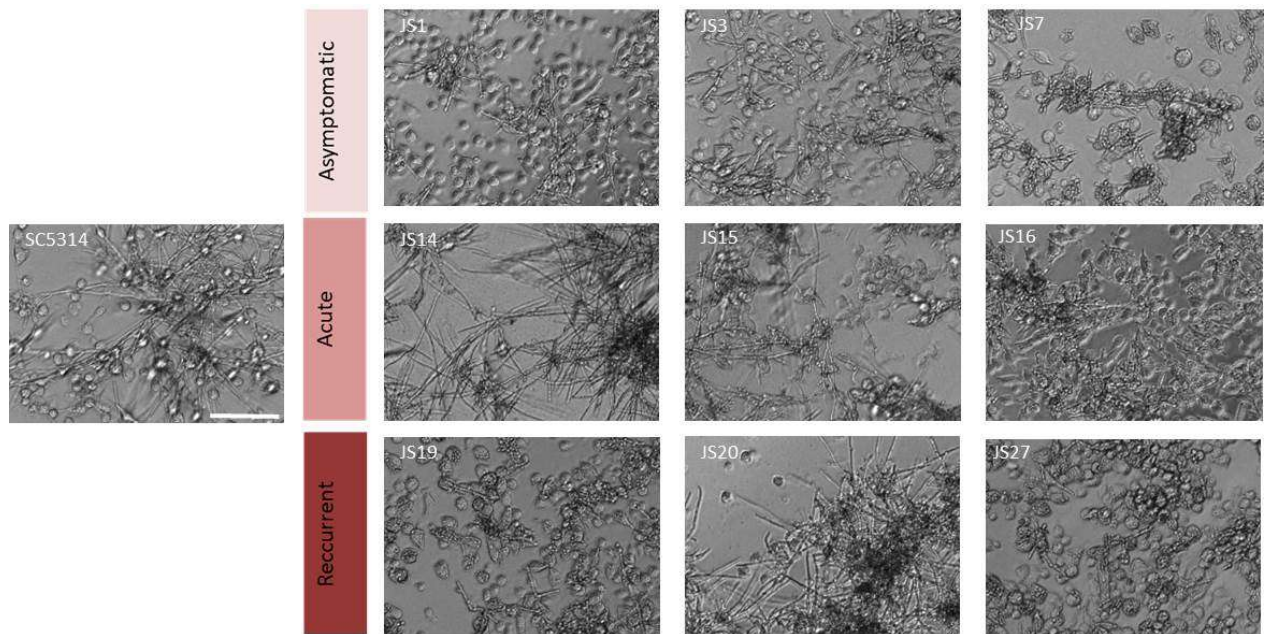
- Pellon A, Sadeghi Nasab SD, Moyes DL. 2020. New insights in *Candida albicans* innate immunity at the mucosa: toxins, epithelium, metabolism, and beyond. *Front Cell Infect Microbiol* 10:81. <https://doi.org/10.3389/fcimb.2020.00081>.
- Willems HME, Ahmed SS, Liu J, Xu Z, Peters BM. 2020. Vulvovaginal candidiasis: a current understanding and burning questions. *J Fungi (Basel)* 6:27. <https://doi.org/10.3390/jof6010027>.
- Sobel JD. 1997. Vaginitis. *N Engl J Med* 337:1896–1903. <https://doi.org/10.1056/NEJM199712253372607>.
- Denning DW, Kneale M, Sobel JD, Rautemaa-Richardson R. 2018. Global burden of recurrent vulvovaginal candidiasis: a systematic review. *Lancet Infect Dis* 18:e339–e347. [https://doi.org/10.1016/S1473-3099\(18\)30103-8](https://doi.org/10.1016/S1473-3099(18)30103-8).
- Foxman B, Barlow R, D'Arcy H, Gillespie B, Sobel JD. 2000. *Candida* vaginitis: self-reported incidence and associated costs. *Sex Transm Dis* 27:230–235. <https://doi.org/10.1097/00007435-200004000-00009>.
- Sobel JD, Faro S, Force RW, Foxman B, Ledger WJ, Nyirjesy PR, Reed BD, Summers PR. 1998. Vulvovaginal candidiasis: epidemiologic, diagnostic, and therapeutic considerations. *Am J Obstet Gynecol* 178:203–211. [https://doi.org/10.1016/s0002-9378\(98\)80001-x](https://doi.org/10.1016/s0002-9378(98)80001-x).
- Rosati D, Bruno M, Jaeger M, Ten Oever J, Netea MG. 2020. Recurrent vulvovaginal candidiasis: an immunological perspective. *Microorganisms* 8:144. <https://doi.org/10.3390/microorganisms8020144>.
- Teshima S, Rokutan K, Takahashi M, Nikawa T, Kido Y, Kishi K. 1995. Alteration of the respiratory burst and phagocytosis of macrophages under protein malnutrition. *J Nutr Sci Vitaminol (Tokyo)* 41:127–137. <https://doi.org/10.3177/jnsv.41.127>.
- Childers DS, Avelar GM, Bain JM, Larcombe DE, Pradhan A, Budge S, Heaney H, Brown AJP. 2019. Impact of the environment upon the *Candida albicans* cell wall and resultant effects upon immune surveillance. *Curr Top Microbiol Immunol* https://doi.org/10.1007/82_2019_182.
- Rastogi R, Su J, Mahalingam A, Clark J, Sung S, Hope T, Kiser PF. 2016. Engineering and characterization of simplified vaginal and seminal fluid simulants. *Contraception* 93:337–346. <https://doi.org/10.1016/j.contraception.2015.11.008>.
- Ballou ER, Avelar GM, Childers DS, Mackie J, Bain JM, Wagener J, Kastora SL, Panea MD, Hardison SE, Walker LA, Erwig LP, Munro CA, Gow NA, Brown GD, MacCallum DM, Brown AJ. 2016. Lactate signalling regulates fungal beta-glucan masking and immune evasion. *Nat Microbiol* 2:16238. <https://doi.org/10.1038/nmicrobiol.2016.238>.
- Ene IV, Adya AK, Wehmeier S, Brand AC, MacCallum DM, Gow NA, Brown AJ. 2012. Host carbon sources modulate cell wall architecture, drug resistance and virulence in a fungal pathogen. *Cell Microbiol* 14: 1319–1335. <https://doi.org/10.1111/j.1462-5822.2012.01813.x>.
- Zangl I, Pap IJ, Aspöck C, Schuller C. 2019. The role of *Lactobacillus* species in the control of *Candida* via biotrophic interactions. *Microb Cell* 7:1–14. <https://doi.org/10.15698/mic2020.01.702>.
- Uwamahoro N, Verma-Gaur J, Shen HH, Qu Y, Lewis R, Lu J, Bamberg K, Masters SL, Vince JE, Naderer T, Traven A. 2014. The pathogen *Candida albicans* hijacks pyroptosis for escape from macrophages. *mBio* 5:e00003–14. <https://doi.org/10.1128/mBio.00003-14>.
- Cheng SC, Joosten LA, Kullberg BJ, Netea MG. 2012. Interplay between *Candida albicans* and the mammalian innate host defense. *Infect Immun* 80:1304–1313. <https://doi.org/10.1128/IAI.06146-11>.
- Brown GD, Taylor PR, Reid DM, Willment JA, Williams DL, Martinez-Pomares L, Wong SY, Gordon S. 2002. Dectin-1 is a major beta-glucan receptor on macrophages. *J Exp Med* 196:407–412. <https://doi.org/10.1084/jem.20020470>.
- Bain JM, Louw J, Lewis LE, Okai B, Walls CA, Ballou ER, Walker LA, Reid D, Munro CA, Brown AJ, Brown GD, Gow NA, Erwig LP. 2014. *Candida albicans* hypha formation and mannan masking of beta-glucan inhibit macrophage phagosome maturation. *mBio* 5:e01874. <https://doi.org/10.1128/mBio.01874-14>.
- Gantner BN, Simmons RM, Underhill DM. 2005. Dectin-1 mediates macrophage recognition of *Candida albicans* yeast but not filaments. *EMBO J* 24:1277–1286. <https://doi.org/10.1038/sj.emboj.7600594>.
- Childers DS, Avelar GM, Bain JM, Pradhan A, Larcombe DE, Netea MG, Erwig LP, Gow NAR, Brown AJP. 2020. Epitope shaving promotes fungal immune evasion. *mBio* 11:e00984–20. <https://doi.org/10.1128/mBio.00984-20>.
- Vylkova S, Lorenz MC. 2014. Modulation of phagosomal pH by *Candida albicans* promotes hyphal morphogenesis and requires Stp2p, a regulator of amino acid transport. *PLoS Pathog* 10:e1003995. <https://doi.org/10.1371/journal.ppat.1003995>.
- Wheeler RT, Fink GR. 2006. A drug-sensitive genetic network masks fungi from the immune system. *PLoS Pathog* 2:e35. <https://doi.org/10.1371/journal.ppat.0020035>.

Hypha formation in different hypha-inducing media conditions (37°C)										
Isolate type	Laboratory Strain	Asymptomatic			Acute			Recurrent		
Strain	SC5314	JS1	JS3	JS7	JS14	JS15	JS16	JS19	JS20	JS27
M199, pH 7.5 *	+++	++	++	++	++	+	+	+	++	+++
2% GlcNac *	+++	++	++	+++	++	++	++	++	+	+
Human serum #	+++	+++	+++	+++	-	-	+++	+++	-	++++
Spider #	+++	+	+	+	-	-	-	-	-	++

*Liquid, 6h; # Solid 2 d

FIG S1

Filamentation of vaginal isolates in different hypha-inducing media. Color coding indicates the isolate type. Degree of hyphal formation (DMEM with macrophages, 24 h, 37°C) is indicated by pattern of the bar: +++, hyphae length exceeds SC5314; +++, SC5314-like hypha length with branching; ++, moderate hyphae length with marginal branching; +, short hyphae; -, no hyphae or sporadic germ tubes. Incubation time was 6 h (liquid) or 2 days (solid). Composition of media: GlcNac (2% *N*-acetyl-d-glucosamine, 0.5% ammonium sulfate, 0.17% YNB), human serum (10% heat-inactivated human serum, 0.5% ammonium sulfate, 0.17% YNB, 2% glucose, 2% agar), or Spider (1% nutrient broth, 1% mannitol, 0.2% K₂HPO₄, 2% agar [pH 7.2])

**FIG S2**

Filamentation of vaginal isolates with J774.1 macrophages in DMEM. *C. albicans* strains were cocultured with J774.1 macrophages in DMEM (MOI of 5, 24 h). Pictures were taken after conducting the macrophage killing assay. Between the three infection-related groups (asymptomatic, acute, and recurrent isolates), various isolates showed group-independent filamentation defects. Scale bar, 100 μm.

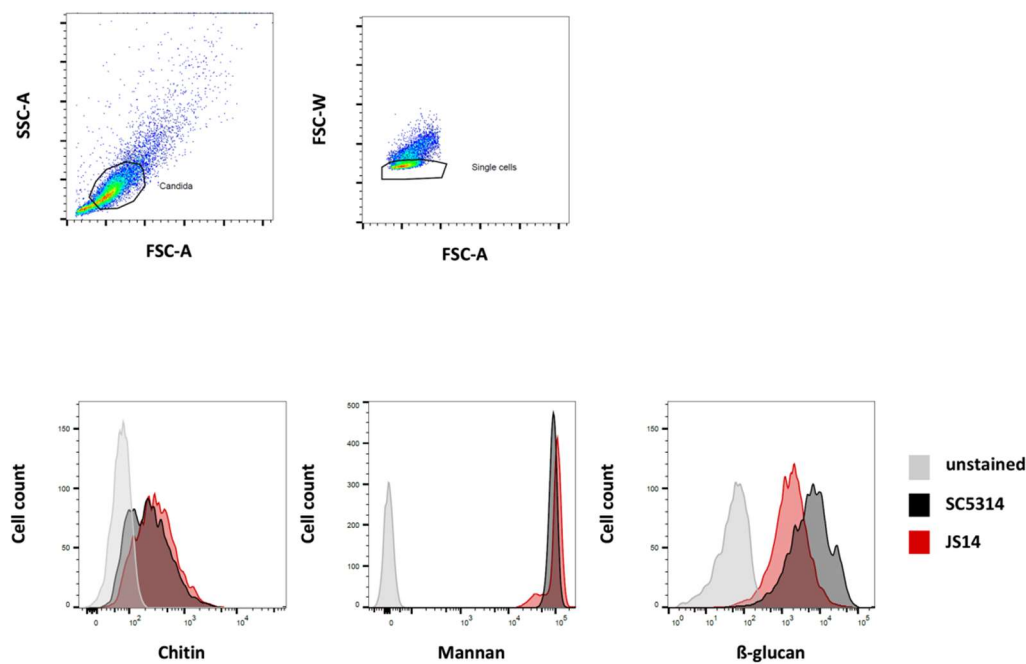


FIG S3

Gating strategy for staining of *C. albicans* cell wall components. *C. albicans* was incubated as indicated in YPD or VSM; stained for the respective cell wall components chitin, mannan, and β -glucan; and analyzed with a FACSVerse (BD Biosciences) counting 10,000 single yeast cells. Gating was performed to exclude debris and doublets. The median fluorescence intensity (MFI) was quantified and compared to an unstained control. Data analysis was performed using FlowJo 10.6.2 software. Exemplary measurements for YPD-grown strains SC5314 and JS14 are shown.

3.2. Manuscript II: Machata *et al.*, Front. Immunol., 2021

Significant Differences in Host-Pathogen Interactions Between Murine and Human Whole Blood

Silke Machata, Sravya Sreekantapuram, Kerstin Hänniger, Oliver Kurzai, **Christine Dunker**, Katja Schubert, Wibke Krüger, Bianca Schulze-Richter, Cornelia Speth, Günter Rambach, and Ilse D. Jacobsen

Frontiers in Immunology. 2021 Jan 15. 11:565869. doi: 10.3389/fimmu.2020.565869

Summary

Systemic candidiasis is often arising as consequence of dissemination of fungal cells *via* the bloodstream. In this study, a human whole-blood model was adapted to murine blood to study the complex host-pathogen interplay *ex vivo*. This publication shows that murine blood significantly differs from human blood not only with regards to its composition: While neutrophils are the most abundant leukocytes in human blood, lymphocytes are the most frequent cell type in murine blood. In contrast to human blood, murine blood was not able to kill fungal cells, and was less able to prevent hyphae formation by *C. albicans*. However, less efficient killing was neither due to hypha formation by *C. albicans* nor due to the reduced number of neutrophils in comparison to human blood. Therefore, caution has to be paid when translating data obtained in one host with another.

The candidate is:

First author, Co-first author, Corresponding author, Coauthor.

Estimated authors' contributions in %:

Author	Conception	Data analysis	Experimental	Writing	Provision of the material
Silke Machata	50	53	64	46	50
Sravya Sreekantapuram			8		
Kerstin Hänniger		5	5		
Oliver Kurzai					
Christine Dunker		6	8	5	10
Katja Schubert			2		
Wibke Krüger		6	2		
Bianca Schulze-Richter			1		
Cornelia Speth		10	5	2	10
Günter Rambach		10	5	2	10
Ilse D. Jacobsen	50	10		45	20



Significant Differences in Host-Pathogen Interactions Between Murine and Human Whole Blood

Silke Machata¹, Sravya Sreekantapuram¹, Kerstin Hünninger^{2,3}, Oliver Kurzai^{2,3}, Christine Dunker¹, Katja Schubert¹, Wibke Krüger¹, Bianca Schulze-Richter^{1†}, Cornelia Speth⁴, Günter Rambach⁴ and Ilse D. Jacobsen^{1,5*}

OPEN ACCESS

Edited by:

Markus M. Heimesaat,
Charité-Universitätsmedizin Berlin,
Germany

Reviewed by:

Caroline N. Jones,
The University of Texas at Dallas,
United States
Sunil Shaw,
Brown University, United States

*Correspondence:

Ilse D. Jacobsen
ilse.jacobsen@leibniz-hki.de

†Present address:

Bianca Schulze-Richter,
Institute of Immunology, Molecular
Pathogenesis, Center for
Biotechnology and Biomedicine (BBZ),
College of Veterinary Medicine,
University of Leipzig, Leipzig, Germany

Specialty section:

This article was submitted to
Microbial Immunology,
a section of the journal
Frontiers in Immunology

Received: 26 May 2020

Accepted: 30 November 2020

Published: 15 January 2021

Citation:

Machata S, Sreekantapuram S,
Hünninger K, Kurzai O, Dunker C,
Schubert K, Krüger W,
Schulze-Richter B, Speth C,
Rambach G and Jacobsen ID (2021)
Significant Differences in
Host-Pathogen Interactions Between
Murine and Human Whole Blood.
Front. Immunol. 11:565869.
doi: 10.3389/fimmu.2020.565869

¹ Research Group Microbial Immunology, Leibniz Institute for Natural Product Research and Infection Biology, Hans Knoell Institute, Jena, Germany, ² Research Group Fungal Septomics, Leibniz Institute for Natural Product Research and Infection Biology, Hans Knoell Institute, Jena, Germany, ³ Institute for Hygiene and Microbiology, University of Würzburg, Würzburg, Germany, ⁴ Institute of Hygiene and Medical Microbiology, Medical University of Innsbruck, Innsbruck, Austria, ⁵ Institute of Microbiology, Friedrich Schiller University Jena, Jena, Germany

Murine infection models are widely used to study systemic candidiasis caused by *C. albicans*. Whole-blood models can help to elucidate host-pathogen interactions and have been used for several *Candida* species in human blood. We adapted the human whole-blood model to murine blood. Unlike human blood, murine blood was unable to reduce fungal burden and more substantial filamentation of *C. albicans* was observed. This coincided with less fungal association with leukocytes, especially neutrophils. The lower neutrophil number in murine blood only partially explains insufficient infection and filamentation control, as spiking with murine neutrophils had only limited effects on fungal killing. Furthermore, increased fungal survival is not mediated by enhanced filamentation, as a filament-deficient mutant was likewise not eliminated. We also observed host-dependent differences for interaction of platelets with *C. albicans*, showing enhanced platelet aggregation, adhesion and activation in murine blood. For human blood, opsonization was shown to decrease platelet interaction suggesting that complement factors interfere with fungus-to-platelet binding. Our results reveal substantial differences between murine and human whole-blood models infected with *C. albicans* and thereby demonstrate limitations in the translatability of this *ex vivo* model between hosts.

Keywords: whole blood *ex vivo* model, host-pathogen interaction, *Candida albicans*, neutrophils, mice

INTRODUCTION

Dissemination of pathogens from a primary site of colonization or infection can occur *via* different routes, including lymphatic vessels and the blood stream (1). The hematogenous is by far the most frequent route for systemic infections of various bacterial and fungal pathogens, in the most severe cases leading to blood stream infections (2). Survival in blood can thus be considered a major virulence trait in the development of systemic infections. However, our understanding of how pathogens interact with cellular and humoral host factors in blood is limited, mainly due to

technical issues: While it is relatively easy to study the interaction of pathogens with isolated blood cells, or their survival in serum or plasma, such approaches lack the complexity of interactions between different types of immune cells and additional factors, e.g., complement, present in blood. Assessing host-pathogen interactions *in vivo* in patients is challenging due to ethical and logistic limitations. In mice, as the most commonly used laboratory animal for *in vivo* experiments, the blood volume that can be withdrawn repeatedly is very limited and thereby hampers in depth analysis of interactions within blood. Furthermore, if bacteremia or fungemia occurs transiently or intermittently, pathogens might not be detectable in every blood sample during hematogenous dissemination (3). Therefore, we previously established an *ex vivo* human whole-blood infection model that allowed us to define which immune cells interact with the human fungal pathogen *Candida albicans* (4), to identify cross-talk between different components of the host response (5), and to detect substantial differences between related fungal pathogens (6).

Candida infections (candidiasis) caused by *C. albicans* commonly arise from endogenous strains that colonize mucosal surfaces as a commensal in healthy individuals. Risk factors for candidiasis are microbiota imbalance, impaired mucosal barrier function, and immunosuppression (7, 8). In the majority of cases the fungus causes relatively benign mucosal infections such as oral and vaginal candidiasis (9). Life-threatening infections arise from dissemination *via* the blood stream resulting in deep-seated or systemic candidiasis (8). Disseminated candidiasis is associated with high mortality rates that can exceed 50% despite antifungal therapy (10, 11). Dissemination from the gut into internal organs can be triggered in mice by a combination of intestinal barrier disruption and immunosuppression (12), but the most commonly used model to study systemic candidiasis is intravenous infection of mice (13). This model is considered a gold standard tool for detailed investigations of fungal virulence and of host immune responses, and largely resembles catheter-associated disseminated candidiasis in men (13, 14). However, the initial interaction of *C. albicans* with murine blood and its impact on the development of systemic candidiasis is not well understood. Following intravenous infection, *C. albicans* rapidly disappears from circulating peripheral blood (15, 16), yet it is unknown whether this is due to killing of circulating fungal cells, adhesion to endothelium, rapid invasion of internal organs, or a combination of these factors.

In the human whole-blood model, neutrophils predominantly associate with and phagocytose *C. albicans* (4). Fungal killing in the human whole-blood model is to 98% accountable to neutrophils (4) and mediated by phagocytosis, degranulation and formation of extracellular traps. However, murine blood differs significantly from human blood in the abundance of neutrophils: These cells are the most abundant leukocytes in human blood (55–70%) while murine blood is dominated by lymphocytes (70–80%) with neutrophils accounting only for 8% to 24% of all leukocytes (17). To elucidate whether these differences affect interaction of *C. albicans* with whole blood, we adapted our protocol established for human blood for application to mice. Our results show significant differences

between humans and mice in the *ex vivo* model, including lower association of the fungus with leukocytes, higher association with thrombocytes, and substantially less killing of *C. albicans* in murine blood.

MATERIALS AND METHODS

Ethics Statement

Human peripheral blood was collected from healthy volunteers with written informed consent. This study was conducted in accordance with the Declaration of Helsinki and all protocols were approved by the Ethics Committee of the University Hospital Jena (permit number: 273-12/09). All animals used for the project were held in accordance with the European Convention for the Protection of Vertebrate Animals Used for Experimental and Other Scientific Purposes and the experiments performed in accordance with European and German regulations. The sacrifice of mice for blood withdrawal was performed under §4 “removal of organs” of the German Animal Welfare Act and was approved by the local animal welfare officer (no specific permit number issued). The systemic candidiasis model was approved by the Thuringian authority and ethics committee (Thüringer Landesamt für Verbraucherschutz, permit number 03-007/13 and HKI-19-003).

Strains and Culture Conditions

C. albicans GFP-expressing strains M137 (18) (pACT1-GFP) and *C. albicans* Δ *efg1* Δ *cph1* + pADH1-GFP were used. To construct *C. albicans* Δ *efg1* Δ *cph1* + pADH1-GFP a CaGFP-caSAT1 construct with homology regions for the integration into the *C. albicans* *ADH1* locus was excised with *AscI/SacI* from the plasmid pSK-ADH1prom-CaGFP-SAT1 (4) and then transformed into the *EFG1/CPH1* double mutant HLC52 (19). Transformation was performed with the established lithium acetate protocol (20). Transformants were grown for two days on YPD with 200 mg/ml nourseothricine and verified by PCR and microscopy. For experiments *C. albicans* over-night cultures grown in YPD medium (2% peptone, 1% yeast extract, 2% glucose) at 30°C and 180 rpm were diluted 1:50 in YPD medium and sub-cultured for another 3 to 4 h into the mid-log phase under the same conditions. Yeast cells were washed three times with PBS, counted and diluted in PBS to 5×10^7 /ml or 5×10^6 /ml, as indicated.

GFP-expressing *S. aureus* [6850/pALC1743 (21, 22)] and *Escherichia coli* ATCC 25922 (23) were cultivated overnight at 37°C, 180 rpm in LB medium. The overnight culture was inoculated 1:100 into fresh LB medium and incubated at 37°C, 180 rpm until OD_{600} 0.6 to 0.7 was reached. The cultures were then washed three times with PBS and bacterial cell numbers were calculated based on OD_{600} -CFU correlations. Cultures were diluted to desired concentrations with PBS before inoculation of whole blood.

Whole-Blood Model

Human peripheral blood from healthy donors was collected in hirudin-monovettes (Sarstedt, Germany, 2.7 ml volume). Hirudin was used as an anti-coagulant as it was previously

shown to have no effect on complement activation (24). Due to their size, direct use of the hirudin-monovettes was not feasible for the collection of murine blood. Therefore, three hirudin-monovettes were rinsed with total volume of 500 μ l sterile saline (0.9% NaCl) to solubilize the hirudin. Needles and syringes rinsed with hirudin-NaCl were then used to collect blood from female BALB/c mice (8–12 weeks old, Charles River, Germany) or from C57BL/6J mice (8–12 weeks old, Service Unit Experimental Biomedicine, Friedrich-Schiller-University Jena, Germany) by heart puncture immediately after sacrifice by intraperitoneal application of an overdose of ketamine (500 mg/kg) and xylazine (25 mg/kg). The blood was then immediately transferred to a falcon tube containing 500 μ l hirudin-NaCl, in which blood from ten animals was pooled for each experiment. Pilot experiments analyzing fungal CFU in whole blood of female and male C57BL/6J mice revealed no sex-specific differences; thus, both male and female mice were used for the experiments.

The human whole-blood infection assay was performed as described previously (4), and murine blood was infected in the same way. Briefly, 1/50 volume fungal or bacterial suspensions prepared as described above were added to murine or human blood, resulting in an infectious dose of 1×10^6 /ml for most experiments or 1×10^5 /ml for lower infection dose experiments. The incubation of the whole blood was carried out at 37°C under slow constant motion on a rolling device (Phoenix instrument RS_TR05) for time points from 10 min to 480 min. Survival of the pathogens was determined by plating on agar plates (YPD for *C. albicans*, LB for *E. coli* and *S. aureus*) using serial dilutions in PBS and counting colony forming units. To determine the effect of ketamine/xylazine on phagocytosis and association of *C. albicans* with immune cells, 40 μ g/ml ketamine and 2 μ g/ml xylazine were added to human blood directly before the experiment. 40 μ g/ml ketamine is equivalent to fivefold the maximal serum concentration in mice after intraperitoneal application of 100 mg/kg ketamine (25).

Blood Analysis and Flow Cytometry

Generally hematology analysis of murine samples was performed using a BC-5300Vet (Mindray) configured for murine blood. For murine samples, blood smears were prepared for each time point and stained by May-Gruenwald-Giemsa staining (Roth). Filamentation and interaction with platelets were observed by light microscopy. Further analyses were performed by differential staining and subsequent measurement with a flow cytometer. For murine blood, differential staining was performed with CD45-PerCP (Cat. no. 557235, clone 30-F11, 12 μ g/ml, BD Biosciences), CD19-APC-Cy7 (Cat. no. 115530, clone 1D3; 12 μ g/ml, Biolegend) for B-cells, CD3e-V500 (Cat. no. 560771, clone 500A2, 12 μ g/ml, BD Biosciences) for T-cells, Ly6G-PE (Cat. no. 127608, clone 1A8, 12 μ g/ml final conc; Biolegend) for neutrophils, NK1.1-BV421 (for C57BL/6J mice: Cat. no. 108731, clone PK136, 12 μ g/ml, Biolegend) or CD335-BV421 (for BALB/C mice: Cat. no. 562850, Clone 29A1.4, 12 μ g/ml, BD Biosciences) for NK cells, CD11b-APC (Cat. no. 130-091-241, clone M1/70.15.11.5, 30 μ g/ml, Miltenyi) for monocytes and neutrophils, CD41 (Cat. no. 133906, clone MWReg30, 12 μ g/ml, Biolegend) for platelets, and CD69-PE vio770 (Cat. no. 130-103-

944, clone H1.2F3, 30 μ g/ml, Miltenyi) and CD62-PE-Vio779 (Cat. no. 130-105-537, clone REA 344, 30 μ g/ml, Miltenyi) as platelet activation markers. In parallel, staining with the appropriate isotype controls (APC Rat IgG2b, κ Isotype Control, clone RTK5430, Cat. no. 400611, Biolegend; V500: Syrian hamster IgG2 κ Isotype Control, clone B81-3, Cat. no. 560785, BD Bioscience; PE: rat IgG2a κ Isotype Control, clone RTK2758, Cat. no. 400507, Biolegend; PerCP rat IgG2b κ Isotype Control, clone A95-1, Cat. no. 552991, BD Bioscience; APC-Cy7 rat IgG2a κ Isotype Control, clone RTK2758, Cat. no. 400524, Biolegend; V450 rat IgG2a κ Isotype Control, clone R35-95, Cat. no. 560377, BD Bioscience; V450 mouse IgG2a κ Isotype Control, clone G155-178, Cat. no. 560550, BD Bioscience; PE Vio770 hamster IgG1 Isotype Control, clone G235-2356, Cat. no. 553956, BD Bioscience; PE rat IgG1 κ Isotype Control, clone RTK2071, Cat. no. 400407, Biolegend; APC human IgG1 Isotype Control, clone QA16A12, Cat. no. 403505, Biolegend) was performed as a binding specificity control. After staining the erythrocytes were removed using the BD FACS Lysing solution and fixed samples were analyzed on a FACSVerser (BD Biosciences) flow cytometer after two washing steps in PBS supplemented with 3% FCS.

Human whole-blood was analyzed with a BD FACSCanto II flow cytometer. Platelets were specifically identified by CD42b⁺ staining (mouse anti-human CD42b-APC antibody, clone HIP-1, Cat. no. 303912, BioLegend). Co-staining with mouse anti-human CD66b-V450 antibody (clone G10F5, Cat. no. 561649, BD Bioscience) identified platelets associated with neutrophils. Activation of human platelets was investigated by changes in surface CD62P expression (mouse anti-human CD62P-PE antibody, clone AK-4, Cat. no. 555524, BD Bioscience). In parallel, staining with the appropriate isotype controls (APC mouse IgG1, κ Isotype Ctrl, clone MOPC-21, Cat. no. 400122, BioLegend; V450 mouse IgM, κ Isotype Control, clone G155-228, Cat. no. 560861, BD Bioscience and PE Mouse IgG1, κ Isotype Control, clone MOPC-21, Cat. no. 555749, BD Bioscience) was performed as a binding specificity control. Stained blood samples were treated with BD FACS Lysing solution followed by washing and harvesting cells in BD CellWASH solution. FlowJo10 was used for analysis of all samples.

Neutrophil Isolation From Murine Bone Marrow

Neutrophils were isolated from bone marrow of femur and tibia of three to four female 8- to 12-week-old BALB/c mice as previously described (26). Briefly, bone marrow was flushed with RPMI 1640 supplemented with Penicillin/Streptomycin (Sigma) and homogenized using a 40 μ m cell strainer. Lysis of erythrocytes was carried out for 1 min on ice using a lysis buffer containing 8 mg/ml NH₄Cl, 1 mg/ml K₂CO₃ and 0.01% EDTA. Neutrophils were purified using a Percoll gradient of 52%, 69%, and 78% in PBS and cells were collected from the 69% to 78% interface. After washing with HBSS neutrophils were resuspended in HBSS, analyzed on a BC-5300Vet (Mindray) and stored on ice until usage for a maximum of 1 h. The purity of isolated neutrophils was roughly 70%.

Analysis of Platelets From Mice With Systemic Candidiasis

Six- to eight-week-old female specific-pathogen-free BALB/c mice (16 to 18 g) purchased from Charles River (Germany) were housed in groups of five in individually ventilated cages with free access to food and water. Mice were infected with 2.5×10^4 *C. albicans* CFU/g body weight in 100 μ l DPBS via the lateral tail vein at day 0. Groups of mice were sacrificed at the indicated time points post infection by intraperitoneal application of an overdose of ketamin (500 mg/kg) and xylazin (25 mg/kg). 100 μ l of blood were collected under terminal anesthesia by retro-orbital bleeding, immediately transferred into a tube containing 10 μ l EDTA solution (1.6 mg/ml), and gently mixed. 20 μ l of the sample were analyzed on a BC-5300Vet (Mindray) to determine platelet counts and mean platelet volume. Platelet-rich plasma (RPP) was prepared from 40 μ l of whole-blood by centrifugation at 135 g for 15 min at room temperature. To detect platelet activation, platelets were stained for 30 min with fluorescence-labeled antibodies (BioLegend) directed against CD41 (clone HIP8, Cat. no. 303710, 0.1 μ g/ml) as platelet marker and CD63 (clone H5C6, Cat. no. 353006, 8 μ g/ml) as activation marker, followed by fixation with 1% formaldehyde. Surface expression of CD62P, fibrinogen binding and C3c binding were determined as described for CD63 using fluorescence-labeled antibodies (CD62P: BioLegend, clone AK4, Cat. no. 304906, 1.5 μ g/ml; fibrinogen: BioRad, polyclonal, Cat. no. 4440-8004F, 100 μ g/ml; C3c: Dako, polyclonal, Cat. no. F0201, 400 μ g/ml). Non-activated unstained cells and non-activated and activated stained cells were used to calibrate the flow cytometer using single stains and combined stains. Plasma was prepared by centrifugation of 40 μ l whole-blood at 1500 g for 15 min at room temperature. Plasma concentrations of soluble CD62P were determined using the Quantikine[®] ELISA Mouse sP-Selectin/CD62P kit (R&D Systems, USA) performed according to manufacturer instructions.

Isolation of Platelets and Confrontation Assay

Venous blood of healthy human volunteers was collected in sodium citrate monovettes (Sarstedt) and directly centrifuged at $80 \times g$ for 20 min (without break). Supernatants were collected and treated with 0.25 mg/ml acetylsalicylic acid (Sigma Aldrich) for 30 min followed by addition of 1 mM Prostaglandin E1 (Sigma Aldrich), both to prevent pre-activation of the containing platelets. Centrifugation at $400 \times g$ for 8 min pelleted platelets that were afterwards suspended in HEPES-Tyroses buffer (10 mM HEPES, 137 mM NaCl, 2.8 mM KCl, 1 mM MgCl₂·6H₂O, 12 mM NaHCO₃, 0.4 mM Na₂HPO₄·2H₂O, 5.5 mM Glucose, 0.35% BSA, without Ca²⁺). Purified platelets were treated again with 1 mM Prostaglandin E1, centrifuged at $400 \times g$ for 10 min and suspended either in RPMI 1640 medium containing 20% autologous active or heat-inactivated plasma. Autologous human plasma was collected after centrifugation of Hirudin-anticoagulated blood from the same donor at $16,000 \times g$ for 10 min. To inactivate complement proteins, autologous human plasma was incubated for 1 h at 56°C. Murine platelets were prepared from freshly collected blood of healthy mice as

concentrates by thrombocytapheresis with Amicus cell separator (Baxter, Vienna, Austria) by the Department of Immunology and Blood Transfusion (Innsbruck Medical University, Innsbruck, Austria). The platelet concentration was determined by a hemocytometer and adjusted to a concentration of 1.2 to 1.4×10^9 /ml. Murine serum was collected by centrifugation of blood samples from (i) SPF mice without any treatment, (ii) mice systemically infected with a sublethal dose of 1×10^4 *C. albicans* CFU/g body weight on days 8 to 21 after infection (see 2.6), (iii) C3-deficient mice (B6.129S4-C3^{tm1Crj}/J). Pooled serum of 5 to 12 mice per group was used for experiments with isolated platelets.

Confrontation of isolated platelets with *C. albicans* was performed at a ratio of platelets to fungal cells of 10:1 for the indicated time points (37°C, constant rolling at 5 rpm). Mock-infected platelets with the two different media served as controls.

Quantification of Cytokines

Plasma samples were generated from whole-blood aliquots that were incubated on ice for 45 min to 1 h and subsequently centrifuged at 4°C for 10 min at $10,000 \times g$. Supernatants were stored at -80°C until further use. Concentration of IFN- γ , IL-1 β , TNF- α , IL-6, and KC (CXCL1) in murine samples was determined by ELISA (Invitrogen, Thermo Fisher Scientific) performed according to manufacturer's instructions.

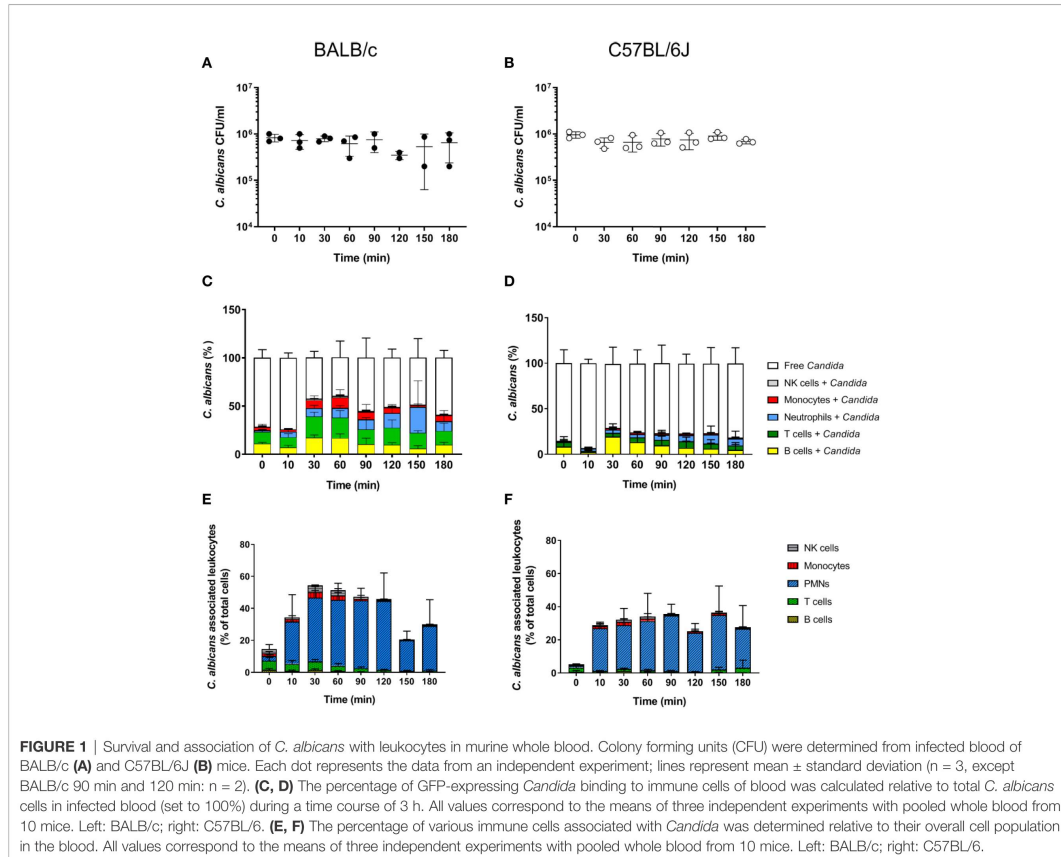
RESULTS

C. albicans Survives in Murine Whole Blood

The fate of *C. albicans* upon exposure to murine blood was analyzed in whole blood collected from two of the most commonly used mouse strains for infection experiments, BALB/c and C57BL/6J. As described by Hünigler et al. for the human whole-blood model (4), whole blood was inoculated with 1×10^6 /ml of yeast-grown *C. albicans* and fungal survival was determined by counting colony forming units (CFU) at various time points over a time course of 3 h. In contrast to human blood in which a 50% decrease of the initial CFUs within the first hour of contact was observed (4), the fungal burden did not decrease during incubation in neither BALB/c nor C57BL/6J mouse blood but remained stable throughout the experiment (Figures 1A, B). Of note, ketamine and xylazin were used to euthanize mice prior to blood collection. As ketamine has been shown to affect antimicrobial functions of macrophages and neutrophils in a dose-dependent manner (27–30), we added ketamine and xylazin to human blood and quantified fungal killing. At the used dose (40 μ g/ml ketamine and 2 μ g/ml xylazin) ketamine/xylazin treatment did not affect fungal killing (Figure S1).

Less Immune Cells Interact With *C. albicans* in Murine Compared to Human Blood

In order to determine whether the higher fungal survival in murine compared to human blood was associated with



differences in the interaction with immune cells, we analyzed the number of immune cells and association of *C. albicans* with leukocytes. Quantification of total leukocyte numbers using a hematology analyzer showed a moderate, non-significant decline over time in both mouse strains (Figure S2A). While the numbers of CD45⁺ leukocytes in relation to all blood cells showed no obvious changes throughout the infection (Figure S2B), the numbers of neutrophils decreased by almost 50% within the first 10 min after addition of *C. albicans* (Figure S2C). This was not the case for mock-infected control samples (Figure S2D). In contrast, the number of other types of leukocytes remained stable over time (Figure S3). Note that the relative abundance of neutrophils was significantly lower in the blood of B57BL/6J ($4.56 \pm 1.3\%$) than of BALB/c mice ($8.63 \pm 1.58\%$; $p = 0.02$).

Using a strain constitutively expressing green fluorescent protein the association of *C. albicans* with leukocytes was determined by flow cytometry. Within 30 min, more than 50% of *C. albicans* cells were associated with immune cells in BALB/c whole blood (Figure 1C). The proportion of fungal cells

associated with immune cells remained relatively stable until the end of the experiments (Figure 1C). A similar trend was observed in blood of C57BL/6J mice; however, the rate of association was lower and did not exceed 40%. Surprisingly, a large proportion of *C. albicans* cells were found to be associated with B- and T-cells in both mouse lines (Figures 1C, D). This contrasts results from the human whole-blood model in which monocytes and neutrophils were the dominant types of immune cells physically interacting with *C. albicans* (4). Since the ratio of the different immune cell populations in blood differs significantly between humans and mice, we speculated that the association to lymphocytes could be the consequence of the higher abundance of these types of immune cells in murine blood rather than the result of specific interactions. We thus calculated the percentage of host cells interacting with *C. albicans* within the different immune cell populations (Figures 1E, F). Although only a small fraction of *C. albicans* cells were associated with neutrophils, up to 50% and 40% of all neutrophils associated to fungal cells in blood from BALB/c and C57BL/6J mice, respectively. In contrast, only a minor fraction of the B- and

T-cell populations interacted with the fungus, suggesting that the observed association is indeed a stochastic physical event rather than the result of specific interactions.

The Reduced Fungal Killing in Murine Blood Is Only Partially Due to Lower Neutrophil Numbers

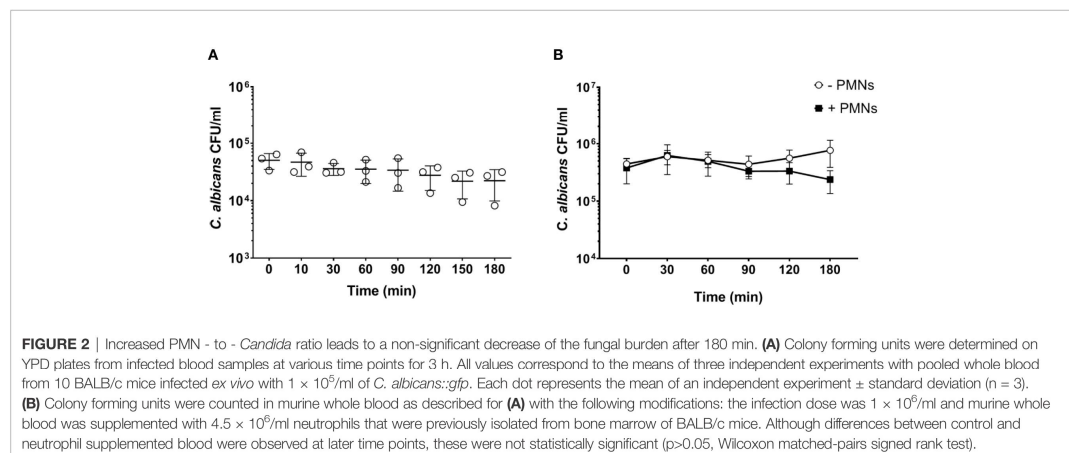
Neutrophils are the most active immune cells interacting with *C. albicans* in both human and murine blood, and have been shown to be critical for killing of the fungus in the human whole-blood model (4). However, the absolute number of neutrophils is approximately 10-fold lower in murine ($0.4 \times 10^6/\text{ml}$) than human blood ($4 \times 10^6/\text{ml}$; according to reference values and determined by a hematology analyzer). Using the same infection dose ($1 \times 10^6/\text{ml}$) in both models thus resulted in a pathogen to neutrophil ratio of 2.5 in murine but 0.25 in human blood. We hypothesized that the higher microbe to neutrophil ratio in the murine whole-blood model overwhelmed the capacity of the neutrophils to interact with and control *C. albicans*. Therefore, we analyzed fungal survival in whole blood of BALB/c mice using a 10-fold lower infection dose ($1 \times 10^5/\text{ml}$), which is comparable to the ratio used previously in human whole blood (4). With the reduced infection dose there was a moderate reduction of the fungal burden by 30% within 3 h of infection (Figure 2A). A similar effect was observed when murine blood was supplemented with neutrophils isolated from bone marrow to reach cell numbers comparable to human blood ($4.4 \pm 0.51 \times 10^9/\text{L}$ of cells, determined by a hematology analyzer) (Figure 2B). Thus, both the addition of external neutrophils and the lower infection dose led to increased fungal killing, but survival of *C. albicans* after 180 min was still substantially higher (>40%) than in a human whole-blood model (10% (4)). Furthermore, fungal burden decreased only slowly in murine blood, whereas 50% of fungal cells were killed within the first 60 min in human blood (4). To exclude effects mediated by ketamine/xylazine, ketamine and xylazine were added to human

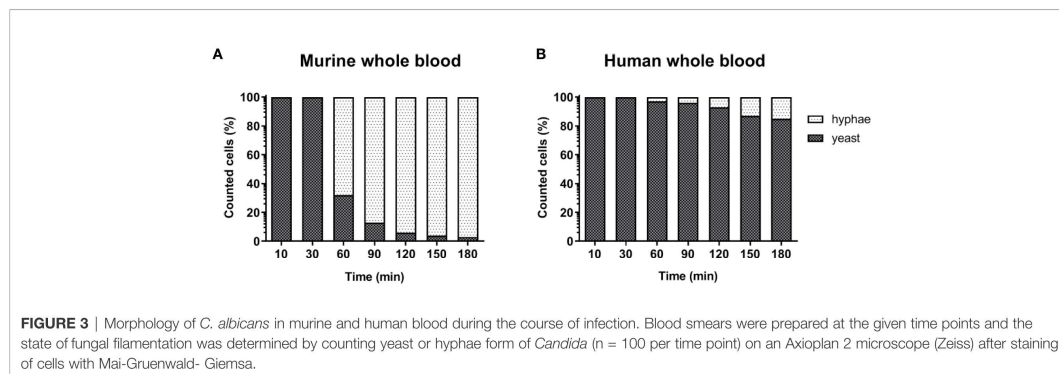
blood; this did not affect association rates with neutrophils and monocytes (Figure S4).

Filamentation of *C. albicans* in Whole Blood Is Not Effectively Inhibited by Murine Neutrophils but Fungal Survival Does Not Require Filamentation

The lower number of neutrophils in murine compared to human blood did not fully explain the lower killing of *C. albicans* in murine blood. However, functional differences between human and murine neutrophils have been described: A previous study from Ermert et al. (31) described a reduced efficiency of murine neutrophils to kill *Candida* species due to the fact that mice lack β -defensins and produce lower amounts of myeloperoxidase. They also showed that internalized *C. albicans* can escape from murine but not from human neutrophils by outgrowing neutrophils through filamentation and subsequent rupture of the neutrophil membrane (31). We therefore analyzed *C. albicans* morphology in whole blood by microscopy. Following infection with yeast cells, after 60 min the majority of *C. albicans* (~70%) in murine blood were hyphae and after 180 min nearly all (>90%) fungal cells grew as filaments (Figure 3A). In contrast, hyphal morphology was observed only for 10% and 20% of all *C. albicans* cells in human blood after 60 and 180 min, respectively (Figure 3B).

C. albicans morphology has been shown to affect recognition by neutrophils (5, 32) and monocytes (33). Furthermore, while human neutrophils prevent *C. albicans* filamentation and escape following phagocytosis (31), human monocytes and macrophages do not, and intracellular filamentation leads to immune cell lysis and fungal escape (34). Given the higher rate of *C. albicans* filamentation observed in murine blood, and the role of morphology for immune escape, we used a yeast-locked *C. albicans* $\Delta\text{efg1}/\Delta\text{cph1}$ mutant expressing GFP (19) in the murine whole-blood infection model to determine if the higher filamentation rate could explain higher survival of *C. albicans*





in murine blood. Surprisingly, no decrease in CFU counts was observed with this strain and fungal numbers even increased 2.5-fold from 60 to 180 min (**Figure 4A**). The increasing fungal burden correlated with a decrease in CD45⁺ cells (**Figure 4B**), and especially neutrophils (**Figure 4C**), at later time points (150 min and 180 min). The percentage of *C. albicans* Δ efg1/ Δ cph1 cells not associated with any type of immune cell (~80%, **Figure 4D**) was significantly higher compared to the wild type strain (~50%, **Figure S2A**). This is in contrast to experiments with human blood, in which similar association of wild type and mutant with immune cells was observed (4, 5). However, more than 25% of all neutrophils were associated with this mutant after 2 h (**Figure 4E**), and the release of cytokines upon infection with the mutant was comparable to or higher than *C. albicans* wild type infection (**Figure S4**). Thus, the large number of free Δ efg1/ Δ cph1 cells cannot be explained by an inability of immune cells to recognize mutant yeast cells.

Rapid Platelet Aggregation and Activation in Murine Blood Upon Exposure to *C. albicans*

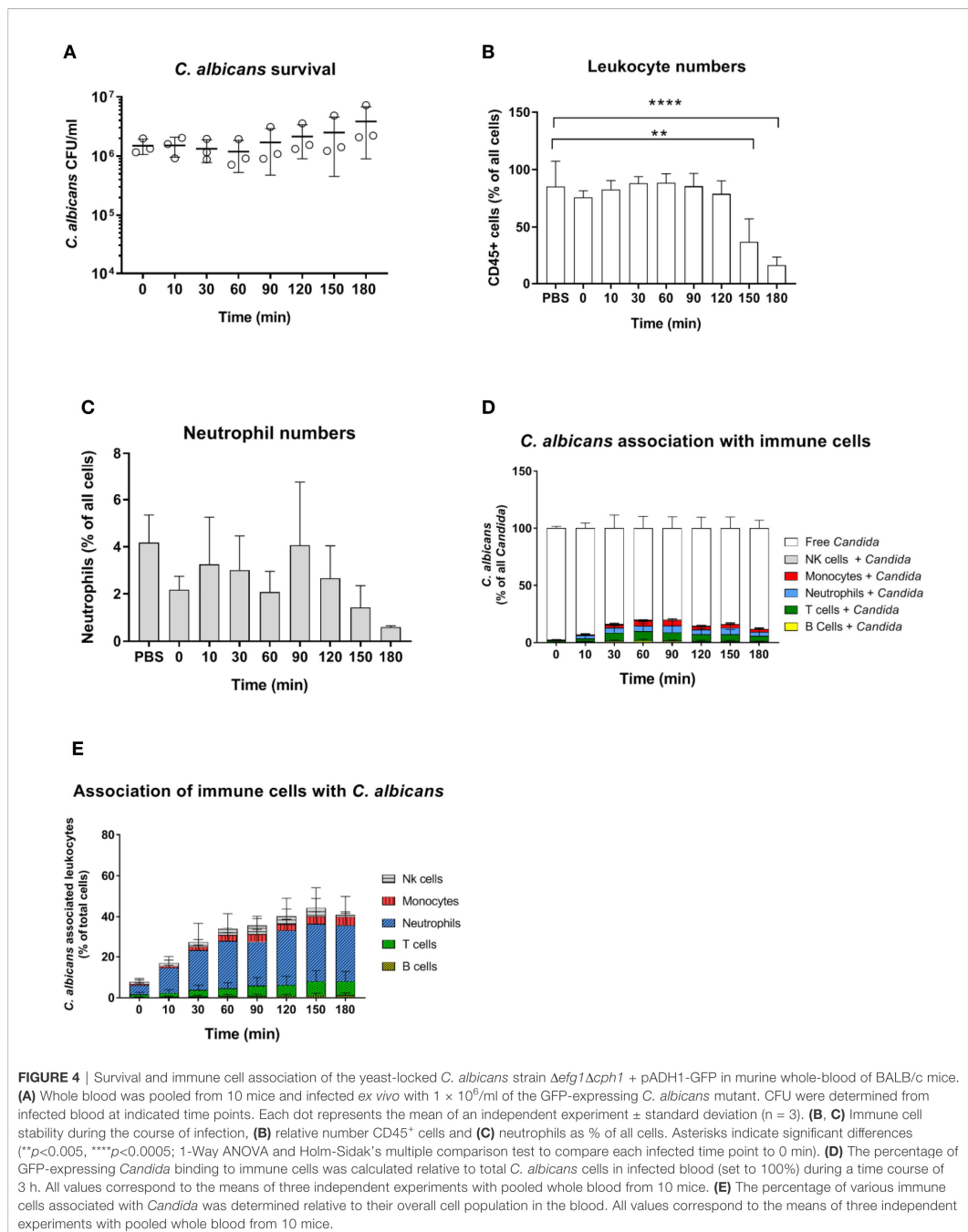
In addition to fungal filamentation, microscopic analysis revealed aggregates of platelets around *C. albicans* cells (**Figure 5A**). This interaction was confirmed and quantified by flow cytometry (**Figure 5B**): Within 10 min almost 60% of *C. albicans* cells were associated with platelets. The association rate slowly decreased over time to 40% after 3 h. At early time points, over 35% of the fungal-associated platelets expressed the activation marker CD69 on their surface (**Figure 5C**). We also observed increased expression of CD62 on the surface of *C. albicans* bound platelets, however in only 20% of all platelets (**Supplementary Figure S6**). To exclude that platelet activation was an artefact of the *ex vivo* situation, blood samples of intravenously (i. v.) infected mice were analyzed. *In vivo*, platelet counts increased significantly over a course of three days post infection (**Figure 6A**). Transient platelet activation was observed at 6 h post infection characterized by a significant increase of complement C3c, indicating opsonization, the platelet aggregation factor fibrinogen, and the activation markers CD63 and CD62P on the surface of platelets (**Figures 6B–E**). While at later time points

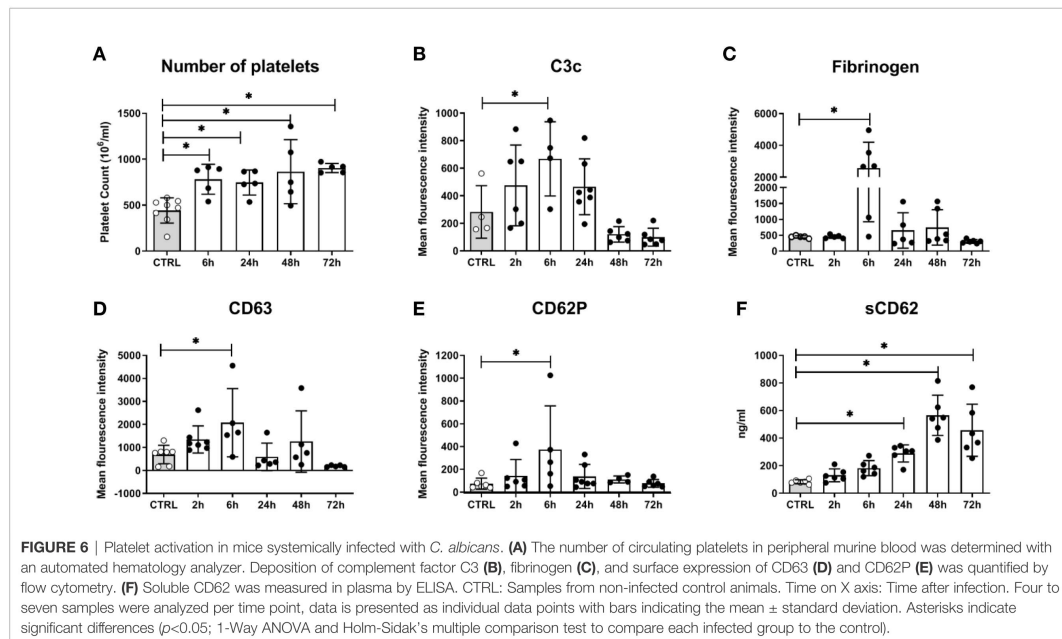
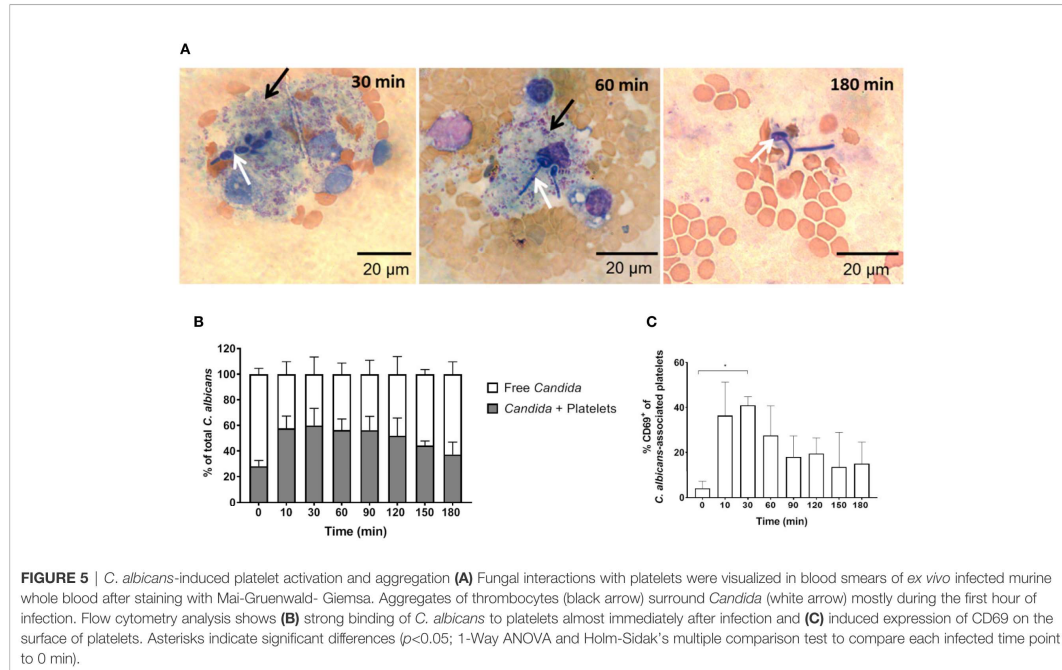
expression of these markers was comparable to control samples, increased concentrations of soluble CD62 were detectable in the plasma of infected mice from 1 to 3 days post infection by ELISA (**Figure 6F**). Taken together, these data demonstrate interaction and activation of platelets following infection with *C. albicans* in murine blood *ex vivo* and *in vivo*.

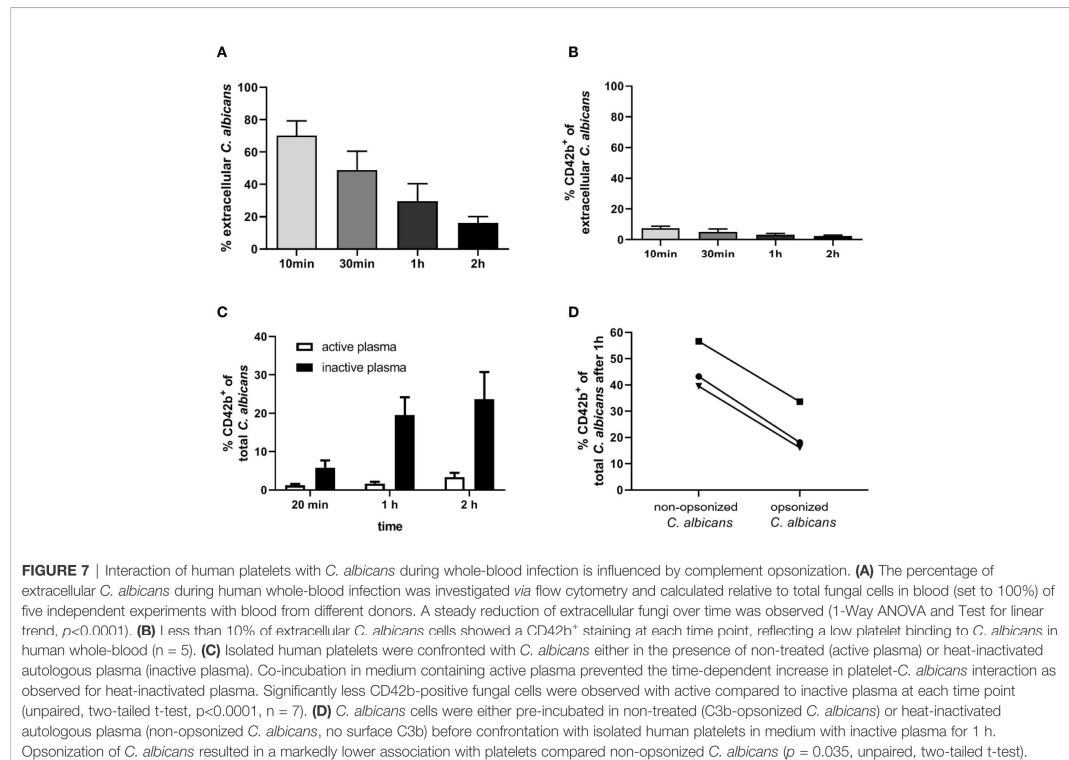
Opsonization of *C. albicans* in Human Blood Leads to Low Platelet Association

Our next aim was to determine if interaction with thrombocytes also occurs in human blood. Consistent with previous findings (4), we observed decreasing numbers of *C. albicans* cells not associated with host cells in human blood over time (**Figure 7A**). Only a small proportion (less than 10%) of fungal cells directly associated with platelets (**Figure 7B**). This was in sharp contrast to the results we obtained in murine blood. To investigate the potential influence of human blood components on fungal-platelet interaction, confrontation of isolated human platelets with *C. albicans* cells was performed in the presence of non-treated (active) or heat-inactivated autologous plasma and showed a time-dependent increase in platelet-*C. albicans* interaction when plasma proteins were inactivated (**Figure 7C**). In contrast, the presence of non-treated plasma containing active complement proteins resulted in a low platelet association. Consequently, we tested if opsonization of fungal cells interferes with platelet binding. Indeed, pre-opsonized *C. albicans* showed a significantly reduced interaction with isolated platelets compared to non-opsonized *C. albicans* (**Figure 7D**) indicating that opsonization of extracellular *C. albicans* during human whole-blood infection prevents the binding of platelets. In a comparable experiment using isolated murine thrombocytes and murine serum, active but not inactive serum significantly increased the binding of thrombocytes to *C. albicans* (**Figure 8A**).

The observation that inactivation of human plasma increases interaction of thrombocytes with *C. albicans* suggests that complement factors interfere with binding of human platelets to the fungus. While it remains unclear how complement becomes activated in active human plasma upon contact with *C. albicans*, the classical, antibody-mediated complement activation pathway







might be involved. Specific-pathogen free mice, as used in this study, are usually not colonized by *C. albicans* (35) and show comparatively low colonization with fungi (36), resulting in very low detectable anti-*Candida* antibodies in SPF mice (37). Thus, due to the absence of antibodies, whole murine blood and serum might lack the level of opsonization mediated by normal human plasma and, in consequence, lower opsonization could result in higher interaction with platelets. To test this hypothesis, we compared the binding of isolated thrombocytes to *C. albicans* in the presence of active serum from normal SPF mice (naïve mice) and mice that survived a sublethal systemic *C. albicans* infection (reconvalescent mice). The binding of thrombocytes to fungal cells was significantly higher with serum from naïve mice; furthermore, naïve serum and serum from C3-deficient mice induced similar binding of thrombocytes to *C. albicans* (Figure 8B), supporting the hypothesis that the lack of prior contact to the fungus in SPF mice contributes to the observed differences between human and murine whole blood regarding interaction with thrombocytes.

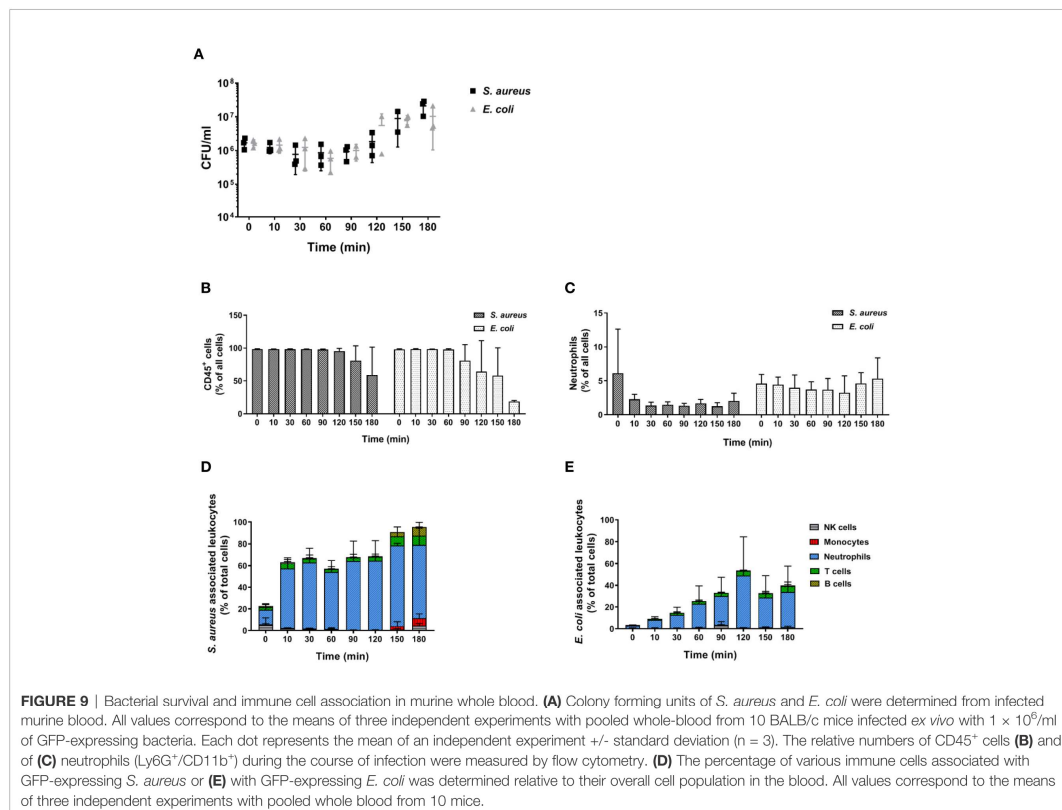
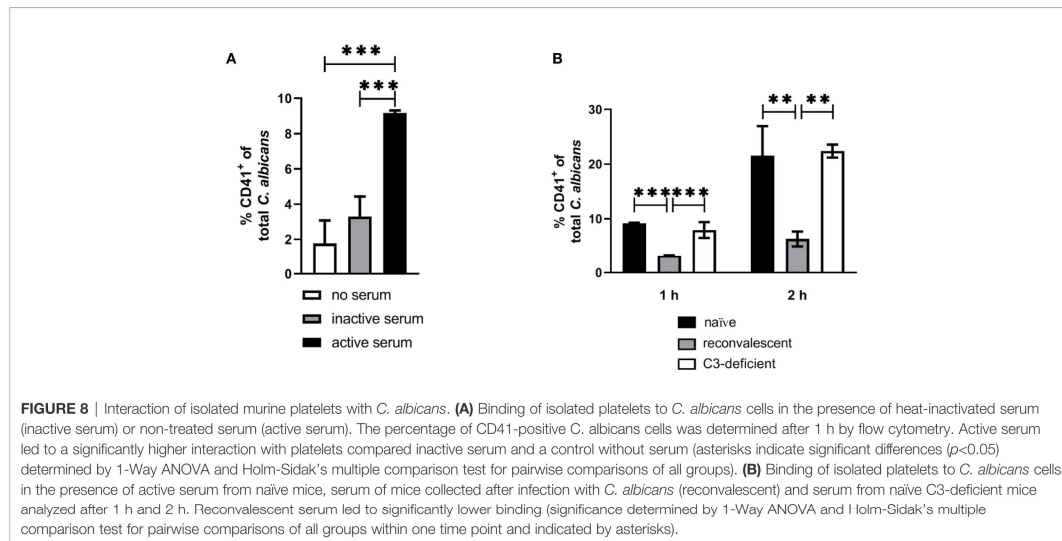
Whole Murine Blood Is Not Able to Clear Bacterial Infections *Ex Vivo*

In order to determine whether the inability of murine blood to control infections *ex vivo* is restricted to *C. albicans*, we performed infections with *S. aureus* and *E. coli* as models for

Gram-positive and Gram-negative bacteria, respectively. Similar to our observations with the filament-deficient *C. albicans* strain, CFU counts for both bacterial pathogens remained stable for the first 90 min followed by a steady increase (Figure 9A). This increase in pathogen load was even more pronounced than that observed for *C. albicans* $\Delta efg1 \Delta cph1$ (Figure 4A), and was also seen with a 10-fold lower infection dose, albeit at a lesser extent (Figure S7). Also similar to infection with the yeast-locked *C. albicans* mutant was the reduction of leukocyte numbers (Figure 9B), and for *S. aureus* especially neutrophil counts (Figure 9C), at late time points. The association of bacteria to immune cells varied quite drastically between both bacterial strains: While almost 60% of neutrophils were rapidly bound to *S. aureus* within 10 min and almost all neutrophils were attached to these Gram-positive bacteria 1.5 h post infection (Figure 9D), bacterial host cell association occurred much later for *E. coli* and a maximum of 50% of neutrophils were attached to bacteria at 2 h post infection (Figure 9E).

DISCUSSION

Intravenous infection of mice is the most commonly used model to study candidiasis (13). It is known that *C. albicans* disappears



quickly from circulating blood within a few minutes to hours after infection (15, 16, 38), but the mechanisms underlying this phenomenon and the fungal interaction with blood components are not fully understood. We have previously employed a human whole-blood model to determine the interaction of *C. albicans* with leukocytes and the fate of the fungus. In this study, the model was adapted to mice to elucidate host-fungal interactions in whole blood over a period of 3 h.

One of the most striking differences observed between the murine and human whole-blood experiments was the lack of *C. albicans* killing in murine blood, both at the infectious dose used in our previous study on human blood (1×10^6 /ml) and at a 10-fold lower dose (1×10^5 /ml). A commonly used infectious dose in the intravenous mouse model is 2.5×10^4 CFU/g body weight, equivalent to 5×10^5 CFU for a 20 g mouse (13, 16). The approximate blood volume of a 20 g mouse is 1.6 ml (39), resulting in approximately 3×10^5 CFU injected per ml of blood. Thus, the doses used in this study are relevant for the *in vivo* mouse model. Consequently, the inability of murine blood to effectively eliminate the fungus cannot be explained by an inadequately high infectious dose. Furthermore, as comparable results were obtained with blood from BALB/c and C57BL/6 mice, low fungal killing is unlikely to be a consequence of the specific genetic background.

Differences were also observed in the interaction with immune cells: A higher proportion of fungal cells was not associated to any leukocytes in murine (40–50%) compared to human blood (10–20% (4)). Especially the proportion of *C. albicans* cells associated with neutrophils was substantially lower in mouse blood (<30% compared to >60% (4)). Neutrophils are known to be the major effector cells mediating *C. albicans* killing in human whole-blood infection (4), and they are essential for host defense against disseminated candidiasis both in humans (40, 41) and mice (42, 43). It is unlikely that the low number of *C. albicans* interacting with neutrophils is due to insufficient recognition, as the high proportion of neutrophils associated with *C. albicans* indicated that these leukocytes responded to the fungus. The lower absolute numbers, however, lead to a pathogen-to-neutrophil ratio that might have been too high to allow efficient infection control. Contrary to this hypothesis, reducing the infectious dose did not substantially increase fungal killing. It is possible that the abundance of other immune cells blocked physical contact between neutrophils and *Candida*. Consistent with this, many fungal cells were associated with lymphocytes during high dose infection, even though the proportion of lymphocytes interacting with *Candida* was low, indicating limited directed activity. We therefore increased the absolute number of murine neutrophils to that in human blood, thereby also altering the neutrophil-lymphocyte ratio. As this had only a minor impact on fungal killing, functional differences between murine and human immune cells are likely to contribute to fungal survival in murine blood.

While human and murine neutrophils share many characteristics, they differ in some functional aspects. For example, murine neutrophils do not produce defensins (44), express less myeloperoxidase and lysozyme (45), and differ in the

expression and production of pattern recognition receptors, cytokines, and chemokines [summarized in (46)]. Ermert et al. showed that this translates into functional differences: Isolated murine neutrophils were less efficient in killing *C. albicans in vitro* than their human counterparts (31). Furthermore, while neutrophils were shown to be responsible for preventing hyphae development in human blood (18), isolated murine neutrophils fail to inhibit filamentation of phagocytosed yeast, resulting in fungal escape (31). Consistent with this, we observed substantial filamentation of *C. albicans* in murine, but not human blood. Thus, the higher filamentation rate in murine blood might be the consequence of an inability of murine neutrophils to control filamentation not only *in vitro* but also in the more complex *ex vivo* model. Killing of neutrophils by *C. albicans* filamentation after phagocytosis would furthermore explain the decline of neutrophil numbers over time in infected murine blood. However, extracellular filamentation has been shown to also occur in human blood (4), and we can therefore not exclude that the increased filamentation observed in murine blood is due to the lower number of fungal cells interacting with immune cells.

Although long filaments are more difficult to phagocytose due to their size (47), it is unlikely that filamentation alone is responsible for the lack of fungal killing, as survival and even proliferation in murine whole blood was observed for a filament-deficient *C. albicans* mutant. This was surprising because mutants lacking either of the genes (*EFG1* and *CPH1*) deleted in the mutant used here were previously reported to display reduced survival in human blood (18), and the double mutant is avirulent in a systemic mouse infection model (48). The association rate of this mutant with leukocytes was however lower compared to wild type fungi (<25% compared to up to 50%). This is indicative of lower phagocytosis rates and likely leads to less phagocytosis-dependent fungal killing. The lower association rates could be due to the generally less efficient recognition of yeast *versus* hyphal cells by neutrophils (32, 49). The specific gene deletions furthermore affect the exposure of cell wall components serving as pathogen-associated molecular patterns (50–52). As the percentage of neutrophils interacting with the non-filamentous mutant was however only slightly less than for the wild type, it appears unlikely that altered recognition alone is responsible for proliferation of the filament-deficient mutant. This is supported by the cytokine measurements that demonstrate similar or higher responses of murine whole blood to the mutant compared to the wildtype, and is consistent with the higher cytokine release by monocytes and PBMCs in response to yeast cells observed by others (33, 53).

While our results overall suggest a very limited capacity of murine neutrophils to control *C. albicans* in murine blood, it should be noted that we observed a reduction of fungal burden at late time points in murine whole blood with added neutrophils. Although not statistically significant, this is in agreement with other studies demonstrating some efficacy of isolated murine neutrophils against this fungus (31, 54). In this context it should be noted that neutrophils are primed during recruitment to a site of inflammation, leading to increased expression of pattern recognition receptors and enhanced effector functions (55, 56).

TABLE 1 | Summary of the key differences between the murine and human whole-blood model for *C. albicans*.

	Murine whole blood	Human whole blood
<i>C. albicans</i> killing	Not detectable	≥50% within 60 min, ≥80% within 180 min (4)
Association <i>C. albicans</i> with leukocytes	Approx. 40–60% max. (mouse strain-dependent)	Approx. 80% max (4).
Association with neutrophils relative to all leukocytes	≥50% (time point-dependent)	≥80% (4)
Association with monocytes relative to all leukocytes	≥25% (time point-dependent)	≤15% (4)
Association with lymphocytes relative to all leukocytes	≥50% (time point-dependent)	Not detectable (4)
% association neutrophils with <i>C. albicans</i>	40–50% (mouse strain-dependent)	Not determined
Filamentation (% hyphae)	≥60% after 60 min; ≥ 90% after 180 min	≤10% after 60 min; ≤20% after 180 min
Interaction with platelets		
<i>C. albicans</i> association with platelets in whole blood	≤60% after 10 min; 40% after 180 min	≤10%

Thus, the limited impact of neutrophils in murine whole blood cannot be transferred to neutrophil efficacy in tissue *in vivo*. However, our results suggest that the rapid decline of *C. albicans* CFU numbers in the peripheral blood of intravenously infected mice is not due to fungal killing within circulating blood. Possibly, interaction between *C. albicans* and murine blood leukocytes *in vivo* occurs only after fungal attachment to endothelial cells (57, 58).

Host-dependent differences in the interaction of *C. albicans* with leukocytes were also observed for platelets: In the murine whole-blood model, aggregation of platelets around and adhesion to fungal cells was observed which was associated with platelet activation. Transient activation of platelets was also observed *in vivo* in mice, consistent with previous observations by others (38). In contrast, only few platelets associated with *C. albicans* in human blood, supporting recent findings by Eberl et al. (59). The absence of the formation of obvious platelet aggregates around fungal elements in human blood is consistent with other studies (60, 61), and might be mediated by fungal chitin (62). Importantly, others showed that only those human platelets that bound to *C. albicans* became activated (59). The low number of bound platelets likely results in a very small increase of activation in the overall platelet population. This could explain why several studies described that this fungus does not activate human platelets (60, 63, 64), whereas we detected a significant increase of released platelet effector molecules. Interestingly, we found that the physical interaction between *C. albicans* and human platelets was enhanced by plasma inactivation, suggesting that complement factors interfere with binding of human platelets to the fungus. In this context our observation that prior exposure of mice to *C. albicans* significantly affected the impact of their serum on the rate of interaction between the fungus and thrombocytes might be of relevance not only for this, but also for other studies and might have implications beyond *C. albicans* infection: SPF mice, which are commonly used to study infections, lack contact to common opportunistic pathogens and thus adaptive immune response to these microbes. As demonstrated here, this could explain some of the differences observed between mice and men, and might also contribute to the limited efficacy of murine whole blood to eliminate *E. coli* and *S. aureus* shown in this study. Even though *S. aureus* has been isolated from laboratory SPF mice colonies, over 70% of tested animals were found to be free of this opportunistic pathogen (65). It can also be assumed that SPF mouse colonies are free from pathogenic *E. coli* and thus naïve to

the strain used in this study. Further research is clearly needed to investigate to which extent the lack of prior exposure affects host responses of mice in infection models.

In summary, we present here a thorough analysis of host-pathogen interaction in a murine whole-blood model, the first point of fungal interaction with the host immune system in experimental candidiasis, and provide time-resolved data on fungal survival and association to immune cells. Our results indicate substantial differences to the host-fungal interactions shown in a human whole-blood model (summarized in **Table 1**), thereby limiting the translatability of data obtained in a murine whole-blood model to human infections—even though the murine systemic infection model recapitulates several important aspects of systemic infection in humans. This could be at least in part due to the lack of *C. albicans* colonization of SPF mice.

DATA AVAILABILITY STATEMENT

The original contributions presented in the study are included in the article/**Supplementary Material**. Further inquiries can be directed to the corresponding author.

ETHICS STATEMENT

The studies involving human participants were reviewed and approved by Ethics Committee of the University Hospital Jena, permit number: 273-12/09. The patients/participants provided their written informed consent to participate in this study. The animal study was reviewed and approved by Thüringer Landesamt für Verbraucherschutz, permit number 03-007/13 and HKI-19-003.

AUTHOR CONTRIBUTIONS

SM, SS, IJ, BS-R, OK, KH, and CS conceived the study. SM, SS, CD, KS, WK, KH, CS, and GR performed the experiments. SM, KH, CS, and IJ analyzed the data. SM, CD, and IJ drafted the manuscript. SM, SS, KH, OK, CD, KS, WK, BS-R, CS, GR, and IJ revised and approved the manuscript. All authors contributed to the article and approved the submitted version.

FUNDING

Part of this project was funded by the funding line Strategic Networking in the Leibniz Association within the framework of the Leibniz Science Campus "InfectoOptics" (Project BLOODi to IJ) in Jena. CS was supported by the FWF Austrian Science Fund (Project Nr. P26117-B20). Work in the lab of OK and IJ was supported by the German Research Foundation (DFG; TRR 124 FungiNet, "Pathogenic fungi and their human host: Networks of Interaction," DFG project number 210879364, Project C3 to OK and C5 to IJ). Funders had no role in study design, analyses and interpretation of data, in the writing of the report, and in the decision to submit the article for publication.

REFERENCES

- Watson KG, Holden DW. Dynamics of growth and dissemination of *Salmonella in vivo*. *Cell Microbiol* (2010) 12:1389–97. doi: 10.1111/j.1462-5822.2010.01511.x
- Martinez RM, Wolk DM. Bloodstream Infections. *Microbiol Spectr* (2016) 4. doi: 10.1128/microbiolspec.DMIH2-0031-2016
- Reimer LG, Wilson ML, Weinstein MP. Update on detection of bacteremia and fungemia. *Clin Microbiol Rev* (1997) 10:444–65. doi: 10.1128/CMR.10.3.444
- Hünninger K, Lehnert T, Bieber K, Martin R, Figge MT, Kurzai O. A virtual infection model quantifies innate effector mechanisms and *Candida albicans* immune escape in human blood. *PLoS Comput Biol* (2014) 10:e1003479. doi: 10.1371/journal.pcbi.1003479
- Hünninger K, Bieber K, Martin R, Lehnert T, Figge MT, Löffler J, et al. A second stimulus required for enhanced antifungal activity of human neutrophils in blood is provided by anaphylatoxin C5a. *J Immunol (Baltimore Md: 1950)* (2015) 194:1199–210. doi: 10.4049/jimmunol.1401845
- Duggan S, Essig F, Hünninger K, Mokhtari Z, Bauer L, Lehnert T, et al. Neutrophil activation by *Candida glabrata* but not *Candida albicans* promotes fungal uptake by monocytes. *Cell Microbiol* (2015) 17:1259–76. doi: 10.1111/cmi.12443
- Viscoli C. Bloodstream Infections: The peak of the iceberg. *Virulence* (2016) 7:248–51. doi: 10.1080/21505594.2016.1152440
- Pappas PG, Lionakis MS, Arendrup MC, Ostrosky-Zeichner L, Kullberg BJ. Invasive candidiasis. *Nat Rev Dis Primers* (2018) 4:18026. doi: 10.1038/nrdp.2018.26
- Vazquez JA, Sobel JD. Mucosal candidiasis. *Infect Dis Clin North Am* (2002) 16:793–820, v. doi: 10.1016/S0891-5520(02)00042-9
- Perlroth J, Choi B, Spellberg B. Nosocomial fungal infections: epidemiology, diagnosis, and treatment. *Med Mycol* (2007) 45:321–46. doi: 10.1080/13693780701218689
- Pfäler M, Neofytos D, Dickema D, Azie N, Meier-Kriesche HU, Quan SP, et al. Epidemiology and outcomes of candidemia in 3648 patients: data from the Prospective Antifungal Therapy (PATH Alliance(R)) registry, 2004–2008. *Diagn Microbiol Infect Dis* (2012) 74:323–31. doi: 10.1016/j.diagmicrobio.2012.10.003
- Koh AY, Köhler JR, Coggshall KT, Van Rooijen N, Pier GB. Mucosal damage and neutropenia are required for *Candida albicans* dissemination. *PLoS Pathog* (2008) 4:e35. doi: 10.1371/journal.ppat.0040035
- MacCallum DM. Hosting infection: experimental models to assay *Candida* virulence. *Int J Microbiol* (2012) 2012:363764. doi: 10.1155/2012/363764
- Lionakis MS. New insights into innate immune control of systemic candidiasis. *Med Mycol* (2014) 52:555–64. doi: 10.1093/mmy/myu029
- Lionakis MS, Lim JK, Lee CCR, Murphy PM. Organ-Specific Innate Immune Responses in a Mouse Model of Invasive Candidiasis. *J Innate Immun* (2011) 3:180–99. doi: 10.1159/000321157
- MacCallum DM, Odds FC. Temporal events in the intravenous challenge model for experimental *Candida albicans* infections in female mice. *Mycoses* (2005) 48:151–61. doi: 10.1111/j.1439-0507.2005.01121.x

ACKNOWLEDGMENTS

We thank Joanna M. Niemiec for help with neutrophil isolation, and Philipp Kaemmer for technical assistance. SS is a member of the Jena School for Microbial Communication (JSMC).

SUPPLEMENTARY MATERIAL

The Supplementary Material for this article can be found online at: <https://www.frontiersin.org/articles/10.3389/fimmu.2020.565869/full#supplementary-material>

- Doering DC, Borowicz JL, Crockett ET. Gender dimorphism in differential peripheral blood leukocyte counts in mice using cardiac, tail, foot, and saphenous vein puncture methods. *BMC Clin Pathol* (2003) 3:3. doi: 10.1186/1472-6890-3-3
- Fradin C, De Groot P, MacCallum D, Schaller M, Klis F, Odds FC, et al. Granulocytes govern the transcriptional response, morphology and proliferation of *Candida albicans* in human blood. *Mol Microbiol* (2005) 56:397–415. doi: 10.1111/j.1365-2958.2005.04557.x
- Lo HJ, Kohler JR, DiDomenico B, Loebenberg D, Cacciapuoti A, Fink GR. Nonfilamentous *C. albicans* mutants are avirulent. *Cell* (1997) 90:939–49. doi: 10.1016/S0092-8674(00)80358-X
- Walther A, Wendland J. An improved transformation protocol for the human fungal pathogen *Candida albicans*. *Curr Genet* (2003) 42:339–43. doi: 10.1007/s00294-002-0349-0
- Balwit JM, van Langevelde P, Vann JM, Proctor RA. Gentamicin-Resistant Menadione and Hemin Auxotrophic *Staphylococcus aureus* Persist within Cultured Endothelial Cells. *J Infect Dis* (1994) 170:1033–7. doi: 10.1093/infdis/170.4.1033
- Kahl BC, Goulian M, van Wamel W, Herrmann M, Simon SM, Kaplan G, et al. *Staphylococcus aureus* RN6390 replicates and induces apoptosis in a pulmonary epithelial cell line. *Infect Immun* (2000) 68:5385–92. doi: 10.1128/IAI.68.9.5385-5392.2000
- Sreekantapuram S, Lehnert T, Praufte MTE, Berndt A, Berens C, Figge MT, et al. Dynamic Interplay of Host and Pathogens in an Avian Whole-Blood Model. *Front Immunol* (2020) 11:500. doi: 10.3389/fimmu.2020.00500
- Mollnes TE, Brekke OL, Fung M, Fure H, Christiansen D, Bergseth G, et al. Essential role of the C5a receptor in E coli-induced oxidative burst and phagocytosis revealed by a novel leprudin-based human whole blood model of inflammation. *Blood* (2002) 100:1869–77.
- Ganguly S, Panetta JC, Roberts JK, Schuetz EG. Ketamine Pharmacokinetics and Pharmacodynamics Are Altered by P-Glycoprotein and Breast Cancer Resistance Protein Efflux Transporters in Mice. *Drug Metab Dispos* (2018) 46:1014–22. doi: 10.1124/dmd.117.078360
- Ermert D, Urban CF, Laube B, Goosmann C, Zychlinsky A, Brinkmann V. Mouse neutrophil extracellular traps in microbial infections. *J Innate Immun* (2009) 1:181–93. doi: 10.1159/000205281
- Davidson JA, Boom SJ, Pearsall FJ, Zhang P, Ramsay G. Comparison of the effects of four i.v. anaesthetic agents on polymorphonuclear leucocyte function. *Br J Anaesth* (1995) 74:315–8. doi: 10.1093/bja/74.3.315
- Heller A, Heller S, Blecken S, Urbaschek R, Koch T. Effects of intravenous anesthetics on bacterial elimination in human blood in vitro. *Acta Anaesthesiol Scand* (1998) 42:518–26. doi: 10.1111/j.1399-6576.1998.tb05160.x
- Nishina K, Akamatsu H, Mikawa K, Shiga M, Maekawa N, Obara H, et al. The inhibitory effects of thiopental, midazolam, and ketamine on human neutrophil functions. *Anesth Analg* (1998) 86:159–65. doi: 10.1097/0000539-199801000-00032
- Chang Y, Chen TL, Sheu JR, Chen RM. Suppressive effects of ketamine on macrophage functions. *Toxicol Appl Pharmacol* (2005) 204:27–35. doi: 10.1016/j.taap.2004.08.011

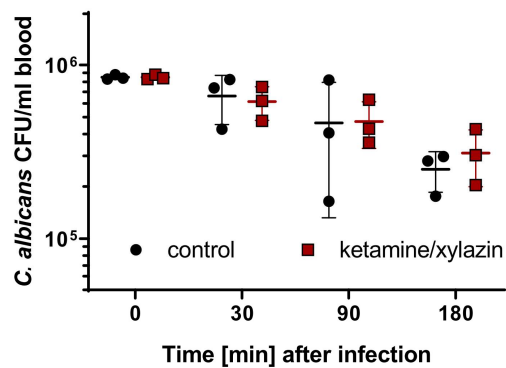
31. Ermert D, Niemiec MJ, Rohm M, Glenthøj A, Borregaard N, Urban CF. *Candida albicans* escapes from mouse neutrophils. *J Leukoc Biol* (2013) 94:223–36. doi: 10.1189/jlb.0213063
32. Wozniok I, Hornbach A, Schmitt C, Froesch M, Einsele H, Hube B, et al. Induction of ERK-kinase signalling triggers morphotype-specific killing of *Candida albicans* filaments by human neutrophils. *Cell Microbiol* (2008) 10:807–20. doi: 10.1111/j.1462-5822.2007.01086.x
33. Mukaremera L, Lee KK, Mora-Montes HM, Gow NAR. *Candida albicans* Yeast, Pseudohyphal, and Hyphal Morphogenesis Differentially Affects Immune Recognition. *Front Immunol* (2017) 8:629. doi: 10.3389/fimmu.2017.00629
34. Jiménez-López C, Lorenz MC. Fungal immune evasion in a model host-pathogen interaction: *Candida albicans* versus macrophages. *PLoS Pathog* (2013) 9:e1003741. doi: 10.1371/journal.ppat.1003741
35. Iliiev ID, Funari VA, Taylor KD, Nguyen Q, Reyes CN, Strom SP, et al. Interactions between commensal fungi and the C-type lectin receptor Dectin-1 influence colitis. *Science (New York NY)* (2012) 336:1314–7. doi: 10.1126/science.1221789
36. Yeung F, Chen YH, Lin JD, Leung JM, McCauley C, Devlin JC, et al. Altered Immunity of Laboratory Mice in the Natural Environment Is Associated with Fungal Colonization. *Cell Host Microbe* (2020) 27(5):809–22. doi: 10.1016/j.chom.2020.02.015
37. Huertas B, Prieto D, Pitarch A, Gil C, Pla J, Díez-Orejás R. Serum Antibody Profile during Colonization of the Mouse Gut by *Candida albicans*: Relevance for Protection during Systemic Infection. *J Proteome Res* (2017) 16:335–45. doi: 10.1021/acs.jproteome.6b00383
38. Robert R, Nail S, Marot-Leblond A, Cottin J, Miegville M, Quenouillere S, et al. Adherence of platelets to *Candida* species in vivo. *Infect Immun* (2000) 68:570–6. doi: 10.1128/IAI.68.2.570-576.2000
39. Mitruka BM, Rawnsley HM. *Clinical biochemical and hematological reference values in normal experimental animals*. New York: Masson Publishing USA Inc. (1977).
40. Horn DL, Neofytos D, Anaissie EJ, Fishman JA, Steinbach WJ, Olyaei AJ, et al. Epidemiology and outcomes of candidemia in 2019 patients: data from the prospective antifungal therapy alliance registry. *Clin Infect Dis* (2009) 48:1695–703. doi: 10.1086/599039
41. Gazendam RP, van de Geer A, Roos D, van den Berg TK, Kuijpers TW. How neutrophils kill fungi. *Immunol Rev* (2016) 273:299–311. doi: 10.1111/imr.12454
42. Romani L, Mencacci A, Cenci E, Puccetti P, Bistoni F. Neutrophils and the adaptive immune response to *Candida albicans*. *Res Immunol* (1996) 147:512–8. doi: 10.1016/S0923-2494(97)85216-9
43. Han Y, Cutler JE. Assessment of a mouse model of neutropenia and the effect of an anti-candidiasis monoclonal antibody in these animals. *J Infect Dis* (1997) 175:1169–75. doi: 10.1086/516455
44. Eisenhauer PB, Lehrer RI. Mouse neutrophils lack defensins. *Infect Immun* (1992) 60:3446–7. doi: 10.1128/IAI.60.8.3446-3447.1992
45. Rausch PG, Moore TG. Granule enzymes of polymorphonuclear neutrophils: A phylogenetic comparison. *Blood* (1975) 46:913–9. doi: 10.1182/blood.V46.6.913.bloodjournal466913
46. Tecchio C, Micheletti A, Cassatella MA. Neutrophil-derived cytokines: facts beyond expression. *Front Immunol* (2014) 5:508. doi: 10.3389/fimmu.2014.00508
47. Branzk N, Lubojemska A, Hardison SE, Wang Q, Gutierrez MG, Brown GD, et al. Neutrophils sense microbe size and selectively release neutrophil extracellular traps in response to large pathogens. *Nat Immunol* (2014) 15:1017–25. doi: 10.1038/ni.2987
48. Lo HJ, Köhler JR, DiDomenico B, Loebenberg D, A. Cacciapuoti, and G.R. Fink. Nonfilamentous *C. albicans* mutants are avirulent. *Cell* (1997) 90:939–49. doi: 10.1016/S0092-8674(00)80358-X
49. Rudkin FM, Bain JM, Walls C, Lewis LE, Gow NA, Erwig LP. Altered dynamics of *Candida albicans* phagocytosis by macrophages and PMNs when both phagocyte subsets are present. *mBio* (2013) 4:e00810–13. doi: 10.1128/mBio.00810-13
50. Zavrel M, Majer O, Kuchler K, Rupp S. Transcription factor Efg1 shows a haploinsufficiency phenotype in modulating the cell wall architecture and immunogenicity of *Candida albicans*. *Eukaryot Cell* (2012) 11:129–40. doi: 10.1128/EC.05206-11
51. Cottier F, Sherrington S, Cockerill S, Del Olmo Toledo V, Kissane S, Tournu H, et al. Remasking of *Candida albicans* β -Glucan in Response to Environmental pH Is Regulated by Quorum Sensing. *mBio* (2019) 10. doi: 10.1128/mBio.02347-19
52. Wartenberg A, Linde J, Martin R, Schreiner M, Horn F, Jacobsen ID, et al. Microevolution of *Candida albicans* in macrophages restores filamentation in a nonfilamentous mutant. *PLoS Genet* (2014) 10:e1004824. doi: 10.1371/journal.pgen.1004824
53. Torosantucci A, Chiani P, Cassone A. Differential chemokine response of human monocytes to yeast and hyphal forms of *Candida albicans* and its relation to the beta-1,6 glucan of the fungal cell wall. *J Leukoc Biol* (2000) 68:923–32.
54. Behnsen J, Narang P, Hasenberg M, Gunzer F, Bilitewski U, Klippel N, et al. Environmental dimensionality controls the interaction of phagocytes with the pathogenic fungi *Aspergillus fumigatus* and *Candida albicans*. *PLoS Pathog* (2007) 3:e13. doi: 10.1371/journal.ppat.0030013
55. Yao Y, Matsushima H, Ohtola JA, Geng S, Lu R, Takashima A. Neutrophil priming occurs in a sequential manner and can be visualized in living animals by monitoring IL-1 β promoter activation. *J Immunol (Baltimore Md: 1950)* (2015) 194:1211–24. doi: 10.4049/jimmunol.1402018
56. Miralda I, Uriarte SM, McLeish KR. Multiple Phenotypic Changes Define Neutrophil Priming. *Front Cell Infect Microbiol* (2017) 7:217. doi: 10.3389/fcimb.2017.00217
57. Grubb SE, Murdoch C, Sudbery PE, Saville SP, Lopez-Ribot JL, Thornhill MH. *Candida albicans*-endothelial cell interactions: a key step in the pathogenesis of systemic candidiasis. *Infect Immun* (2008) 76:4370–7. doi: 10.1128/IAI.00332-08
58. Filler SG, Pfunder AS, Spellberg BJ, Spellberg JP, Edwards JE Jr. *Candida albicans* stimulates cytokine production and leukocyte adhesion molecule expression by endothelial cells. *Infect Immun* (1996) 64:2609–17. doi: 10.1128/IAI.64.7.2609-2617.1996
59. Eberl C, Speth C, Jacobsen ID, Hermann M, Hagleitner M, Deshmukh H, et al. *Candida*: Platelet Interaction and Platelet Activity in vitro. *J Innate Immun* (2019) 11:52–62. doi: 10.1159/000491030
60. Schultz CM, Goel A, Dunn A, Knauss H, Huss C, Launder D, et al. Stepping Up to the Plate(let) against *Candida albicans*. *Infect Immun* (2020) 88:00784–19. doi: 10.1128/IAI.00784-19
61. Willcox MD, Webb BC, Thakur A, Harty DW. Interactions between *Candida* species and platelets. *J Med Microbiol* (1998) 47:103–10. doi: 10.1099/00222615-47-2-103
62. Leroy J, Bortolus C, Lecoqte K, Parny M, Charlet R, Sendid B, et al. Fungal Chitin Reduces Platelet Activation Mediated via TLR8 Stimulation. *Front Cell Infect Microbiol* (2019) 9:383. doi: 10.3389/fcimb.2019.00383
63. Bertling A, Niemann S, Uekötter A, Fegeler W, Lass-Flörl C, von Eiff C, et al. *Candida albicans* and its metabolite gliotoxin inhibit platelet function via interaction with thiols. *Thromb Haemost* (2010) 104:270–8. doi: 10.1160/TH09-11-0769
64. Woth G, Tökés-Füzesi M, Magyarlaki T, Kovács GL, Vermes I, Mühl D. Activated platelet-derived microparticle numbers are elevated in patients with severe fungal (*Candida albicans*) sepsis. *Ann Clin Biochem* (2012) 49:554–60. doi: 10.1258/acb.2012.011215
65. Schulz D, Grumann D, Trübe P, Pritchett-Corning K, Johnson S, Repschläger K, et al. Laboratory Mice Are Frequently Colonized with *Staphylococcus aureus* and Mount a Systemic Immune Response—Note of Caution for *In vivo* Infection Experiments. *Front Cell Infect Microbiol* (2017) 7:152. doi: 10.3389/fcimb.2017.00152

Conflict of Interest: The authors declare that the research was conducted in the absence of any commercial or financial relationships that could be construed as a potential conflict of interest.

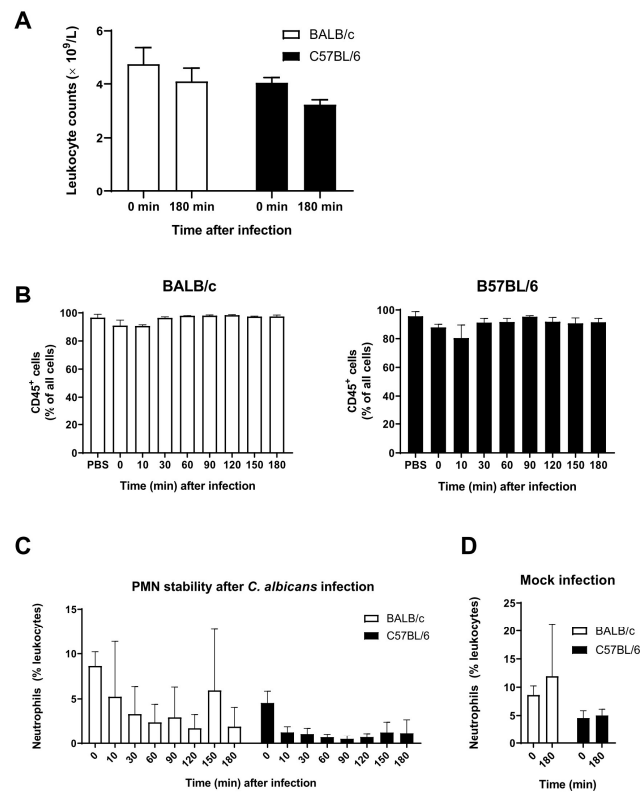
Copyright © 2021 Machata, Sreekantapuram, Himmiger, Kurzai, Dunker, Schubert, Krüger, Schulze-Richter, Speth, Rambach and Jacobsen. This is an open-access article distributed under the terms of the Creative Commons Attribution License (CC BY). The use, distribution or reproduction in other forums is permitted, provided the original author(s) and the copyright owner(s) are credited and that the original publication in this journal is cited, in accordance with accepted academic practice. No use, distribution or reproduction is permitted which does not comply with these terms.

Supplementary Material

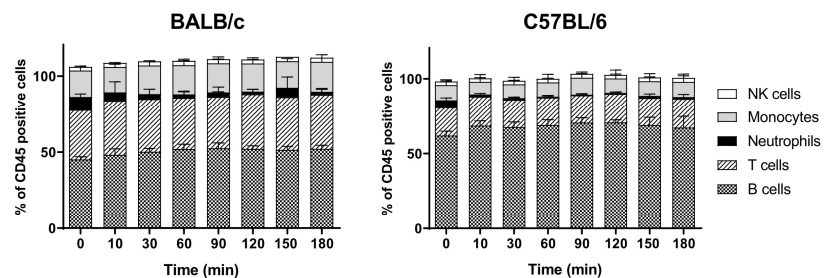
1 Supplementary Figures



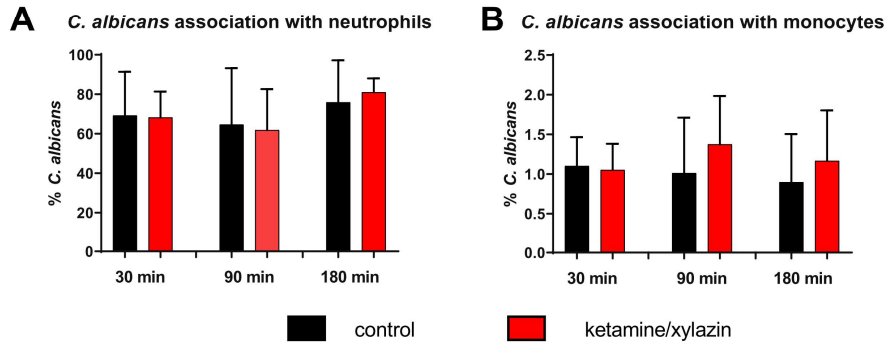
Supplementary Figure 1. Effect of ketamine and xylazine on *C. albicans* killing in the human whole-blood model. Blood from healthy human volunteers was left untreated (control, black circle) or 40 $\mu\text{g/ml}$ ketamine and 2 $\mu\text{g/ml}$ xylazine (ketamine/xylazine, red square) were added just before infection with *C. albicans*. Samples collected at the indicated time points were plated in serial dilution and CFU were quantified. Three experiments using different donors were performed with the control and ketamine/xylazine treatment performed in parallel. Mean \pm standard deviation are indicated by the lines. Statistical analysis was performed by paired, two-tailed t test comparing control and ketamine/xylazine for each time point and showed no significant difference between the groups.



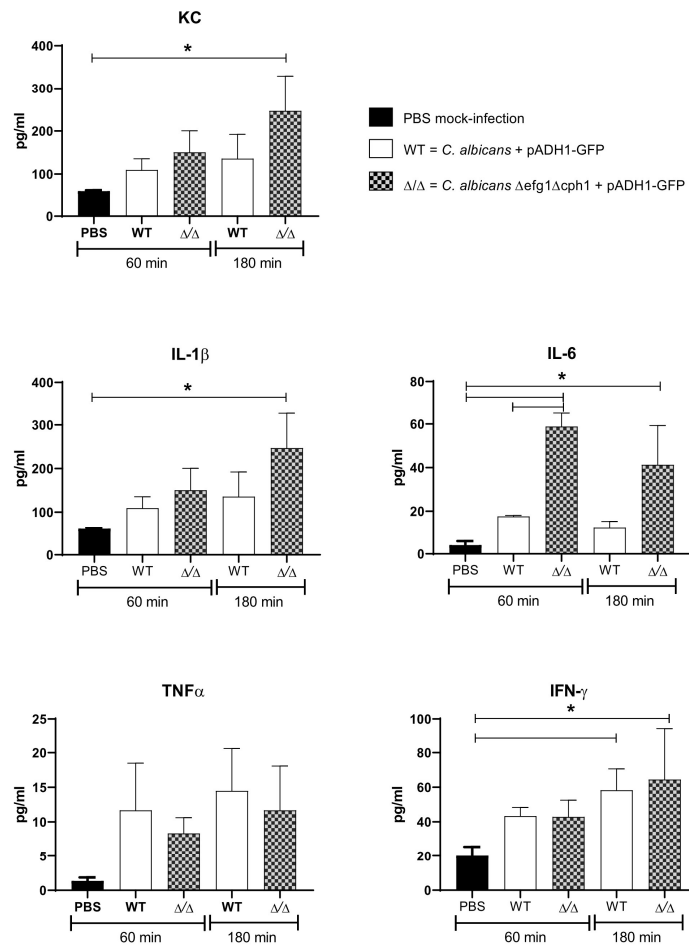
Supplementary Figure 2. Immune cell numbers in infected murine whole blood. (A) Total leukocyte counts were determined with an automated hematology analyzer. Changes over time were not statistically significant (unpaired t test corrected for multiple comparisons using the Holm-Sidak method). (B) The relative numbers of CD45⁺ cells in blood were measured by flow cytometry. (C, D) Relative numbers of neutrophils (Ly6G⁺/CD11b⁺) in infected blood (C) and blood mock-infected with PBS (D) measured by flow cytometry. Data from three independent experiments is presented as mean \pm standard deviation in each graph.



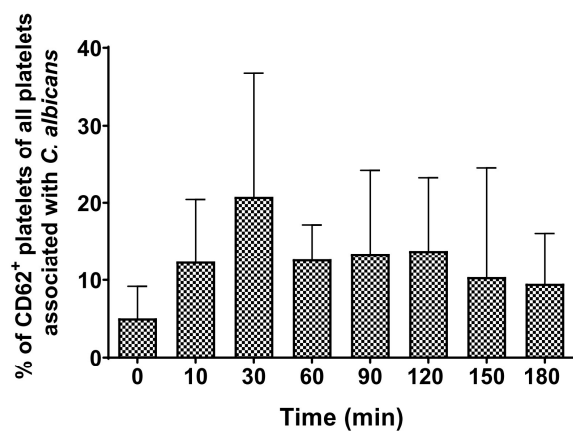
Supplementary Figure 3. Immune cell stability in murine whole blood upon exposure to *Candida*. Cell populations were measured by flow cytometry following *ex vivo* *C. albicans* infection of blood from BALB/c (A) and C57BL/6 mice (B). Statistical analysis was performed by unpaired, two-tailed t test.



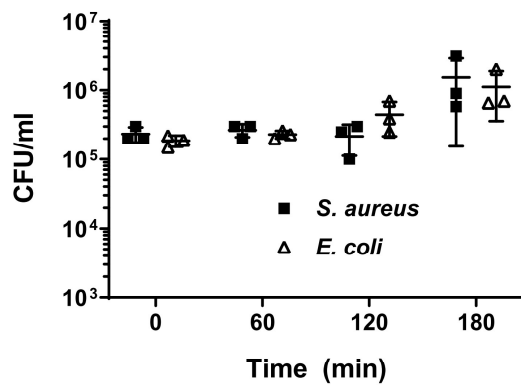
Supplementary Figure 4. Effect of ketamine and xylazine on association of *C. albicans* with neutrophils and monocytes in the human whole-blood model. Blood from healthy human volunteers was left untreated (control, black) or 40 $\mu\text{g/ml}$ ketamine and 2 $\mu\text{g/ml}$ xylazine (ketamine/xylazine, red) were added just before infection with *C. albicans*. Samples collected at the indicated time points were analyzed by flow cytometry. Three experiments using different donors were performed with the control and ketamine/xylazine treatment performed in parallel. The percentage of GFP-expressing *Candida* binding to immune cells of blood was calculated relative to total *C. albicans* cells in infected blood (set to 100 %) during a time course of three hours and is depicted as mean \pm standard deviation. Statistical analysis was performed by paired, two-tailed t test comparing control and ketamine/xylazine for each time point and showed no significant difference between the groups.



Supplementary Figure 5. Cytokine response to *C. albicans* infection in murine blood. Blood from BALB/c mice was infected with GFP-expressing *C. albicans* wild type (white) or *efg1 Δ cph1 Δ* double mutant (grey, square pattern). PBS-mock infection served as control. Cytokines were quantified in plasma at the indicated time points. Asterisks indicate significant differences ($p < 0.05$; 1-Way ANOVA and Holm-Sidak's multiple comparison test for comparison of infected to control blood; unpaired, two-tailed t test for comparison of the two strains at one time point). Mean \pm standard deviation of two to three independent experiments are shown.



Supplementary Figure 6. Numbers of CD62-activated platelets associated with *C. albicans* during the time of infection. Cells were differentially stained in whole blood and activated platelets (CD41⁺ CD62⁺) that were also positive for GFP were included in the analysis. Activated platelets are shown in relative amounts to all positive platelets (CD41⁺).



Supplementary Figure 7. Bacterial survival in murine whole blood at lower infection dose. Colony forming units of *S. aureus* and *E. coli* were determined from infected murine blood. All values correspond to the means of three independent experiments with pooled whole-blood from 10 BALB/c mice infected *ex vivo* with 1×10^5 /ml of GFP-expressing bacteria. Each dot represents the mean of an independent experiment \pm standard deviation (n=3).

3.3. Manuscript III: Dunker *et al.*, Nat. Commun., 2021

Rapid proliferation due to better metabolic adaptation results in full virulence of a filament-deficient *Candida albicans* strain

Christine Dunker, Melanie Polke, Bianca Schulze-Richter, Katja Schubert, Sven Rudolphi, A. Elisabeth Gressler, Tony Pawlik, Juan P. Prada Salcedo, M. Joanna Niemiec, Silvia Slesiona-Künzel, Marc Swidergall, Ronny Martin, Thomas Dandekar & Ilse D. Jacobsen

Nature Communications. 2021 June 23 . 12(1): 3899. doi: 10.1038/s41467-021-24095-8.

Summary

The yeast-to-hypha transition of *C. albicans* is considered to be a key virulence factor. This study shows that hyphae are required for tissue invasion, damage, and virulence in invasion-based infection models. However, hypha formation is not required for virulence in systemic candidiasis, as filament-deficient mutants lacking *EED1* (expression) were as virulent as the wild type in murine infection models resembling catheter-associated candidiasis in humans. Retained virulence of the *eed1Δ/Δ* mutant was associated with rapid yeast proliferation, which is likely the result of better metabolic adaptation and increased fitness, leading to high organ fungal burden and disease progression indistinguishable from infections caused by the *C. albicans* wild type. These data challenge the central dogma that hypha formation is *per se* essential for pathogenesis.

The candidate is:

First author, Co-first author, Corresponding author, Coauthor.

Estimated authors' contributions in %:

	Conception	Data analysis	Experimental	Writing	Provision of the material
Christine Dunker	50	69	68	90	72
Melanie Polke	10	5	5		10
Bianca Schulze-Richter		5	4		
Katja Schubert			4		
Sven Rudolphi		3	3		
A. Elisabeth Gressler		3	3		
Tony Pawlik		2	1		
Juan P. Prada Salcedo		5	2		2
M. Joanna Niemiec			1		
Silvia Slesiona-Künzel			2		
Marc Swidergall		3	2		2
Ronny Martin					2
Thomas Dandekar					2
Ilse D. Jacobsen	40	5	5	10	10



ARTICLE


<https://doi.org/10.1038/s41467-021-24095-8>

OPEN

Rapid proliferation due to better metabolic adaptation results in full virulence of a filament-deficient *Candida albicans* strain

Christine Dunker ¹, Melanie Polke ^{1,5}, Bianca Schulze-Richter ^{1,6}, Katja Schubert ¹, Sven Rudolphi ¹, A. Elisabeth Gressler ^{1,6}, Tony Pawlik ¹, Juan P. Prada Salcedo ², M. Joanna Niemiec ¹, Silvia Slesiona-Künzel ¹, Marc Swidergall ³, Ronny Martin ⁴, Thomas Dandekar ² & Ilse D. Jacobsen ¹✉

The ability of the fungal pathogen *Candida albicans* to undergo a yeast-to-hypha transition is believed to be a key virulence factor, as filaments mediate tissue damage. Here, we show that virulence is not necessarily reduced in filament-deficient strains, and the results depend on the infection model used. We generate a filament-deficient strain by deletion or repression of *EED1* (known to be required for maintenance of hyphal growth). Consistent with previous studies, the strain is attenuated in damaging epithelial cells and macrophages in vitro and in a mouse model of intraperitoneal infection. However, in a mouse model of systemic infection, the strain is as virulent as the wild type when mice are challenged with intermediate infectious doses, and even more virulent when using low infectious doses. Retained virulence is associated with rapid yeast proliferation, likely the result of metabolic adaptation and improved fitness, leading to high organ fungal loads. Analyses of cytokine responses in vitro and in vivo, as well as systemic infections in immunosuppressed mice, suggest that differences in immunopathology contribute to some extent to retained virulence of the filament-deficient mutant. Our findings challenge the long-standing hypothesis that hyphae are essential for pathogenesis of systemic candidiasis by *C. albicans*.

¹Research Group Microbial Immunology, Leibniz Institute for Natural Product Research and Infection Biology - Hans Knoell Institute, Beutenbergstraße 11a, Jena, Germany. ²Department of Bioinformatics, Biocenter, Am Hubland, University of Würzburg, Würzburg, Germany. ³The Lundquist Institute for Biomedical Innovation at Harbor UCLA Medical Center, David Geffen School of Medicine at UCLA, Los Angeles, CA, USA. ⁴Institute for Hygiene and Microbiology, University of Würzburg, Würzburg, Germany. ⁵Present address: Laboratory Dr. Wisplinghoff, Department of Molecular Biology, Horbeller Strasse 18-20, Cologne, Germany. ⁶Present address: Institute of Immunology, Molecular Pathogenesis, Center for Biotechnology and Biomedicine (BBZ), College of Veterinary Medicine, Leipzig University, Deutscher Platz 5, Leipzig, Germany. ✉email: ilse.jacobsen@hki-jena.de

The polymorphic yeast *Candida albicans* colonizes up to 70% of the human population as a commensal on mucosal surfaces^{1,2}. As an opportunistic fungal pathogen, however, *C. albicans* is able to cause superficial as well as life-threatening systemic infections promoted by disturbances in the microbiota and impaired host defenses^{3,4}. Despite antifungal therapy, disseminated candidiasis is associated with high mortality rates of up to 50%^{5,6}.

The reversible transition of spherical budding yeast to pseudo-hyphal or hyphal filaments is promoted *in vivo* by body temperature, serum, physiological pH and elevated CO₂ concentration^{7,8}. Nevertheless, both morphologies are present in tissues during systemic infection⁹. While filaments facilitate tissue invasion, damage and escape from host cells^{10,11}, yeast cells are believed to be important for mucosal colonization, dissemination through the bloodstream, adherence to endothelial cells and biofilm formation¹². Furthermore, yeast and hyphae are recognized differentially by immune cells¹³. Saville et al. dissected the relative contribution of *C. albicans* filamentation to virulence during systemic infection by using a regulable expression system, placing one copy of the negative regulator of filamentation *NRG1* under the control of a tetracycline-regulable promoter¹⁴. Mice challenged intravenously with the tet-*NRG1* strain succumbed to infection when hyphal growth was permitted but survived when fungal cells were enforced to grow in the yeast form. Similarly, other *C. albicans* yeast-locked mutants, such as the *cph1Δ/Δ* *efg1Δ/Δ* double and *hgc1Δ/Δ* mutant have been shown to be avirulent or are strongly attenuated in virulence^{15,16}. On the other hand, mutants locked in the filamentous form like *tup1Δ/Δ* or *nrg1Δ/Δ* are less virulent as well^{17–19}, implying that morphological plasticity is essential for virulence in murine disseminated candidiasis.

One of the factors required for maintenance of hyphal growth, invasion and damage of *C. albicans* is encoded by *EED1* (Epithelial Escape and Dissemination 17²⁰). A homozygous *eed1Δ/Δ* deletion mutant is still able to initiate germ tube formation, but fails to elongate these into hyphae and eventually switches back to yeast cell growth^{7,20,21}. Here we show that the *eed1Δ/Δ* mutant is fully virulent in a murine model of systemic candidiasis and confirmed this finding using a tetracycline-regulable expression system to induce or repress *EED1* in *C. albicans* *in vivo*. Virulence of these filament-deficient mutants is associated with high yeast proliferation rates *in vivo* and enhanced growth *in vitro* on nutrient sources likely encountered in the host, suggesting metabolic adaptation as the underlying mechanism for retained virulence in the absence of filamentation. Analysis of host responses furthermore supports a contribution of altered immunopathology to *C. albicans* virulence in the absence of filamentation.

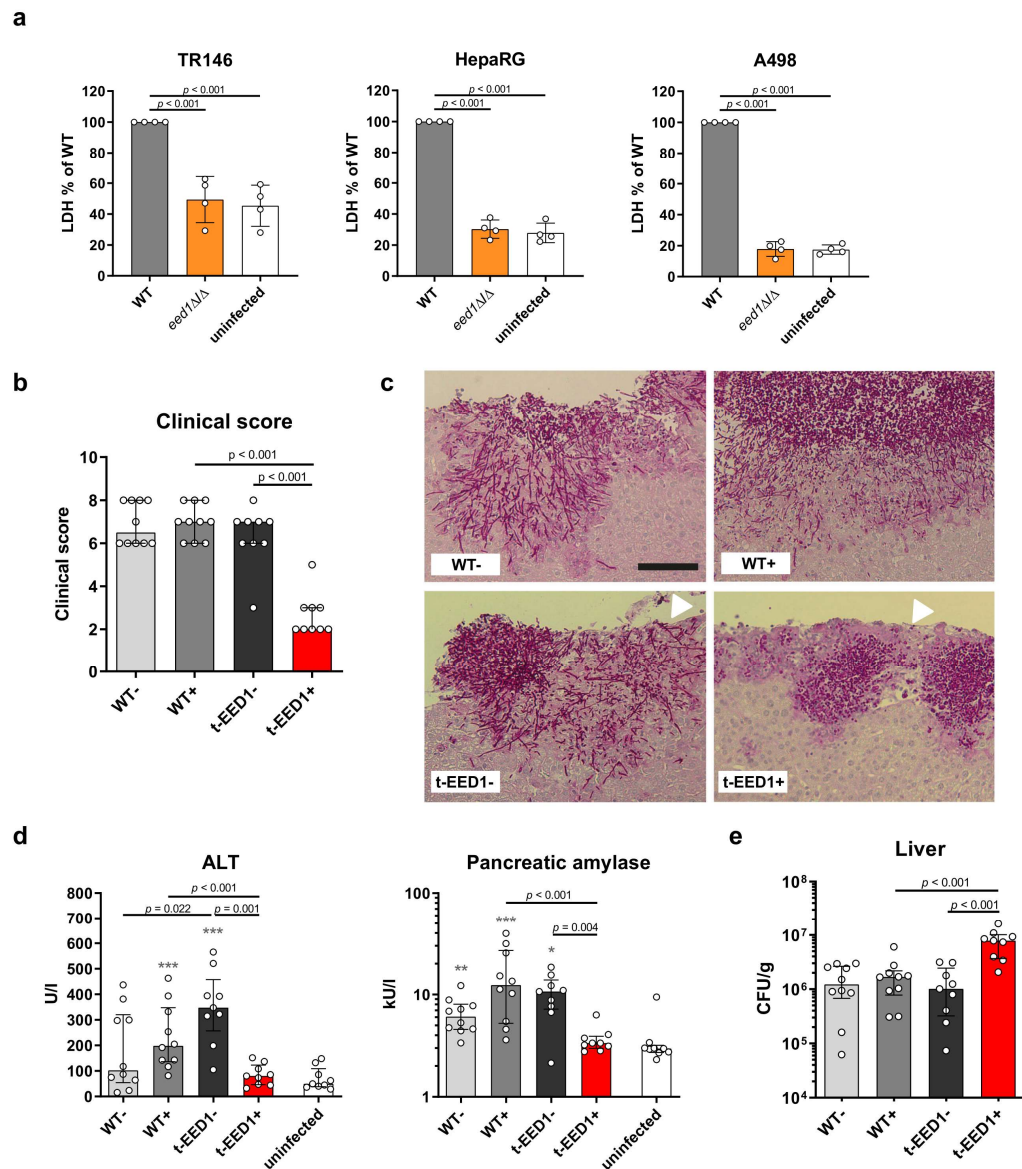
Results

***EED1* is required for virulence in a murine intraperitoneal infection model.** Hypha formation has been shown to be essential for tissue invasion and damage *in vitro* and *in vivo*^{11,14,22}. Consistent with this, the *eed1Δ/Δ* mutant, unable to maintain hyphal growth, was not able to damage renal, hepatic and oral epithelial cells *in vitro* within 24 h of co-incubation (Fig. 1a). To assess the impact of *EED1* for tissue invasion and damage *in vivo*, we employed an intraperitoneal infection model. In this model, *C. albicans* filamentation facilitates invasion from the peritoneal cavity into intraperitoneal organs such as liver, spleen and pancreas²³. In line with the *in vitro* results, deletion of *EED1* led to reduced damage of liver and pancreatic tissue indicated by lower serum levels of tissue-specific enzymes and lower clinical scores compared to mice infected with the wild type strain

(WT; Supplementary Fig. 1). This attenuated virulence phenotype was confirmed using a conditional knock out mutant (t-*EED1*), in which one *EED1* allele was deleted and the other was placed under the control of a tet-OFF promoter¹⁴. In the presence of doxycycline (t-*EED1* +), repressed *EED1* expression leads to yeast cell growth. In absence of doxycycline (t-*EED1* –), the gene is constitutively expressed resulting in increased filamentation on solid media (Supplementary Fig. 2a) and filamentation comparable to the WT in liquid media (Supplementary Fig. 2b). In the presence of doxycycline, mice developed significantly less clinical symptoms after intraperitoneal infection with the t-*EED1*+ yeast compared to the WT and the t-*EED1*– filamentous strain 24 h post infection (p.i.) (Fig. 1b). Histological analysis showed t-*EED1*+ yeast that remained in the upper tissue layers below the liver capsule whereas WT and t-*EED1*– hyphae invaded deeply into liver parenchyma (Fig. 1c). Furthermore, infection with WT and t-*EED1*– induced significantly increased serum levels of alanine aminotransaminase (ALT) and pancreatic amylase indicating liver and pancreatic injury, respectively (Fig. 1d). In contrast, reduced tissue invasion of the t-*EED1*+ yeast resulted in serum enzyme levels of ALT and pancreatic amylase comparable to the uninfected control. Interestingly, a significantly higher fungal burden was recovered from liver tissue of mice infected with either the t-*EED1*+ or *eed1Δ/Δ* mutant compared to the respective WT (Fig. 1e and Supplementary Fig. 1c). Thus, tissue damage and clinical symptoms correlated with the ability to form hyphae in the intraperitoneal infection model, and deletion or repression of *EED1* resulted in attenuation of virulence despite a higher liver fungal burden.

Deletion of *EED1* affects dissemination from the gastrointestinal tract in immunosuppressed mice. It is generally believed that the gastrointestinal tract is the main reservoir for *C. albicans* in humans^{24,25}. In order to disseminate systemically, the fungus needs to translocate across the mucosal barrier^{24,25}. Consistent with the *in vitro* results for renal, hepatic and oral epithelial cells, deletion of *EED1* significantly reduced the ability of *C. albicans* to damage enterocytes under normoxic and hypoxic conditions (Fig. 2a), resulting in maintained barrier function and reduced translocation *in vitro* (Fig. 2b, c). Colonization of the intestinal tract was moderately increased for *eed1Δ/Δ* compared to the WT in antibiotic-treated immunocompetent mice, but not in mice treated with cyclophosphamide (Fig. 2d, e). Dissemination of the *eed1Δ/Δ* mutant to internal organs was, however, only observed upon cyclophosphamide treatment (Fig. 2f), where a significantly higher number of colony forming units (CFU) in kidneys were observed for *eed1Δ/Δ* compared to the WT. Of note, while cyclophosphamide reduces the numbers of immune cells and also impacts the intestinal barrier function^{26,27}, we did not observe any symptoms of disseminated disease in the mice. This suggests that the treatment was not sufficient to induce the level of immunosuppression and/or intestinal damage required for translocation of a sufficiently high number of fungal cells to cause disease²⁷. Nonetheless, these results support the concept that growth in the yeast form is beneficial for intestinal colonization^{28,29} (at least in immunocompetent mice) and dissemination¹², but that filamentation is required for active translocation²².

***EED1* is not essential for virulence in a systemic infection model.** Based on the *in vitro* data and results from the intraperitoneal infection model, we expected the *EED1* mutants also to be attenuated in a murine systemic (intravenous) infection model that mimics catheter-associated disseminated candidiasis in humans. Surprisingly, the *eed1Δ/Δ* mutant showed enhanced



virulence compared to the WT when low infectious doses were used (Fig. 3a) whereas with a high infectious dose mortality was delayed for t-EED1 + yeast (Fig. 3b). Intermediate infectious doses led to virulence and disease progression indistinguishable to the WT when t-EED1 was either forced to grow as yeast or as hyphae (Fig. 3c, Supplementary Fig. 3). Histology confirmed that t-EED1 + grew as yeast in vivo (Fig. 3d). Consistent with previous reports, experiments conducted in parallel with the tet-*NRG1* strain¹⁴ resulted in clinical disease only when filamentation was facilitated by the presence of doxycycline (Supplementary Fig. 4a-c¹⁴). We also noted that mice infected with the WT (THE1-C1p10) reached humane endpoints earlier when receiving

doxycycline; this is likely a consequence of lower water uptake in these groups (see method section for details). Determination of CFU in mice infected with the intermediate dose showed similar initial fungal burden 6 h p.i. in kidney, liver, brain and spleen (Fig. 3e). However, already 24 h p.i. we observed significantly increased (~25-fold higher) fungal burden in the kidneys of mice infected with t-EED1 + yeast compared to the filamentous strains. Likewise, fungal burden increased for tet-*NRG1*- yeast, reaching significantly higher levels 72 h p.i. compared to the WT-, but in comparison to t-EED1 + yeast declined until the end of the experiment (Supplementary Fig. 4d). Furthermore, fungal burden of t-EED1 + yeast in the brain continued to increase until mice

Fig. 1 Hyphal elongation of *C. albicans* is required for tissue damage in vitro and virulence in an intraperitoneal infection model. **a** Damage of oral (TR146), hepatic (HepaRG) and renal (A498) epithelial cells was quantified by measuring the release of lactate dehydrogenase (LDH) into the supernatant after co-incubation for 24 h with WT (SC5314) or *eed1Δ/Δ* mutant. Uninfected cells served as negative control. LDH released by WT was set to 100%. Data are presented as mean ± SD from four biologically independent experiments. Within each experiment, supernatants from three wells infected by the same strain were pooled and LDH was measured. Data was analyzed by two-tailed students t-test. **b–e** t-EED1+ yeasts are attenuated in invasion, damage and virulence potential despite higher organ fungal loads in the intraperitoneal infection model 24 h post infection. Mice were infected intraperitoneally with 1×10^8 cells of WT (THE1-Clp10) or t-EED1 in the presence (+) or absence (–) of doxycycline supplied via the drinking water. Data derived from two independent experiments, WT– and WT+ $n = 10$, t-EED1– and t-EED1+ $n = 9$ animals per group. **b** Repression of *EED1* by doxycycline led to significantly reduced clinical symptoms in mice. The semiquantitative clinical score was determined by assessing fur, coat and posture, behavior and lethargy, fibrin exudation and other symptoms like diarrhea. The score ranges from 0 (no symptoms) to 10 (severe illness). **c** Representative images of periodic acid-Schiff stained histological sections of liver tissue 24 h p.i., fungal cells are stained purple. Arrows point towards the liver surface (capsule, partially destroyed). The scale bar represents 100 μm and applies to all images. **d** Damage of liver and pancreas was quantified by measuring serum levels of alanine aminotransferase (ALT) and pancreatic amylase, respectively. Enzyme levels of uninfected mice ($n = 9$) served as negative control. **e** Fungal burden in the liver. **b, d, e** Median and interquartile range are shown, two-sided Mann-Whitney test. Asterisks above bars represent significant differences compared to the uninfected control * $p \leq 0.05$; ** $p \leq 0.01$; *** $p \leq 0.001$. Source data are provided as a Source Data file.

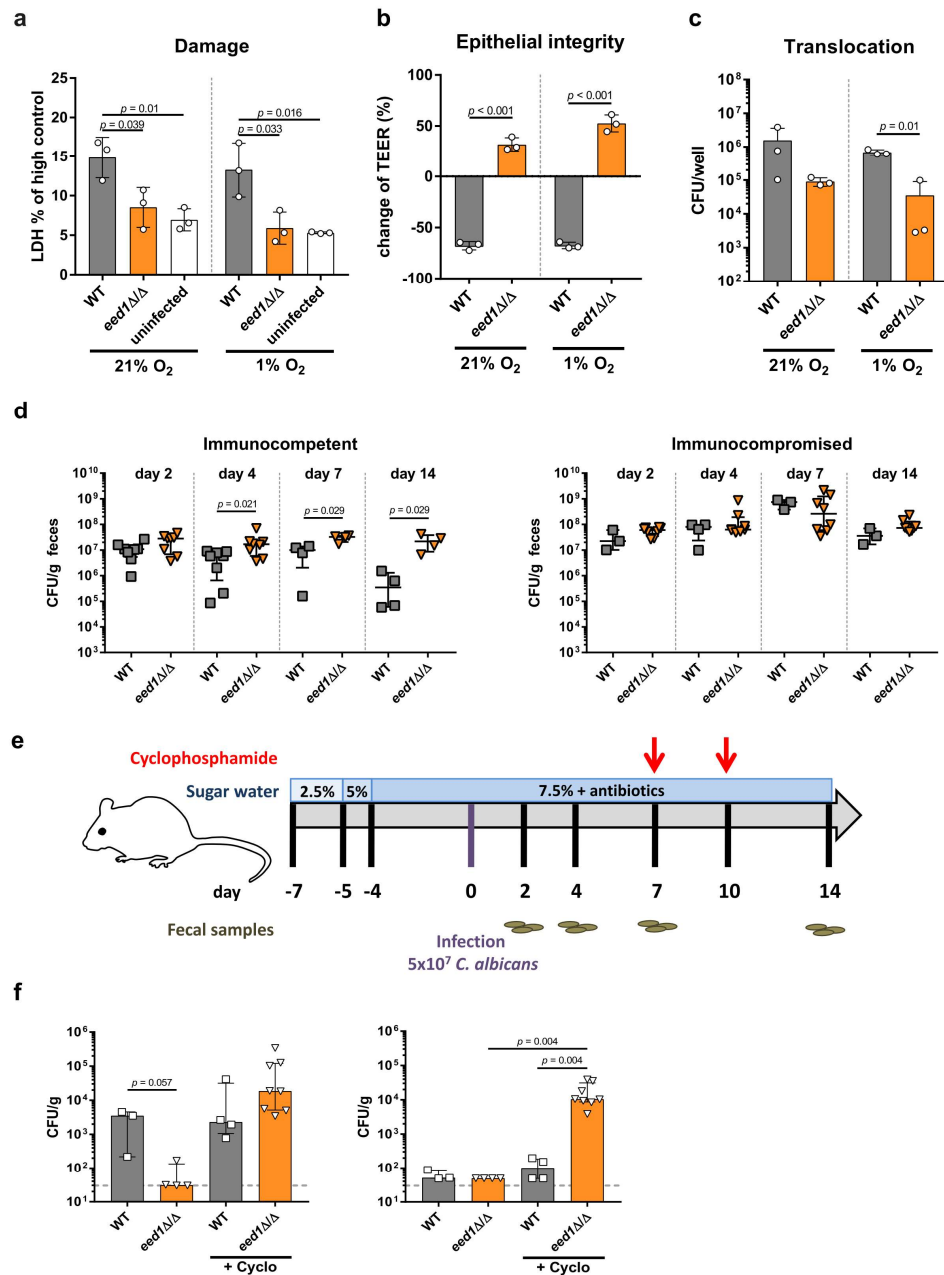
became moribund, whereas after infection with filamentous strains cell numbers peaked 24 h p.i. and were stable or declined thereafter. After an initial decline, the CFU of the t-EED1+ yeast stabilized and increased in liver and spleen while they continuously declined after infection with the WT, t-EED1– or t-*NRG1* yeast or hypha (Fig. 3e; Supplementary Fig. 4d). To test the possibility that differences in fungal load were due to the underestimation of CFU plated from filamentous *C. albicans* strains, we performed quantitative PCR targeting the *C. albicans* 18 S rRNA gene *RDN18* in complex DNA isolated from infected kidney homogenates³⁰. A strong correlation ($R^2 = 0.7076$) between CFU count and DNA content irrespective of the fungal morphology (Supplementary Fig. 5) supports the CFU results.

During hematogenously disseminated candidiasis *EED1* deficiency leads to delayed renal cytokine production but increased immune cell infiltration at later time points. We hypothesized that the increased fungal burden observed for t-EED1+ yeast could be the result of an altered early innate immune response leading to reduced fungal killing. Therefore, we quantified immune cells in the kidney over the course of infection. Leukocytes started to infiltrate kidneys 24 h p.i. and no difference was observed in the overall number or subpopulations of leukocytes 24 and 48 h p.i. between WT+ and t-EED1+ yeast (Supplementary Figs. 6–7). However, morphology-dependent significant differences between WT+ and t-EED1+ were observed 72 h p.i.: Total leukocyte numbers were approximately 2-fold higher in response to t-EED1+ yeast (Fig. 4a), with increased numbers of monocytes (4.5-fold), macrophages (3.2-fold) and DCs and NK cells (2-fold). This coincided with 190-fold higher yeast fungal burden compared to WT+ (Fig. 3e). Interestingly, significantly less leukocytes accumulated in kidneys after infection with the t-EED1– filamentous strain compared to WT– (Supplementary Fig. 8), despite comparable CFU 72 h p.i. (Fig. 3e). While renal cytokine levels induced by the filamentous t-EED1– were comparable to the WT– throughout the course of infection (Supplementary Figs. 9–10), less pro-inflammatory cytokines were induced by t-EED1+ yeast than by WT+ 24 h p.i. (Fig. 4b), despite higher fungal burden of t-EED1+ yeast. In contrast, cytokine levels were comparable 48 h p.i., and a tendency towards increased cytokine release, with significant higher amounts of IL-18, IP-10, RANTES and IFN- γ in response to t-EED1+ yeast, was observed 72 h p.i. (Fig. 4b). In moribund mice no morphology-dependent difference in cytokine levels was observed (Supplementary Fig. 10). To investigate whether the local differences in renal cytokine production were reflected by differences in systemic inflammation, we determined serum levels of the sepsis markers soluble triggering receptor expressed on myeloid cells

(sTREM-1) and neutrophil gelatinase-associated lipocalin (NGAL). NGAL and sTREM-1 levels increased rapidly and throughout the course of infection (Fig. 4c) irrespective of the fungal morphology.

Lower cytokine levels induced by t-EED1+ yeast in the presence of similar leukocyte numbers 24 h p.i. suggested differences in the interaction with leukocytes and/or epithelial cells and their interaction with fungal cells was therefore analyzed in vitro. Murine bone marrow (BM) neutrophils and BM-derived macrophages (BMDMs) were capable of phagocytosing and killing *C. albicans* WT and *eed1Δ/Δ* mutant to the same extent in vitro after 1 h and 2 h, respectively (Fig. 5a, b; Supplementary Fig. 11a). At that time point both strains had formed germ tubes (Supplementary Fig. 11b and Supplementary Fig. 12). After 6 h, the WT maintained filamentation while the *eed1Δ/Δ* mutant had switched back to yeast cell growth (Fig. 5c; Supplementary Fig. 12). Analysis at 6 h showed that a significantly larger proportion of *C. albicans eed1Δ/Δ* was killed by BMDMs compared to the WT. However, we noted that the relative increase in CFU of the *eed1Δ/Δ* mutant from 0 h to 6 h was considerably higher than for the WT both in the presence and absence of macrophages (Fig. 5d). This resulted in significantly higher numbers of *eed1Δ/Δ* than WT cells in the presence of BMDMs. In addition, the *eed1Δ/Δ* mutant showed a reduced capacity to damage BMDMs (Fig. 5e) and to stimulate TNF- α release by BMDMs 24 h p.i. (Fig. 5f). At that time wells that contained the *C. albicans* WT were completely covered by hyphae whereas wells with *eed1Δ/Δ* showed yeasts only and macrophages were visible from time to time (Supplementary Fig. 12). In contrast, activation of murine PMNs determined by the release of IL-10, IL-6 and TNF- α (Supplementary Fig. 11c) and production of reactive oxygen species (ROS; Supplementary Fig. 11d) was comparable between the strains. Infection of renal, hepatic and oral epithelial cells with the *eed1Δ/Δ* mutant induced no increase of pro-inflammatory cytokines compared to uninfected controls (Fig. 5g), likely due to the lack of damage caused by the mutant in this model (Fig. 1a). For oral epithelial cells, no significant increase was observed for the WT either, although a tendency of higher cytokine production was observed. Thus, the initial lower cytokine release in response to t-EED1+ yeast in vivo is likely due to reduced damage of and lower cytokine production by renal and hepatic cells and macrophages, which is balanced by the response of recruited immune cells at later time points.

***eed1Δ/Δ* yeast display enhanced growth on physiologically relevant carbon sources.** *EED1* depleted yeast were able to increase their cell number approximately 100-fold from 6 h to 24 h p.i. in murine kidneys (which equals a generation time of 2.6 h



compared to 7.1 h for the WT). Since we found no evidence for reduced recognition or killing by immune cells, this observation cannot be explained by increased immune evasion resulting in less killing. We thus hypothesized that *EED1*-deficient yeasts are metabolically better adapted to acquire locally available nutrients resulting in increased proliferation. Therefore, we analyzed the growth of *C. albicans* WT and the *eed1Δ/Δ* mutant in the

presence of different fermentable and non-fermentable carbon sources at 37 °C (Fig. 6). Growth of both strains was similar with 2% glucose in complex (YPD) and defined media (SD). However, in the presence of physiological glucose concentrations of 0.1% in SD medium, the mutant reached lower cell densities at stationary phase. In YPD with 0.1% glucose, in contrast, the *eed1Δ/Δ* mutant continued to grow steadily after depletion of glucose

Fig. 2 The *eed1Δ/Δ* mutant shows a reduced translocation capacity in vitro and in a gut dissemination model in immunocompetent but not immunocompromised mice. **a–c** C2BBel cells were infected with *C. albicans* WT (SC5314) or the *eed1Δ/Δ* mutant and incubated under normoxic (21% O₂) or hypoxic (1% O₂) conditions for 24 h. **a** Damage of C2BBel cells was quantified by measurement of LDH and is shown in % of high control (cells lysed with Triton X-100). Uninfected cells served as negative control. **b** Integrity of epithelial barrier was quantified by TEER measurement. Data are expressed as change of TEER 24 h post infection compared to TEER values prior to infection in percent. **c** Translocation across the epithelial barrier was assessed by CFU plating. **a–c** Graphs show the mean ± SD of three independent biological replicates, two-tailed students *t*-test. *p*-values are shown in the graph. **d** Fungal burden in feces of antibiotic-treated immunocompetent and mice rendered immunocompromised by cyclophosphamide treatment. Immunocompetent, day 2 and 4 *n* = 8; day 7 and 14 *n* = 4 mice per group, one experiment. Immunocompromised WT infected *n* = 3; *eed1Δ/Δ* *n* = 8, one experiment. **e** Schematic overview of the timeline for the gastrointestinal dissemination model. **f** Fungal burden in liver (left) and kidneys (right) of immunocompetent or cyclophosphamide-treated immunosuppressed (+Cyclo) mice colonized with either *C. albicans* WT or *eed1Δ/Δ* mutant 14 d post infection. WT *n* = 3, one experiment; WT + Cyclo and *eed1Δ/Δ* *n* = 4, one experiment; *eed1Δ/Δ* + Cyclo *n* = 8 mice, data from two independent experiments. Dashed lines indicate limit of detection. **d, f** Shown is the median with interquartile range, two-sided Mann-Whitney test, *p*-values are shown in the graph. Source data are provided as a Source Data file.

reaching higher ODs than the WT. Importantly, the *eed1Δ/Δ* mutant showed enhanced growth in the presence of the physiological relevant alternative carbon sources lactate, acetate, citrate, amino acids and the amino sugar N-acetyl-glucosamine (GlcNAc). Additionally, the *eed1Δ/Δ* mutant showed faster onset of growth in YCB-BSA compared to the WT indicating that this strain is highly proteolytically active. Furthermore, *eed1Δ/Δ* showed better growth than the WT in murine kidney homogenates. Taken together, these data suggest that the absence of *EED1* results in better metabolic adaptation in vivo, facilitating faster proliferation resulting in increased fungal burden.

To gain information on possible mechanisms mediating the enhanced proliferation of the *eed1Δ/Δ* mutant on alternative carbon sources, we performed RNAseq analysis of cells grown in SD with glucose at 30 °C for 10 h (designated as 0 h time point), followed by a shift to citrate or casamino acids as sole carbon source at 37 °C (2 h, 6 h, and 12 h; Supplementary Fig. 13a). Growth in SD with glucose resulted in yeast morphology for both strains (Supplementary Fig. 13b); on casamino acids, both strains formed germ tubes within 2 h, but only the WT formed hyphae at later time points (Supplementary Fig. 13b). With citrate as sole carbon source, filamentation was observed only for the WT (Supplementary Fig. 13b). In both, citrate and amino acid media, the *eed1Δ/Δ* mutant showed enhanced growth as observed by optical density as well as by determination of dry weight (Supplementary Fig. 14a). Principal component analysis (PCA) of the RNAseq data showed that biological replicates clustered together and that the transcriptome of both strains varied over time (Supplementary Fig. 14b). Comparison of *eed1Δ/Δ* mutant and WT for each condition and time point (with a log₂ fold change of 2.0 as cut off) revealed that only one yet uncharacterized gene (orf19.2962) was differentially expressed during yeast growth at the 0 h time point (2.1-fold down-regulated). After the shift to media containing either citrate or casamino acids as sole carbon sources, relatively few genes (<320) were differentially expressed in the mutant compared to the WT at any given time point, and the majority of differentially expressed genes (DEGs) were down-regulated in *eed1Δ/Δ* compared to the WT (Supplementary Fig. 15). Consistent with differences in morphology, down-regulated genes in both conditions included genes associated with filamentous growth, biofilm formation, and adhesion (e.g. *ECE1*, *HGCI*, *BRG1*, *UME6*, *HYR1*, *SAP5*, *HWPI* and *ALSI*; Supplementary Fig. 16a). The expression of secreted aspartyl proteinases likewise coincided with morphology, with the hypha-associated genes *SAP4-6*³¹ showing reduced transcription while transcription of the yeast-associated genes *SAP1* and *SAP3*³¹ was enhanced in the *eed1Δ/Δ* mutant during growth on casamino acids (Supplementary Fig. 16b). The highest number of DEGs was observed at the 12 h time point (Fig. 7a), when the *eed1Δ/Δ* mutant grew as yeast but also the filamentous WT

switched back to yeast cell growth to some extent (Fig. 7b). Genes that were up-regulated in *eed1Δ/Δ* mutant compared to WT in both media included the ammonium permease *MEP1*, the putative 2-isopropylmalate synthase *LEU4*, the secreted yeast wall protein *YWPI*, the transcription factor *MSS11*, and 5 yet uncharacterized open reading frames. Most of the DEGs showed a medium-specific regulation. After 12 h of growth with citrate as sole carbon source Gene Ontology (GO) term analysis identified enrichment of genes associated with organic acid, (long-chain) fatty acid and small molecule biosynthetic and metabolic processes within the up-regulated DEGs in the *eed1Δ/Δ* mutant (Fig. 7c), which might explain the better growth of the mutant on citrate. Genes that were up-regulated exclusively in citrate included e.g., the dicarboxylic acid transporter *JEN2* and a key enzyme of gluconeogenesis, *PCK1*. Of note, the only significantly enriched GO term after 12 h of growth on casamino acids in the genes up-regulated in *eed1Δ/Δ* was found to be carbohydrate transport. However, individual genes that were significantly up-regulated included the broad specificity amino acid permease *GAP2*, the predicted amino acid transmembrane transporter *UGA5*, the GATA-type transcription factor *GAT1* that regulates nitrogen utilization, and the glyoxylate cycle enzyme isocitrate lyase *ICL1* (Supplementary Data 1), which might contribute to enhanced growth. In addition to *GAT1*, three other transcription factors (TFs) were up-regulated and 13 down-regulated in the *eed1Δ/Δ* mutant 12 h after shift to either citrate or casamino acids (Supplementary Fig. 16c). Several down-regulated TFs were associated with filamentous growth and thus, differential expression likely reflects differences in morphology (e.g., *UME6*, *SFL2*, *BRG1*, *TEC1*, *OFI1*³², *ACE2*³³). Counterintuitively, though, transcription of *MSS11*, encoding a factor interacting with Flo8 to activate transcription of hypha-specific genes³⁴, was higher in the mutant in both citrate and amino acid media. Similarly, expression of *RFX2* was reduced in the *eed1Δ/Δ* mutant – deletion of this gene, however, results in hyper-filamentation and increased expression of hypha-associated genes³⁵. Interestingly, both *WOR1* and *WOR3* were significantly down-regulated after prolonged growth in both media, possibly indicating increased commitment of the *eed1Δ/Δ* mutant to grow as white cells. White cells have been shown to have a metabolic advantage over opaque cells with various nutrients at 37 °C³⁶, lead to higher renal fungal burden, and are more virulent in systemic infection models^{37,38}.

High numbers of yeast cells result in renal damage in vivo. To determine if immune cell recruitment together with high fungal burden during t-EED1 + infection was sufficient to cause renal damage in the absence of invading hyphae, we measured KIM-1, a biomarker for renal proximal tubule injury in the urine of infected mice^{39,40}. KIM-1 levels increased after infection with all strains without significant differences (Fig. 8a). Additionally, we

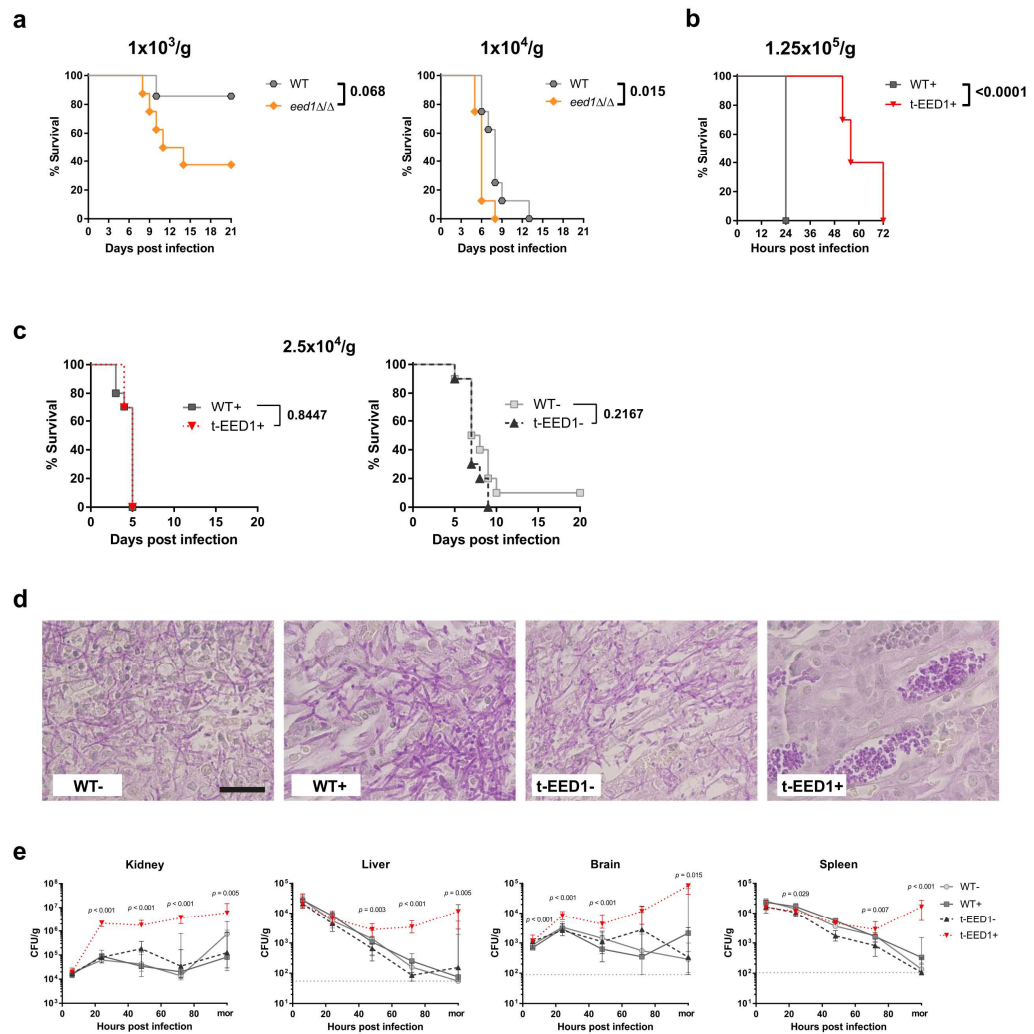
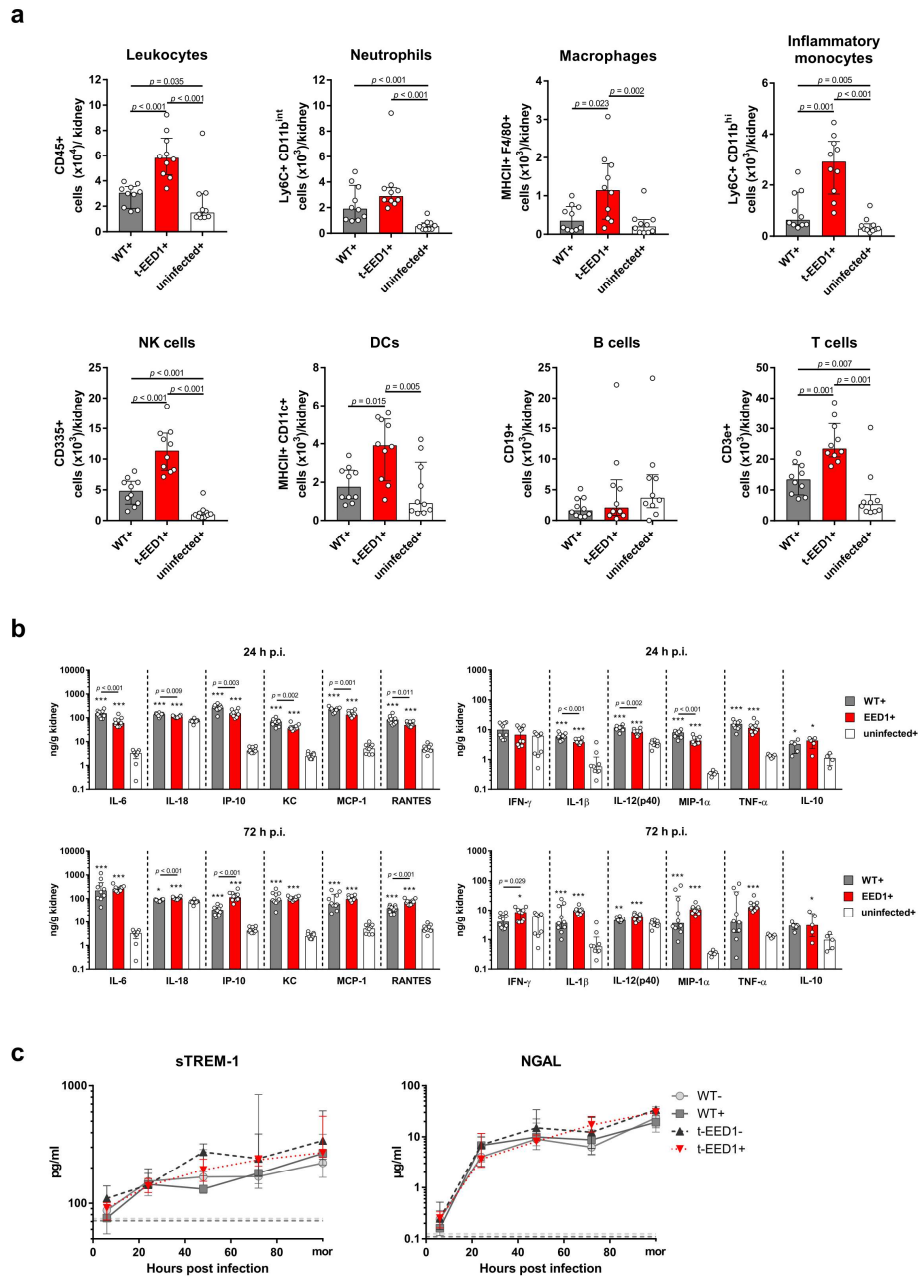


Fig. 3 C. albicans retains its virulence potential in a mouse model of systemic candidiasis even in the absence of hyphal elongation due to repression or deletion of *EED1* accompanied by higher organ fungal loads. Mice were intravenously infected with the following doses: **a** Low doses of 1×10^3 or 1×10^4 CFU/g body weight of WT (SC5314) or *eed1* Δ/Δ mutant. One experiment, $n = 8$ mice per group (except for WT 1×10^3 , $n = 7$). **b** A high dose of 1.25×10^5 CFU/g body weight of WT (THE1-Clp10) or t-EED1 in the presence (+) or absence (-) of doxycycline. One experiment, $n = 10$ mice per group. **a-c** Survival was monitored over a course of 20 or 21 days and is shown as Kaplan-Meier curve. Survival curves were compared using the two-sided Log-rank (Mantel-Cox) test, p -values are shown in the graph. **d** Representative images of PAS stained histological cross sections of kidneys from moribund mice infected with 2.5×10^4 CFU/g body weight with WT (THE1-Clp10) or t-EED1 in the presence (+) or absence (-) of doxycycline. Fungal cells are stained purple. Scale bar represents 20 μ m and applies to all images. **e** Organ fungal loads of mice infected with 2.5×10^4 CFU/g body weight with WT (THE1-Clp10) or t-EED1 in the presence (+) or absence (-) of doxycycline. Shown is the number of CFU per gram organ from mice sacrificed 6, 24, 48 and 72 h post infection and from moribund mice (mor). Data are shown as median with interquartile range. Dashed gray lines indicate limit of detection. Moribund: one experiment, $n = 10$; Kidney: two independent experiments $n = 10$. Liver, spleen, brain: three independent experiments, $n = 15$. Two-sided Mann-Whitney test, asterisks indicate significant changes of t-EED1+ compared to WT+ groups at the indicated time points. * $p \leq 0.05$; ** $p \leq 0.01$; *** $p \leq 0.001$.



evaluated kidney function by measuring serum creatinine and blood urea nitrogen (BUN) levels. Both increased at comparable rates, reaching highly elevated levels indicating severe renal dysfunction^{41,42} in moribund mice only (Fig. 8b, c). Finally, the same extent of apoptosis was observed in the kidneys of moribund mice infected with either WT or t-EED1 (Fig. 8d, c). Therefore, enhanced fungal proliferation can compensate for the

reduced capacity of hypha-mediated damage in *C. albicans* lacking expression of *EED1*.

Rapid yeast proliferation in combination with immunopathology contributes to mortality. To investigate whether mortality caused by the yeast form is the result of high organ fungal loads interfering with organ function or whether

Fig. 4 Increased immune cell infiltration in kidneys of mice 72 h after systemic infection with t-EED1+ yeast coincides with increased local cytokine production while systemic inflammation is not affected. Mice were systemically infected with an intermediate dose of 2.5×10^4 CFU/g body weight of WT (THE1-Clp10), t-EED1 or remained uninfected in the presence (+) of doxycycline. **a** Immune cells infiltrating the kidney 72 h post infection. Shown are absolute numbers of living immune cells per kidney. Two independent experiments, $n = 10$. **b** Cytokine levels were measured in kidney homogenates 24 h and 72 h post infection. Asterisks above bars represent significant differences compared to the uninfected control. Two independent experiments, $n = 10$, except for uninfected+, $n = 9$. MIP-1 α , TNF- α for uninfected+, $n = 5$. IL-10 data derived from one experiment, $n = 5$. **c** Markers for systemic inflammation sTREM-1 and NGAL were quantified by ELISA in serum of mice after 6, 24, 48, 72 h and when mice become moribund (mor). Dashed lines indicate median serum protein levels of uninfected controls in the presence (dark gray) or absence of doxycycline (light gray). Two independent experiments. sTREM-1 $n = 10$, except for 6 h $n = 6$ and mor $n = 5$; for WT- 24 h $n = 8$ and 48 h $n = 9$. NGAL $n = 10$, except for WT- 24 h $n = 9$, t-EED1- 24 h $n = 8$ and 72 h $n = 9$. **a-c** Shown is the median and interquartile range, two-sided Mann-Whitney test. **a, b** p -values are shown in the graph and **b** asterisks indicate significant differences in comparison to the uninfected control (* $p \leq 0.05$; ** $p \leq 0.01$; *** $p \leq 0.001$). Source data are provided as a Source Data file.

immunopathology is the driving force in the pathogenic process, mice successfully depleted of peripheral neutrophils and monocytes (Supplementary Fig. 17) were intravenously infected with low infectious doses (1×10^2 and 1×10^3 CFU/g body weight). Although the *eed1* Δ/Δ mutant led to 100% mortality in immunosuppressed mice, this was significantly delayed in comparison to WT strain infections (Fig. 9a). However, in immunocompetent mice challenged with 1×10^3 CFU/g body weight, the opposite effect was observed: while 6/7 mice survived in the WT, only 3/8 mice survived in the *eed1* Δ/Δ group until the end of the experiment (Fig. 3a). In addition, histological analysis of renal tissue showed more pronounced immune cell infiltrations in response to *eed1* Δ/Δ yeast in immunocompetent mice (Fig. 9b), suggesting some contribution of immunopathology to yeast driven mortality. In the absence of neutrophils and monocytes, fungal burden of WT and *eed1* Δ/Δ mutant progressively increased during the course of infection. However, organ fungal load of the *eed1* Δ/Δ mutant exceeded that of the WT in all organs tested, with significant differences detectable as early as 12 h post infections in liver and kidneys (Fig. 9c). At the humane endpoint, the fungal burden of the *eed1* Δ/Δ mutant exceeded those of the WT in all organs tested (Fig. 9c and Supplementary Fig. 18a) with a 150-fold and 280-fold increase in kidney and spleen fungal burden, respectively. Furthermore, the urinary KIM-1 to creatinine ratio steadily increased after infection with *C. albicans eed1* Δ/Δ , indicating that filaments are not essential for induction of renal injury (Fig. 9d). However, kidney function as determined by measurement of BUN in serum of immunosuppressed mice was not affected at any time after infection with WT or *eed1* Δ/Δ mutant (Supplementary Fig. 18b), possibly because the time to the humane endpoint was too short to allow accumulation of waste products by impaired renal clearance.

Discussion

C. albicans hypha formation has been linked to invasion and damage, and *C. albicans* strains locked in either the yeast or hyphal morphology were repeatedly found to be less virulent in systemic infection models^{15–18}. Consequently, morphological plasticity is considered as an important virulence trait of *C. albicans*^{43,44}. Consistent with the role of filamentation for invasion and damage, repression or absence of *EED1* in *C. albicans*, interfering with hyphal elongation and leading to yeast growth, resulted in significantly reduced capacity to damage epithelial cells in vitro, and reduced virulence in a murine intraperitoneal infection model in vivo although the mutant was present in higher numbers than the WT in the liver. The observation that following intraperitoneal injection *EED1*-deficient cells superficially invaded the liver parenchyma but remained below the liver capsule, without causing detectable damage, resembles the described behavior of the *eed1* Δ/Δ mutant in a reconstituted human epithelium model²⁰. Thus, our results support previous research demonstrating that hyphae are important for tissue

infiltration. In the gut, however, *C. albicans* can be found in both yeast and hyphal form^{28,45,46}. Some studies found higher colonization rates for strains locked in the yeast morphology (e.g., the *cph1* Δ/Δ *efg1* Δ/Δ double mutant and the *hgc1* Δ/Δ mutant²⁸), whereas enforced filamentous growth resulted in lower intestinal colonization (e.g. *C. albicans nrg1* Δ/Δ and *tup1* Δ/Δ mutants^{27,28}, repression of *TUP1*²⁹, and constitutive expression of *UME6*^{28,45}). We likewise observed higher colonization rates for the *eed1* Δ/Δ mutant in immunocompetent mice, supporting the concept that yeast growth favors intestinal colonization. How *C. albicans* is translocating across the intestinal barrier remains unknown. In vitro, translocation requires filamentation²², but low level translocation has been observed in immunocompetent mice independent of fungal morphology²⁸. This has been suggested to be mediated by transport via host cells that sample the intestinal content²⁸. We observed reduced basal dissemination of the *eed1* Δ/Δ mutant to the liver, which might be a consequence of altered interaction of the mutant with dendritic cells or M cells mediating entry into the bloodstream by lumen sampling or transcytosis^{28,47} in the absence of hyphal formation, but this aspect was not investigated further in this study. In contrast, increased fungal burden in liver and kidney was observed in *C. albicans eed1* Δ/Δ colonized mice treated with cyclophosphamide, and in these mice kidney CFU were significantly higher for the *eed1* Δ/Δ compared to the WT. However, this data does not allow any conclusion on the translocation process, as the higher fungal load could also be a consequence of increased proliferation of the mutant within this organ. It should furthermore be noted that the fungal burden in kidneys following translocation from the gut was substantially lower than that observed after intravenous infection, which explains why colonized mice did not develop signs of systemic candidiasis upon cyclophosphamide treatment.

Surprisingly, the filamentation defect caused by *EED1* deficiency did not impair virulence in a systemic infection model when intermediate infectious doses were injected directly into the bloodstream. Remarkably, infectious doses lower than 10^4 cells per gram body weight resulted in increased virulence of the *eed1* Δ/Δ mutant compared to the WT, whereas with high infectious doses or in absence of neutrophils and monocytes mortality was delayed but still reached 100%. In the murine model of hematogenously disseminated candidiasis, infection is established via the lateral tail vein mimicking disseminated *C. albicans* infections in humans⁴⁸. While virtually all organs can get affected during infection the kidney is not able to control fungal growth⁴⁹. The fungus reaches the kidneys via the renal artery and the afferent arterioles. In order to invade into tubules and the renal parenchyma, the fungus needs to adhere to endothelial cells and pass through into the renal cortex. This step probably does not require fungal invasion by hypha formation, as tet-*NRG1*- yeast and a *hgc1* Δ/Δ mutant defective in hyphal formation were shown to traverse from the bloodstream to the renal endothelium^{14,16}. Although attenuated in its damage capacity, the *eed1* Δ/Δ mutant

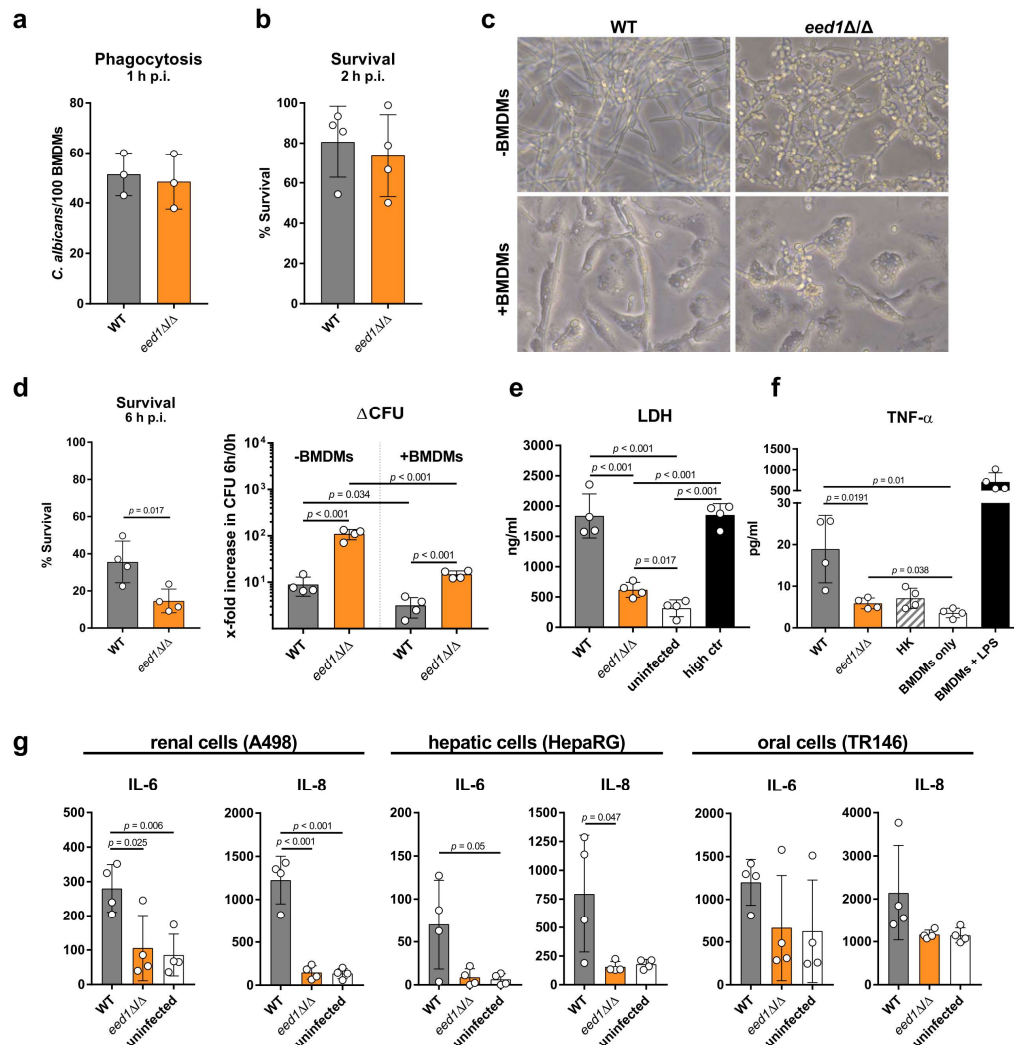


Fig. 5 *eed1Δ/Δ* yeast are less efficient in damaging and inducing cytokine responses of bone marrow-derived macrophages (BMDMs) and epithelial cells. Murine bone marrow-derived macrophages (BMDMs) were infected at an MOI of 1 with *C. albicans* WT (SC5314) or *eed1Δ/Δ* mutant and incubated at 37 °C and 5% CO₂. **a** Phagocytosis calculated as phagocytic index (the number of *C. albicans* cells phagocytosed by 100 BMDMs within 1 h of incubation). Mean \pm SD from three biologically independent experiments. **b** Fungal survival was analyzed after co-incubation with BMDMs for 2 h by CFU plating. Survival was normalized to *C. albicans* controls incubated in the absence of immune cells. **c** Fungal morphology of WT and *eed1Δ/Δ* mutant in the absence (–) or presence (+) of BMDMs after 6 h of incubation. Scale bar represents 20 μm and applies to all images. **d** Fungal survival was analyzed after co-incubation with BMDMs for 6 h by CFU plating. Left: Survival was normalized to *C. albicans* controls incubated in the absence of immune cells. Right: To account for the observation that the mutant replicates faster than the WT in the absence of macrophages, data is shown as fold increase in CFU from 0 h to 6 h with and without BMDMs. **e** Damage of BMDMs was quantified by measuring lactate dehydrogenase (LDH) release into the supernatant after 24 h of co-incubation with *C. albicans* WT or *eed1Δ/Δ* mutant. Uninfected cells served as negative control and Triton X-100 lysed cells served as high control. **f** TNF- α release of BMDMs 24 h after co-incubation with *C. albicans* WT (SC5314), *eed1Δ/Δ* mutant or heat-killed (HK) WT cells. BMDMs were left untreated (BMDM only) or stimulated with 100 ng/ml LPS as positive control. **g** Release of IL-6 and IL-8 by renal (A498), hepatic (HepaRG) and oral (TR146) epithelial cells 24 h after infection with *C. albicans*. Uninfected cells served as negative control. **b, d, e, f, g** Mean \pm SD of four biologically independent experiments are shown. **b, d** In each experiment, three wells were infected with each strain and fungal survival was quantified per well. The mean of these three samples is shown as single point for the individual experiment. Data were analyzed by two-tailed student's *t*-test. *p*-values are shown in the graph. Source data are provided as a Source Data file.

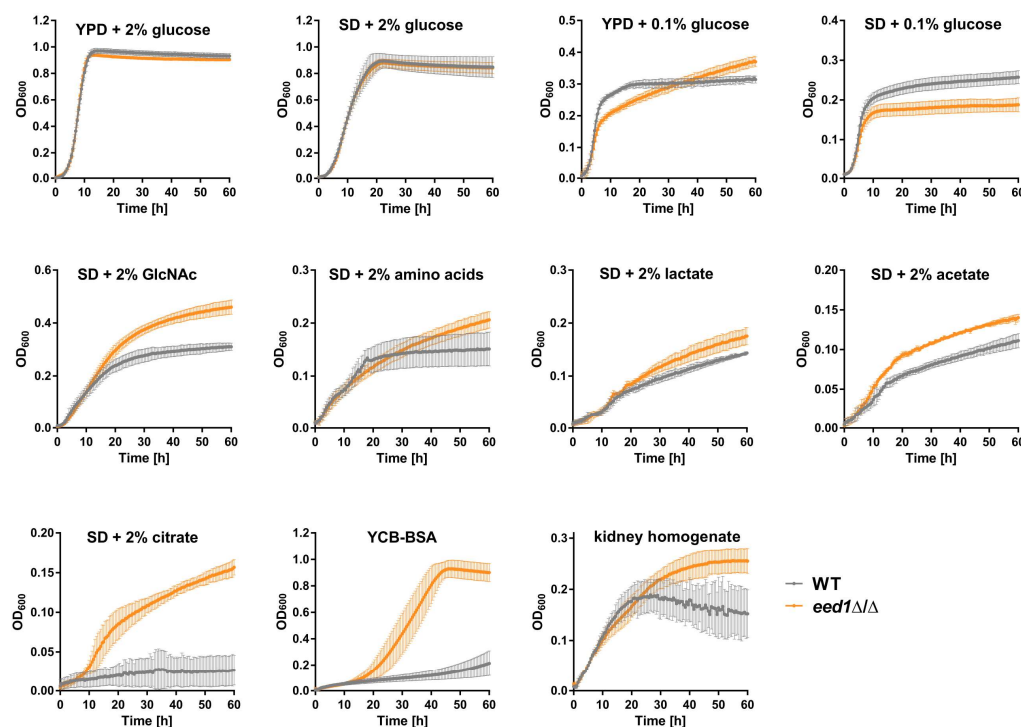


Fig. 6 *eed1Δ/Δ* yeast have a growth advantage on physiologically relevant carbon sources and kidney homogenates and furthermore show enhanced proteolytic activity. Growth curves of *C. albicans* in YPD with 2 or 0.1% glucose or SD medium with different concentrations of sugars or alternative carbon sources as indicated in the graphs. YCB-BSA contained 0.5% of BSA as sole nitrogen source, pH was adjusted to 4.0. For kidney homogenates, kidneys of uninfected mice were removed aseptically, homogenized and diluted to 25 mg/ml in DPBS. Growth was recorded by measuring the optical density at 600 nm in a microplate reader at 37 °C. Measurements were performed in 30 min intervals over a course of 60 h. Graphs show the mean \pm SD of three to five independent biological replicates. Source data are provided as a Source Data file.

is able to adhere and invade into epithelial cells *in vitro*^{20,50}, which might be sufficient to mediate entry into renal tissue *in vivo*. Thus, while filamentation is required for active tissue penetration in the intraperitoneal infection model, it might be dispensable if defensive barriers are breached by direct injection into the blood stream.

Following establishment of the fungus in the kidney in immunocompetent mice, pathogenesis is thought to be driven by both direct fungus-mediated damage and immunopathology. Enhanced immunopathology could compensate for the lack of hypha-mediated fungal damage during pathogenesis; however, in the early time points following infection with an intermediate infectious dose of t-*EED1*+ yeast we rather observed a reduced induction of pro-inflammatory cytokines, likely as a result of the reduced capacity of the yeast to directly damage epithelial cells and macrophages and stimulate cytokine release. Macrophages have been shown to be less prone to killing by hypha-deficient strains⁵¹ and to release less TNF- α after stimulation with *C. albicans* strains unable to germinate;⁵² likewise, murine macrophages produced less TNF- α in response to the *eed1Δ/Δ* mutant. However, the amount of TNF- α in infected kidneys was not affected by absence of *EED1*-driven filamentation and the interaction with murine neutrophils *in vitro* was comparable for WT and *eed1Δ/Δ* mutant. Interestingly, while killing of the mutant by BMDMs was increased after 6 h of co-incubation, the relative

increase in CFU was higher for the *eed1Δ/Δ* mutant than for the WT, suggesting that the increased proliferation is sufficient to compensate for the higher killing rate mediating survival and allowing for continuous organ colonization. It thus appears unlikely that the higher renal fungal burden of the yeast is solely due to reduced fungal clearance as a result of impaired recognition by and/or activation of immune cells.

We hypothesized that increased fitness mediated by better metabolic adaptation to the locally available nutrients facilitated rapid proliferation of *EED1* deficient yeast *in vivo* in the systemic infection model, and that the higher fungal burden in the liver after intraperitoneal infection might likewise reflect increased growth of the mutant. Upon infection *C. albicans* faces a hostile environment with varying nutritional compositions. Preferred carbon sources such as glucose are present only in low concentrations in the bloodstream (0.06–0.1%⁵³), and can become scarce in microenvironments or deprived by phagocytes upon ingestion¹⁰. Consequently, *C. albicans* relies on the assimilation of alternative carbon sources in order to survive and proliferate within the host⁵⁴. As Crabtree-negative yeast, *C. albicans* is able to assimilate glucose and alternative carbon sources such as amino acids, fatty acids, and carboxylic acids, at the same time⁵⁵. This metabolic flexibility is known to increase colonization, resistance to phagocytic recognition⁵⁶ and killing, and enhances pathogenicity^{57,58}. The *eed1Δ/Δ* mutant indeed showed enhanced

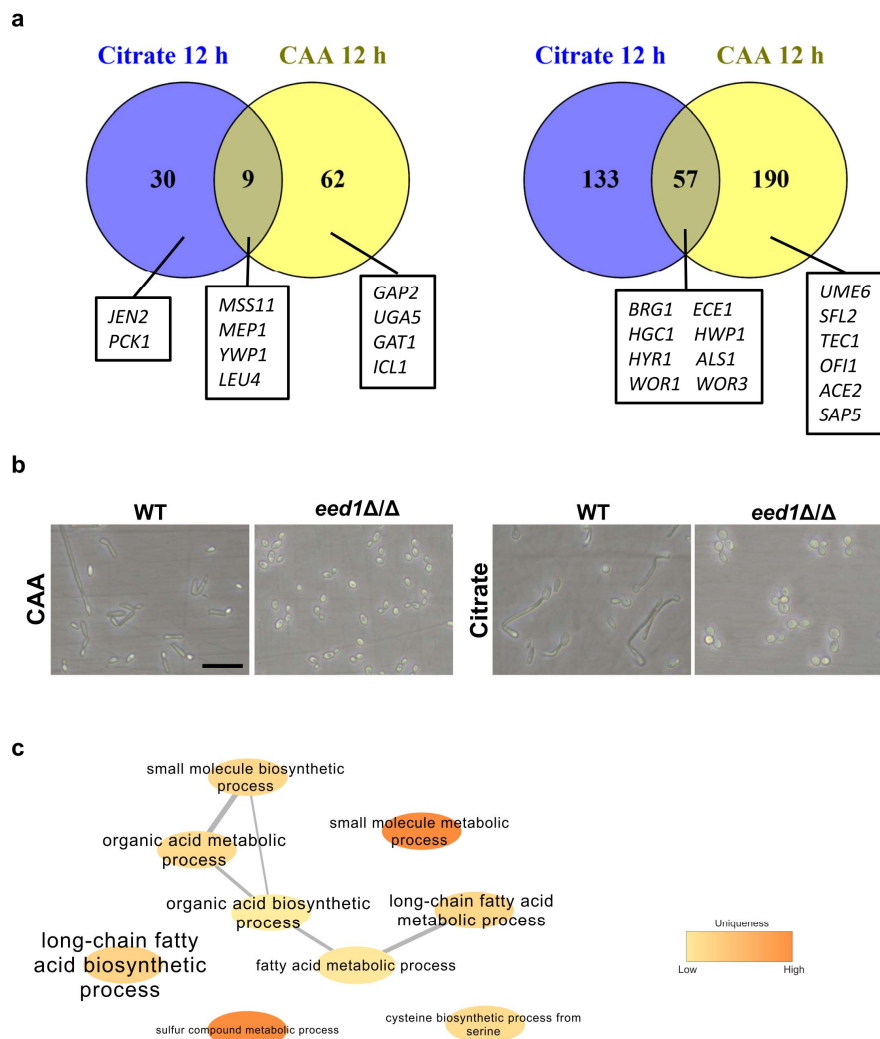


Fig. 7 Transcriptional analysis of the *eed1Δ/Δ* mutant during growth on citrate or casamino acids (CAA) after 12 h at 37 °C. **a Venn diagrams showing the numbers of genes significantly up- or down-regulated ($\pm \log_2 2$ and adjusted p -value < 0.05) in the *eed1Δ/Δ* mutant compared to WT (SC5314) with citrate or CAA as sole carbon source. Genes referred to in the text are highlighted. **b** Morphology of *C. albicans* WT and *eed1Δ/Δ* mutant after 12 h of growth on citrate or CAA. Representative pictures from three biologically independent experiments are shown. Scale bar represents 20 μm and applies to all images. **c** Network analysis of Gene Ontology (GO) term enrichments of significantly up-regulated genes ($+ \log_2 2$ and adjusted p -value < 0.05) in *eed1Δ/Δ* mutant compared to WT after 12 h of growth on citrate. Font size represents the p -value ($p < 0.1$) of the GO term: big letters - small p value, ranging from $p < 2.3 \times 10^{-5}$ to low p -value $p < 0.09$ indicated by small letters. Color is representing the uniqueness, indicating how particular each term is with respect to the set of terms being evaluated (original data analyzed are available in Supplementary Data 1).**

growth in kidney homogenates and in the presence of alternative carbon sources that are available *in vivo*, such as acetate, lactate, amino acids, citrate, and the amino sugar N-acetyl-glucosamine. Additionally, the *eed1Δ/Δ* mutant displayed an enhanced proteolytic activity, possibly supporting utilization of host proteins and immune evasion by degradation of complement proteins and antimicrobial peptides *in vivo*^{59–61}. Whereas hypha-associated SAPs appeared to be down-regulated during growth on casamino acids, enhanced expression of *SAP1*, *SAP3*, *SAP7*, *SAP9* and

SAP10 was observed. Since *Sap1–3*, *Sap4–6* and *Sap9–10* have different pH optima for activity, pH 3–5, pH 5–7 and pH 5–8, respectively, and in addition Saps differ in their substrate specificity^{31,62}, this compensatory gene expression might lead to the earlier onset of BSA utilization observed for the *eed1Δ/Δ* mutant. The increased growth on citrate is especially interesting as citrate is present in blood in a range of 0.05 to 0.3 mM, freely filtered in the glomerulus, and extensively reabsorbed in the nephrons of the kidney⁶³. Therefore, citrate levels are

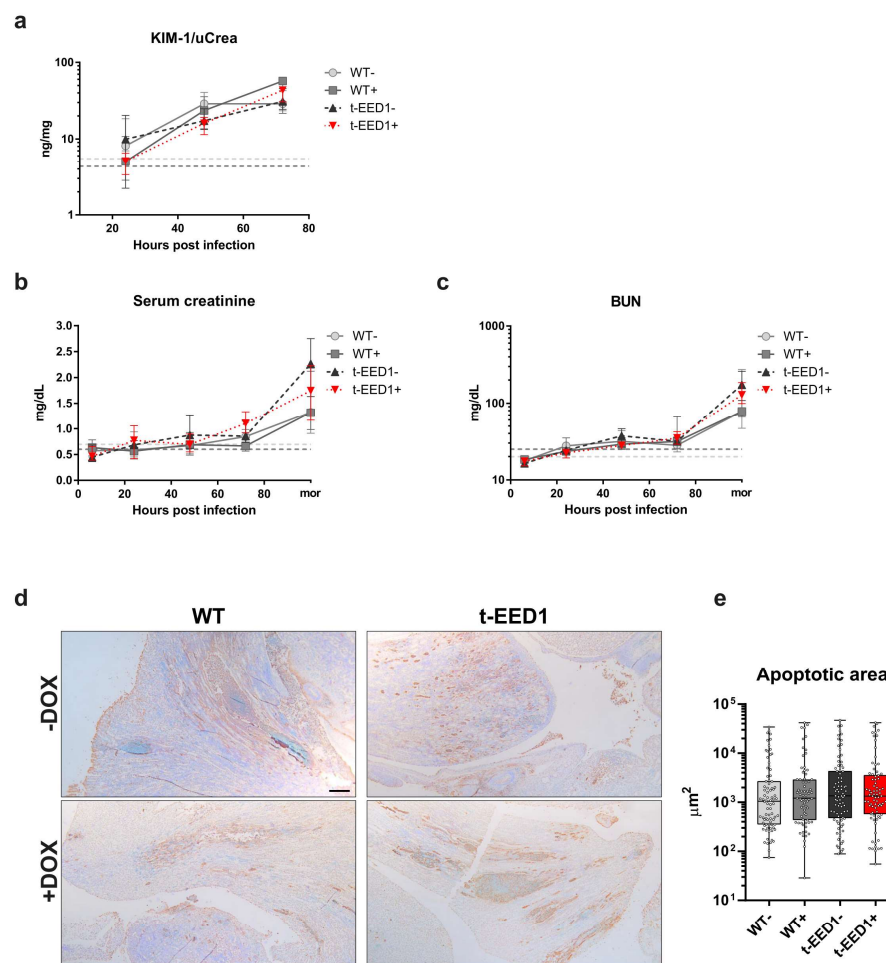
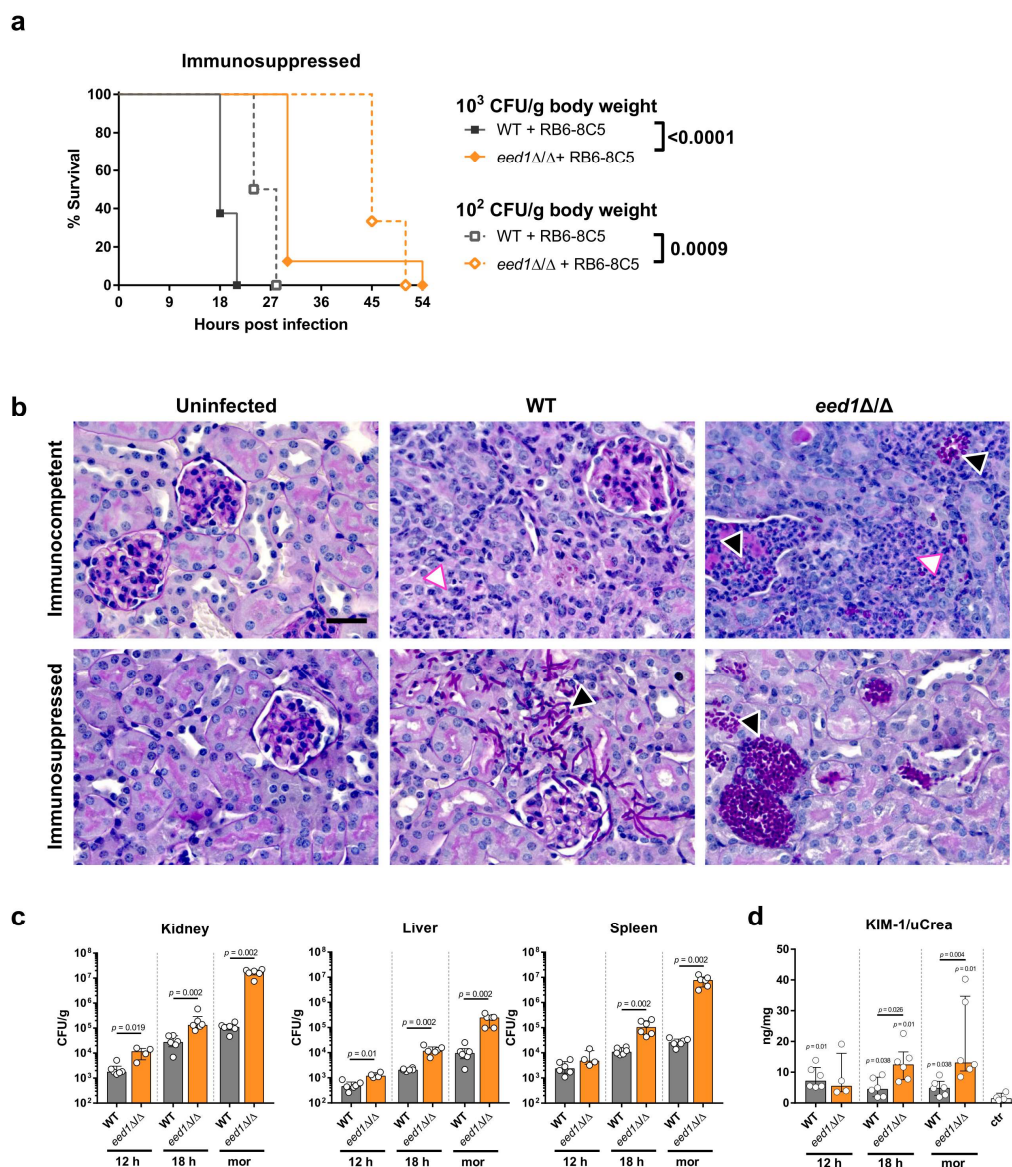


Fig. 8 Kidneys are injured early after intravenous challenge with *C. albicans* by yeast and hyphal forms, while kidney function is not impaired within 72 h post infection. When moribund, mice developed severe renal dysfunction accompanied by renal apoptosis. **a** Kidney injury was quantified by measuring and normalizing urinary KIM-1 level to urinary creatinine 24, 48 and 72 h post infection. Two independent experiments, $n = 10$ per group except for WT- 24 and 48 h and t-EED1+ 72 h: $n = 9$. Biomarkers for kidney function **b** serum creatinine and **c** blood urea nitrogen (BUN) were quantified in serum of mice 6, 24, 48, 72 h post infection and increased especially in serum of moribund (mor) mice. Two independent experiments. Serum creatinine $n = 10$, except for WT- mor, WT+ 24–72 h, t-EED1+ 24 and 48 h $n = 9$, for t-EED1- 6 h and t-EED1+ mor $n = 8$. BUN $n = 10$, except for WT- 24, 48 h and mor $n = 9$, t-EED1+ mor $n = 8$. **a–c** Dashed lines indicate median serum biomarker level of uninfected controls in the presence (+, dark gray) or absence of doxycycline (–, light gray). Data are shown as median and interquartile range. **d** Immunohistochemistry of the renal pelvis of moribund mice identified apoptotic areas stained in brown. Scale bar represents 200 μm . **e** Quantification of apoptotic areas in kidneys of moribund mice ($n = 5$ per group). Shown are apoptotic areas in μm^2 in box-and-whiskers graph with min to max. No significant changes were observed by two-sided Mann-Whitney test. Source data are provided as a Source Data file.

approximately 3–4-fold higher in the renal cortex than in plasma. Furthermore, mice develop metabolic alkalosis early after systemic infection⁴⁸ which is known to further increase citrate concentration in the cortex, and in addition enhances renal citrate excretion 20-fold compared to the steady state⁶³. Therefore, citrate could be an abundant source of carbon available for *C. albicans* in the renal cortex and tubules during the early phase of systemic infection. Thus, enhanced growth on citrate might contribute to the higher renal fungal burden in the absence of *EED1* expression. Transcriptional profiling

during growth of *C. albicans* on citrate as sole carbon source revealed only few genes that were up-regulated in the *eed1 Δ / Δ* mutant compared to the WT after 12 h. These, however, included genes involved in metabolism of carboxylic acids and hence could aid in the metabolism of citrate. Similarly, up-regulation of *GAT1* might be promoting growth on casamino acids. However, many metabolic enzymes are regulated by post-transcriptional modifications to respond quickly to changing environmental conditions^{64,65}, and it is therefore likely that the transcriptional changes described here reflect only in part the



cellular changes leading to enhanced proliferation of the *eed1Δ/Δ* mutant.

Infection with t-EED1+ yeast resulted in higher organ fungal burden, significantly more leukocytes infiltrating the kidneys and increased renal pro-inflammatory cytokine production at later time points contributing to local immunopathology^{49,66}. Markers of systemic inflammation, sTREM-1 and NGAL, increased rapidly in serum of infected mice irrespective of fungal morphology. NGAL thresholds defining sepsis in humans⁶⁷ and sTREM-1 thresholds in mice⁶⁸ were reached within 24 h after infection, while damage of proximal tubular cells measured by KIM-1 became detectable slightly later (between 24 and 48 h p.i.).

Impaired kidney function determined by increased blood urea nitrogen level and serum creatinine was only evident in moribund mice, consistent with findings by Spellberg et al.⁴⁸, again without significant differences between hypha-forming and filament-deficient strains. Histologically, t-EED1+ yeast were found in large numbers mainly within tubules and in the renal pelvis; it appears possible that accumulation of yeast led to obstruction of tubules and the collecting duct system⁶⁹, increasing the intrarenal pressure and thereby, in addition to immunopathology, causes renal tissue damage. This is supported by our data showing that the area of apoptotic tissue in kidneys did not differ between mice infected with WT and t-EED1+ and suggests that the lack of

Fig. 9 Systemic infection with the *C. albicans eed1Δ/Δ* mutant leads to delayed mortality of immunosuppressed mice despite higher fungal burden accompanied by increased kidney injury compared to mice infected with the WT. Mice that were rendered immunosuppressed by depletion of neutrophils and monocytes using the RB6-8C5 antibody were intravenously infected with 1×10^2 , 1×10^3 or 1×10^4 CFU/g body weight of *C. albicans* WT (SC5314) or *eed1Δ/Δ* mutant. **a** Survival of mice was monitored after infection with 1×10^2 CFU/g or 1×10^3 CFU/g body weight for 21 days. Survival of mice infected with 1×10^2 CFU/g ($n = 6$ per group) or 1×10^3 CFU/g body weight ($n = 8$ per group) is shown as Kaplan-Meier curve and curves were compared using the two-sided Log-rank (Mantel-Cox) test. p -values are shown in the graph. **b** Representative images of PAS stained histological cross sections of kidneys from moribund immunocompetent or immunosuppressed mice infected with 10^4 CFU/g body weight of WT or *eed1Δ/Δ* mutant. Immunocompetent and immunosuppressed uninfected control mice were sacrificed 7 d after mock infection. Black arrows point towards purple stained *C. albicans* hyphae (WT) or yeast (*eed1Δ/Δ* mutant), white arrows towards immune cells infiltrating the renal tissue. Scale bar represents 20 μ m and applies to all images. **c** Organ fungal burden of immunosuppressed mice infected with 1×10^2 CFU/g body weight 12 h and 18 h post infection and when moribund (mor). **d** Quantification of kidney injury by measuring and normalizing urinary KIM-1 to urinary creatinine level. **c, d** Two independent experiments, $n = 6$, except for *eed1Δ/Δ* mutant 12 h, $n = 4$; controls, $n = 4$. Data are shown as median with interquartile range and were compared using the two-sided Mann-Whitney test. p -values are shown in the graph. **d** p -values above bars represent significant changes in comparison to the uninfected control. Source data are provided as a Source Data file.

hyphae-driven direct damage can be compensated by enhanced yeast cell growth. The exact molecular mechanisms by which absence of *EEDI* influences both morphogenesis and growth on alternative carbon sources remains unknown; however, it should be noted that retention of some level of virulence in the absence of hyphal elongation is not a unique feature of *EEDI* deficient strains. Homozygous deletion of *UME6*, resulting in a similar filamentation defect as observed for the *eed1Δ/Δ* mutant, leads to significantly attenuated virulence, but still causes lethal infections in mice⁷⁰. Virulence of a *sf12Δ/Δ* mutant was comparable to the WT despite a filamentation defect⁷¹. In contrast to the *eed1Δ/Δ* mutant, systemic infection with the *sf12Δ/Δ* mutant, however, did not result in increased fungal burden, and some filamentation occurs in the absence of *SFL2*^{71,72}. The role of *SFL2* for interaction with immune cells has not been investigated so far, and it thus remains unclear if differences in immunopathology contribute to the virulence of the *sf12Δ/Δ* mutant. Furthermore, a screen of a *C. albicans* deletion library identified mutants with defects in filamentation but with unaltered infectivity⁷³; a detailed analysis of these mutants might reveal additional strains for which virulence in murine systemic candidiasis models does not depend on filamentation.

Of note, significantly higher CFUs in kidneys were also observed for tet-*NRG1*- yeast on day 3 after systemic infection compared to both the parental strain (Supplementary Fig. 4d) and the same strain with doxycycline ($p = 0.001$), consistent with observations by Saville et al.¹⁴. However, the fungal burden of tet-*NRG1*- yeast was approximately 1-log lower than for t-EED1+ yeast at this time point (mean $3.19 \times 10^5 \pm 2.5 \times 10^5$ compared to $3.45 \times 10^6 \pm 1.15 \times 10^5$), and declined over time (Supplementary Fig. 4d). This indicates that while increased proliferation in vivo might be a feature shared by different filament-deficient strains, it quantitatively differs; the lower fungal burden resulting from infection with tet-*NRG1* yeast compared to t-EED1 yeast is likely one factor contributing to the difference in virulence between these two strains. In addition to metabolic fitness, resistance to host defense mechanisms determines the extent to which *C. albicans* can proliferate in vivo. While *C. albicans* locked in the yeast form by constitutive expression of *NRG1* (tet-*NRG1*) were avirulent in immunocompetent mice in this and previous studies^{14,74}, the same strain was capable of inducing lethal infection in mice rendered leukopenic by combined treatment with cyclophosphamide and cortisone acetate⁷⁵. In these mice, the yeast-locked strain reached a significantly higher fungal burden than the corresponding filamentous strain⁷⁵, which was also higher than observed in immunocompetent animals in this study and by others¹⁴. Furthermore, in the same study the fungal load observed in mice with different types of immunosuppression and infected with the filamentous strain was comparable at the

humane endpoint, even though this was reached at different time points after infection⁷⁵. Similarly, MacCallum and Odds⁷⁶ observed comparable kidney burden in mice at the humane endpoint even if animals were challenged with different infectious doses and survived for a different duration. Together, this suggests that a certain number of fungal cells can be tolerated within the kidney, and that this threshold is higher for yeast than for hyphae.

Comparison of tet-*NRG1* and *EEDI*-deficient strains furthermore indicates that, despite a shared morphology, different yeast strains display substantial differences in the ability to proliferate in vivo in the presence of functional innate immunity.

To our knowledge, this is the first study showing that increased metabolic fitness of *C. albicans* not only contributes to virulence in hematogenously disseminated candidiasis, but that enhanced proliferation of yeast cells can result in pathogenesis and mortality indistinguishable from infection with hyphae-forming WT and t-EED1- strains. Of note, the *eed1Δ/Δ* mutant caused 100% mortality in a systemic infection model in immunosuppressed mice, although delayed compared to the WT. In the absence of hypha-mediated damage and overt immunopathology, this indicates that rapid proliferation resulting in high organ fungal loads might be sufficient to drive pathogenesis. Previous studies have reported similar results: tet-*NRG1* yeast, which are avirulent in immunocompetent mice (Supplementary Fig. 4¹⁴), can cause lethal infection in immunosuppressed mice⁷⁵. Whether this was due to increased fungal burden was not determined. The relevance of fungal load for pathogenesis is furthermore supported by the fact that the course of disease and rate of mortality in mice with systemic candidiasis is highly dependent on the initial infection dose^{76,77}. Furthermore, by adjusting the infectious dose of different strains Odds et al. achieved a comparable mean survival time of mice infected either with *C. albicans* SC5314 or an isolate (RV4688) that displayed less filamentation in the murine kidney. Interestingly, less filamentation of RV4688 also coincided with a higher fungal burden compared to SC5314 in this study⁷⁷.

Considering that immunosuppression is a major risk factor for the development of candidemia⁷⁸ the findings in this study might provide some explanation for the virulence of non-*albicans Candida* species, such as *C. glabrata* and *C. auris*, that do not form true hyphae^{79,80}. Interestingly, the yeast form is the virulent cell type in most pathogenic dimorphic fungi, such as *Histoplasma* spp. and *Blastomyces* spp., that grow as mycelia in the environment but switch to yeast upon entering the host⁸¹. While the pathogenicity factors and pathogenesis mechanisms employed by these yeast cells differ significantly from *C. albicans* yeast, this underscores the general concept that yeast cells are not per se less virulent than hyphae.

Methods

C. albicans strains, strain construction and growth conditions. The t-EED1 strain was generated in the THE1⁸² background. Therefore, the *URA3*-tetracycline-regulable (TR) promoter region was amplified from p99CAU1⁸² using primers Eed1-TET-F and Eed1-TET-R (Supplementary Table 1). Fragments were used to replace the endogenous promoter of one allele of *EED1*. The second allele of *EED1* was deleted using the SAT1 flipping method⁸³ with plasmids already containing the *EED1*-flanking regions used to generate the homozygous *eed1Δ/Δ* deletion mutant M1315⁷. Transformants were selected on YPD with 200 mg/ml nourseothricin⁸³ and were verified by PCR and Southern Blot analysis.

The *C. albicans* clinical isolate SC5314⁸⁴, the isogenic *eed1Δ/Δ* mutant⁷, t-EED1 and the respective parental strain THE1-Clp10¹⁸ were maintained as glycerol stocks and grown on YPD (1% yeast extract, 2% peptone, 2% glucose) agar plates. Single colonies were inoculated into liquid YPD and grown overnight at 30 °C with horizontal shaking at 180 rpm. When needed, *C. albicans* cells were grown to exponential phase by diluting liquid cultures to an optical density at 600 nm (OD_{600}) of 0.2, followed by incubation at 30 °C and 180 rpm for 3–4 h. Cultures were washed twice with phosphate buffered saline (PBS) prior to experiments.

For infection experiments, fresh *C. albicans* colonies were inoculated into liquid YPD and grown to late exponential phase (14–16 h) at 30 °C with horizontal shaking at 180 rpm. Doxycycline hyclate (50 µg/ml; Sigma Aldrich) was added to t-EED1 cultures to prevent hypha formation. Cells were washed twice with sterile PBS and resuspended in Dulbecco's Phosphate Buffered Saline (DPBS, Gibco), counted using a hemocytometer and adjusted to the desired concentrations in DPBS. Infectious doses were confirmed by serial dilutions and plating on YPD agar plates.

Morphology of tetracycline-regulable strains in vitro. To investigate fungal morphology of the tet-regulable t-EED1 strain in vitro, THE1-Clp10 and t-EED1 were streaked on YPD plates in the absence or presence of 50 µg/ml doxycycline. Plates were incubated under non-hypha-inducing conditions at 25 °C for 2 days before pictures were taken from single colonies with an inverse microscope (Axio Vert.A1; Zeiss). To test for morphology under hypha-inducing conditions, 5×10^4 cells of the strains were seeded in RPMI1640 in the absence or presence of 50 µg/ml doxycycline per well in 12-well plates and incubated at 37 °C and 5% CO₂. Pictures were taken after various time points by inverse microscopy.

Growth curves. To evaluate growth in the presence of different carbon sources SC5314 and the *eed1Δ/Δ* mutant were diluted to OD_{600} of 0.1 in YPD medium with 2 or 0.1% glucose or in SD minimal medium (0.67% yeast nitrogen base; BD Biosciences) in the presence of 2% glucose, 0.1% glucose, 2% N-acetyl-glucosamine (GlcNAc; Sigma–Aldrich), 2% sodium-DL-lactate (Sigma Aldrich), 2% potassium acetate (Merck), 2% citric acid monohydrate (Roth) or 2% casamino acids (BD Biosciences). For testing of proteolytic activity, *C. albicans* strains were grown in SD medium overnight, washed twice with PBS and OD_{600} was set to 0.1 in YCB-BSA (1.17% Yeast Carbon Base (BD Biosciences), 1% glucose, 0.5% BSA (Serva)), pH 4.0. For growth in kidney homogenates, kidneys of uninfected mice were removed aseptically, homogenized and diluted to 25 mg/ml in DPBS and filtered through 70 µm and 40 µm cell strainers before filter sterilization. Growth was recorded by measuring OD_{600} in a microplate reader at 37 °C. Measurements were performed in 30 min intervals over a course of 60 h. Blank values were subtracted from all measurements.

Sample preparation for RNA isolation, RNA sequencing and analysis of data. For RNAseq, overnight cultures of *C. albicans* WT SC5314 and *eed1Δ/Δ* mutant were grown in SD with 2% glucose at 30 °C and 180 rpm (Supplementary Fig. 13a). To synchronize cultures cells were inoculated at an OD_{600} of 0.1 in SD with 2% glucose and grown at 30 °C and horizontal shaking at 180 rpm. After 10 h samples for the 0 h time point were taken and cells were transferred to SD medium containing 2% of citrate (Roth) or 2% of casamino acids (CAA; BD Bacto) as sole carbon source at an OD_{600} of 0.2 in individual flasks for each time point. Cells were grown at 37 °C and 180 rpm. After 2 h, 6 h and 12 h samples were removed from the cultures and cell pellets for RNA isolation were obtained by centrifugation at 20,000 × g for 3 min and were immediately frozen in liquid nitrogen. Additional samples were taken at these and intermediate time points to determine the optical density at 600 nm, dry mass and morphology of fungal cells. For the determination of dry mass, nylon Whatman® membrane filters with a pore size of 0.2 µm were dried at 55 °C for 24 h in a hybridization oven, weight and placed on a bottle top vacuum filter. Cells were loaded on the membrane by filtration and washed with ddH₂O. After drying for additional 24 h, membranes were weighed again and dry mass was calculated. Experiments were conducted in triplicates and RNA isolation was performed as previously described⁷. In brief, pellets were resuspended in 400 µl AE-buffer (50 mM sodium acetate, 10 mM EDTA) and 40 µl 10% SDS. An equal volume of phenol/chloroform/isoamylalcohol was added followed by incubation at 65 °C for 5 min. Homogenous solutions were frozen at –80 °C for 10 min, transferred to 65 °C for 5 min. Freezing and thawing was repeated once. Solutions were centrifuged for 10 min at 20,800 × g and the upper phase was transferred into a new reaction tube. 10% volume 3 M sodium acetate (pH 5.3) and 1 volume 2-propanol were added. Precipitation of RNA was carried out for 30 min at –20 °C.

After centrifugation for 10 min at 12,000g the supernatant was discarded and RNA pellets were washed twice with 70% ethanol. RNA was solved in RNase free water. RNA quantity was determined with a Nanodrop ND1000 (Peqlab) and quality was assessed using an Agilent 2100 Bioanalyzer (Agilent Technologies). Library preparation and RNA sequencing was carried out at Novogene (UK) Company Limited. Sequencing was performed using an Illumina NovaSeq 6000 system to obtain 150 bp paired-end reads.

Mapping of the fastq files delivered by the company (raw data are accessible at NCBI under BioProject accession number PRJNA714826, <https://www.ncbi.nlm.nih.gov/bioproject/PRJNA714826>) and counting of the gene transcription reads was performed using the European Galaxy server⁸⁵ that is providing an environment and sets of tools for the following analysis steps: First, *FastQC* was used to assess the quality of the sequences and *Cutadapt* was applied. Sequences were mapped to the genome of *C. albicans* WT (SC5314) using the *RNA-Star* tool, the “length of the genomic sequence around annotated junctions” parameter was set to 149. From that analysis, bam files were constructed that were used to quantify gene counts with the *FeatureCount* function. The reverse stranded bam files were processed allowing for fragment counts but not multimapping. The minimum mapping quality per read was set to 10. Final count files were analyzed in R, using the *DESeq2* package⁸⁶ that allows searching for differentially expressed genes (DEGs) by comparing the count tables of different conditions. For this purpose, transcription profiles of the mutant were compared to the WT at the 0 h time point, as well as for each time point in medium containing citrate or casamino acids. The principal component analysis was done using the PCA function from the *DESeq2* package in R. All genes were used for the calculation. Gene Ontology (GO) term enrichment analysis was performed from significantly up- or down-regulated genes (+ or - log₂ and adjusted *p*-value <0.05) in *eed1Δ/Δ* mutant compared to WT using the CGD GO Term Finder⁸⁷. Based on the analysis of GO terms with REVIGO⁸⁸ graphs were created using cytoscape⁸⁹. Venn diagrams were created using Venny2.1 (<https://bioinfo.cnb.csic.es/tools/venny/>).

Mice. All animal experiments were performed in accordance with European and German regulations. Protocols were approved by the Thuringian authority and ethics committee (Thüringer Landesamt für Verbraucherschutz, permit numbers: HKI-19-003, 03-007/13, 03-002/11, 03-004/15, 03-008/13). Eight- to ten-week-old female specific-pathogen-free BALB/c mice (16 to 18 g), purchased from Charles River (Germany), were housed in groups of five in individually ventilated cages at 22 ± 1 °C, 55 ± 10 % relative humidity, 12 h/12 h dark/light cycle, with free access to food and water and autoclavable mouse houses as environmental enrichment.

Intraperitoneal and systemic infection model. For intraperitoneal infection and survival analyses after intravenous infection with THE1-Clp10, t-EED1 and tet-*NRG1*, mice received drinking water containing 5% sucrose without (–) or with (+) 2 mg/ml doxycycline starting 3 days prior to infection. Water was replaced every two days. The low acceptance of doxycycline containing water resulted in a loss of body weight in the doxycycline group only, indicating possible dehydration. This could have aggravated the consequences of impaired renal function caused by systemic infection and likely explains while mice infected with THE1-Clp10 reached the humane endpoints earlier if they received doxycycline (Fig. 2c). Therefore, in further experiments mice received a diet containing 625 mg/kg doxycycline (Envigo Teklad, catalog no. TD.120769). Food was replaced every 5 days; acceptance was high, resulting in body weights comparable to the non-doxycycline groups. For the intraperitoneal infection model, mice were infected intraperitoneally with 1×10^8 CFU in 500 µl DPBS and mice were humanely sacrificed 24 h post infection. For hematogenously disseminated candidiasis mice were infected with 1×10^2 to 1.25×10^5 CFU/g body weight in 100 µl DPBS via the lateral tail vein at day 0. For survival experiments, mice were euthanized when showing signs of severe illness (details described below), and these animals are referred to as “moribund”. Groups of mice (*n* = 5) were sacrificed 6, 24, 48 and 72 h post infection with 2.5×10^4 CFU/g body weight for analysis of fungal burden, immune cell infiltration, renal cytokines, serum and urinary marker protein progression during the acute phase of infection. Uninfected control mice received (ctr +) or did not receive doxycycline (ctr–) containing food. Time point experiments were repeated two to three times.

Induction of neutro- and monocytopenia. To deplete neutrophils and monocytes 100 µg of the InVivo Plus anti-mouse Ly6G/Ly6C (Gr-1) monoclonal antibody (clone RB6-8C5; BioXcell) in 100 µl DPBS were administered intraperitoneally 24 h prior to infection and every 48 h thereafter. Mice were systemically infected with *C. albicans* WT (SC5314) and the *eed1Δ/Δ* mutant using 1×10^2 , 1×10^3 or 1×10^4 CFU/g body weight. Successful depletion of peripheral neutrophils (neutropenia defined as less than 200 PMNs/µl blood⁹⁰) and monocytes was confirmed when animals reached humane endpoints by white blood cell differential count using the hematology analyzer BC-5300Vet (Mindray; Supplementary Fig. 11). Uninfected control groups (*n* = 2) did or did not receive RB6-8C5 and were sacrificed 7 days after they were mock-infected with 100 µl DPBS into the lateral tail vein.

Murine model of gastrointestinal colonization and dissemination. To avoid environmental contamination, cages, bedding, bottles and drinking water were

sterilized prior to use and mice were handled exclusively in laminar flow hoods. Mice received sucrose-containing drinking water and sucrose concentration was increased from 2.5% starting 7 d prior to infection for 2 d to 5% for 1 d. From day -4 until the end of the experiment mice received antibiotics to reduce the intestinal bacterial flora: 1500 U/ml penicillin and 2 mg/ml streptomycin were added to 7.5% sucrose-containing drinking water that was replaced daily. Mice were fed with chow containing 625 mg/kg doxycycline sterilized by irradiation. On day 0, mice were inoculated by gavage with 100 μ l DPBS containing 5×10^7 *C. albicans* WT (SC5314) or *eed1* Δ / Δ . Mice were divided in two groups: one group was only colonized whereas in the other group dissemination was induced by injecting 200 mg/kg body weight cyclophosphamide (Endoxan, Baxter) intraperitoneally on day 7 and 10 post infection. Successful depletion of immune cells was confirmed by white blood cell differential count using the hematology analyzer. Feces were collected from individual mice on day 2, 4, 7 and 14, weighed and plated on YPD agar with or without 80 μ g/ml chloramphenicol for determination of fungal and bacterial CFUs, respectively. On the end of the experiment (14 days p.i.) mice were humanely sacrificed and fungal burden were determined in liver and kidney.

Clinical monitoring and scoring. Body weight and body surface temperature were recorded daily. After infection the health status of the mice was checked at least twice a day. For RB6-8C5 treated immunosuppressed mice, health status was recorded every 3 h for 39 h and every 6 h thereafter. An additive clinical score was determined to evaluate disease severity. For intraperitoneal infection the following parameters were included: fur, coat and posture (normal, 0; fur mildly ruffled, 1; fur strongly ruffled, 2; fur strongly ruffled and hunched posture, 3), lethargy (absent, 0; mild, 1; moderate, 2; severe, 3), intraabdominal fibrin exudation (none, 0; single, small flocks, 1; multiple adhering flocks, removable, 2; multiple adhering flocks, removing causes damage to organ, 3), presence of other symptoms like ocular discharge, diarrhea (absent, 0; present, 1). The maximum possible score was 10. For systemic infections and the colonization and dissemination model the following parameters were included: fur (normal, 0; slightly ruffled, 1; ruffled, 2), lethargy (absent, 0; mild, 1; moderate, 2; severe, 3), body temperature (normal, 0; moderately increased, 1; increased, 2; hypothermia, 3). The maximum possible score was 8. Mice were humanely sacrificed when they reached the humane endpoints defined as (i) severe lethargy, (ii) hypothermia, or (iii) a cumulative clinical score of ≥ 5 . Mice were euthanized with an overdose of ketamine (100 μ l of 100 mg/ml) and xylazine (25 μ l of 20 mg/ml) applied intraperitoneally followed by blood withdrawal.

Determination of serum and urinary biomarkers. Blood was collected by cardiac puncture (intraperitoneal infection and survival experiment) or via the vena cava inferior from mice euthanized at defined time points. Serum enzyme levels of pancreatic amylase and alanine aminotransaminase (ALT) were measured using the EuroLysar CCA 180 Vet system (QinLAB Diagnostik) according to standard methods recommended by the International Federation of Clinical Chemistry. The Mouse TREM-1 ELISA Kit (RayBiotech), DetectX[®] Urea Nitrogen (BUN) Detection Kit (Arbor Assays), Mouse Lipocalin-2 (NGAL) ELISA Kit (RayBiotech) and DetectX[®] Serum Creatinine Kit (Arbor Assays) were used to measure the respective parameters in serum of mice. Urine of mice was collected from mice euthanized 24, 48 and 72 h p.i. from moribund and uninfected mice. Either spontaneous urine was collected or gentle trans-abdominal pressure was applied onto the bladder and urine was collected using untreated glass capillary tubes. Urinary KIM-1 and creatinine levels were measured using the Mouse TIM-1 ELISA Kit (RayBiotech) and the Creatinine Parameter Assay Kit (R&D Systems), respectively. KIM-1 levels were normalized to urinary creatinine to account for differences in urinary concentration.

Quantification of immune cells by flow cytometry. To evaluate immune cell infiltration during the course of infection, organs were perfused with normal saline after withdrawal of blood. Organs were removed and weighed. One half of each kidney was cut into small pieces and digested in the presence of collagenase D (30 μ g/ml; Sigma Aldrich) and DNase I (0.7 mg/ml; Sigma Aldrich) in RPMI (RPMI 1640; Gibco) supplemented with 10% fetal bovine serum (FBS; Bio&Sera), Pen Strep (100 U/ml Penicillin and 100 μ g/ml Streptomycin; Life Technologies), and 1 mM sodium pyruvate (Gibco) for 30 min at 37 °C with moderate horizontal shaking (70 rpm). Single cells were obtained by passing the digested tissue through a 70 μ m cell strainer. Cells were washed and erythrocytes were lysed by addition of red blood cell lysis buffer (0.15 M NH₄Cl, 10 mM KHCO₃, 1 mM Na₂EDTA, pH 7.2). Remaining cells were washed, resuspended in 70% Percoll (GE Healthcare) and layered under 30% Percoll. Leukocytes were enriched by density gradient centrifugation (400g, 20 min, room temperature (RT), acceleration 1, deceleration 0). Leukocytes were collected from the interphase, washed with PBS and volumes were determined. Cells were transferred in a 96-well plate. Leukocytes were stained for flow cytometric analysis and acquired on a FACSVerser (BD Biosciences). The following antibodies were used: PerCP anti-CD45 (30-F11, BD Biosciences), APC anti-CD11b (M1/70, eBioscience), eFluor anti-CD335 (29A1.4, eBioscience), FITC anti-F4/80 (Bm8, eBioscience), PE anti-CD11c (N418, eBioscience), PE-Cy7 anti-MHCII (M5/114.15.2, eBioscience), eFluor anti-Ly-6C (HK1.4, eBioscience) FITC anti-CD19 (1D3, BD Biosciences), PE-Cy7 anti-CD3e (145-2C11, eBioscience). Fc

receptors were blocked by addition of anti-mouse CD16/32 (93; BioLegend) 1:50 to the staining mixture. Dead cells were excluded from analysis using the Fixable Viability Dye eFluor[®] 506 (eBioscience) prior to specific antibody staining. A detailed description of the gating strategy is provided in Supplementary Fig. 19. Data were analyzed using FlowJo V.10.0.8 software.

Histopathology and immunohistochemistry. For histology, longitudinal sections of kidneys were fixed with buffered formalin and embedded in paraffin, cut into 3–4 μ m slices, and stained with periodic acid-Schiff (PAS) staining according to standard protocols. Apoptotic cells in the kidney were detected by immunohistochemistry using the ApopTag in situ apoptosis detection kit (EMD Millipore) following the manufacturer's directions. Briefly, paraffin-embedded sections were rehydrated in Histo-Clear II (National Diagnostics) and alcohols followed by washing with phosphate-buffered saline (PBS). The sections were pre-treated with 20 μ g/ml Proteinase K (Ambion) in PBS for 15 min at RT. Endogenous peroxidases were blocked by incubating slides for 15 min in 3% hydrogen peroxide. Sections were incubated with equilibration buffer (EMD Millipore) for 30 s at RT, followed by terminal deoxynucleotidyl transferase (TdT; EMD Millipore) incubation at 37 °C for 1 h. Sections were further exposed to anti-Digoxigenin (EMD Millipore, Cat Number S7100) for 30 min at RT, and the positive reaction was visualized with DAB 3, 3'-diaminobenzidine (DAB) substrate (Thermo Scientific). After counter-staining the specimens with 0.5% methyl green (Sigma), they were imaged by bright field microscopy. For quantification, apoptotic areas were quantified using PROGRES GRYPHAX[®] software (Jenoptik).

Determination of organ fungal burden and in vivo cytokine production. Weighed organs were homogenized in MPO buffer (200 mM NaCl, 5 mM EDTA, 10 mM TRIS pH 8, 10% glycerol, 1 mM PMSF, 28 μ g/ml Aprotinin, 1 μ g/ml Leupeptin) using an UltraTurrax (Ika). Homogenates were serially diluted and plated onto YPD plates containing 80 μ g/ml chloramphenicol (Roth) for enumeration of CFU. Supernatants were generated by centrifugation (1500 g, 4 °C, 15 min) and frozen at -80 °C until determination of cytokine concentrations. Cytokines were quantified using a customized ProcartaPlex[™] Mix&Match Mouse 12-plex (eBioscience; cytokines that were included: GRO- α (KC), IFN- γ , IL-1 β , IL-10, IL-12p40, IL-18, IL-6, IP-10, MCP-1, MIP-1 α , RANTES, TNF- α). The plex was performed according to manufacturer's instructions using a Luminex Magpix system (Luminex Corporation).

Neutrophil isolation from bone marrow and differentiation of bone marrow-derived macrophages. Bone marrow was obtained from 8–20 week old female BALB/c mice as described previously⁹¹. Briefly, mice were euthanized by cervical dislocation and femora, tibiae and humeri were removed and placed in RPMI supplemented with Pen Strep. Bone marrow was flushed with supplemented RPMI and single cell suspensions were obtained by continuous pipetting. Bone residues were removed by filtration through a 40 μ m pore-size filter. Cells were pelleted and erythrocytes were lysed by addition of RBC lysis buffer. Cells were resuspended in Hanks' balanced saline solution without Ca and Mg (HBSS; Lonza). Mature neutrophils were purified using a discontinuous Percoll gradient consisting of 52%, 69%, and 78% Percoll in HBSS. Mature neutrophils were recovered from the 69%/78% interphase after centrifugation (1500 g, 4 °C, 30 min, acceleration 2, deceleration 2), washed and resuspended in HBSS. Neutrophils were counted using the hematology analyzer. Purity of neutrophils was confirmed by flow cytometry to be between 89 - 95%. For differentiation into macrophages, bone marrow cells were seeded at a density of 5×10^6 cells in 175 cm² cell culture flasks in RPMI containing 10% heat-inactivated (h.i.; 30 min at 56 °C) FBS, Pen Strep and 40 ng/ml recombinant murine M-CSF (ImmunoTools). Cells were incubated in a humidified incubator at 37 °C with 5% CO₂ and medium was exchanged every 2–3 days. After 7 days, adherent cells were detached in RPMI + FBS by scrapping. Viable cells were counted using trypan blue exclusion and diluted to desired concentrations. For phagocytosis assays 5×10^5 neutrophils or macrophages were allowed to adhere to sterile coverslips in a 24-well plate for 1–2 h at 37 °C, 5% CO₂ in a humidified incubator. To increase the adherence of neutrophils, coverslips were pre-treated with 0.1% gelatin and incubated at 4 °C overnight. Wells were washed twice with PBS before seeding. For cytokine measurement, survival and damage assays 8×10^4 neutrophils or macrophages were seeded in 96-well plates in RPMI supplemented with 1% mouse serum. Cells were allowed to adhere to the substrate by culturing them for 1–2 h at 37 °C, 5% CO₂ in a humidified incubator prior to infection.

Phagocytosis, survival and damage assays. To quantify phagocytosis, cells were infected with *C. albicans* at a multiplicity of infection (MOI) of 1 in the presence of 1% murine serum in a total volume of 500 μ l. After 1 h of co-incubation at 37 °C with 5% CO₂, cells were fixed with 2% paraformaldehyde. Extracellular *C. albicans* cells were stained with Alexa Fluor 647-conjugated Concanavalin A (Thermo Fisher Scientific) for 30 min, intra- and extracellular fungal cells were stained with Calcofluor White (Sigma-Aldrich) after permeabilization of immune cells with 0.5% Triton X-100. Coverslips were mounted with ProLong Gold antifade reagent (Thermo Fisher Scientific) and fluorescence images were recorded using the Axio Observer.Z1 (Carl Zeiss Microscopy). The phagocytic index was determined by counting the numbers of *C. albicans* cells phagocytosed by 100 immune cells.

Fungal survival in the presence of immune cells was determined by infecting macrophages or neutrophils with *C. albicans* (MOI1) in the presence of 1% murine serum in a total volume of 150 μ l. After 2 or 6 h, immune cells were lysed by addition of 50 μ l 5% Triton X-100. Fungal cells were resuspended by rigorously pipetting and lysates were diluted and plated onto YPD plates and incubated for 48 h at 37 °C. Survival rates were calculated by normalization from control wells containing no immune cells and the increase in fungal CFU was calculated by normalization to the starting inoculum for cells in the presence or absence of BMDMs. Fungal morphology was recorded by inverse microscopy using an Axio Vert.A1 microscope (Zeiss) after various time points. To quantify damage and TNF- α , BMDMs were co-incubated with *C. albicans* (MOI1) for 24 h. For total LDH release (high control), BMDMs were lysed by addition of 20 μ l 5% Triton X-100, incubated for 10 min at 37 °C. Supernatants were obtained by centrifugation at 300 \times g for 10 min. LDH was quantified using the Cytotoxicity Detection Kit (Roche) and TNF- α was quantified by ELISA (Ready-SET-Go, eBioscience) according to manufacturer's instructions.

Cytokine and ROS production. Macrophages and neutrophils were infected with living or heat-killed (HK; 70 °C, 10 min) *C. albicans* WT cells (MOI1) in a total volume of 200 μ l. Unstimulated immune cells and cells treated with 100 nM phorbol 12-myristate 13-acetate (PMA; Sigma Aldrich) or 100 ng/ml lipopolysaccharide (LPS; Sigma Aldrich) served as negative and positive controls, respectively. After co-incubation for 24 h at 37 °C with 5% CO₂ supernatants were recovered after centrifugation (1500 \times g, 4 °C, 15 min) and TNF- α , IL-6 and IL-10 were determined by commercially available ELISA kits (Invitrogen) according to manufacturer's instructions.

Total ROS accumulation by neutrophils was quantified by luminol-enhanced chemiluminescence. Therefore, 5 \times 10⁴ freshly isolated neutrophils were seeded into white clear-bottom 96-well plates (Corning) in RPMI without phenol red (Gibco). Cells were allowed to attach for 30 min at 37 °C and 5% CO₂ prior to infection. Neutrophils were infected with *C. albicans* (MOI1) left untreated or were stimulated with PMA as positive control. Immediately after stimulation, 50 μ l of RPMI without phenol red containing 200 mM luminol (Fluka) and 16 U horseradish peroxidase (Sigma Aldrich) were added. Luminescence was recorded every 2.5 min for 190 min at 37 °C in a Tecan Infinite microplate reader. The area under the curve was calculated with GraphPad Prism 7.

Epithelial cell infection. The following human epithelial cell lines were used in this study: Hepatic epithelial cells (HepaRG; Gibco) were maintained in William's Medium E with GlutaMAX and HepaRG Thaw, Plate & General Purpose Medium Supplement; renal epithelial cells (A498; DSMZ) were cultivated in Minimum Essential Medium with L-glutamine supplemented with 10% h.i. FBS; oral epithelial cells (TR146; Episkin) were cultivated in Dulbecco's Modified Eagle Medium (DMEM) with high glucose supplemented with 10% h.i. FBS; intestinal epithelial cells (Caco-2 clone type C2BBE1; ATCC®CRL-2102™) were maintained in DMEM supplemented with 10% h.i. FBS and 10 μ g/ml human holotransferrin (Merck Millipore). Cells were cultured in a humidified incubator at 37 °C with 5% CO₂ under normoxic conditions (21% O₂) if not stated otherwise. In addition, C2BBE1 cells were cultivated under hypoxic conditions (1% O₂) in a temperature controlled Hypoxystation (H35, Don Whitley Scientific) to mimic physiological intestinal O₂ concentrations. For damage assays and the quantification of cytokines, cells were detached and 2 \times 10⁴ cells (TR146, A498) or 4 \times 10⁴ cells (HepaRG) were seeded in 96-well plates 2 d prior to infection. Cells were washed and infected with exponentially grown *C. albicans* strains at a MOI of 1 in a volume of 200 μ l. Medium without fungal cells served as mock control. After 24 h of co-incubation, supernatants were recovered after centrifugation (200 \times g, 5 min). To measure epithelial integrity and translocation, Corning® Transwell® polycarbonate membrane inserts with 5 μ m pore size and 6.5 mm in diameter were coated with 100 μ l of 10 μ g/ml collagen I for 2 h at RT before they were washed twice and placed in a 24-well plate filled with 600 μ l supplemented DMEM. 2 \times 10⁴ C2BBE1 cells were seeded in 200 μ l supplemented DMEM in inserts and cultivated for 14 d at 37 °C, 5% CO₂ with 21% O₂ or 1% O₂. Medium was replaced on day 5 and every second day thereafter. Epithelial cells were infected by adding 1 \times 10⁵ *C. albicans* cells to the upper compartment and incubated for 24 h at the conditions mentioned above. To measure epithelial integrity, the trans-epithelial electrical resistance (TEER) was quantified using a chopstick electrode connected to the Epithelial VoltOhmmeter EVOM2 (WPI) before and 24 h post infection. TEER measurements from inserts containing medium only served as blank values and were subtracted from all measurements. Supernatants of the upper compartment were kept for measurement of lactate dehydrogenase (LDH). To quantify the potential of the different *C. albicans* strains to translocate through the C2BBE1 cell layer, 24 h after infection the lower compartment was treated with 20 U/l zymolyase (Amsbio) for 2 h at 37 °C and 5% CO₂. Detached fungal cells were plated on YPD agar and CFUs were counted. Epithelial cell damage was quantified by measurement of LDH in supernatants using the Cytotoxicity Detection Kit (Roche). Uninfected cells served as negative control. For total cells lysis (high control) 10 μ l of 5% Triton X-100 were added. Human IL-6 and IL-8 were quantified by ELISA (Invitrogen) according to the manufacturer's instructions.

Quantitative PCR. DNA was isolated from kidneys infected with either the WT (THE1-Cip10) or t-EED1 in the presence of doxycycline. Kidneys were homogenized and centrifuged for 15 min at 1500 \times g. DNA was extracted from pellets using the Yeast DNA Extraction Kit (Thermo Scientific) following manufacturer's instructions. For amplification of the *C. albicans* 18S rRNA gene *RDNI8* the following primers were used: sense amplification primer, 5'-GGACCCAGCCGAGCCCTT-3' and antisense amplification primer, 5'-AAGTAAAAGTCTGGTTCGCCA-3'³⁰. Quantitative PCR was conducted using 1 μ l of template DNA and the QPCR Mix EvaGreen (Bio&SELL) on a CFX 96 Real time System (BioRad). The following condition were used for product amplification: 95 °C for 15 min, 40 cycles of each 95 °C for 15 s, 59 °C for 15 s and 72 °C for 15 s. To confirm PCR product specificity, a melting curve was generated. The resulting Ct values were plotted against the CFU determined from the homogenized tissue.

Statistical analysis. GraphPad Prism 7 was used to analyze all data sets. Shown are either the mean and standard deviation (SD) or the median and the inter-quartile range as indicated in the figure legends. The two-tailed student's *t*-test or the Mann-Whitney test was used to test for statistical significances. *p*-values \leq 0.05 were considered significant, **p* \leq 0.05; ***p* \leq 0.01; ****p* \leq 0.001. Survival curves were compared using the Log-rank (Mantel-Cox) test.

Reporting summary. Further information on research design is available in the Nature Research Reporting Summary linked to this article.

Data availability

The RNAseq data that support the findings of this study are available at NCBI under BioProject accession number PRJNA714826 (<https://www.ncbi.nlm.nih.gov/bioproject/PRJNA714826>). Source data are provided with this paper.

Received: 19 June 2020; Accepted: 28 May 2021;

Published online: 23 June 2021

References

- Huffnagle, G. B. & Noverr, M. C. The emerging world of the fungal microbiome. *Trends Microbiol.* **21**, 334–341 (2013).
- Kim, J. & Sudbery, P. *Candida albicans*, a major human fungal pathogen. *J. Microbiol.* **49**, 171–177 (2011).
- Brusselsaers, N., Blot, S. & Vogelaers, D. Deep-seated *Candida* infections in the intensive care unit. *Neth. J. Crit. Care* **15**, 183–189 (2011).
- Spellberg, B., Marr, K. A., Filler, S. G. *Candida*: What should clinicians and scientists be talking about? In: *Candida and Candidiasis, Second Edition*. (American Society of Microbiology, 2012).
- Horn, D. L. et al. Epidemiology and outcomes of Candidemia in 2019 patients: data from the prospective antifungal therapy alliance registry. *Clin. Infect. Dis.* **48**, 1695–1703 (2009).
- Perlotto, J., Choi, B. & Spellberg, B. Nosocomial fungal infections: epidemiology, diagnosis, and treatment. *Med Mycol.* **45**, 321–346 (2007).
- Martin, R. et al. The *Candida albicans*-specific gene *EED1* encodes a key regulator of hyphal extension. *PLoS ONE* **6**, e18394 (2011).
- Ernst, J. F. Transcription factors in *Candida albicans* – environmental control of morphogenesis. *Microbiology* **146**, 1763–1774 (2000).
- Cleary, I. A. et al. Examination of the pathogenic potential of *Candida albicans* filamentous cells in an animal model of haematogenously disseminated candidiasis. *FEMS Yeast Res.* **16**, <https://doi.org/10.1093/femsyr/fow011> (2016).
- Lorenz, M. C., Bender, J. A. & Fink, G. R. Transcriptional response of *Candida albicans* upon internalization by macrophages. *Eukaryot. Cell* **3**, 1076–1087 (2004).
- Rooney, P. J. & Klein, B. S. Linking fungal morphogenesis with virulence. *Cell Microbiol.* **4**, 127–137 (2002).
- Thompson, D. S., Carlisle, P. L. & Kadosh, D. Coevolution of morphology and virulence in *Candida* species. *Eukaryot. Cell* **10**, 1173–1182 (2011).
- Mukaremera, L., Lee, K. K., Mora-Montes, H. M. & Gow, N. A. R. *Candida albicans* yeast, pseudohyphal, and hyphal morphogenesis differentially affects immune recognition. *Front Immunol.* **8**, 629–629 (2017).
- Saville, S. P., Lazzell, A. L., Monteagudo, C. & Lopez-Ribot, J. L. Engineered control of cell morphology in vivo reveals distinct roles for yeast and filamentous forms of *Candida albicans* during infection. *Eukaryot. Cell* **2**, 1053–1060 (2003).
- Lo, H.-J. et al. Nonfilamentous *C. albicans* mutants are avirulent. *Cell* **90**, 939–949 (1997).
- Zheng, X., Wang, Y. & Wang, Y. Hgc1, a novel hypha-specific G1 cyclin-related protein regulates *Candida albicans* hyphal morphogenesis. *EMBO J.* **23**, 1845–1856 (2004).

17. Braun, B. R., Head, W. S., Wang, M. X. & Johnson, A. D. Identification and characterization of *TUP1*-regulated genes in *Candida albicans*. *Genetics* **156**, 31–44 (2000).
18. Braun, B. R., Kadosh, D. & Johnson, A. D. *NRG1*, a repressor of filamentous growth in *C. albicans*, is down-regulated during filament induction. *EMBO J.* **20**, 4753–4761 (2001).
19. Murad, A. M. et al. *NRG1* represses yeast-hypha morphogenesis and hypha-specific gene expression in *Candida albicans*. *EMBO J.* **20**, 4742–4752 (2001).
20. Zakikhany, K. et al. In vivo transcript profiling of *Candida albicans* identifies a gene essential for interepithelial dissemination. *Cell Microbiol* **9**, 2938–2954 (2007).
21. Polke, M. et al. A functional link between hyphal maintenance and quorum sensing in *Candida albicans*. *Mol. Microbiol* **103**, 595–617 (2017).
22. Allert, S. et al. *Candida albicans*-induced epithelial damage mediates translocation through intestinal barriers. *mBio* **9**, e00915–e00918 (2018).
23. Felk, A. et al. *Candida albicans* hyphal formation and the expression of the Efg1-regulated proteinases Sap4 to Sap6 are required for the invasion of parenchymal organs. *Infect. Immun.* **70**, 3689–3700 (2002).
24. Nucci, M. & Anaissie, E. Revisiting the source of candidemia: skin or gut? *Clin. Infect. Dis.* **33**, 1959–1967 (2001).
25. Miranda, L. N. et al. *Candida* colonisation as a source for candidaemia. *J. Hosp. Infect.* **72**, 9–16 (2009).
26. Owari, M., Wasa, M., Oue, T., Nose, S. & Fukuzawa, M. Glutamine prevents intestinal mucosal injury induced by cyclophosphamide in rats. *Pediatr. Surg. Int.* **28**, 299–303 (2012).
27. Koh, A. Y., Köhler, J. R., Cogshall, K. T., Van Rooijen, N. & Pier, G. B. Mucosal damage and neutropenia are required for *Candida albicans* dissemination. *PLoS Pathog.* **4**, e35 (2008).
28. Vautier, S. et al. *Candida albicans* colonization and dissemination from the murine gastrointestinal tract: the influence of morphology and Th17 immunity. *Cell Microbiol.* **17**, 445–450 (2015).
29. Román, E., Huertas, B., Prieto, D., Díez-Orejas, R. & Pla, J. *TUP1*-mediated filamentation in *Candida albicans* leads to inability to colonize the mouse gut. *Future Microbiol.* **13**, 857–867 (2018).
30. Bowman, J. C. et al. Quantitative PCR assay to measure *Aspergillus fumigatus* burden in a murine model of disseminated aspergillosis: demonstration of efficacy of caspofungin acetate. *Antimicrob. Agents Chemother.* **45**, 3474–3481 (2001).
31. Naglik, J., Albrecht, A., Bader, O. & Hube, B. *Candida albicans* proteinases and host/pathogen interactions. *Cell Microbiol* **6**, 915–926 (2004).
32. Du, H., Li, X., Huang, G., Kang, Y. & Zhu, L. The zinc-finger transcription factor, Of1, regulates white–opaque switching and filamentation in the yeast *Candida albicans*. *Acta Biochim. Biophys. Sin.* **47**, 335–341 (2015).
33. Wakade R. S., Ristow L. C., Stammes M. A., Kumar A., Krysan D. J. The Ndr1/LATS kinase Cbk1 regulates a specific subset of Ace2 functions and suppresses the hypha-to-yeast transition in *Candida albicans*. *mBio* **11**, e01900–20 (2020).
34. Su, C., Li, Y., Lu, Y. & Chen, J. Mss11, a transcriptional activator, is required for hyphal development in *Candida albicans*. *Eukaryot. Cell* **8**, 1780–1791 (2009).
35. Hao, B. et al. *Candida albicans* RFX2 encodes a DNA binding protein involved in DNA damage responses, morphogenesis, and virulence. *Eukaryot. Cell* **8**, 627–639 (2009).
36. Ene, I. V. et al. Phenotypic profiling reveals that *Candida albicans* opaque cells represent a metabolically specialized cell state compared to default white cells. *mBio* **7**, e01269–01216 (2016).
37. Kvaal, C. A., Srikantha, T. & Soll, D. R. Misexpression of the white-phase-specific gene *WH11* in the opaque phase of *Candida albicans* affects switching and virulence. *Infect. Immun.* **65**, 4468–4475 (1997).
38. Tao, L. et al. Discovery of a “White-Gray-Opaque” tristable phenotypic switching system in *Candida albicans*: roles of non-genetic diversity in host adaptation. *PLoS Biol.* **12**, e1001830 (2014).
39. McLroy David, R., Wagener, G., Lee, H. T. & Riou, B. Biomarkers of acute kidney injury: an evolving domain. *Anesthesiology* **112**, 998–1004 (2010).
40. Sabbiseti, V. S. et al. Novel assays for detection of urinary KIM-1 in mouse models of kidney injury. *Toxicol. Sci.* **131**, 13–25 (2013).
41. Leventhal, J. S. et al. Autophagy limits endotoxemic acute kidney injury and Alters renal tubular epithelial cell cytokine expression. *PLoS ONE* **11**, e0150001 (2016).
42. Singer, M. et al. The third international consensus definitions for sepsis and septic shock (Sepsis-3). *JAMA* **315**, 801–810 (2016).
43. Kadosh, D. Control of *Candida albicans* morphology and pathogenicity by post-transcriptional mechanisms. *Cell Mol. Life Sci.* **73**, 4265–4278 (2016).
44. Desai, J. V. *Candida albicans* hyphae: from growth initiation to invasion. *J. Fungi (Basel)* **4**, 10–19 (2018).
45. Böhm, L. et al. The yeast form of the fungus *Candida albicans* promotes persistence in the gut of gnotobiotic mice. *PLoS Pathog.* **13**, e1006699 (2017).
46. Witchley, J. N. et al. *Candida albicans* morphogenesis programs control the balance between gut commensalism and invasive infection. *Cell Host Microbe* **25**, 432–443.e436 (2019).
47. Albac, S. et al. *Candida albicans* is able to use M cells as a portal of entry across the intestinal barrier in vitro. *Cell Microbiol* **18**, 195–210 (2016).
48. Spellberg, B., Ibrahim, A. S., Edwards, J. E. Jr. & Filler, S. G. Mice with disseminated candidiasis die of progressive sepsis. *J. Infect. Dis.* **192**, 336–343 (2005).
49. Lionakis, M. S., Lim, J. K., Lee, C. C. & Murphy, P. M. Organ-specific innate immune responses in a mouse model of invasive candidiasis. *J. Innate Immun.* **78**, 3, 180–199 (2011).
50. Wächtler, B., Wilson, D., Haedicke, K., Dalle, F. & Hube, B. From attachment to damage: defined genes of *Candida albicans* mediate adhesion, invasion and damage during interaction with oral epithelial cells. *PLoS ONE* **6**, e17046 (2011).
51. McKenzie, C. G. et al. Contribution of *Candida albicans* cell wall components to recognition by and escape from murine macrophages. *Infect. Immun.* **78**, 1650–1658 (2010).
52. Blasi, E., Pitzurra, L., Bartoli, A., Puliti, M. & Bistoni, F. Tumor necrosis factor as an autocrine and paracrine signal controlling the macrophage secretory response to *Candida albicans*. *Infect. Immun.* **62**, 1199–1206 (1994).
53. Brown, A. J. P., Brown, G. D., Netea, M. G. & Gow, N. A. R. Metabolism impacts upon *Candida* immunogenicity and pathogenicity at multiple levels. *Trends Microbiol* **22**, 614–622 (2014).
54. Askew, C. et al. Transcriptional regulation of carbohydrate metabolism in the human pathogen *Candida albicans*. *PLoS Pathog.* **5**, e1000612 (2009).
55. Sandai, D. et al. The evolutionary rewiring of ubiquitination targets has reprogrammed the regulation of carbon assimilation in the pathogenic yeast *Candida albicans*. *mBio* **3**, e00495–00412 (2012).
56. Ballou, E. R. et al. Lactate signalling regulates fungal β -glucan masking and immune evasion. *Nat. Microbiol* **2**, 16238–16238 (2016).
57. Childers, D. S. et al. The rewiring of ubiquitination targets in a pathogenic yeast promotes metabolic flexibility, host colonization and virulence. *PLoS Pathog.* **12**, e1005566 (2016).
58. Ene, I. V., Brunke, S., AJP, Brown & Hube, B. Metabolism in fungal pathogenesis. *Cold Spring Harb. Perspect. Med.* **4**, a019695 (2014).
59. Miramón, P. & Lorenz, M. C. A feast for *Candida*: metabolic plasticity confers an edge for virulence. *PLoS Pathog.* **13**, e1006144 (2017).
60. Meiller, T. F. et al. A novel immune evasion strategy of *Candida albicans*: proteolytic cleavage of a salivary antimicrobial peptide. *PLoS ONE* **4**, e5039 (2009).
61. Gropp, K. et al. The yeast *Candida albicans* evades human complement attack by secretion of aspartic proteases. *Mol. Immunol.* **47**, 465–475 (2009).
62. Schild, L. et al. Proteolytic cleavage of covalently linked cell wall proteins by *Candida albicans* Sap9 and Sap10. *Eukaryot. Cell* **10**, 98–109 (2011).
63. Simpson, D. P. Citrate excretion: a window on renal metabolism. *Am. J. Physiol.* **244**, F223–F234 (1983).
64. Kochanowski, K., Sauer, U. & Noor, E. Posttranslational regulation of microbial metabolism. *Curr. Opin. Microbiol* **27**, 10–17 (2015).
65. Leach, M. D. & Brown, A. J. Posttranslational modifications of proteins in the pathobiology of medically relevant fungi. *Eukaryot. Cell* **11**, 98–108 (2012).
66. Swidergall, M. et al. Candidalysin is required for neutrophil recruitment and virulence during systemic *Candida albicans* infection. *J. Infect. Dis.* **220**, 1477–1488 (2019).
67. Angeletti S. et al. Plasma neutrophil gelatinase-associated lipocalin (NGAL) in combination with procalcitonin (PCT) and MR-proadrenomedullin (MR-proADM) in the diagnosis and prognosis of sepsis and sepsis associated acute kidney injury. *J. Immunol. Tech. Infect. Dis.* **5**, https://www.scitechnol.com/peer-review/plasma-neutrophil-gelatinaseassociated-lipocalin-ngal-incombination-with-procalcitonin-pct-and-mrproadrenomedullin-mrproadm-in-the-d-mrMK.php?article_id=4674 (2016).
68. Horst, S. A. et al. Prognostic value and therapeutic potential of TREM-1 in *Streptococcus pyogenes*-induced sepsis. *J. Innate Immun.* **5**, 581–590 (2013).
69. Boulanger, Y., Ghuysen, M.-S., Nchimi, A., Lewin, M. & Khamis, J. Ultrasound diagnosis and follow-up of neonate renal candidiasis. *J. Belg. Soc. Radio.* **100**, 113–113 (2016).
70. Banerjee, M. et al. *UME6*, a novel filament-specific regulator of *Candida albicans* hyphal extension and virulence. *Mol. Biol. Cell* **19**, 1354–1365 (2008).
71. Spiering, M. J. et al. Comparative transcript profiling of *Candida albicans* and *Candida dubliniensis* identifies *SFL2*, a *C. albicans* gene required for virulence in a reconstituted epithelial infection model. *Eukaryot. Cell* **9**, 251–265 (2010).
72. McCall, A. D., Kumar, R. & Edgerton, M. *Candida albicans* Sfl1/Sfl2 regulatory network drives the formation of pathogenic microcolonies. *PLoS Pathog.* **14**, e1007316 (2018).
73. Noble, S. M., French, S., Kohn, L. A., Chen, V. & Johnson, A. D. Systematic screens of a *Candida albicans* homozygous deletion library decouple morphogenetic switching and pathogenicity. *Nat. Genet.* **42**, 590–600 (2010).

74. Saville, S. P., Lazzell, A. L., Chaturvedi, A. K., Montegudo, C. & Lopez-Ribot, J. L. Efficacy of a genetically engineered *Candida albicans tet-NRG1* strain as an experimental live attenuated vaccine against hematogenously disseminated candidiasis. *Clin. Vaccin. Immunol.* **16**, 430–432 (2009).
75. Saville, S. P., Lazzell, A. L., Chaturvedi, A. K., Montegudo, C. & Lopez-Ribot, J. L. Use of a genetically engineered strain to evaluate the pathogenic potential of yeast cell and filamentous forms during *Candida albicans* systemic infection in immunodeficient mice. *Infect. Immun.* **76**, 97–102 (2008).
76. MacCallum, D. M. & Odds, F. C. Temporal events in the intravenous challenge model for experimental *Candida albicans* infections in female mice. *Mycoses* **48**, 151–161 (2005).
77. Odds, F. C., Van Nuffel, L. & Gow, N. A. R. Survival in experimental *Candida albicans* infections depends on inoculum growth conditions as well as animal host. *Microbiology* **146**, 1881–1889 (2000).
78. Yapar, N. Epidemiology and risk factors for invasive candidiasis. *Ther. Clin. Risk Manag* **10**, 95–105 (2014).
79. Ho H.-I. & Haynes K. *Candida glabrata*: new tools and technologies—expanding the toolkit. *FEMS Yeast Res.* **15**, fov066, <https://doi.org/10.1093/femsyr/fov066> (2015).
80. Bravo Ruiz, G., Ross, Z. K., Gow, N. A. R. & Lorenz, A. Pseudohyphal growth of the emerging pathogen *Candida auris* Is triggered by genotoxic stress through the S phase checkpoint. *mSphere* **5**, e00151–00120 (2020).
81. Sil, A. & Andrianopoulos, A. Thermally dimorphic human fungal pathogens—polyphyletic pathogens with a convergent pathogenicity trait. *Cold Spring Harb. Perspect. Med.* **5**, a019794 (2014).
82. Nakayama, H. et al. Tetracycline-regulatable system to tightly control gene expression in the pathogenic fungus *Candida albicans*. *Infect. Immun.* **68**, 6712–6719 (2000).
83. Reuß, O., Vik, Å., Kolter, R. & Morschhäuser, J. The SAT1 flipper, an optimized tool for gene disruption in *Candida albicans*. *Gene* **341**, 119–127 (2004).
84. Gillum, A. M., Tsay, E. Y. H. & Kirsch, D. R. Isolation of the *Candida albicans* gene for orotidine-5'-phosphate decarboxylase by complementation of *S. cerevisiae ura3* and *E. coli pyrF* mutations. *MGG* **198**, 179–182 (1984).
85. Afgan, E. et al. The Galaxy platform for accessible, reproducible and collaborative biomedical analyses: 2018 update. *Nucleic Acids Res.* **46**, W537–w544 (2018).
86. Love, M. I., Huber, W. & Anders, S. Moderated estimation of fold change and dispersion for RNA-seq data with DESeq2. *Genome Biol.* **15**, 550–571 (2014).
87. Skrzypek, M. S. et al. The *Candida* Genome Database (CGD): incorporation of Assembly 22, systematic identifiers and visualization of high throughput sequencing data. *Nucleic Acids Res.* **45**, D592–D596 (2017).
88. Supek, F., Bošnjak, M., Škunca, N. & Šmuc, T. REVIGO summarizes and visualizes long lists of gene ontology terms. *PLOS ONE* **6**, e21800 (2011).
89. Shannon, P. et al. Cytoscape: a software environment for integrated models of biomolecular interaction networks. *Genome Res* **13**, 2498–2504 (2003).
90. Han, Y. & Cutler, J. E. Assessment of a mouse model of neutropenia and the effect of an anti-candidiasis monoclonal antibody in these animals. *J. Infect. Dis.* **175**, 1169–1175 (1997).
91. Ermert, D. et al. Mouse neutrophil extracellular traps in microbial infections. *J. Innate Immun.* **1**, 181–193 (2009).

Acknowledgements

We would like to thank Birgit Weber, Nadja Jablonowski, Stephanie Wisgott and Elisabeth Rättsch for excellent technical assistance. Furthermore, we want to thank all members of the Research Group Microbial Immunology (HKI) for technical support with the animal

experiments as well as the Department of Microbial Pathogenicity Mechanisms (HKI) and Franziska Gerwien for encouraging discussions. The work was financially supported by the German Research Foundation (DFG; JA1960/1-1 to IDJ); and in part through the TRR 124 FungiNet, “Pathogenic fungi and their human host: Networks of Interaction,” DFG project number 210879364, Project C5 to IDJ and B2 to TD). CD was supported by the International Leibniz Research School for Microbial and Biomolecular Interactions (ILRS). M.S. was supported in part by NIH grant R00DE026856.

Author contributions

Conception and design of the study was performed by C.D., M.P. and I.D.J. All authors contributed with data acquisition and analysis: C.D., M.P., B.S., K.S., S.R., A.E.G., T.P., S.S., R.M. and I.D.J. were involved in animal experiments; T.P. and A.G. performed epithelial co-infections; C.D. and B.S. performed flow cytometry; M.S. performed immunohistochemistry; C.D., K.S. and M.I.N. performed neutrophil experiments. C.D. and K.S. prepared samples for RNAseq. J.P.P. and T.D. performed differential gene expression analysis. Data were interpreted by C.D., M.P., B.S., T.P., M.S., S.R., A.E.G. and I.D.J. C.D. and I.D.J. wrote and all authors commented on the manuscript.

Funding

Open Access funding enabled and organized by Projekt DEAL.

Competing interests

The authors declare no competing interests.

Additional information

Supplementary information The online version contains supplementary material available at <https://doi.org/10.1038/s41467-021-24095-8>.

Correspondence and requests for materials should be addressed to I.D.J.

Peer review information *Nature Communications* thanks the anonymous reviewers for their contribution to the peer review of this work. Peer reviewer reports are available.

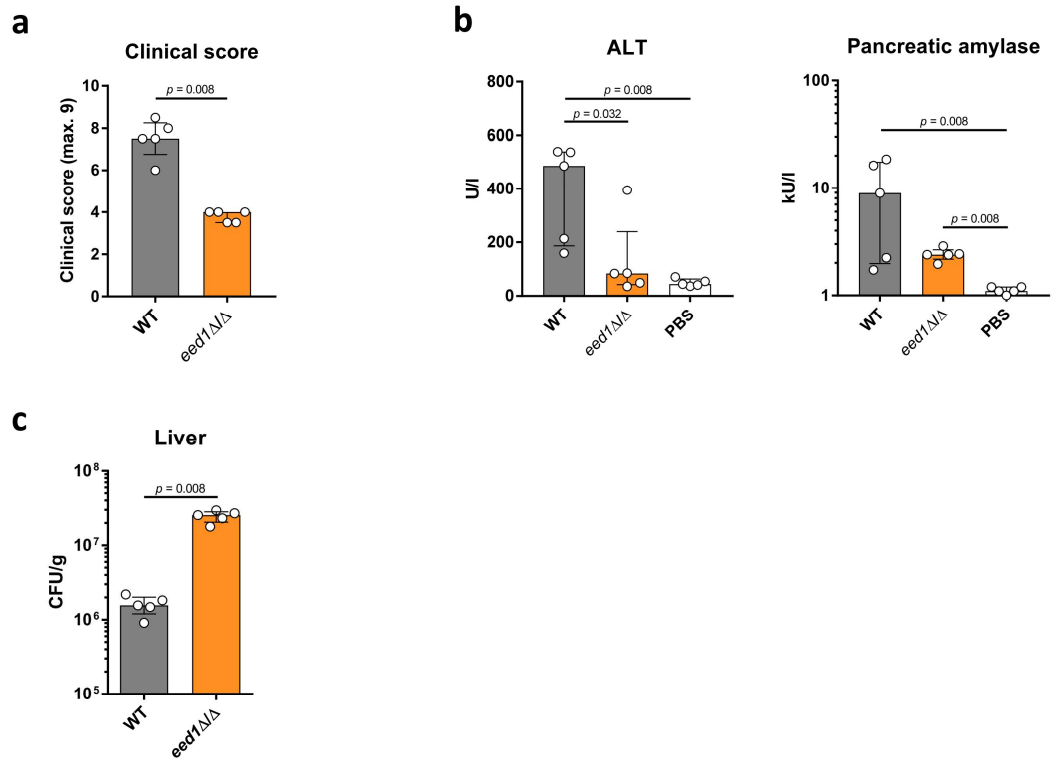
Reprints and permission information is available at <http://www.nature.com/reprints>

Publisher's note Springer Nature remains neutral with regard to jurisdictional claims in published maps and institutional affiliations.

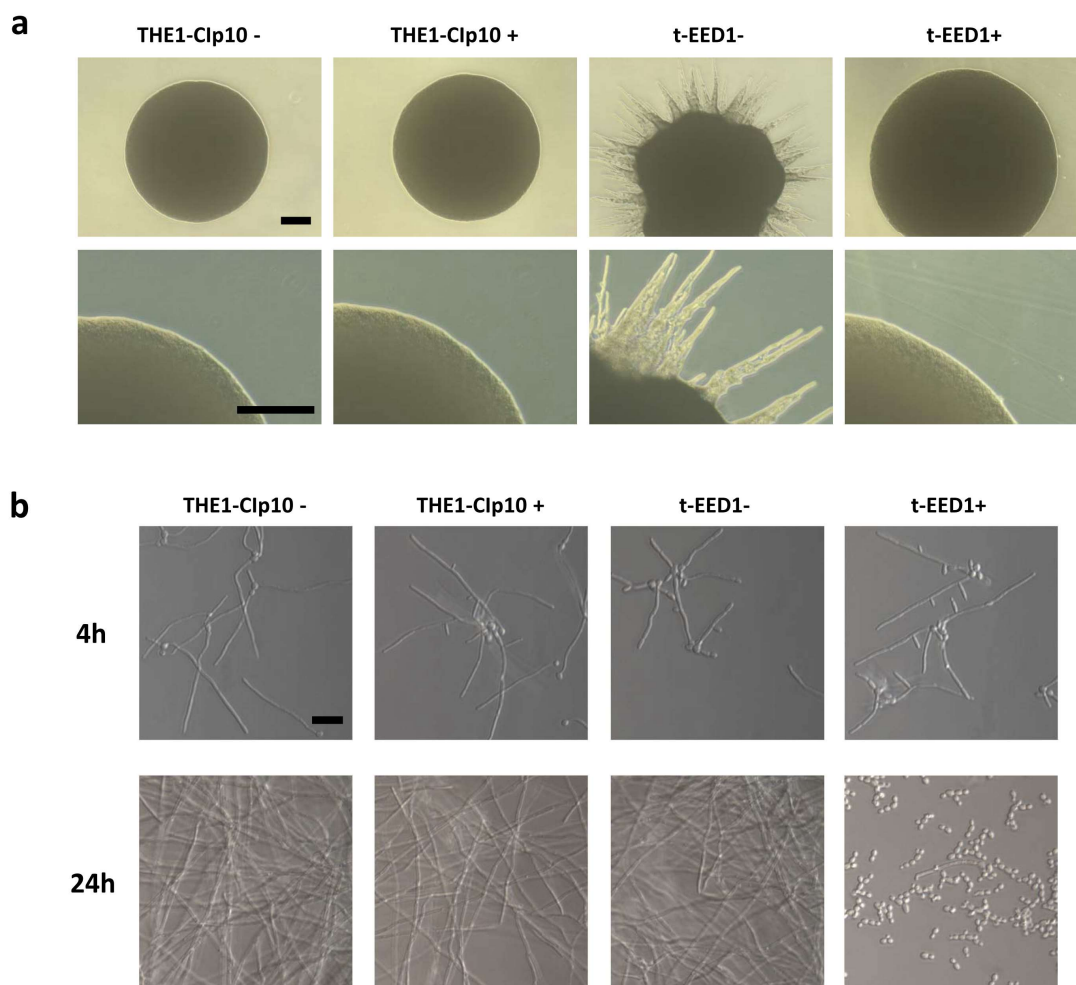


Open Access This article is licensed under a Creative Commons Attribution 4.0 International License, which permits use, sharing, adaptation, distribution and reproduction in any medium or format, as long as you give appropriate credit to the original author(s) and the source, provide a link to the Creative Commons license, and indicate if changes were made. The images or other third party material in this article are included in the article's Creative Commons license, unless indicated otherwise in a credit line to the material. If material is not included in the article's Creative Commons license and your intended use is not permitted by statutory regulation or exceeds the permitted use, you will need to obtain permission directly from the copyright holder. To view a copy of this license, visit <http://creativecommons.org/licenses/by/4.0/>.

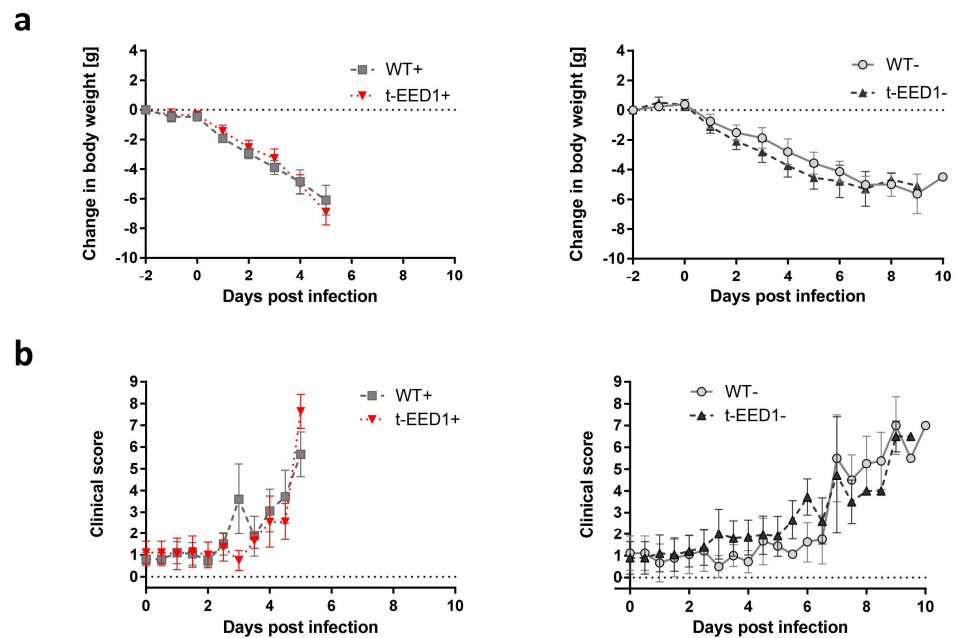
© The Author(s) 2021



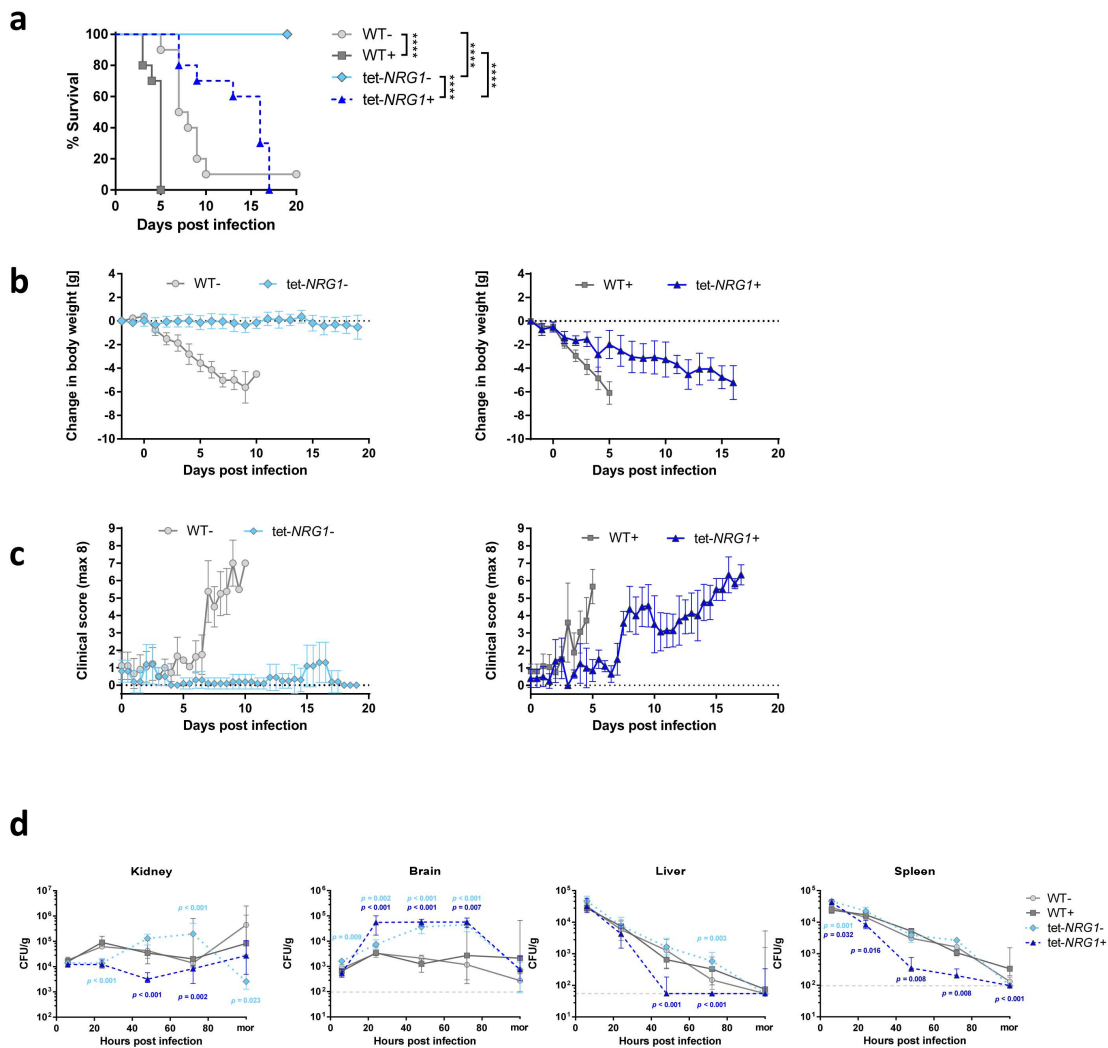
Supplementary Fig. 1 An *eed1Δ/Δ* mutant is attenuated in damage and virulence potential in the intraperitoneal infection model 24 h post infection. Mice were infected intraperitoneally with 1×10^8 cells of the WT (SC5314), or *eed1Δ/Δ* mutant or were mock infected with PBS (n=5 per group). a) The semiquantitative clinical score was determined by assessing fur, coat and posture, behavior and lethargy, fibrin exudation and other symptoms like diarrhea. The score ranges from 0 (no symptoms) to 10 (severe illness). b) Damage of liver and pancreas was quantified by measuring serum levels of alanine aminotransaminase (ALT) and pancreatic amylase, respectively. c) Fungal burden of the liver. a-c) Data are shown as median with interquartile range and were statistically analyzed using the two-sided Mann-Whitney test, *p*-values are shown in the graphs. Source data are provided as a Source Data file.



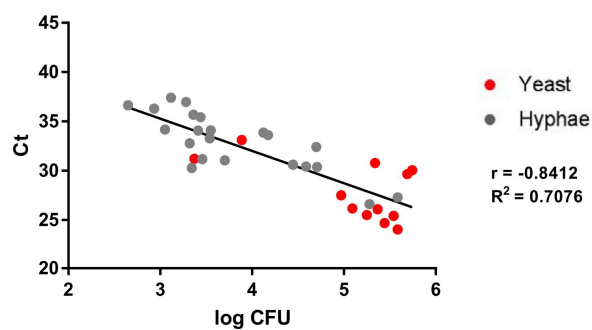
Supplementary Fig. 2 In the absence of doxycycline t-EED1 is hyper-filamentous on solid medium but forms filaments comparable to the WT in liquid medium. Representative pictures of three biologically independent experiments are shown. a) Colony morphology of *C. albicans* WT (THE1-Clp10) and t-EED1 grown for 2 days on YPD agar at 25 °C in the presence (+) or absence (-) of doxycycline. Bars represent 200 μm (upper row) and 100 μm (lower row). b) Morphology of *C. albicans* WT (THE1-Clp10) and t-EED1 grown for 4 h and 24 h in RPMI at 37 °C and 5% CO₂ in the presence (+) or absence (-) of doxycycline. Scale bar represents 20 μm and applies to all images.



Supplementary Fig. 3 Development of clinical symptoms and change in body weight during the course of systemic infection with WT and t-EED1. Mice were intravenously infected with 2.5×10^4 CFU/g body weight with WT (THE1-Clp10) or t-EED1 in the presence (+) or absence of doxycycline (-) supplied to mice via the drinking water. a) Change in body weight relative to body weight at day-3 (start of doxycycline treatment). At day 0, mice were infected intravenously with the indicated *C. albicans* strains. b) Development of clinical symptoms during the course of infection. The semiquantitative clinical score was determined by assessing fur, body surface temperature, behavior and lethargy. The score ranges from 0 (no symptoms) to 8 (severe illness). a,b) Shown is the mean \pm SD. One experiment, n=10 mice per group. The surviving mouse in the WT- group (Fig. 3c) was excluded from analysis.

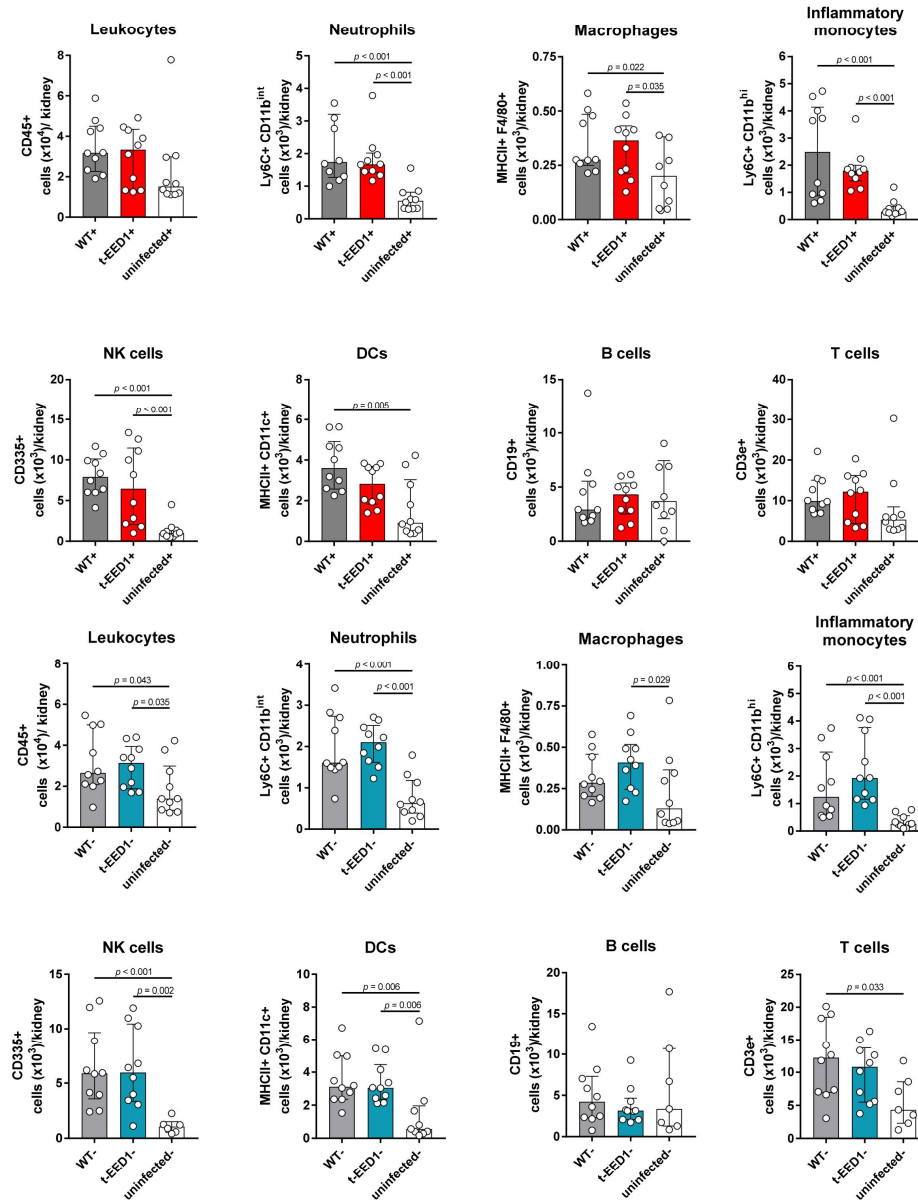


Supplementary Fig. 4: tet-*NRG1*- yeast are avirulent whereas tet-*NRG1*+ hyphae lead to delayed mortality in a mouse model of systemic candidiasis. Mice were intravenously infected with 2.5×10^4 CFU/g body weight with WT (THE1-Clp10) or tet-*NRG1* in the presence (+) or absence (-) of doxycycline supplied to mice via the drinking water. a) Survival was monitored over a period of 20 days and is shown as Kaplan-Meier curve. Survival curves were analyzed using the two-sided Log-rank (Mantel-Cox) test, two curves were compared at a time; **** $p < 0.0001$. b) Change in body weight relative to body weight at day -3 (start of doxycycline treatment). At day 0, mice were infected intravenously with the indicated *C. albicans* strains. c) Development of clinical symptoms during the course of infection. The semiquantitative clinical score was determined by assessing fur, body surface temperature, behavior and lethargy. The score ranges from 0 (no symptoms) to 8 (severe illness). a-c) Shown is the mean \pm SD. The surviving mouse in the WT- group was excluded from analysis. d) Organ fungal loads in mice sacrificed 6, 24, 48 and 72 h post infection and in moribund mice (mor). Mice challenged with tet-*NRG1*- were humanely sacrificed 19 days post infection. Data are shown as median with interquartile range. Dashed lines indicate limit of detection. Moribund: one experiment, $n=10$; kidney: two independent experiments, $n=10$; liver and brain: two independent experiments, $n=10$; spleen: one experiment, $n=5$. Two-sided Mann-Whitney test, significant differences at time points are indicated by asterisks: light blue, tet-*NRG1*- yeast compared to WT-; dark blue, tet-*NRG1*+ filamentous cells compared to WT+. Source data are provided as a Source Data file.



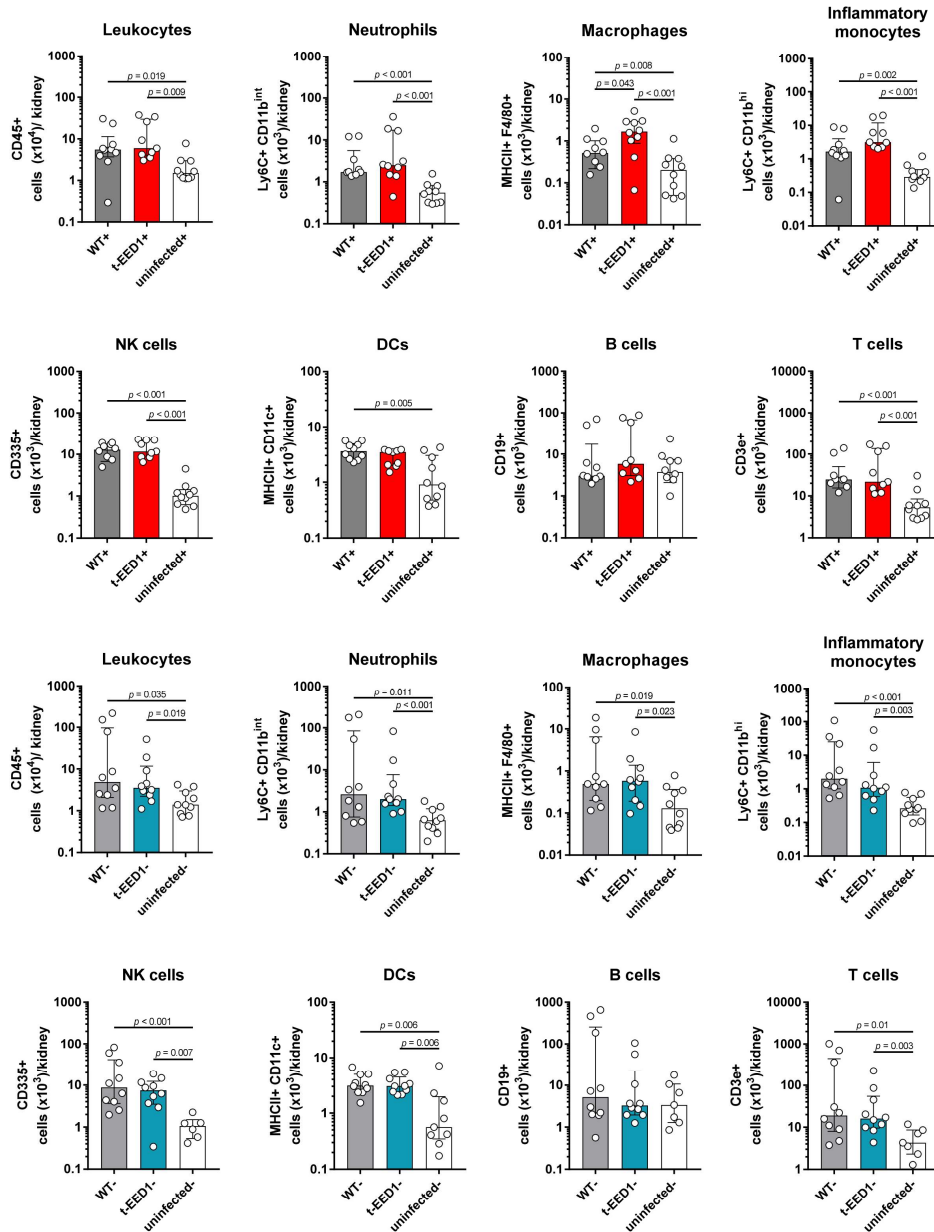
Supplementary Fig. 5 Correlation between fungal DNA content and CFU count from homogenized renal tissues of intravenously infected mice. Renal tissue was homogenized for enumeration of CFU and for DNA isolation to quantitative fungal DNA by PCR, targeting the *C. albicans* 18S rRNA gene *RDN18*. The resulting cycle threshold (Ct) values were plotted against the log transformed CFU counts from the respective samples. A strong correlation ($R^2=0.7076$) between CFU count and DNA content irrespective of the fungal morphology was observed. Source data are provided as a Source Data file.

Kidney infiltrating leukocytes 24 h p.i.



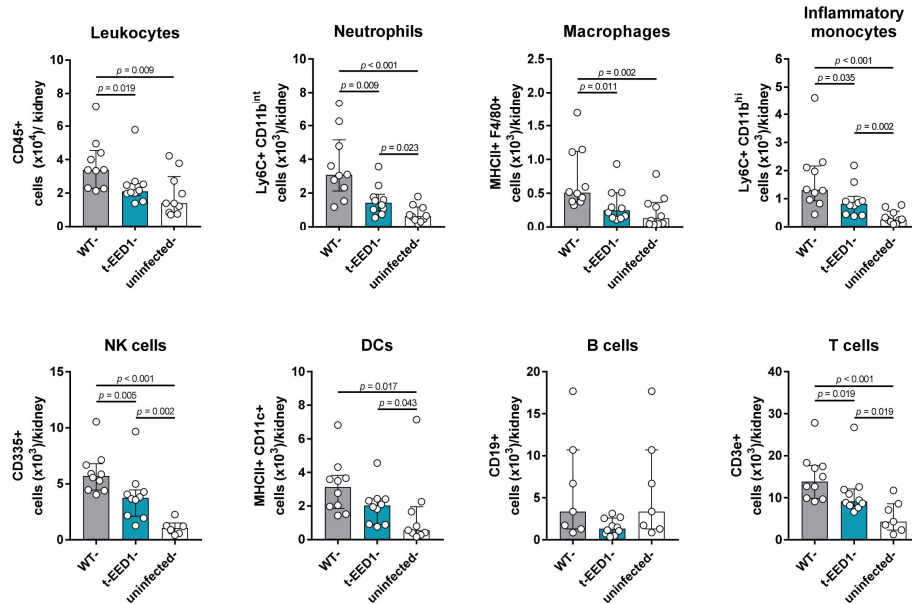
Supplementary Fig. 6 Renal leukocyte infiltration in mice intravenously infected with 2.5×10^4 CFU/g body weight of WT or t-EED1 and in uninfected controls in the presence (+) or absence of doxycycline (-) 24 h post infection. The absolute number of living immune cells per kidney is shown as median and interquartile range. Two independent experiments, $n=10$, except for uninfected- NK cells $n=6$, DCs $n=9$, B cells and T cells $n=7$. Two-sided Mann-Whitney test, p -values are shown in the graphs. Source data are provided as a Source Data file.

Kidney infiltrating leukocytes 48 h p.i.

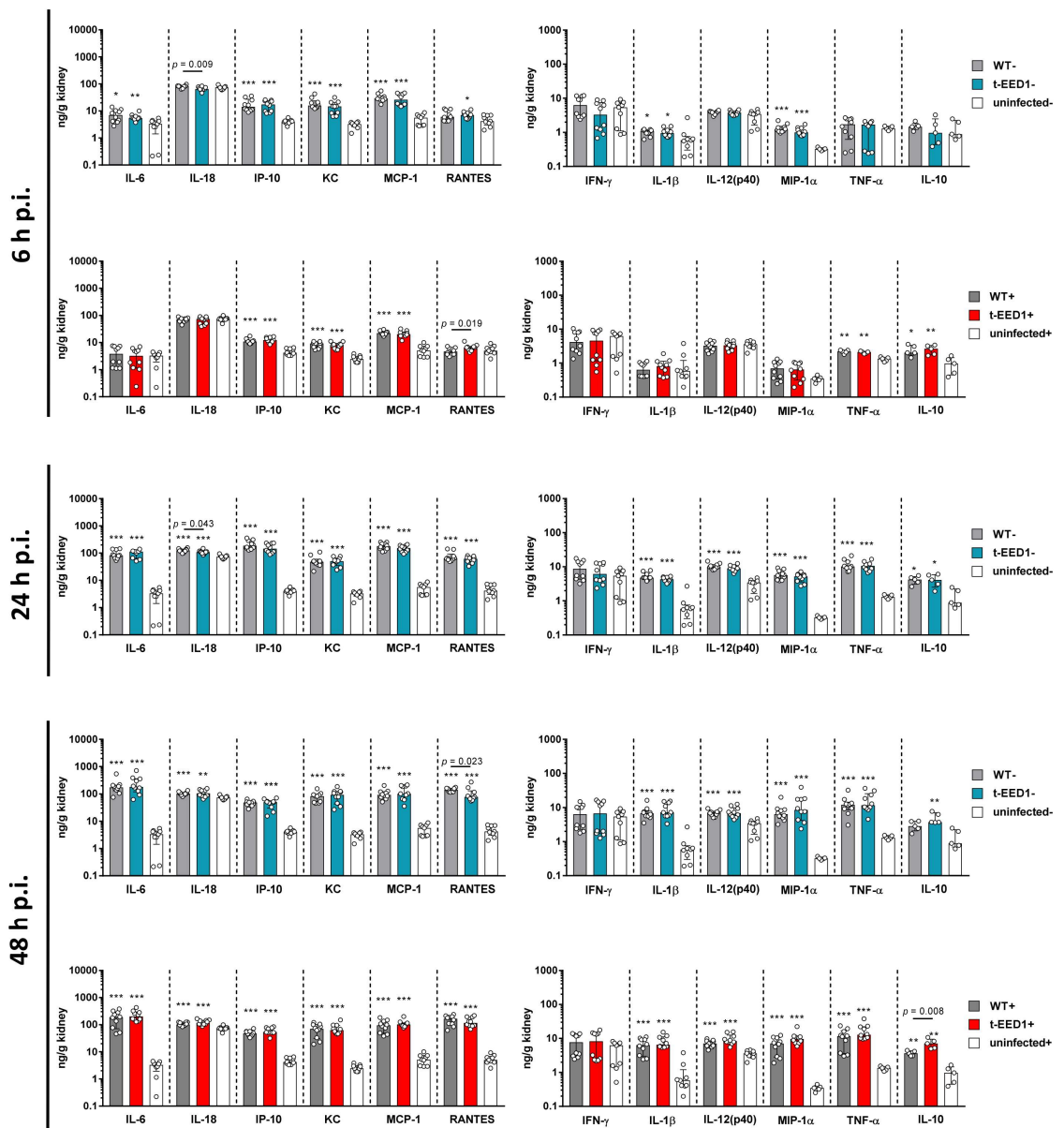


Supplementary Fig. 7 Renal leukocyte infiltration in mice intravenously infected with 2.5×10^4 CFU/g body weight of WT or t-EED1 and in uninfected controls in the presence (+) or absence of doxycycline (-) 48 h post infection. The absolute number of living immune cells per kidney is shown as median and interquartile range. Two independent experiments, $n=10$, except for t-EED1+ $n=9$ and uninfected- NK cells $n=6$, DCs $n=9$, B cells and T cells $n=7$. Two-sided Mann-Whitney test, p -values are shown in the graphs. Source data are provided as a Source Data file.

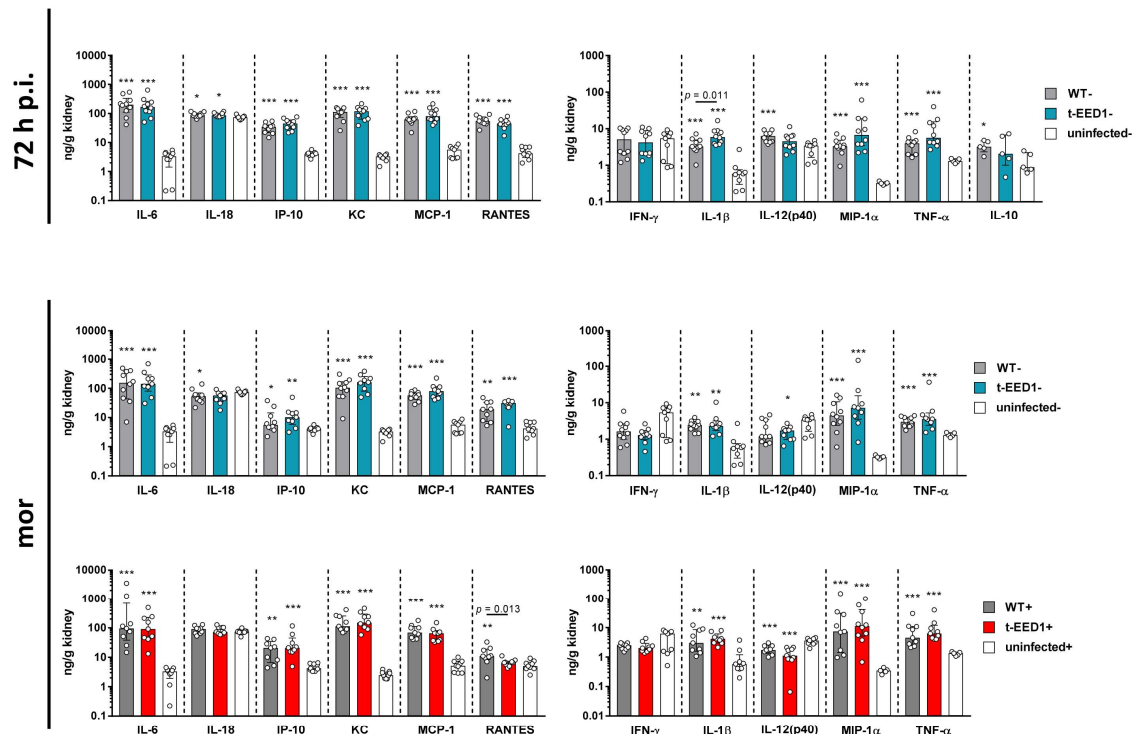
Kidney infiltrating leukocytes 72 h p.i.



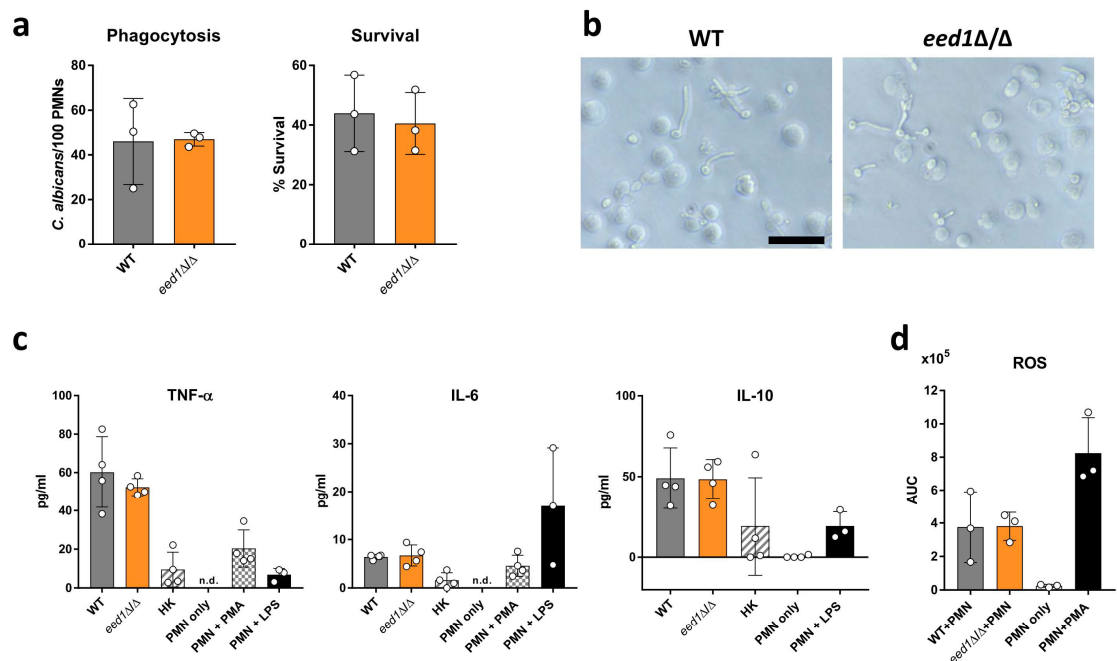
Supplementary Fig. 8 Renal leukocyte infiltration in mice intravenously infected with 2.5×10^4 CFU/g body weight of WT or t-EED1 and in uninfected controls in absence of doxycycline (-) 72 h post infection. The absolute number of living immune cells per kidney is shown as median and interquartile range. Two independent experiments, $n=10$, except for uninfected- NK cells $n=6$, DCs $n=9$, B cells and T cells $n=7$. Two-sided Mann-Whitney test, p -values are shown in the graphs. Source data are provided as a Source Data file.



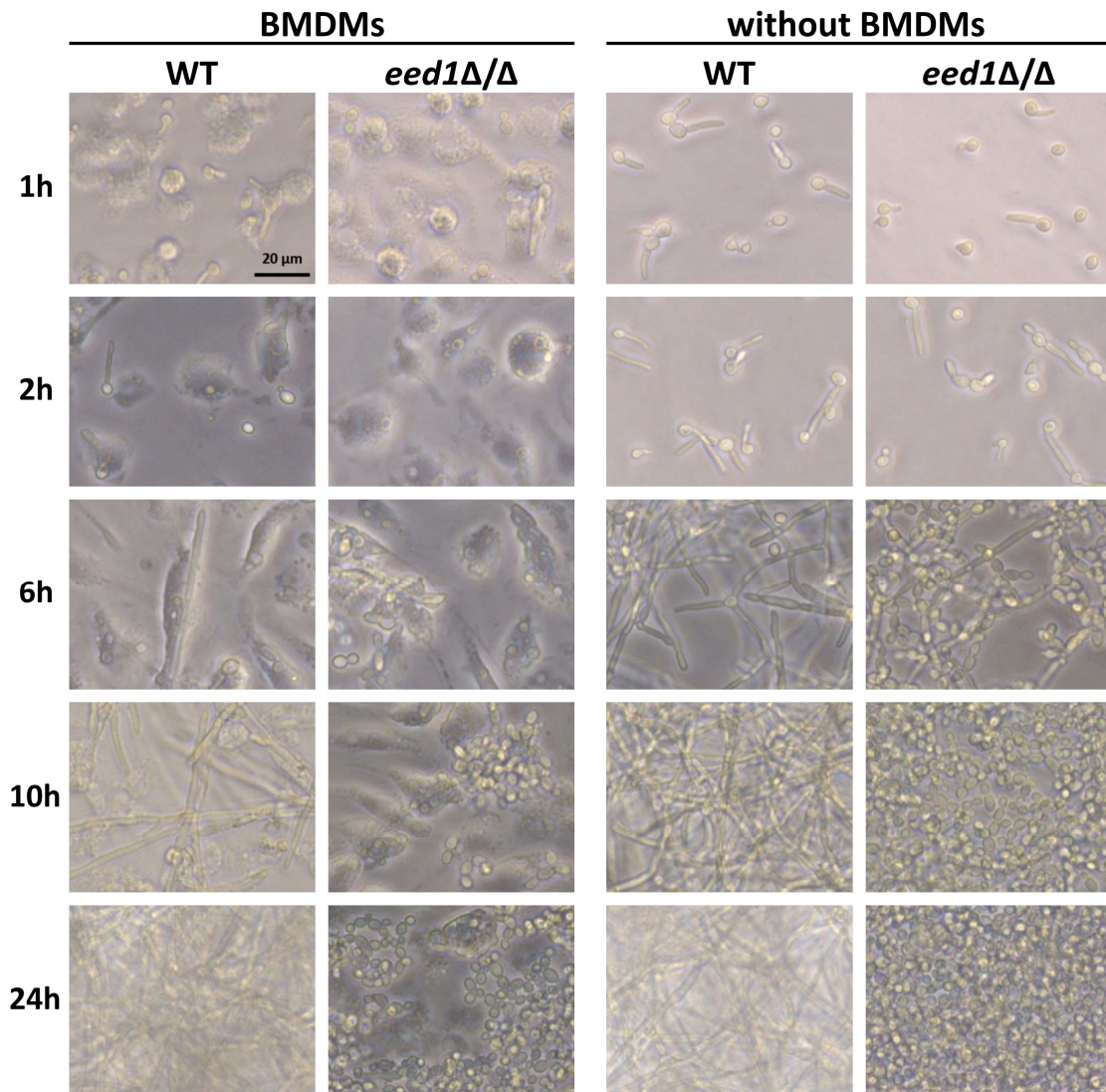
Supplementary Fig. 9 Local cytokine production in kidneys of mice intravenously infected with 2.5×10^4 CFU/g body weight of WT or t-EED1 6, 24, 48 h post infection and in uninfected controls in the presence (+) or absence of doxycycline (-). Cytokine concentrations were determined in kidney homogenates. Shown is the median with interquartile range from two independent experiments. $n=10$, except for uninfected controls $n=9$; MIP-1 α , TNF- α uninfected controls $n=5$. IL-10 data derived from one experiment, $n=5$. Two-sided Mann-Whitney test. Asterisks above bars represent significant differences compared to the uninfected control, * $p \leq 0.05$; ** $p \leq 0.01$; *** $p \leq 0.001$. Source data are provided as a Source Data file.



Supplementary Fig. 10 Local cytokine production in kidneys of mice intravenously infected with 2.5×10^4 CFU/g body weight of WT or t-EED1 72 h post infection, in moribund animals (mor) and in uninfected controls in the presence (+) or absence of doxycycline (-). Cytokine concentrations were determined in kidney homogenates. Shown is the median and interquartile range from two independent experiments. $n=10$, except for uninfected controls $n=9$; MIP-1 α , TNF- α uninfected controls $n=5$. IL-10 data derived from one experiment, $n=5$. Two-sided Mann-Whitney test. Asterisks above bars represent significant differences compared to the uninfected control, * $p \leq 0.05$; ** $p \leq 0.01$; *** $p \leq 0.001$. Source data are provided as a Source Data file.

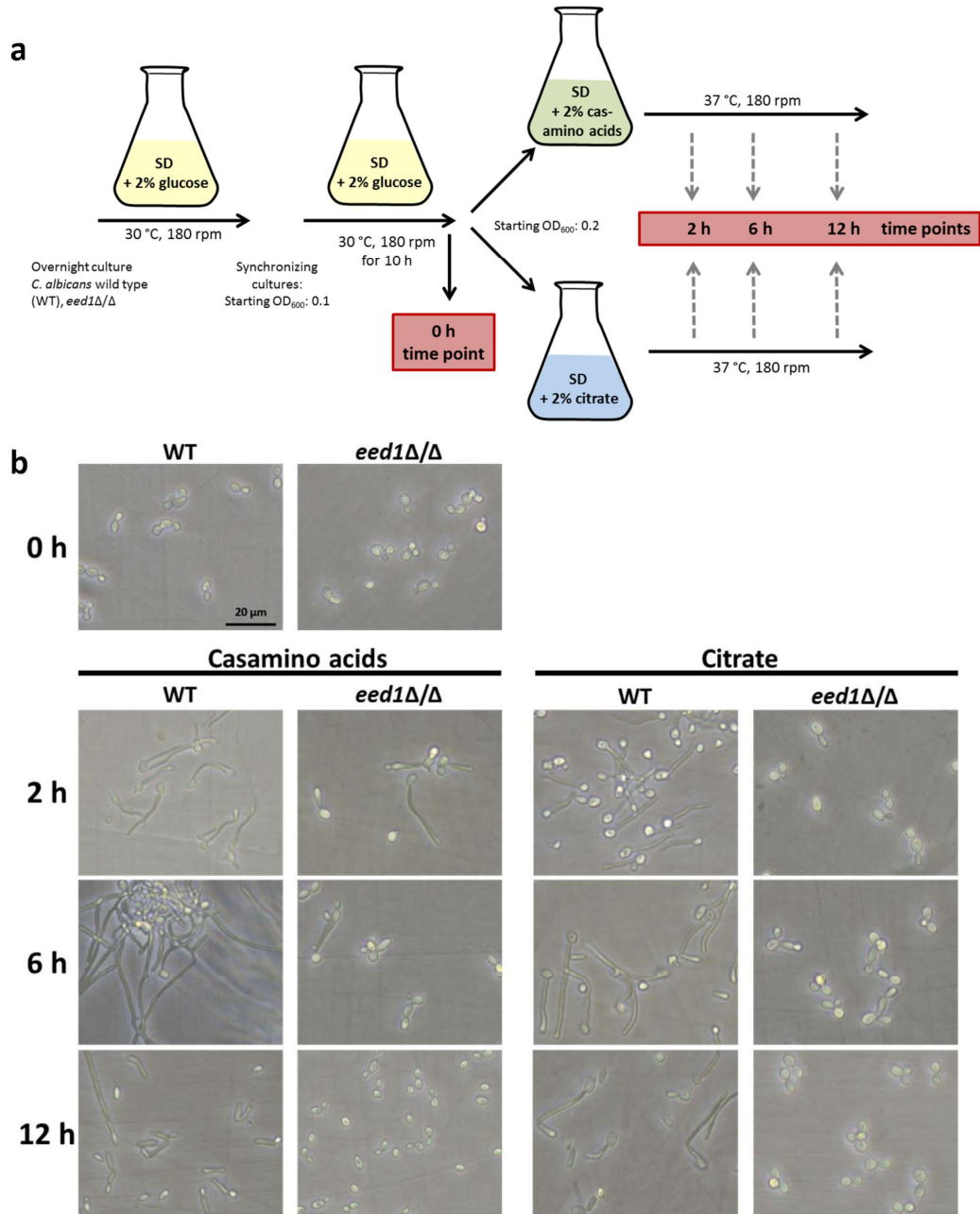


Supplementary Fig. 11 Interaction of *C. albicans* WT and *eed1Δ/Δ* mutant with murine bone marrow neutrophils (PMNs). PMNs were infected at a MOI of 1. a) The phagocytic index is the number of *C. albicans* cells phagocytosed by 100 PMNs within 1 h of incubation at 37 °C and 5% CO₂. Fungal survival was analyzed after co-incubation with PMNs at 37 °C and 5% CO₂ for 2 h by CFU plating. Survival was normalized to *C. albicans* controls incubated in the absence of immune cells. Graphs show the mean \pm SD of three independent biological replicates. b) Morphology of *C. albicans* strains during co-incubation with PMNs after 3 h. Representative pictures of two biologically independent experiments are shown. Scale bar represents 20 μ m and applies to all images. c) Cytokines released by PMNs after co-incubation for 24 h with living or heat-killed (HK) *C. albicans* WT cells. PMNs were left untreated (PMN only) as negative or stimulated with 100 nM PMA or 100 ng/ml LPS as positive controls. d) Release of reactive oxygen species (ROS) by PMNs upon stimulation with *C. albicans* was quantified by luminol-enhanced chemiluminescence assay in 2.5 min intervals over a period of 190 min using a microplate reader. The graph shows the calculated area under the curve (AUC). As negative and positive control, PMNs were left untreated or stimulated with 100 nM PMA, respectively. Shown is the mean \pm SD from a,d) three or c) four independent biological replicates except for PMN+LPS n=3. Source data are provided as a Source Data file.

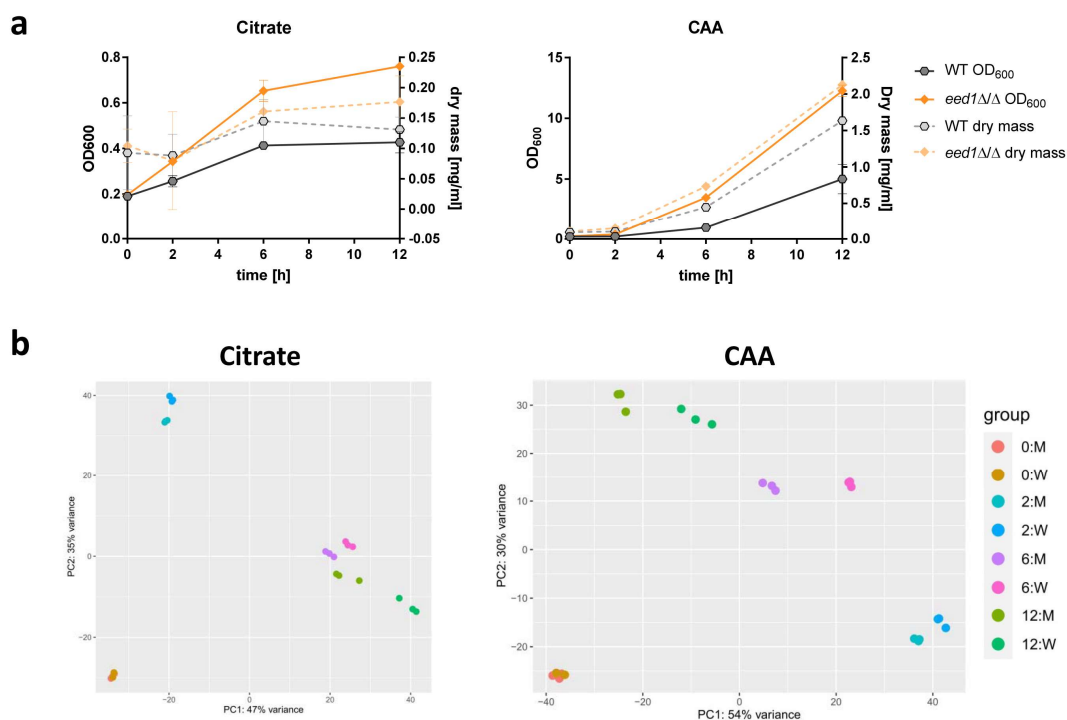


Supplementary Fig. 12 Morphology of *C. albicans* WT and *eed1Δ/Δ* mutant in the presence of bone marrow-derived macrophages (BMDMs; left) or without BMDMs (right). BMDMs were infected at a MOI of 1 and cells were incubated at 37 °C and 5% CO₂. Representative pictures of three biologically independent experiments are shown. Pictures were taken after various time points as indicated on the left. Scale bar applies to all images.

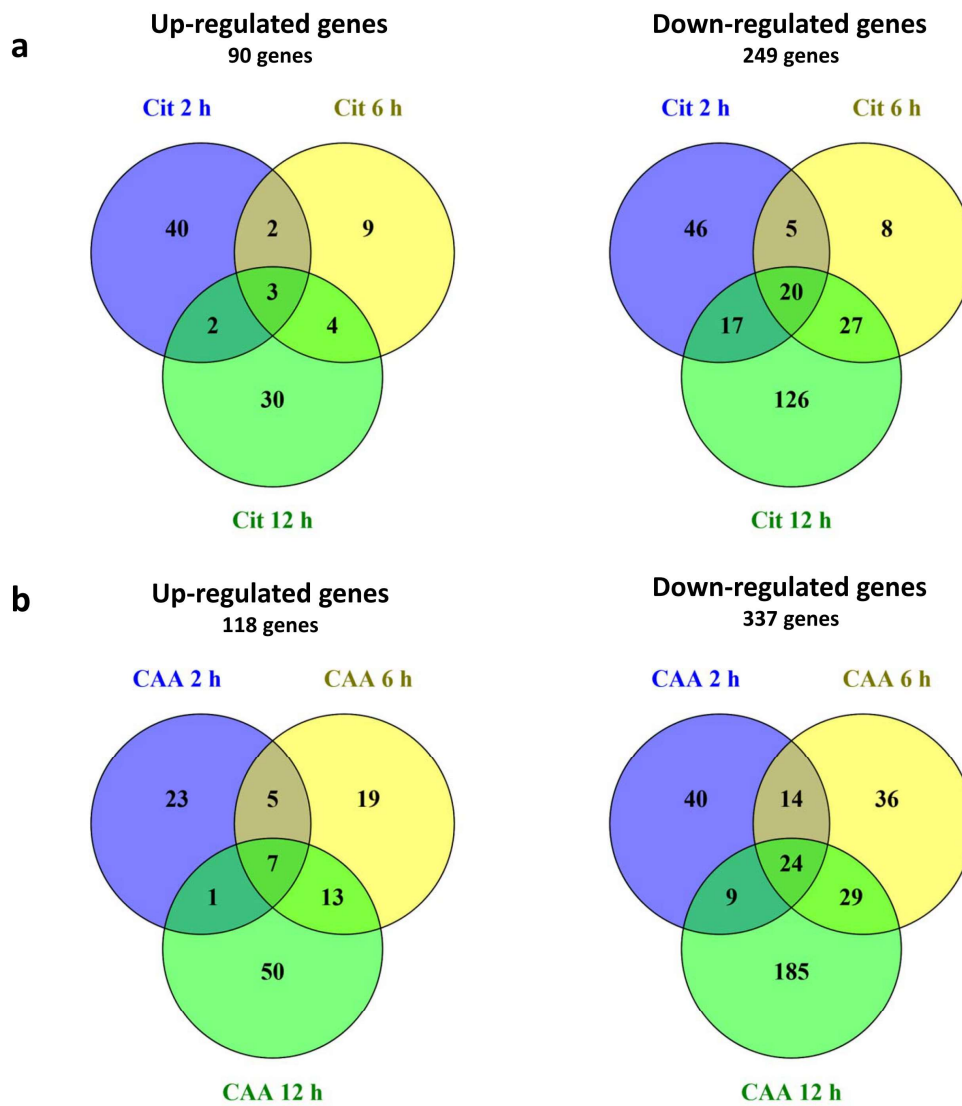
Supplementary Fig. 13



Supplementary Fig. 13 Sample preparation for RNAseq analysis and fungal morphology at the time of sampling. a) *C. albicans* WT (SC5314) and *eed1Δ/Δ* mutant were grown over night in Synthetic Minimal Media (SD) containing glucose as sole carbon source at 30 °C and 180 rpm. Cultures were synchronized in the same media and cultivated for 10 h at 30 °C (0 h). Cultures were then shifted to SD medium containing either casamino acids (CAA) or citrate as sole carbon source and incubated at 37 °C and 180 rpm. After 2 h, 6 h and 12 h samples were taken. b) Morphology of *C. albicans* WT (SC5314) and *eed1Δ/Δ* mutant during growth on citrate or casamino acids as sole carbon source at 37 °C and 180 rpm. Representative pictures of three biologically independent experiments are shown. The scale bar applies to all images.

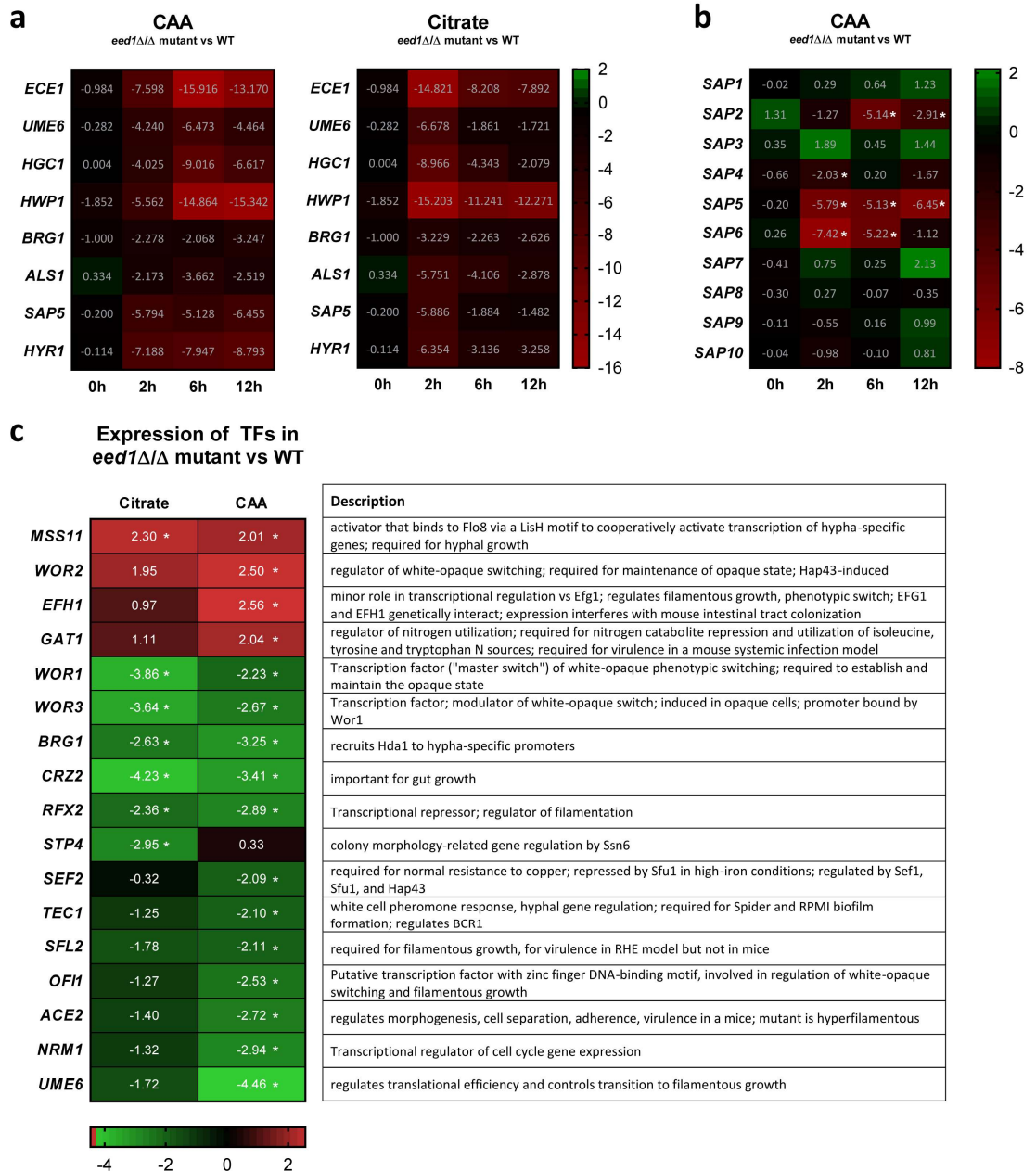


Supplementary Fig. 14 The *eed1Δ/Δ* mutant grows better on the alternative carbon sources citrate and casamino acids and shows differences in expression profiles compared to the WT. a) Growth of WT (SC5314) and *eed1Δ/Δ* mutant on citrate and casamino acids as sole carbon source at 37 °C and 180 rpm was recorded by OD measurement at 600 nm and the determination of dry mass. Mean \pm SD from three biologically independent experiments (one flask per strain and experiment) are shown. Source data are provided as a Source Data file. b) Principal component analysis (PCA) of expression data obtained by RNAseq from *C. albicans* WT (W; SC5314) and *eed1Δ/Δ* mutant (M) grown on citrate or casamino acids for 0, 2, 6 and 12 h.

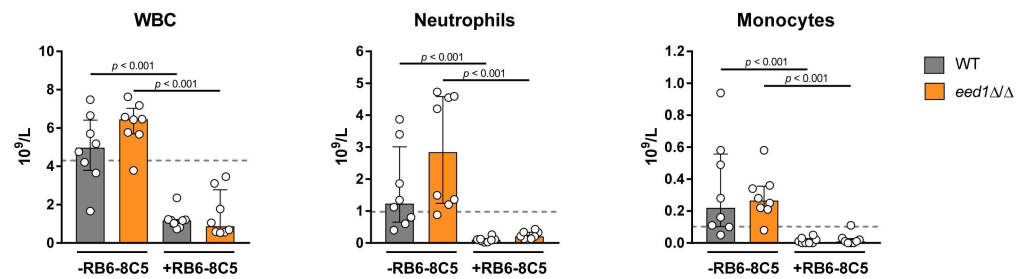


Supplementary Fig. 15 Venn diagrams showing the number of genes significantly up- and down-regulated ($\pm \log_2 2$ and adjusted p -value < 0.05) in the *eed1Δ/Δ* mutant compared to WT (SC5314) during growth for 2, 6 and 12 h with a) citrate (Cit) or b) casamino acids (CAA) as sole carbon source at 37 °C.

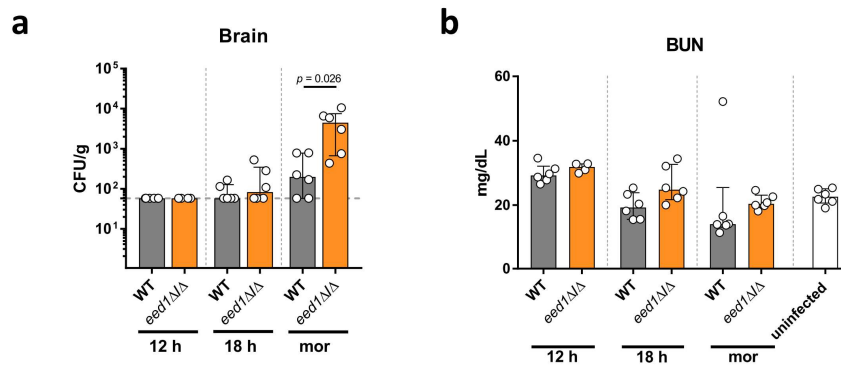
Supplementary Fig. 16



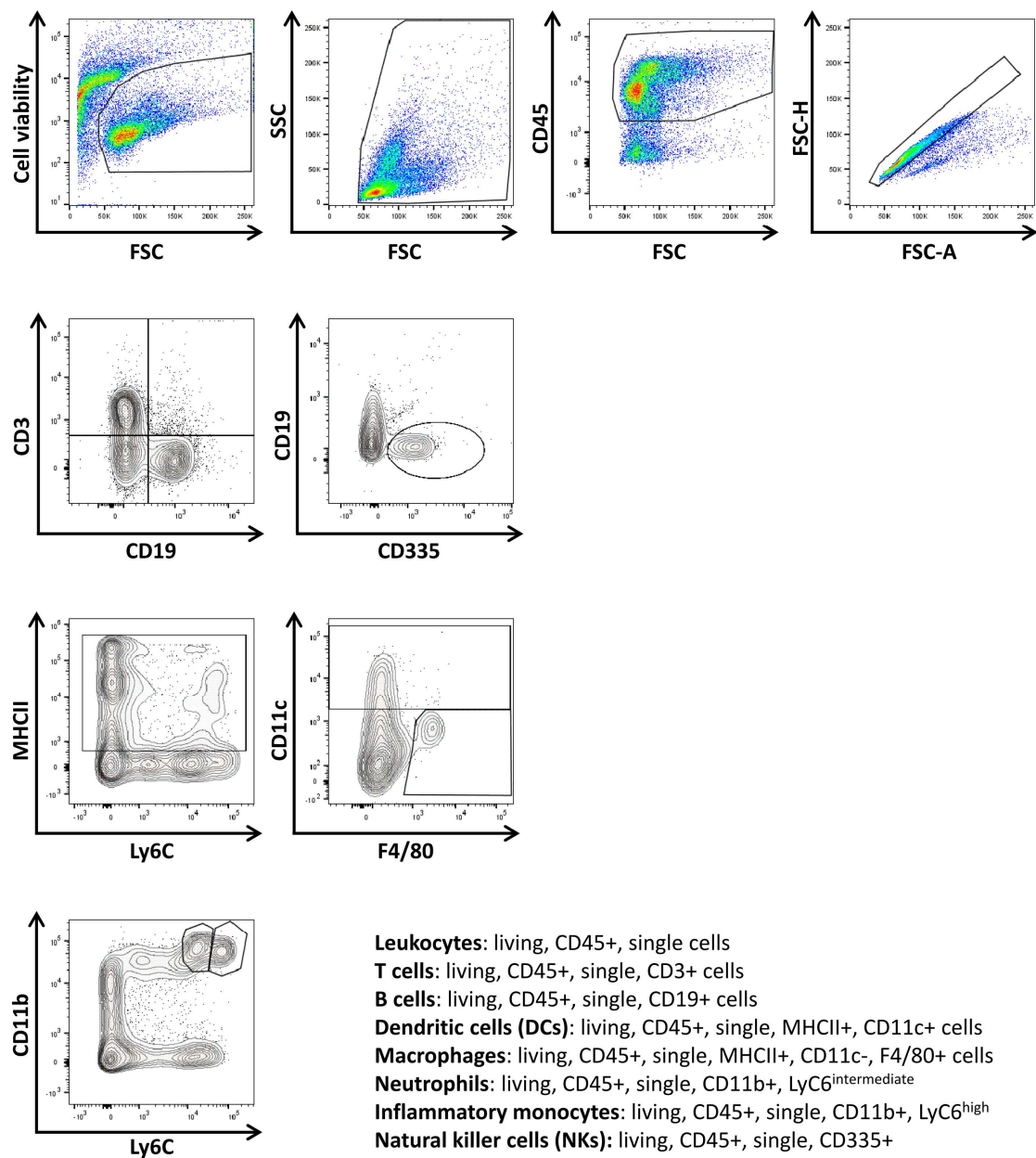
Supplementary Fig. 16 Heat plots showing transcriptional regulation of a) hypha-associated genes in *eed1Δ/Δ* mutant compared to WT (SC5314) in medium containing casamino acids (CAA; left) or citrate (right) as sole carbon source after different time points; b) the secreted aspartic proteinase (*SAP*) gene family in *eed1Δ/Δ* mutant compared to WT (SC5314) during growth with casamino acids as sole carbon source; c) transcription factors (TFs) in *eed1Δ/Δ* mutant compared to WT (SC5314) after 12 h of growth with citrate or casamino acids (CAA). The description is modified from the "Candida Genome Database" (<http://www.candidagenome.org/>). b,c) Asterisks indicate significant regulation ($\pm \log_2 2$ and adjusted p -value < 0.05) as determined by two-sided Wald test, p -values were corrected for multiple comparisons using the Benjamini and Hochberg method.



Supplementary Fig. 17 Neutrophils and monocytes were successfully depleted in RB6-8C5 treated mice. Immunocompetent or RB6-8C5 treated mice were systemically infected with 1×10^3 CFU/g body weight of WT (SC5314) or *eed1Δ/Δ* mutant. Absolute numbers of white blood cells (WBC), neutrophils and monocytes determined at the humane endpoint are shown. One experiment, $n=8$ mice per group. Dashed lines indicate median values from 10 uninfected immunocompetent mice. Shown is the median and interquartile range, two-sided Mann-Whitney test. p -values are shown in the graphs. Source data are provided as a Source Data file.



Supplementary Fig. 18 Fungal burden in brain and determination of kidney function in immunosuppressed mice after systemic infection. Mice depleted of neutrophils and monocytes by using the antibody RB6-8C5 were infected with 1×10^2 CFU/g body weight of *C. albicans* WT (SC5314) or *eed1Δ/Δ* mutant. Mice were humanely sacrificed 12 and 18 h post infection and a) organ fungal burden was determined by CFU plating. Kidney function was measured by quantification of blood urea nitrogen (BUN) in serum of mice. Uninfected mice served as control (ctr). a,b) Two independent experiments, $n=6$, except for *eed1Δ/Δ* mutant at 12 h, $n=4$. Shown is the median with interquartile range, two-sided Mann-Whitney test. *p*-values are shown in the graphs. Source data are provided as a Source Data file.



Supplementary Fig. 19 Gating strategy for the differentiation of immune cell populations after flow cytometry. Dead cells were excluded from analysis by staining with the Fixable Viability Dye eFluor® 506. Living Fixable Viability Dye^{low} cells were gated on size and granularity to exclude debris. CD45+ single cells were used to further discriminate different immune cell populations. T and B cells were identified by expression of CD3 and CD19, respectively. Dendritic cells were identified by expression of MHCII and CD11c and macrophages were characterized as MHCII+, CD11c-, F4/80+ cells. Neutrophils and inflammatory monocytes were identified by co-expression of CD11b and Ly6C and differentiated by the level of Ly6C expression: neutrophils as Ly6C^{int} and inflammatory monocytes as Ly6C^{hi} cells. Natural killer cells (NKs) were identified by expression of CD335.

Supplementary Table 1: Primers used in this study

Name	Primer sequences (5' → 3')	Used for
Eed1-TET-F	GCTTTAACTTTCACCTTTCATTTTCAATTTGTTTGCTGCTTGTCTAACAGTTTA TTATCATTTTGCTTTTTTTTTTCATACTACAATTAAGTACAAGTAATACGACTC ACTATAGGG	Amplification of <i>URA3</i> - TR promoter region from p99CAU1 (Nakayama et al 2000)
Eed1-TET-R	ggatctgggagtcttacgaggacgcctgtccgttctaagtggatgtgtaaattgtcttcttc catggtgaaatccaacgagaatgatgaagCTAGTTTTCTGAGATAAAGCT	Amplification of <i>URA3</i> - TR promoter region from p99CAU1 (Nakayama et al 2000)

4. Additional results related to Manuscript III

4.1. tet-*NRG1*- yeast are avirulent in a murine intraperitoneal infection model

C. albicans t-EED1+ yeast are reduced in their capacity to damage epithelial cells and show a reduced virulence potential in the intraperitoneal infection model (Manuscript III, Fig.1). Comparable to the attenuated phenotype of t-EED1+ yeast, the tet-*NRG1* strain, which in the absence of doxycycline (tet-*NRG1*-) is solely growing in the yeast form is incapable of damaging oral epithelial cells *in vitro* (Fig. 3).

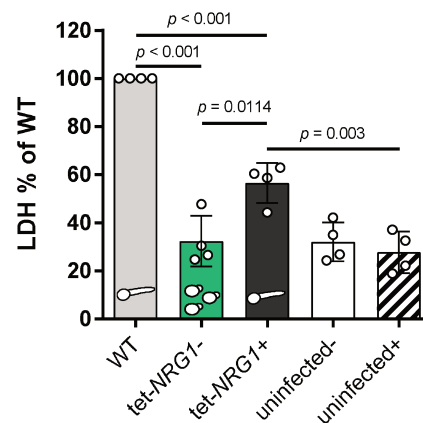


Fig. 3: tet-*NRG1*- yeast are unable to damage oral epithelial cells. Damage of oral epithelial cells (TR146) caused by *C. albicans* was quantified by measuring the release of lactate dehydrogenase (LDH) into the supernatant after co-incubation for 24 h with *C. albicans* WT (THE1-Clp10) or tet-*NRG1* strains in the presence (+) or absence (-) of doxycycline. Respective fungal morphologies are depicted in the graph. Uninfected cells served as negative control. LDH released by WT was set to 100%. Data are presented as mean \pm SD from four biologically independent experiments. Within each experiment, supernatants from three wells infected by the same strain were pooled and LDH was measured. Data were analyzed by two-tailed students t-test, *p* values are shown in the graph.

In accordance with the reduced ability to damage epithelial cells *in vitro*, the tet-*NRG1*- yeast showed an attenuated virulence potential in the invasion-based intraperitoneal infection model in mice in comparison to the filament-forming WT+/- and tet-*NRG1*+ strain (Fig. 4). Mice infected with tet-*NRG1*- yeast showed less clinical symptoms (Fig. 4a) and reduced serum enzyme levels of ALT and pancreas amylase indicating liver and pancreas damage, respectively (Fig. 4b). Although

attenuated in the intraperitoneal infection model, a higher liver fungal burden was observed for tet-*NRG1*- yeast in comparison to the respective WT (Fig. 4c).

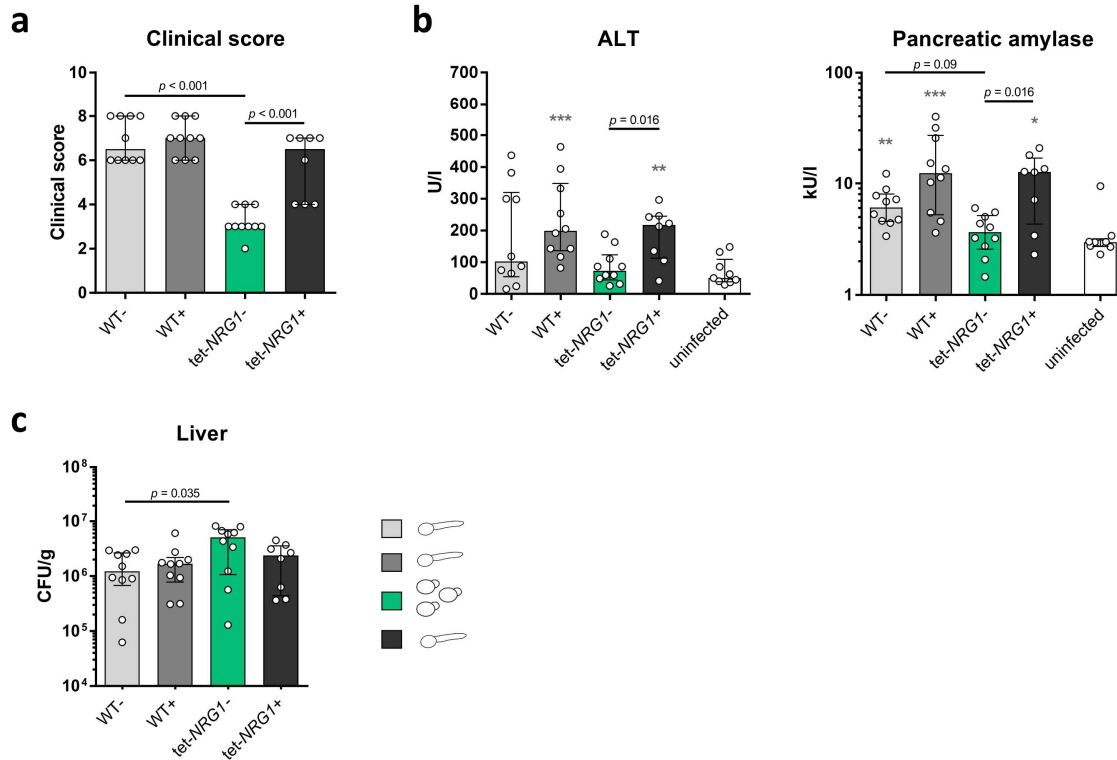


Fig. 4: tet-*NRG1*- yeasts are attenuated in the murine intraperitoneal infection model despite higher liver fungal burden. Mice were infected intraperitoneally with 1×10^8 cells of *C. albicans* WT (THE1-Clp10) or tet-*NRG1* in the presence (+) or absence (-) of doxycycline supplied *via* the drinking water. **a)** Infection with tet-*NRG1*- yeast resulted in significantly reduced clinical symptoms in mice. The semiquantitative clinical score was determined by assessing fur, coat and posture, behavior and lethargy, fibrin exudation and other symptoms like diarrhea. The score ranges from 0 (no symptoms) to 10 (severe illness). **b)** Damage of liver and pancreas was quantified by measuring serum levels of alanine aminotransaminase (ALT) and pancreatic amylase, respectively. Enzyme levels of uninfected mice ($n = 9$) served as negative control. **c)** Fungal burden in the liver. **a-c)** Respective fungal morphologies are depicted in the graph. Data derived from two independent experiments, WT+/- doxycycline and tet-*NRG1*- $n = 10$, tet-*NRG1*+ $n = 8$ animals per group. Shown is the median and interquartile range, two-sided Mann-Whitney test. p values are shown in the graph, asterisks above bars represent significant differences compared to the uninfected control * $p \leq 0.05$; ** $p \leq 0.01$; *** $p \leq 0.001$.

4.2 The initial fungal load in kidney, liver and spleen is higher than in the brain

In the early stages of experimentally induced systemic infection with *C. albicans* the fungus disseminates *via* the bloodstream and can be found in all internal organs. When mice were challenged with an intermediate infectious dose of 2.5×10^4 CFU/g body weight with *C. albicans* WT and t-EED1+ yeast kidney, liver and spleen were uniformly affected in terms of fungal load 6 h p.i. mirroring the infectious dose (Fig. 5). In contrast, the brain showed an approximately 10-fold lower fungal burden compared to the other organs tested.

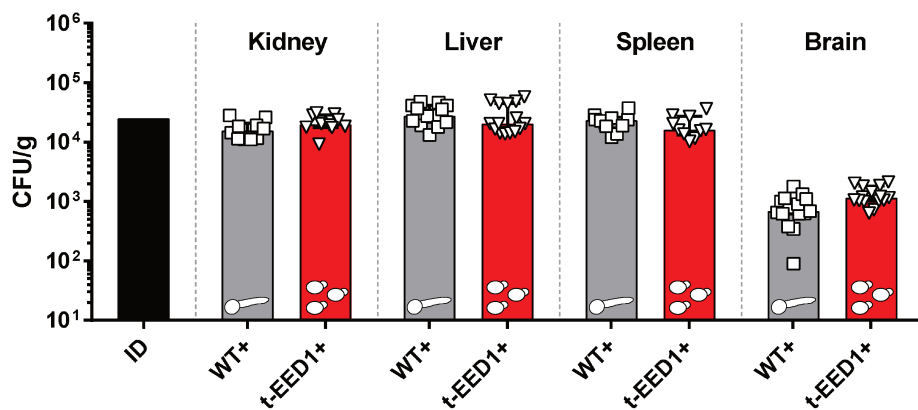


Fig. 5: Organ fungal load 6 h after systemic infection with an intermediate infectious dose (ID) of *C. albicans*. Mice were infected intravenously with 2.5×10^4 CFU/g body weight of *C. albicans* WT (THE1-Clp10) and t-EED1 in the presence (+) of doxycycline. Respective fungal morphologies are depicted in the graph. Shown is the median with interquartile range. Kidney: Two independent experiments $n = 10$. Liver, spleen, brain: Three independent experiments, $n = 15$.

4.3. Kidney fungal loads are similar in moribund mice

When mice become moribund following systemic infection with *C. albicans* the kidney is the organ most severely affected by fungal growth. In fact among the liver and the spleen, the kidney is the organ with the lowest number of CD45+ leukocytes (Fig. 6), probably having an impact on the ability of the kidney to withstand fungal growth.

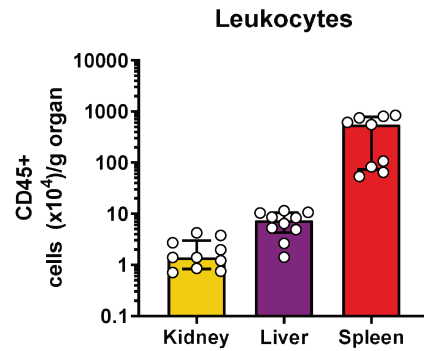


Fig. 6: The kidney is the organ with the lowest number of leukocytes. Number of living CD45+ leukocytes per gram kidney, liver or spleen of uninfected immunocompetent mice were determined by flow cytometry analysis. For kidney samples, one half of each kidney was pooled together. n= 10 mice per group from two independent experiments, except for spleen, n=9.

Interestingly, when challenged with infectious doses ranging from 10^2 to 2.5×10^4 CFU/g bodyweight kidney fungal burden in immunocompetent and immunosuppressed mice reached similar levels when mice become moribund. It is known from the literature that threshold levels of 10^7 CFU/g kidney are incompatible with survival of mice (MacCallum and Odds 2005). Interestingly, the threshold level reached differed between *C. albicans* WT and strains repressing or lacking *EED1*: WT infection led to renal fungal burden in the range from 10^5 to 4×10^5 /g kidney (Fig. 7), whereas infection with strains unable to express *EED1* reached level between 6×10^6 to 2×10^7 /g kidney (Fig. 8). For both strains, the time to reach threshold levels extended with decreasing infectious doses. Thresholds were reached much faster in immunosuppressed mice treated with the monoclonal RB6-8C5 antibody to deplete mice of neutrophils and monocytes (Fig. 7 and Fig. 8). Since the infectious dose (ID) closely resembles the CFU/g present in the kidneys 6 h p.i. (Fig. 5) the increase over the ID was calculated. In order to reach the threshold level, *EED1* repressing/deleted strains had to replicate faster (Fig. 8).

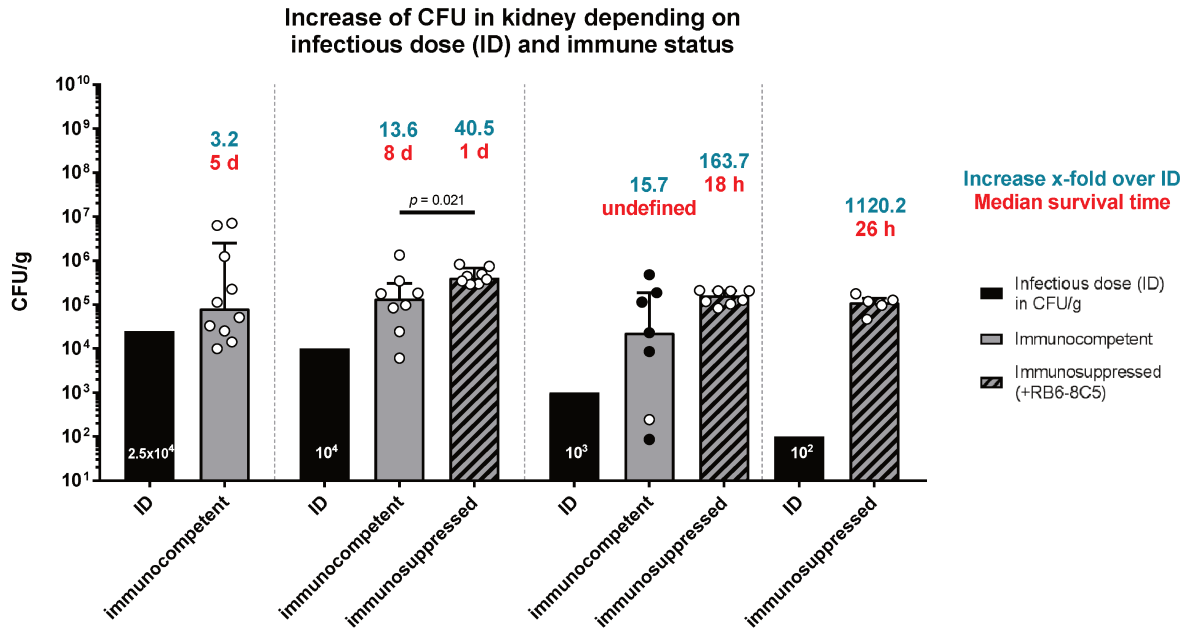


Fig. 7: CFUs in kidneys of moribund immunocompetent or immunosuppressed mice systemically infected with different infectious doses of *C. albicans* WT. CFU per g kidney were evaluated at the time mice became moribund. One exception are immunocompetent mice infected with 10^3 CFU/g body weight: 6/7 mice survived until the end of the experiment (21 days). Median survival times in hours or days are indicated in the graphs in red. Survival times could not be calculated in groups containing surviving mice and therefore are undefined. Relative increases in CFU compared to the infectious dose are shown in blue. Note that experiments were conducted with the SC5314 WT strain except for the experiment using 2.5×10^4 CFU/g body weight, where the THE1-C1p10 WT was used. White circles: CFU of moribund mice. Black circles: CFU of surviving mice sacrificed at the end of the experiment (d21). Shown is the median and interquartile range, two-sided Mann–Whitney test. p values are shown in the graph. Data were generated from one experiment. 2.5×10^4 CFU/g body weight, $n=10$. 10^3 and 10^4 CFU/g body weight immunocompetent and immunosuppressed, $n=8$. 10^2 CFU/g body weight, $n=6$.

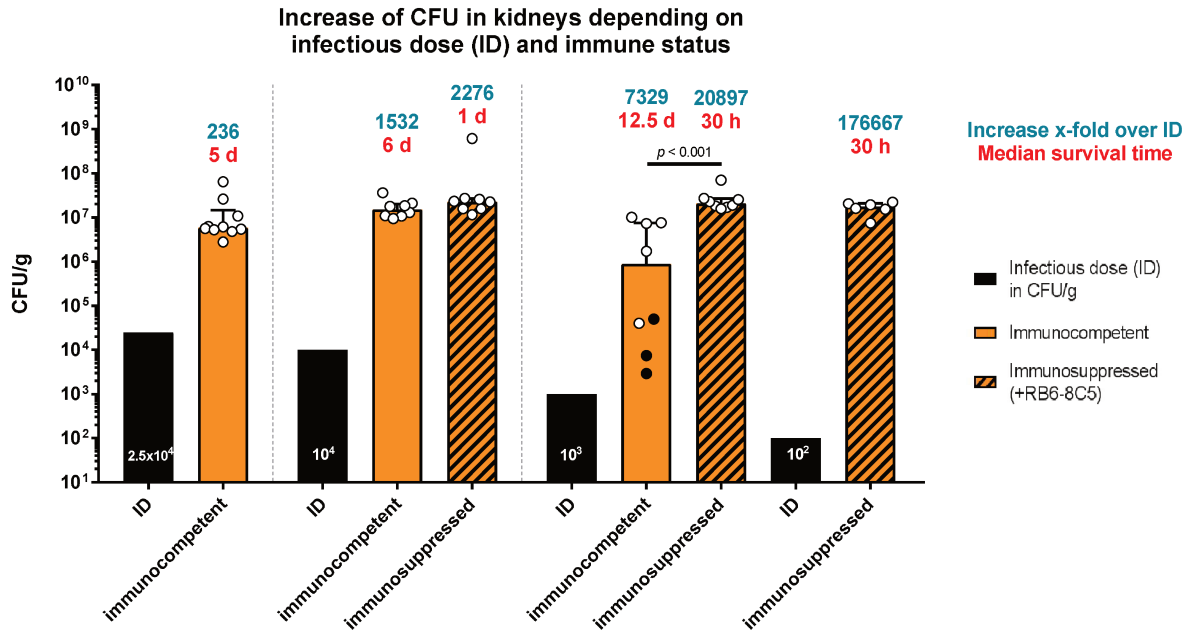


Fig 8: CFUs in kidneys of moribund mice systemically infected with different infectious doses of *C. albicans eed1Δ/Δ* mutant or t-EED1+. CFU per g kidney were evaluated at the time mice became moribund. One exception are immunocompetent mice infected with 10^3 CFU/g body weight: 3/8 mice survived until the end of the experiment (21 days). Median survival times in hours or days are indicated in the graphs in red. Relative increases in CFU compared to the infectious dose are shown in blue. Note that experiments were conducted with the *eed1Δ/Δ* mutant except for the experiment using 2.5×10^4 CFU/g body weight were the t-EED1 strain in the presence of doxycycline (+) was used. White circles: CFU of moribund mice. Black circles: CFU of surviving mice sacrificed at the end of the experiment (d21). Shown is the median and interquartile range, two-sided Mann-Whitney test. *p* values are shown in the graph. Data were generated from one experiment. 2.5×10^4 CFU/g body weight, $n=10$. 10^3 and 10^4 CFU/g body weight immunocompetent and immunosuppressed, $n=8$. 10^2 CFU/g body weight, $n=6$.

4.4. Organ fungal burden in mice challenged with low infectious doses

Mice infected with a low infectious dose of 10^3 CFU/g body weight were able to better cope with systemic candidiasis. After infection with the *C. albicans* WT (SC5314) 6/7 mice and 3/8 mice infected with the *eed1Δ/Δ* survived until the end of the experiment (21d). As observed with higher infectious doses, fungal replication was primarily observed in the kidneys for both *C. albicans* strains (Fig. 9). Whereas the WT was cleared from the liver, spleen and brain, the *eed1Δ/Δ* mutant was often detected in these organs, primarily in mice that succumbed to the infection.

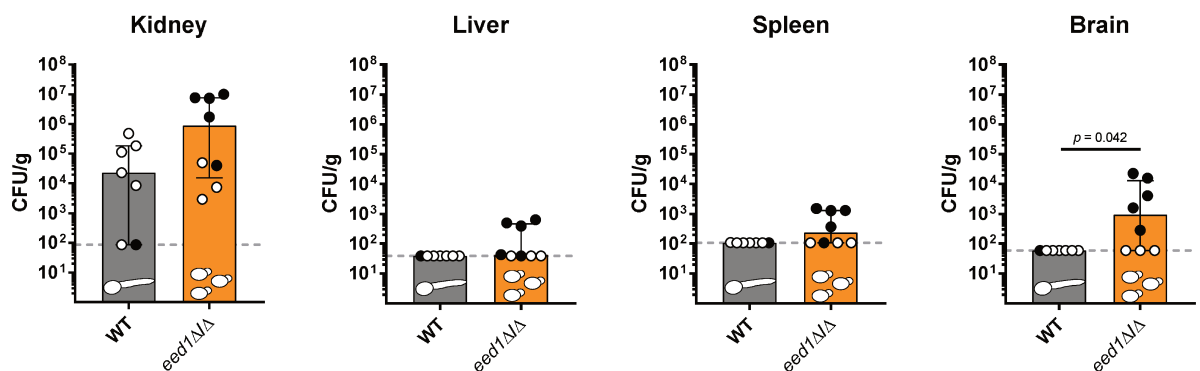


Fig. 9: Organ fungal burden in moribund mice systemically infected with a low dose of 10^3 CFU/g body weight of *C. albicans* WT (SC5314) or *eed1Δ/Δ* mutant. Respective fungal morphologies are depicted in the graph. One experiment, WT n= 7, *eed1Δ/Δ* mutant n=8 mice per group. Black circles: Fungal burden of mice that had to be sacrificed before the end of the experiment, white circles: Fungal burden of mice that survived until the end of the experiment (21 d). Dashed gray lines indicate limit of detection. Median and interquartile range are shown. Two-sided Mann-Whitney test, *p* values are indicated in the graph.

4.5. Neutrophil activation in kidneys of systemically infected mice is comparable between WT+ and t-EED1+ yeast

Kidneys of mice systemically infected with the t-EED1+ yeast showed increased leukocyte infiltrations 72 h p.i. To determine whether the enhanced infiltration was accompanied by an increased activation of immune cells, especially neutrophils, the concentration of the myeloperoxidase (MPO) in supernatants of kidney homogenates was determined. MPO concentrations 6 h p.i. was in the range of uninfected controls and at that time, no immune cell infiltration had occurred. MPO concentrations started to increase significantly 24 h p.i. for all strains tested (Fig. 10) coinciding with an increased immune cell infiltration of the kidneys (**Manuscript III**, Supplementary Fig. 6). No significant differences were observed 24 and 72 h p.i. between WT+ and

t-EED1+ yeast cells, only 48 h p.i. MPO concentrations were elevated in kidneys of mice infected with the t-EED1+ yeast.

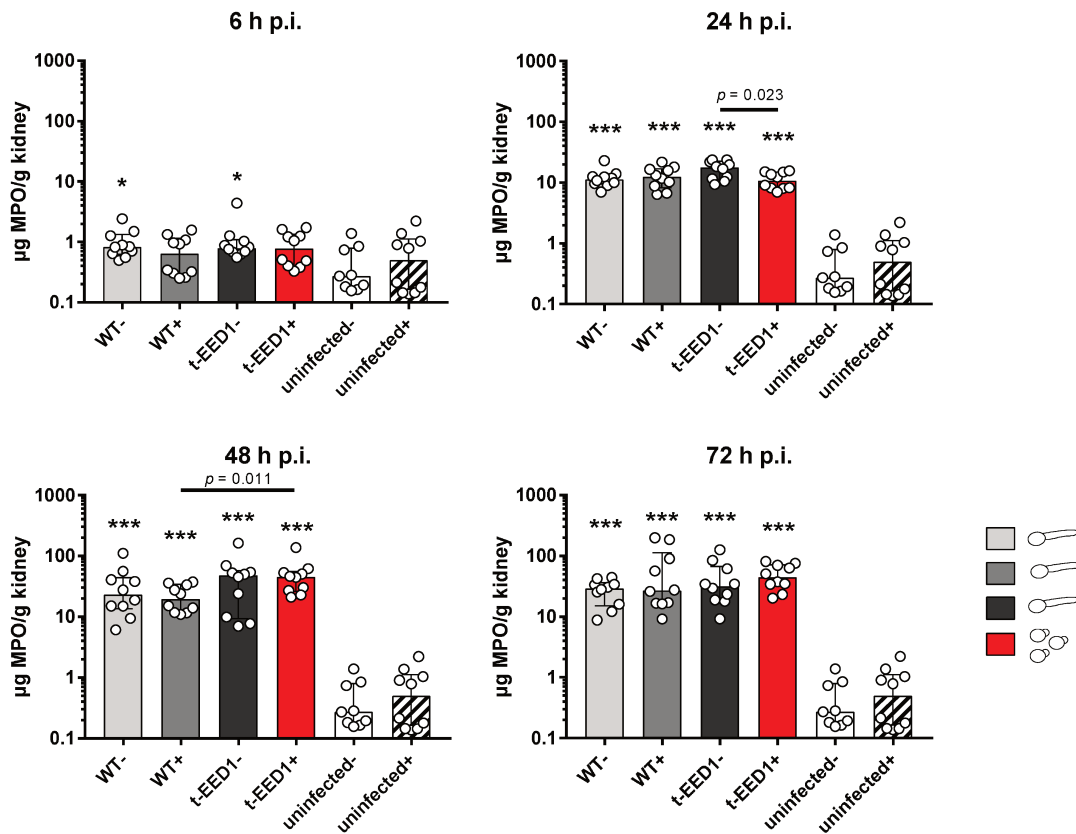


Fig. 10: Immune cell activation, measured by MPO concentrations, in kidneys of systemically infected mice is comparable between *C. albicans* WT and t-EED1+ yeast. Immunocompetent mice were systemically infected with *C. albicans* WT or t-EED1 in the presence (+) or absence (-) of doxycycline with an intermediate infectious dose of 2.5×10^4 CFU/g body weight. Respective fungal morphologies are depicted in the graph. MPO concentrations were determined by ELISA in supernatants of kidney homogenates 6, 24, 48 and 72 h post infection. Data was generated from two independent experiments, $n=10$. Shown is the median and interquartile range, two-sided Mann-Whitney test. p values are shown in the graph, asterisks above bars represent significant differences compared to the respective uninfected control * $p \leq 0.05$; ** $p \leq 0.01$; *** $p \leq 0.001$.

5. Discussion

The transition from yeast to hypha is considered to be one of the key virulence factors of *C. albicans* as it facilitates tissue invasion and damage as well as escape from phagocytes. *C. albicans* strains that are locked in the yeast or the hyphal morphology were repeatedly found to be attenuated or avirulent in systemic infection models (Lo et al. 1997, Zheng, Wang, and Wang 2004, Braun et al. 2000, Braun, Kadosh, and Johnson 2001). Hence, it was argued that the morphological transition in either direction is required for full virulence in systemic infections (Kadosh and Lopez-Ribot 2013). However, a *C. albicans eed1Δ/Δ* mutant, although unable to maintain hyphal growth, retains its virulence in a murine systemic infection model challenging the central dogma that hypha formation is *per se* essential for pathogenesis.

5.1. Yeast growth of *C. albicans* results in decreased damage and virulence in invasion-based infection models

Invasion and damage of epithelial and endothelial cells by *C. albicans* is directly coupled to hypha-formation associated with the expression of hypha-associated genes (HAGs) and production of the Ece1-derived peptide toxin Candidalysin (Richardson et al. 2018, Moyes et al. 2016, Swidergall et al. 2019). It is therefore not surprising, that mutants unable to maintain filamentation (*eed1Δ/Δ*, *hgc1Δ/Δ*), strains unable to filament at all (*tet-NRG1-*, *efg1Δ/Δcph1Δ/Δ*), but also the Candidalysin-deficient *ece1Δ/Δ* mutant, which forms normal filaments, show a reduced capacity to damage epithelial and/or endothelial cells *in vitro* (Wächtler et al. 2011, Moyes et al. 2016, Dunker et al. 2021). Consistent with *in vitro* observations, infection models in mice mimicking superficial candidiasis (OPC and VVC) showed the inability of the yeast morphology to induce damage and disease, whereas strains able to filament and produce Candidalysin induced tissue damage, which coincided with immune cell infiltration, inflammation, and disease progression (Moyes et al. 2016, Peters et al. 2014).

In the *eed1Δ/Δ* mutant, the switch back to yeast cell growth after hyphal initiation is linked to the down-regulation of hypha-associated genes such as *ECE1* (Martin et al. 2011). In another filament-deficient *C. albicans* strain, the *hgc1Δ/Δ* mutant, expression of HAGs and filamentation appears uncoupled as the mutant is able to express *ECE1*, *HYR1* and *HWP1* after 5 h of growth at 37 °C (Zheng, Wang, and Wang 2004). Still, this mutant is not able to damage epithelial cells (Wächtler et al. 2011), implying that expression of HAGs alone does either not lead to production of a sufficient quantity of damaging factors, or these factors are not directed to the hyphal tip in sufficient concentrations and therefore cannot unfold their full damage potential. Importantly, although

adhesion to and invasion into epithelial and endothelial cells by the *eed1Δ/Δ* mutant appeared to be unaltered (Wächtler et al. 2011), the transient germ tube formation seems not sufficient to generate damage.

Since *in vitro* models cannot mimic all aspects of the *in vivo* situation, the *C. albicans* t-EED1 and the tet-*NRG1* strains were tested in an intraperitoneal infection model to evaluate the importance of hyphal formation (Fig. 4 and **Manuscript III**, Fig. 1). To induce *Candida* peritonitis, *C. albicans* is injected into the otherwise sterile peritoneal cavity of immunocompetent mice. The model mimics e.g. catheter-induced *C. albicans* peritonitis after peritoneal dialysis, required in patients with restricted kidney function or end-stage kidney disease (Hu et al. 2019, Prasad and Gupta 2005). From the peritoneal cavity *C. albicans* is able to cross the peritoneum and invades deeply into the underlying intraperitoneal organs such as the liver and the pancreas *via* hyphal formation. In contrast to filamenting strains (WT± doxycycline, tet-*NRG1*+, t-EED1-), yeast strains (t-EED1+ and tet-*NRG1*-) were unable to cause liver and pancreas damage as measured by the concentration of tissue specific enzymes in the blood of the mice in comparison to the WT. However, although not able to form proper hyphae, t-EED1+ yeast were detected below the liver capsule (**Manuscript III**, Fig. 1c) indicating that either hyphal formation was not required or that transient filamentation was sufficient for superficial invasion into this organ. These results are in line with observations made in a RHE model *in vitro* by Zakikhany *et al.*: The *eed1Δ/Δ* mutant was able to invade into the uppermost cell layer, proliferated within these cells but caused no detectable damage (Zakikhany et al. 2007). Replication in the liver tissue resulted in higher CFU levels for the t-EED1+ but also for tet-*NRG1*- yeast when compared to the respective WT (Fig. 4c and **Manuscript III**, Fig. 1e). However, liver fungal burden for t-EED1+ yeast was approximately 7-fold higher than for tet-*NRG1*- yeast, indicating that either the genetic basis of filament-deficiency affects the ability to proliferate, or that transient filamentation provides access to tissue that provides a better nutrient source. Since both mutants were attenuated in their ability to cause organ damage, it can be concluded that hyphal formation is required for deep invasion of tissues *in vivo*, ultimately resulting in measurable tissue damage.

5.2. In the absence of *EED1* expression, *C. albicans* yeast retain their virulence potential in a murine systemic infection model

Systemic fungal infections are a serious concern especially in the ICU (Girmenia et al. 2011). Two mouse models to study invasive Candidiasis and investigate fungal virulence and the complex host-pathogen interplay in mice exist: The systemic, intravenous infection model and the gastrointestinal colonization model in which stable colonization is obtained by antibiotic and dissemination is

subsequently induced by antibiotic and immunosuppressive treatment (Koh et al. 2008, MacCallum 2012). The GI tract is the main reservoir of *C. albicans* in humans and is suggested to be the primary endogenous source of systemic infection (Nucci and Anaissie 2001, Miranda et al. 2009). In the commensal state *C. albicans* is primarily found in the GI tract in the yeast morphology (Vautier et al. 2015) although hyphal forms can be observed as well (Vautier et al. 2015, Böhm et al. 2017, Witchley et al. 2019). When mice were colonized orally with the *eed1Δ/Δ* mutant, colonization levels in the GI tract were higher than for the WT in immunocompetent antibiotic-treated mice (**Manuscript III**, Fig. 2d). This is in accordance with previous data showing that the yeast-locked *efg1Δ/Δcph1Δ/Δ* and the *hgc1Δ/Δ* mutant reach higher colonization levels in the murine GI tract (Vautier et al. 2015). In contrast, the filamentous *nrg1Δ/Δ* and *tup1Δ/Δ* mutant showed reduced colonization levels (Koh et al. 2008, Vautier et al. 2015). In addition, the regulable *tetO-UME6* strain colonized the GI tract comparable to the WT, when kept in the yeast morphology by addition of doxycycline to the drinking water. However, when the strain was enforced to filament by withdrawal of doxycycline, colonization level rapidly declined but recovered to normal levels when doxycycline was administered again and the yeast morphology was recovered (Vautier et al. 2015), further emphasizing the importance of yeast cell growth for colonization. In the healthy host, the mucosal barrier in addition to a functional immune system prevents *C. albicans* translocation. When the mucosal barrier is breached e.g. by gastrointestinal surgery and/or the individual is severely immunosuppressed e.g. due to myelosuppressive cancer therapy (Moore, Leef, and Pang 2003) *C. albicans* is able to translocate from the GI tract. It still remains unknown how *C. albicans* is translocating across the intestinal barrier. Filamentation is required for translocation of epithelial cells *in vitro* (Allert et al. 2018), and has been suggested to be required for translocation by Koh *et al. in vivo* in conjunction with disturbed barrier function and immunosuppression (Koh et al. 2008). However, in the study by Koh *et al.*, a WT strain was compared with the non-filamentous *efg1Δ/Δcph1Δ/Δ* mutant that is avirulent in murine systemic infection models (Lo et al. 1997). Since survival after dissemination served as read out, it appears possible that this mutant might had translocated to the same extent as the WT but, due to its intrinsic virulence defect, was nonetheless unable to cause lethal disease. In another study, translocation (based on organ fungal burden) has been observed in immunocompetent mice independent of fungal morphology (Vautier et al. 2015). Translocation from the GI tract is primarily resulting in dissemination to the liver *via* the hepatic portal circulation manifesting as hepatosplenic candidiasis (Moore, Leef, and Pang 2003), but in principle every organ can get affected. In accordance with that, low level dissemination of the WT to the liver but not to the kidney was observed in immunocompetent mice, whereas in only 1/4 mice dissemination to the liver was observed for the *eed1Δ/Δ* mutant (**Manuscript III**, Fig. 2f). This

suggests that *in vivo*, as *in vitro*, hyphae are required for active translocation. However, increased dissemination of the WT and the *eed1Δ/Δ* mutant to the kidneys and the liver was observed upon cyclophosphamide treatment, a drug that, in combination with other medications, is used by clinicians to treat hematological malignancies (Miyazaki and Hirano 1996). Cyclophosphamide reduces the numbers of immune cells but, as unwanted side effect disturbs the intestinal barrier function (Koh et al. 2008, Owari et al. 2012, Yang et al. 2013), in consequence likely resulting in the dispensability of hyphal formation for the translocation process. Interestingly, fungal burden of the *eed1Δ/Δ* mutant in the kidney were significantly higher than fungal burden of the WT in antibiotic-treated immunosuppressed mice (**Manuscript III**, Fig. 2f). However, whether this is due to enhanced translocation or due to increased proliferation within the kidney (see also discussion below), remains speculative. Therefore, the fungal morphology is likely irrelevant for translocation in an immunosuppressed host but might rather decide how the infection progresses once *C. albicans* disseminates *via* the blood stream and reaches deeper tissues.

Another common route of systemic infection in the nosocomial setting is catheter-associated systemic candidiasis in humans. The mouse model of systemic candidiasis is the gold standard model used to study host-pathogen interactions and pathogenesis during systemic infections (MacCallum 2012, Spellberg et al. 2005). Surprisingly, *EED1* deficient/repressing *C. albicans* mutants, unable to maintain hyphal growth were as virulent as the WT in systemic infection in mice when intermediate infectious doses were used (**Manuscript III**, Fig. 3c). This finding is in stark contrast to the generally accepted assumption that hyphal formation is a prerequisite for the virulence potential of *C. albicans* in this model. In addition, another interesting observation was made: When infectious doses were lower or higher an inverse correlation was observed. Lower infectious doses led to enhanced virulence of the *eed1Δ/Δ* mutant whereas infection with high doses of t-EED1+ yeast resulted in delayed mortality compared to infections caused by the WT (**Manuscript III**, Fig. 3a,b). These findings challenge the long-standing hypothesis that *C. albicans* yeast cells are *per se* less or even avirulent. In fact, in the yeast-locked mutants that were found to be avirulent in systemic infections, important transcription factors have been deleted (*efg1Δ/Δcph1Δ/Δ* mutant) (Lo et al. 1997), or a transcriptional repressor of hyphal formation was constitutively expressed (tet-*NRG1* without doxycycline) (Saville et al. 2008, Saville et al. 2003). Efg1 and Cph1 represent downstream transcription factors of the cAMP-PKA and MAPK pathway, respectively, which function not only on the level of filamentation. Efg1, for example, is also responsible for the regulation of metabolic genes, for the expression of genes in response to hypoxia (Doedt et al. 2004), and genes involved in cell wall biogenesis (Doedt et al. 2004, Sohn et al. 2003). It is therefore not surprising that this filament-deficient mutant, which is lacking two central TFs, shows

attenuated fitness and virulence in the systemic infection model, likely as combined consequence of the absence of hypha formation and other pleiotropic effects (Saville et al. 2003). The tet-*NRG1* strain is unable to form hypha in the absence of doxycycline due to the continuous expression of the transcription factor and repressor of hyphal formation Nrg1 (Saville et al. 2008, Saville et al. 2003, Cleary and Saville 2010). Mice even survived when systemically challenged with doses as high as 1.7×10^6 CFU/mouse of tet-*NRG1*- yeast (equaling approximately 8.5×10^5 CFU/g bodyweight assuming that mice weigh approximately 20 g) (Saville et al. 2008). As Nrg1 is regulating the expression of various hypha-associated genes such as *HWP1* and *ALS3*, it cannot be excluded that other processes dependent on *NRG1* led to the observed phenotype (Cleary and Saville 2010, Saville et al. 2003). Taken together, strains that were used in the past to analyze the importance of the yeast morphology for systemic infection are likely biased as the genes that were deleted encoded important regulators regulating more than just fungal morphology. Pleiotropic effects of *EED1*-deficiency cannot be excluded as well. Unfortunately, the molecular function of *EED1* is still unknown (Martin et al. 2011, Polke et al. 2017). *EED1* is considered a unique gene of *C. albicans* with a distant uncharacterized ortholog found in *C. dubliniensis* (Polke 2017) and is likely not coding for a transcription factor as no DNA-binding domains were identified (Martin et al. 2011). *EED1* is distantly related to *S. cerevisiae* *DEF1* (Polke 2017), coding for a RNA polymerase II degradation factor with multiple biological functions (Stepchenkova, Shiriaeva, and Pavlov 2018). The only motif of the Eed1 protein that could indicate a cellular function is a central glutamine- and proline-rich region (Martin et al. 2011, Polke 2017), which could be involved in protein-protein interactions (Martin et al. 2011, Tanaka, Clouston, and Herr 1994, Xiao and Jeang 1998). Nevertheless, *C. albicans* *EED1*-deficient or repressing cells are the first mutants that are fully virulent in systemic infection models in immunocompetent mice despite the lack of hyphal maintenance.

In this study, all *C. albicans* strains were injected into the bloodstream *via* the lateral tail vein of mice in the yeast morphology to induce systemic candidiasis. Systemic distribution of fungal yeast cells over the bloodstream happens fast: A 20 g mouse has an approximate blood volume of 1.2-1.6 ml (6-8% of bodyweight) and a cardiac output of 14.3 ml/min (Wiesmann et al. 2000), hence the blood volume is circulating 9-12 times per minute. *C. albicans* is rapidly disappearing from circulating blood, with only 10% of the initial inoculum present 10 min p.i. (MacCallum and Odds 2005), and less than 1% present 1 h p.i. (Lionakis et al. 2011). Using low infectious doses, viable *C. albicans* cells were no longer found in murine blood 5 h p.i., and only occasionally thereafter, when intermediate infectious doses were administered (MacCallum and Odds 2005). The first host cells *C. albicans* encounters in the systemic infection model are blood cells. As murine blood, in stark contrast to human blood, is not able to kill *C. albicans* in whole-blood infection models *in vitro*

(**Manuscript II**, Fig. 1a,b), disappearance of *C. albicans* from the blood stream after infection is likely due to adhesion to the endothelium lining the blood vessels (and subsequent escape into deeper tissues) rather than to the result of extensive killing by circulating immune cells. Resident macrophages of the spleen (marginal zone macrophages) and the liver (Kupffer cells) contribute to filter *C. albicans* from the blood, as depletion of these cells in mice slowed down the clearance of fungal cells from the blood system (Qian et al. 1994) and increased the number of fungal cells deposited in the kidneys (Sun et al. 2019). As fast as *C. albicans* is disappearing from the blood stream, it can be found in all internal organs (MacCallum and Odds 2005, Lionakis et al. 2011). In order to establish deep-seated infections, following adhesion *C. albicans* needs to traverse from the bloodstream through the endothelium (Filler et al. 1995). Evidence exists that hyphae perform better in adhering to epithelial and endothelial cells than yeast cells under static conditions because they express hypha-associated adhesins such as Als3 and Hwp1 (Wilson, Naglik, and Hube 2016). However, under flow conditions which more closely resemble the *in vivo* situation in the blood stream, it has been shown that yeast cells adhere better than hyphae (Wilson and Hube 2010, Grubb et al. 2009). In addition, an *als3Δ/Δ* mutant that is still forming hypha is defective in adhesion to endothelial and epithelial cells under static condition (Zhao et al. 2004). In contrast, under flow conditions yeast and hyphal cells of an *als3Δ/Δ* mutant adhered to the same extent as the WT to endothelial cells (Cleary et al. 2011). Nonetheless, hyphal formation is likely not required for traversal from the blood stream *in vivo* as all yeast-locked strains and strains unable to maintain hyphal growth were detected within kidney parenchyma after intravenous challenge in this study and by others (Saville et al. 2003, Wartenberg et al. 2014, Zheng, Wang, and Wang 2004, Grubb et al. 2009). *C. albicans* can induce its own endocytosis by vascular endothelial cells, a passive process that requires no metabolically active cells since living and killed fungal cells can be taken up (Filler et al. 1995). Two mechanisms of escape from endothelial cells to the abluminal side exist: On the one hand *C. albicans* can form hyphae upon contact with endothelial cells leading to invasion, cell damage and subsequent translocation to the other side. On the other hand endothelial cells can transport fungal cells, as upon phagocytosis by endothelial cells, *C. albicans* was found in phagocytic vacuoles that opened up at the abluminal side, which was observed for killed yeast as well (Filler et al. 1995). The latter would also explain how non-filamentous species such as *C. auris* and *C. glabrata* are able to establish systemic candidiasis and reach deeper tissues. Therefore, *C. albicans* can traverse the endothelial lining independent of the fungal morphology. However, given the fact that induced endocytosis happens within 2 h p.i. *in vitro* (Filler et al. 1995), *C. albicans* cells lacking or repressing *EED1* likely traversed before differences in morphology in comparison to the WT become

apparent (*EED1*-deficient strains switch back to yeast cell growth after approximately 4 h), a view that is supported by Grubb *et al.* (Grubb *et al.* 2009).

Within 6 h p.i. with an intermediate infectious dose, WT+ and t-EED1+ yeast had traversed successfully and reached similar fungal burden in kidney, liver and spleen, which was in the range of the infectious dose whereas the brain showed an initial 10-fold lower involvement (Fig. 5). In accordance with previous work by others (Lionakis *et al.* 2011, MacCallum and Odds 2005), after reaching all internal organs fungal burden progression was organ-specific: Fungal burden declined in liver and spleen of WT-infected mice but not in the kidney and in the brain. The highest fungal burden was detected in the kidney, the main target organ of disseminated candidiasis in mice (**Manuscript III**, Fig. 3e). Different reasons could explain why the kidney is the primary target organ: (I) Despite their small size, kidneys of mice receive 9-22% of the cardiac output. Most of the blood is directed to the glomerular capillaries within the cortex (Munro, Hohenstein, and Davies 2017), probably resulting in high numbers of *C. albicans* cells concentrated within this tight area of the kidney. (II) Fungal traversal from the blood stream might be eased in the kidneys by fenestrations in the endothelium (Grubb *et al.* 2008), transcellular holes with 60-70 nm in diameter that enable blood filtration (Satchell and Braet 2009). (III) The kidney possesses a lower number of tissue residential immune cells compared to other organs (Fig. 6). In combination with a delay in immune cell infiltration (Lionakis *et al.* 2011) these factors might explain why the kidneys are especially vulnerable to systemic candidiasis. Fungal replication in the kidney starts already 10 h after experimentally induced systemic infection (MacCallum and Odds 2005). Surprisingly, the *eed1Δ/Δ* mutant massively proliferated, especially in the kidney of mice reaching 25-fold higher levels than the WT and filamentous t-EED1- strain after 24 h p.i. Within a short time frame of 18 h (between 6 h p.i. and 24 h p.i.), the fungal burden of t-EED1+ yeast increased 100-fold in immunocompetent mice (**Manuscript III**, Fig. 3e). The fungal burden of tet-*NRG1*- yeast increased as well, reaching highest levels 72 h p.i (**Manuscript III**, Supplementary Fig. 4d). However, for this mutant the onset of fungal replication started later (after 24 h p.i.) than observed for t-EED1+ yeast (after 6 h p.i.). In addition, with a 10-fold lower fungal burden in the kidneys, tet-*NRG1*- yeast never reached the high fungal burden found for t-EED1+ yeast. Similar observations have been made by others for the avirulent *efg1Δ/Δcph1Δ/Δ* mutant, that was shown to be able to replicate *in vivo* (Chen *et al.* 2006). However, fungal burden remained 10-fold lower compared to the respective WT (Chen *et al.* 2006) and 10-fold lower than observed for *EED1* deficient/repressing *C. albicans* yeast. These results indicate that yeast can proliferate *in vivo* in the absence of hypha formation. However, although they share the same morphology, these yeast cells differ: Deletion or repression of *EED1* in *C. albicans* led to the highest kidney fungal burden observed with a filament-deficient mutant. As

the WT and the t-EED1- filamenting strain, in moribund mice t-EED1+ yeast were found in the renal pelvis. Whereas filamentous strains diffusely grew through the tissue, t-EED1+ yeast were found in large numbers mainly within tubules (**Manuscript III**, Fig. 3d). Accumulation of cells within close proximity or aggregate formation might display a mechanism of immune evasion as it hinders phagocytosis of fungal cells by immune cells, a mechanism that has been proposed to promote virulence of *C. auris* (Xin et al. 2019). Noteworthy, while the liver and the spleen were able to initially restrict growth of t-EED1+ yeast after infection with intermediate doses, both organs were unable to completely contain yeast growth as t-EED1+ yeast started to replicate after 48 h and 72 h, respectively, in stark contrast to WT cells and the t-EED1- filaments (**Manuscript III**, Fig. 2e). Therefore, in t-EED1+ yeast infected mice, multi-organ involvement could contribute to multi-organ failure, whereas for WT and t-EED1- infections the kidney was the primarily affected organ.

Interestingly, with lower infectious doses (10^4 and 10^3 CFU/g body weight) the *eed1Δ/Δ* mutant appeared to be even more virulent than the WT strain in immunocompetent mice (**Manuscript III**, Fig. 3a). Fungal burden increased rapidly in the kidney as well: When moribund after challenge with 10^4 CFU/g body weight, the renal fungal burden had increased 1532-fold in *eed1Δ/Δ* mutant and only 13.6-fold in WT infected mice with median survival times of 6 d and 8 d, respectively (Fig. 7 and Fig. 8). With an infectious dose of 10^3 CFU/g body weight the majority of the mice infected with the WT (6/7) survived until the end of the experiment (**Manuscript III**, Fig. 3a), an effect that had been described before to happen with infectious doses lower than 10^4 /g body weight by MacCallum and Odds (MacCallum and Odds 2005). Again, the kidneys were the organs most affected by fungal growth, whereas the WT was cleared from liver spleen and brain (Fig. 9). Although most of the WT-infected mice survived the challenge until the end of the experiment, the kidneys showed a fungal burden comparable to mice that succumbed to infection with higher infectious doses (Fig. 7). Since for fungal burden determination both kidneys were sampled together, it cannot be excluded that unilateral kidney involvement, that can be observed with low infectious doses (MacCallum and Odds 2005), is the reason for the high fungal burden in surviving mice. This is supported by gross pathology as in 4/7 mice one kidney appeared healthy and normal in weight, whereas the other appeared partly or completely pale, swollen and showed an increase in size and weight. In contrast, only 3/8 mice survived in the *eed1Δ/Δ* mutant-infected group (median survival time 12.5 d; **Manuscript III**, Fig. 3a). In all mice infected with the *eed1Δ/Δ* mutant fungal cells could be recovered from the kidney, although mice that survived showed a lower kidney fungal burden (Fig. 9). In addition, fungal cells could be recovered from mice that succumbed to infection from the brain, whereas liver and spleen were less affected by fungal growth with 3/8 and 4/8 mice affected, respectively. Consequently, the *eed1Δ/Δ* mutant rapidly proliferated in murine kidneys

independent of the infectious dose applied; however, the time to reach the threshold of *eed1Δ/Δ* yeast cells in the kidney incompatible with survival of mice was longer with lower infectious doses.

5.3. The *eed1Δ/Δ* mutant rapidly proliferates *in vivo*

In order to replicate rapidly *in vivo*, the *C. albicans EED1* deficient/repressing yeast must be able to withstand the attack of phagocytes that form the first line of the host defense, and gain access to nutrients. As phagocytosis was not affected by the absence of *EED1* and killing by macrophages after 6 h was even higher for the mutant *in vitro* (**Manuscript III**, Fig. 5), decreased fungal killing could not be the reason for the rapid increase in fungal burden. Immune cells are the first cells in the blood as well as in tissues after systemic infections that encounter fungal cells. After phagocytosis by professional phagocytes, fungal cells are contained in phagosomes that mature by fusion with lysosomes into phagolysosomes. These phagolysosomes generate an acidic, hostile environment that is poor in nutrients (Lorenz, Bender, and Fink 2004). *C. albicans* is able to initiate the yeast-to-hypha transition within the phagosome and eventually grows out by piercing the membrane of macrophages (Miramón, Kasper, and Hube 2013, Ghosh et al. 2009). In addition, *C. albicans* can trigger macrophages to undergo pyroptosis, an inflammasome-mediated programmed cell death. Although pyroptosis is a hypha-independent killing mechanism, filaments induce higher levels of pyroptosis than yeast (Wellington, Koselny, and Krysan 2012, Wellington et al. 2014, Krysan, Sutterwala, and Wellington 2014). Overall, *C. albicans* strains able to robustly form hyphae have a greater capacity to damage macrophages than strains that show impaired or no hypha formation (**Manuscript I**, Fig. 1a)(McKenzie et al. 2010). Although not able to escape by hypha formation, the yeast-locked *C. albicans efg1Δ/Δcph1Δ/Δ* mutant, the non-filamentous *Candida* species *C. glabrata*, (Kaur, Ma, and Cormack 2007, Seider et al. 2011, Rai et al. 2012, Wartenberg et al. 2014, Lorenz, Bender, and Fink 2004) and *C. auris* (personal communication with Dr. Stefanie Allert) as well as the dimorphic opportunistic fungal pathogen *Talaromyces marneffeii*, which grows as yeast in the host (Pongpom et al. 2017) have been shown to replicate within macrophages, giving rise to the assumption that sufficient nutrients are present. The exact composition of nutrients in phagolysosomes is not known (Lorenz, Bender, and Fink 2004), but it is reasonable to assume that they contain carboxylic acids, proteins, peptides, amino acids, fatty acids, and the amino sugar GlcNAc, a potent inducer of hyphal formation (Alvarez and Konopka 2007, Vesely et al. 2017, Lorenz and Fink 2001, Williams and Lorenz 2020, Min, Naseem, and Konopka 2019). *C. albicans* mutants unable to import or catabolize GlcNAc and amino acids have been shown to be more prone to killing by macrophages (Vesely et al. 2017, Vylkova and Lorenz 2014), and are attenuated in virulence in murine systemic infection models (Singh, Ghosh, and

Datta 2001, Vylkova and Lorenz 2014) indicating that both nutrients are available carbon sources in macrophages and *in vivo*. Evidence exists that the *eed1Δ/Δ* mutant, which shows enhanced growth on amino acids, GlcNAc and citrate (**Manuscript III**, Fig. 6), is able to replicate within macrophages (Wittig 2016; Polke and Dunker *et al.*, unpublished): 6 h after infection of human monocyte-derived macrophages, the number of *eed1Δ/Δ* mutant cells contained per macrophage increased in comparison to 1 h whereas for the WT the number of internalized cells remained unaltered over time (Wittig 2016). In addition, time-lapse microscopy showed that the *eed1Δ/Δ* mutant can escape from some macrophages by intracellular replication leading eventually to the rupture of the macrophage membrane within approximately 10-12 h, while the WT is able to pierce the membrane of some macrophages after 6-9 h (Wittig 2016; Polke and Dunker *et al.*, unpublished). These observations are currently under further investigation. During the infection of tissues *C. albicans* is able to metabolize carbon by glycolysis, gluconeogenesis, the glyoxylate cycle, amino acid degradation and fatty acid β -oxidation (Miramón and Lorenz 2017). It is assumed that especially early in infection, phagocytosed fungal cells shift their metabolism from glycolysis to gluconeogenesis and the glyoxylate cycle (Williams and Lorenz 2020, Barelle et al. 2006, Lorenz, Bender, and Fink 2004). In later stages of infection, fungal cells heterogeneously perform mainly glycolysis but also gluconeogenesis (Barelle et al. 2006), indicating that to some extent glycolytic substrates must be available in tissues. Mutants with defects in either pathway are attenuated to some degree in virulence during systemic candidiasis suggesting that all pathways contribute to the virulence potential of *C. albicans* (Lorenz and Fink 2001, Barelle et al. 2006, Ramírez and Lorenz 2007). In tissues, preferred glycolytic substrates like glucose are scarce and *C. albicans*, in addition, has to compete with infiltrating immune cells as well, which in order to unfold their full antimicrobial potential are dependent on glucose metabolism (Tucey et al. 2018). Sources of energy for *C. albicans* might derive from metabolism of carboxylic acids such as citrate, likely abundant in the renal cortex (discussed in detail in **Manuscript III**), of amino acids as break down products of proteins, but also from the amino sugar GlcNAc that can be fed into glycolysis (Min, Naseem, and Konopka 2019). GlcNAc is part of glycosaminoglycans such as hyaluronic acid and thereby present in the extracellular matrix of all tissues and organs (Frantz, Stewart, and Weaver 2010, Bülow and Boor 2019). During systemic candidiasis, infection with the WT leads to the accumulation of hyaluronic acid (Ruhela et al. 2015), likely as a result of kidney injury that actively triggers its production (Jiang, Liang, and Noble 2011). *Via* the hexokinase Hex1 *C. albicans* is able to degrade hyaluronic acid *in vitro* and *in vivo* resulting in the release and free availability of GlcNAc (Ruhela et al. 2015) that could fuel the fungal metabolism. The importance of GlcNAc metabolism is demonstrated by a mutant lacking *HEX1*, which shows attenuated virulence in the systemic

infection model (Ruhela et al. 2015). It is therefore likely, that enhanced GlcNAc assimilation by *EED1* deficient or repressing yeast cells contributes to intracellular replication in macrophages but also to the replication in tissues *in vivo*. The importance of proteins and their breakdown products (amino acids) as carbon and nitrogen sources *in vivo* is displayed by the fact that amino acid auxotrophies of *C. albicans* strains had no impact on virulence in systemic infections (Noble and Johnson 2005) suggesting that amino acids are available in adequate concentrations *in vivo*. In the presence of bovine serum albumin (BSA) as sole nitrogen source (Staib et al. 2008) the *eed1Δ/Δ* mutant showed an early onset of growth indicating that the mutant is proteolytically more active than the WT *in vitro* (**Manuscript III**, Fig. 6). However, it has to be noted that *in vitro* growth experiments were conducted at pH 4, the optimal pH for the activity of the proteases Saps1-3 that are primarily yeast-associated (Naglik et al. 2004). Not surprisingly, the *SAP1* and *SAP3* genes were up-regulated during growth on amino acids at 37°C in the *eed1Δ/Δ* mutant *in vitro* (**Manuscript III**, Supplementary Fig. 16b), which might explain the observed phenotype. The pH of 4 differs greatly from physiological pH 7.4 in tissues; however, inflammation is known to reduce the local pH, although it drops only as low as pH 6 in tissue (Dong et al. 2013). This is still within the pH optimum of the hypha-associated Saps 4-6 which is pH 5-7 (Naglik et al. 2004). It might nevertheless be possible, that the *eed1Δ/Δ* mutant benefits from higher proteolytic activity e.g. in the acidic environment of the phagolysosomes of macrophages that has a pH between 4.5-5.5 (Seider et al. 2011). If this contributes to immune evasion remains to be determined.

Another factor that could have an impact on fungal proliferation, especially of the *eed1Δ/Δ* mutant, is farnesol. The quorum sensing molecule has been shown to be produced by the *eed1Δ/Δ* mutant in high amounts *in vitro* and is in part contributing to the defect in hyphal maintenance: When FOH was not able to accumulate in the supernatant due to flow conditions, the maintenance of filamentation of the *eed1Δ/Δ* mutant was prolonged leading to longer initial filaments than under static conditions (Polke et al. 2017). It is conceivable that *C. albicans* is producing FOH *in vivo* (Hornby et al. 2001). This might be especially true for the *eed1Δ/Δ* mutant that endogenously produces high amounts of FOH *in vitro* (Polke et al. 2017) and reaches high cell densities especially in the kidneys as shown in this thesis. It is, however, uncertain, which concentrations of FOH are produced and present in *C. albicans* infected tissues as FOH is able to diffuse and integrate into host membranes (Langford, Atkin, and Nickerson 2009, Nickerson et al. 2012). The presence of FOH in tissues could have many implications on pathogenesis. FOH has been shown to: (I) attract macrophages *in vitro* and *in vivo* (Hargarten et al. 2015), (II) low-grade activate neutrophils and monocytes (without having an impact on fungal phagocytosis or killing) (Leonhardt et al. 2015), (III) induce the formation of neutrophil extracellular traps (NETs) *in vitro* (Zawrotniak, Wojtalik, and

Rapala-Kozik 2019), which are web-like structures, decorated with antimicrobial granule proteins, able to trap and kill *C. albicans* (Mantovani et al. 2011, Urban et al. 2006); (IV) alter the differentiation of monocytes into DCs (Leonhardt et al. 2015), (V) shift the immune response towards an unprotective Th2 rather than a protective pro-inflammatory Th1 response (Navarathna, Nickerson, et al. 2007), (VI) protect *C. albicans* from oxidative stress *in vitro* (Westwater, Balish, and Schofield 2005), and (VII) modulate the fungal metabolism (Han, Cannon, and Villas-Bôas 2012a). The attraction of higher numbers of immune cells at later time points in response to *C. albicans* t-EED1+ yeast (**Manuscript III**, Fig. 4b) might therefore be also a consequence of increased FOH production by the yeast cells. Han *et al.*, showed, that when yeast growth of *C. albicans* was enforced under hypha-inducing conditions by addition of FOH, pathways involved in central carbon and energy metabolism were overall up-regulated (Han, Cannon, and Villas-Bôas 2012a), whereas the transition from yeast to hyphal growth is associated with down-regulation of metabolism accompanied by lower ATP production (Han, Cannon, and Villas-Bôas 2012b). This might, in part, explain the better initial growth of the *eed1Δ/Δ* mutant in the presence of different carbon sources (**Manuscript III**, Fig. 6). Interestingly, exogenous addition of FOH to the WT dose-dependently promoted the growth of the WT to almost *eed1Δ/Δ* mutant level in media containing citrate as sole carbon source and led to a dose-dependent earlier onset of growth in media with BSA as sole nitrogen source at 37 °C (Zeuch 2019). Thus, the production of FOH by the *eed1Δ/Δ* mutant *in vivo* might be advantageous as it potentially allows the mutant to better use alternative carbon sources, thereby increasing the fitness of the mutant in the absence of filamentation. Because FOH is able to block one of the most important virulence traits, the yeast-to-hypha transition, and prevents biofilm formation, it was considered to be a useful therapeutic target to lower the pathogenic potential of *C. albicans*. (Hornby et al. 2001). While in superficial candidiasis models FOH was proven to have a positive impact on disease progression (Hisajima et al. 2008), in systemic infection the obverse effect was observed: Administration of FOH either intraperitoneally or orally in the drinking water promoted infection and led to accelerated mortality (Navarathna, Hornby, et al. 2007). Likewise, strains producing higher FOH concentrations *in vitro* turned out to be more virulent in systemic infection than strains that endogenously produce less FOH like an *dpp3Δ/Δ* mutant, that despite proper hyphal formation showed attenuated virulence (Navarathna, Hornby, et al. 2007). Interestingly, the application of exogenous FOH resulted in early and rapid fungal replication in the kidneys of infected mice (Navarathna, Hornby, et al. 2007), similar to what was observed in this thesis with *C. albicans* strains lacking or repressing *EED1*. Fungal replication in the kidney started between 8 and 12 h p.i. when FOH was administered to mice, whereas infection with the same strain in absence of FOH reached these high fungal burdens only 48 h later, indicating that FOH acts

as a virulence factor of *C. albicans* in systemic infection (Navarathna, Hornby, et al. 2007, Navarathna, Nickerson, et al. 2007). It is therefore likely that the increased FOH production by *C. albicans* in absence of *EED1* speeds up fungal replication in the kidneys, probably by altering fungal metabolism. Exogenously applied FOH to mice, however, had no effect on fungal morphology of the WT (Navarathna, Hornby, et al. 2007). It might be possible, that FOH concentration necessary to affect fungal metabolism is lower than the level for filamentation; in that case WT metabolism could be altered despite hyphal formation. However, it cannot be excluded that other factors, e.g. immunomodulation, contribute to the observed phenomenon.

Interestingly though, the filamentous *nrg1Δ/Δ* and *tup1Δ/Δ* mutants are producing high amounts of FOH (Kebaara et al. 2008) but show reduced virulence in a systemic infection model (Murad et al. 2001, Braun, Kadosh, and Johnson 2001). In contrast to an *eed1Δ/Δ* mutant, however, both mutants are unresponsive to FOH with regards to fungal morphology (Kebaara et al. 2008). Consequently, the *nrg1Δ/Δ* and the *tup1Δ/Δ* mutant grow constitutively as hyphae or pseudohyphae respectively, even under non-hypha inducing conditions and in the presence of FOH (Braun et al. 2000, Cleary et al. 2016, Braun, Kadosh, and Johnson 2001, Kebaara et al. 2008). In fact, filamentous mutants such as the *nrg1Δ/Δ* mutant are cleared more efficiently from infected tissue after injection in the filamentous form (Cleary et al. 2016). Regulable strains, such as the tet-*NRG1* strain allow injection in the yeast form with subsequent regulation of morphology *via* gene expression *in vivo* by doxycycline (Saville et al. 2003, Saville et al. 2008, Cleary et al. 2016). In the systemic infection model the fungal burden of the tet-*NRG1*+ filamentous strain, in which only one allele of *NRG1* is repressed (Saville et al. 2003), initially dropped between 6 and 48 h p.i., increased thereafter in the kidney until mice become moribund, but never exceeded 2×10^4 CFU/g body weight (WT+ reached median renal burden of 8×10^4 CFU/g body weight; **(Manuscript III, Supplementary Fig. 4d)**). Fungal burden for the tet-*NRG1*+ filamentous strain continuously decreased over time in liver and spleen even faster than observed for the WT. It might therefore be possible that the *nrg1Δ/Δ* and the *tup1Δ/Δ* mutants are not reaching sufficiently high numbers of cells in tissue to produce concentrations of FOH that are necessary to exert a biological effect. On the other hand, the unresponsiveness of the *nrg1Δ/Δ* and the *tup1Δ/Δ* mutant to FOH (Kebaara et al. 2008), in contrast to *C. albicans* *EED1*-deficient mutants, might render these strains unable to benefit from an FOH-mediated altered metabolism.

In summary, in the absence of *EED1* (expression) *C. albicans* is able to rapidly replicate in the host environment, especially in the kidney, likely because of better metabolic adaptation to the nutritional environment of the host that could be in part shaped by higher local FOH concentrations.

5.4. High numbers of *EED1*-repressing yeast damage kidneys to the same extent as the WT

Progression of systemic candidiasis in the mouse model is associated with a steady increase in kidney fungal burden, hyphal formation and the attraction of leukocytes to the site of infection that contribute to renal damage, organ dysfunction and eventually lead to sepsis and death (Spellberg et al. 2005, Lionakis et al. 2011). Considering the reduced capacity of an *eed1Δ/Δ* mutant to damage different epithelial cells *in vitro*, initial early damage of kidney tissue *in vivo* is likely reduced as well. This explains the lower induction of renal pro-inflammatory cytokines observed 24 h p.i. in comparison to WT (**Manuscript III**, Fig. 4b). Initial lower cytokine responses might also be the consequence of the lack of *ECE1* expression in the *eed1Δ/Δ* mutant, as lower renal cytokine levels have been observed after systemic infection with an *ece1Δ/Δ* mutant despite hyphal formation and a higher kidney fungal burden in comparison to the WT 24 h p.i. (Swidergall et al. 2019). Kidney damage, detected by determination of urinary Kidney Injury Molecule-1 (KIM-1) concentrations was measurable 48 h p.i. with an intermediate infectious dose of *C. albicans* WT and *eed1Δ/Δ* mutant (**Manuscript III**, Fig. 8a). The type 1 transmembrane protein KIM-1 serves as an early biomarker of proximal tubular injury in men and mice (Han et al. 2002, Sabbisetti et al. 2013b) and is negatively correlating with kidney function (Edelstein 2008). KIM-1 (mRNA and protein) is expressed at low levels in the healthy kidney but is highly expressed upon kidney injury (Edelstein 2008, Sabbisetti et al. 2013a). The ectodomain of KIM-1 is shed into the urine, and by noninvasive measurement of urinary KIM-1 levels, sensitive detection of injury is possible within 12 h after the insult (Han et al. 2002, Sabbisetti et al. 2013a). Therefore, it is reasonable that kidney damage by *C. albicans* occurred within the time frame of 24-36 h. Twenty four hours p.i. t-EED1+ yeast already had a 25-fold higher kidney fungal burden than the WT, however, immune cell infiltration and neutrophil activation as measured by renal MPO concentrations (Fig. 10) was comparable between WT and t-EED1+ yeast 24 h p.i. KIM-1 level further increased until 72 h p.i. indicative of progressing kidney disease. Whereas kidney damage was detected early p.i., kidney function, measured by blood urea nitrogen (BUN) and serum creatinine level, was impaired only in moribund mice infected with *C. albicans* (**Manuscript III**; Fig. 8b,c), which is in accordance with Spellberg *et al.* (Spellberg et al. 2005). Both markers are known for their late response and lack of sensitivity and specificity during kidney injury (Sabbisetti et al. 2013a): BUN and serum creatinine level in mice rise only when 70-75% of the nephrons are dysfunctional (Perše and Večerić-Haler 2018). However, both markers increased to the same degree in WT and t-EED1+ yeast-infected mice, indicating that kidneys were severely damaged in moribund mice irrespective of the fungal morphology. In addition, immunohistochemistry showed similar areas of apoptotic renal tissue (**Manuscript III**, Fig. 8d,e). Of

note, kidneys of mice infected with t-EED1+ yeast were damaged to the same extent as kidneys of WT-infected mice, although the fungal burden of t-EED1+ yeast were higher, indicating that (I) a higher number of yeast cells are necessary to cause similar damage, and (II) that yeast can damage the kidney in the absence of filamentation. It might be reasonable, that fungal intracellular replication, like observed in the RHE model by Zakikhany *et al.* (Zakikhany et al. 2007), is sufficient to damage the kidney to an extent leading to KIM-1 levels comparable to WT infections early after infection, although damage was not observed *in vitro* (Zakikhany et al. 2007).

5.5. Contribution of immunopathology to virulence of the *eed1Δ/Δ* mutant

Damage during progressing infection in immunocompetent mice can be enhanced by immunopathology, driven by recruitment and activation of immune cells such as neutrophils, whose antimicrobial activities can cause collateral tissue damage (Kruger et al. 2015). In fact, 72 h p.i. higher numbers of immune cells infiltrated the kidneys of t-EED1+ yeast infected mice in comparison to WT-infected mice. Abscesses containing high numbers of immune cells were also observed by histological analysis of moribund immunocompetent mice, infected with low infectious doses of the *eed1Δ/Δ* mutant (**Manuscript III**, Fig. 9b), indicating that immunopathology might play a more prominent role in pathogenesis during disease progression at later stages. In moribund mice, t-EED1+ yeast were found in large numbers mainly within tubules and in the renal pelvis; it appears possible that massive replication of yeast led to obstruction of tubules and the collecting duct system (Boulanger et al. 2016). Together with an increased immune cell infiltration in the kidneys, which possess rigid capsules, this could generate high intrarenal pressure possibly contributing to kidney damage in the progressing disease. Although e.g. neutrophils can contribute to immunopathology, their importance in combating systemic candidiasis becomes most obvious when they are absent reflected by neutropenia being a major risk factor for systemic candidiasis (Pfaller 1996, Abi-Said et al. 1997, Gilbert, Wheeler, and May 2014). In contrast to the situation in humans, lymphocytes and not neutrophils are the most abundant cell type in murine blood (**Manuscript II**). However, neutrophils are as important to fight experimentally induced systemic candidiasis in mice as in humans (Fulurija, Ashman, and Papadimitriou 1996, Han and Cutler 1997). In addition, monocytes and macrophages contribute to antifungal defense as well, as their absence is associated with increased mortality in experimental candidiasis (Qian et al. 1994). While neutrophils mediate protective effects especially early after infection, their continuous infiltration into and activation within the kidney drives immunopathology and accelerates disease progression (Lionakis et al. 2011, Lionakis et al. 2012). Interestingly, whereas immune cell infiltration in response to infection with the t-EED1+ yeast was comparable to the WT early after infection, the

number of infiltrating immune cells increased for t-EED1+ yeast 72 h p.i. likely due to the higher kidney fungal load. The larger number of leukocytes is also likely the explanation for the increased concentrations of pro-inflammatory cytokines observed at that time point. Systemic inflammation measured by serum neutrophil gelatinase-associated lipocalin (NGAL) and soluble triggering receptor expressed on myeloid cells (sTREM-1) levels was detected early after infection (24 h p.i.) and rose until mice become moribund (**Manuscript III**, Fig. 4c). However, both markers were not affected by the increased local renal inflammation 72 h p.i., as their levels did not differ in serum of mice infected with intermediate doses of either *C. albicans* WT, t-EED1+ yeast, or t-EED1- hyphae. To test whether the renal damage caused by the *eed1Δ/Δ* mutant was driven by immunopathology, mice rendered immunosuppressed by the antibody-mediated depletion of neutrophils and monocytes were infected with *C. albicans* WT or *eed1Δ/Δ* mutant. Although the infectious dose was lowered to 10^3 and 10^2 CFU/g body weight, disease started early and progressed rapidly, especially in response to WT infections (**Manuscript III**, Fig. 9a). The *eed1Δ/Δ* mutant showed a delayed onset of disease compared to the WT; nonetheless, the mutant caused lethal infection in all mice. Fungal burden of mice infected with the WT increased rapidly until a certain threshold was reached that was incompatible with survival of the mice. Interestingly, the threshold level was approximately in the same range as for immunocompetent mice only that the time required to reach this threshold was markedly reduced in immunosuppressed mice (Fig. 7), underscoring the importance of neutrophils and monocytes to restrict fungal growth early after infection. Hyphae detected by histopathology were found frequently in the renal cortex and were much shorter than hyphae observed in immunocompetent mice. This is due to the reduced time the fungus was able to perform unconstrained growth in immunosuppressed mice, however, the shortened time was likely compensated by the amount of cells that began germinating and filamenting in the renal cortex in consequence leading to early onset of disease.

Like observed after WT infection in immunosuppressed mice, fungal burden increased rapidly after challenge with the *eed1Δ/Δ* mutant, especially in the kidneys but also in the spleen and in the liver (**Manuscript III**, Fig. 9c). Twelve hours p.i. renal fungal burden of the *eed1Δ/Δ* mutant was already 10-fold higher in comparison to the WT. Interestingly, higher *eed1Δ/Δ* yeast burden in the kidney correlated with increased kidney damage measured by urinary KIM-1 level (**Manuscript III**, Fig. 9d), suggesting that yeast cells are able to damage renal tissue in the absence of an overt inflammation. Histology showed massive yeast replication especially in the tubules of cells (**Manuscript III**, Fig. 9b) what could impede kidney function (Fulurija, Ashman, and Papadimitriou 1996).

The delay in disease onset observed after infection with the *eed1Δ/Δ* mutant is likely the consequence of the time required to reach detrimental fungal densities within the kidneys after

challenge with a low infectious dose. Interestingly, tet-*NRG1*- yeast were also found capable of inducing lethal infection in neutropenic mice: Although avirulent in immunocompetent mice, tet-*NRG1*- yeast led to 100% mortality in cyclophosphamide-cortisone acetate treated leukopenic mice, with a slight delay in onset of mortality in comparison to tet-*NRG1*+ filaments, too (Saville et al. 2008). In addition, tet-*NRG1*- yeast reached similar levels (2.1×10^7 CFU/g) (Saville et al. 2008) as the *eed1* Δ/Δ mutant (2.0 - 2.2×10^7 CFU/g) in immunosuppressed mice. However, in comparison to the low dose of the *eed1* Δ/Δ mutant applied (10^3 CFU/g body weight), that led to a medium survival of 30 h, Saville *et al.*, infected mice with a 85-fold higher infectious dose (8.5×10^4 CFU/g body weight) resulting in 100% mortality within two days. Hence, it appears likely that the rapidly proliferating *eed1* Δ/Δ mutant is more virulent than tet-*NRG1*- yeast in immunosuppressed mice. Nevertheless, immunosuppressed mice are equally susceptible to both, the yeast and the hyphal morphology of *C. albicans*. The results of this thesis hint towards a partial contribution of immunopathology to pathogenesis of systemic infection by *C. albicans* *EED1* deficient or repressing yeast but not during tet-*NRG1*- yeast infection: Whereas tet-*NRG1*- yeast can be cleared in immunocompetent mice (Saville et al. 2006), in mice challenged with the t-*EED1*+ yeast fungal burden increased rapidly in the presence of immune cells, which continuously infiltrated the kidneys in the later stages of infection and likely accelerated disease progression.

5.6. Conclusion

The transition of yeast to hypha is considered to be the key virulence factor of *C. albicans*. Hyphae are likely required for the traversal from the gastrointestinal tract and are essential for deep invasion of tissue in invasion-based murine infection models. In addition, hyphal formation allows *C. albicans* to escape from immune cells and therefore represents an immune evasion strategy.

Strikingly however, hyphae are not essential for virulence in systemic infections as filament-deficient *C. albicans* strains unable to express *EED1* retain their virulence in immunosuppressed, but also in immunocompetent mice. It is therefore likely, that in a susceptible host the fungal morphology is less important during systemic candidiasis than previously thought. The results obtained in this thesis challenge the central dogma that hypha formation is *per se* essential for pathogenesis. This thesis further shows that, although different *C. albicans* mutants share the same yeast morphology, they can differ with regards to their virulence potential.

Retained virulence of *C. albicans* mutants unable to express *EED1* was associated with rapid proliferation in the yeast morphology especially within the kidneys, likely the consequence of a better adaptation to the local environment and increased metabolic fitness. In addition, like the non-filamentous species *C. glabrata*, *C. auris* and the *C. albicans* mutant *efg1Δ/Δcph1Δ/Δ* (Kaur, Ma, and Cormack 2007, Seider et al. 2011, Rai et al. 2012, Wartenberg et al. 2014, Lorenz, Bender, and Fink 2004), the *eed1Δ/Δ* mutant is able to replicate inside macrophages. Whether the ability of the *eed1Δ/Δ* mutant to intrinsically produce high amounts of farnesol (Polke et al. 2017) contributes to the metabolic fitness and rapid replication *in vivo* remains elusive. However, evidence exists that exogenously supplied FOH improves the growth of the WT on certain physiologically relevant carbon sources *in vitro* (Zeuch 2019), implying that FOH could contribute to the virulence phenotype observed. High renal fungal burden of *C. albicans* *EED1* deficient or repressing yeast resulted in tissue damage indistinguishable to infections caused by the filamentous WT, which, to a certain degree is attributable to immunopathology.

Although the molecular function of Eed1 remains unclear, the *eed1Δ/Δ* mutant allows studying the importance of the yeast morphology during pathogenesis. This work further shows how well *C. albicans* is able to adapt to its environment. In addition, this work provides some explanations how non-albicans species that are not able to form filaments establish serious systemic infections. A better understanding of the processes that lead to pathogenesis in the absence of hyphal formation could aid in finding strategies to combat fungal infections other than blocking filamentation.

6. References

- Abi-Said, Dima, Elias Anaissie, Omrum Uzun, Issam Raad, Helio Pinzcowski, and Shahe Vartivarian. 1997. "The Epidemiology of Hematogenous Candidiasis Caused by Different *Candida* Species." *Clin. Infect. Dis.* 24 (6):1122-1128. doi: 10.1086/513663.
- Akpan, A., and R. Morgan. 2002. "Oral candidiasis." *Postgrad. Med. J.* 78 (922):455-459. doi: 10.1136/pmj.78.922.455.
- Alberts, Bruce, Alexander Johnson, Julian Lewis, Martin Raff, Keith Roberts, and Peter Walter. 2002. *Molecular biology of the cell, 4th edition; Helper T Cells and Lymphocyte Activation*. New York: Garland Science.
- Allert, Stefanie, Toni M. Förster, Carl-Magnus Svensson, Jonathan P. Richardson, Tony Pawlik, Betty Hebecker, Sven Rudolphi, Marc Juraschitz, Martin Schaller, Mariana Blagojevic, Joachim Morschhäuser, Marc Thilo Figge, Ilse D. Jacobsen, Julian R. Naglik, Lydia Kasper, Selene Mogavero, and Bernhard Hube. 2018. "*Candida albicans*-Induced Epithelial Damage Mediates Translocation through Intestinal Barriers." *mBio* 9 (3):e00915-18. doi: 10.1128/mBio.00915-18 %J mBio.
- Almeida, Fausto, Marcio L. Rodrigues, and Carolina Coelho. 2019. "The Still Underestimated Problem of Fungal Diseases Worldwide." *Front. Microbiol.* 10:214-214. doi: 10.3389/fmicb.2019.00214.
- Alvarez, F. J., and J. B. Konopka. 2007. "Identification of an N-acetylglucosamine transporter that mediates hyphal induction in *Candida albicans*." *Mol. Biol. Cell* 18 (3):965-975. doi: 10.1091/mbc.e06-10-0931.
- Balish, E., R. D. Wagner, A. Vázquez-Torres, C. Pierson, and T. Warner. 1998. "Candidiasis in Interferon- γ Knockout (IFN- γ -/-) Mice." *J. Infect. Dis.* 178 (2):478-487. doi: 10.1086/515645.
- Ballou, Elizabeth R., Gabriela M. Avelar, Delma S. Childers, Joanna Mackie, Judith M. Bain, Jeanette Wagener, Stavroula L. Kastora, Mirela D. Panea, Sarah E. Hardison, Louise A. Walker, Lars P. Erwig, Carol A. Munro, Neil A. R. Gow, Gordon D. Brown, Donna M. MacCallum, and Alistair J. P. Brown. 2016. "Lactate signalling regulates fungal β -glucan masking and immune evasion." *Nat. Microbiol.* 2:16238-16238. doi: 10.1038/nmicrobiol.2016.238.
- Banerjee, Mohua, Delma S. Thompson, Anna Lazzell, Patricia L. Carlisle, Christopher Pierce, Carlos Monteagudo, José L. López-Ribot, and David Kadosh. 2008. "*UME6*, a novel filament-specific regulator of *Candida albicans* hyphal extension and virulence." *Mol. Biol. Cell* 19 (4):1354-1365. doi: 10.1091/mbc.E07-11-1110.
- Barelle, Caroline J., Claire L. Priest, Donna M. Maccallum, Neil A. R. Gow, Frank C. Odds, and Alistair J. P. Brown. 2006. "Niche-specific regulation of central metabolic pathways in a fungal pathogen." *Cell. Microbiol.* 8 (6):961-971. doi: 10.1111/j.1462-5822.2005.00676.x.
- Bensasson, Douda, Jo Dicks, John M. Ludwig, Christopher J. Bond, Adam Elliston, Ian N. Roberts, and Stephen A. James. 2019. "Diverse Lineages of *Candida albicans* Live on Old Oaks." *Genetics* 211 (1):277-288. doi: 10.1534/genetics.118.301482.
- Berberi, Antoine, Ziad Noujeim, and Georges Aoun. 2015. "Epidemiology of Oropharyngeal Candidiasis in Human Immunodeficiency Virus/Acquired Immune Deficiency Syndrome Patients and CD4+ Counts." *J. Int. Oral Health* 7 (3):20-23.
- Berman, Judith. 2006. "Morphogenesis and cell cycle progression in *Candida albicans*." *Curr. Opin. Microbiol.* 9 (6):595-601. doi: 10.1016/j.mib.2006.10.007.
- Biswas, Subhrajit, Patrick Van Dijck, and Asis Datta. 2007. "Environmental Sensing and Signal Transduction Pathways Regulating Morphopathogenic Determinants of *Candida albicans*." *Microbiol. Mol. Biol. Rev.* 71 (2):348-376. doi: 10.1128/MMBR.00009-06.
- Blankenship, Jill R., and Aaron P. Mitchell. 2006. "How to build a biofilm: a fungal perspective." *Curr. Opin. Microbiol.* 9 (6):588-594. doi: 10.1016/j.mib.2006.10.003.

- Bockmühl, D. P., and J. F. Ernst. 2001. "A potential phosphorylation site for an A-type kinase in the Efg1 regulator protein contributes to hyphal morphogenesis of *Candida albicans*." *Genetics* 157 (4):1523-1530.
- Böhm, L., S. Torsin, S. H. Tint, M. T. Eckstein, T. Ludwig, and J. C. Pérez. 2017. "The yeast form of the fungus *Candida albicans* promotes persistence in the gut of gnotobiotic mice." *PLoS Pathog.* 13 (10):e1006699. doi: 10.1371/journal.ppat.1006699.
- Böttcher, Bettina, Christine Pöllath, Peter Staib, Bernhard Hube, and Sascha Brunke. 2016. "Candida species Rewired Hyphae Developmental Programs for Chlamydospore Formation." *Front. Microbiol.* 7 (1697):1-17. doi: 10.3389/fmicb.2016.01697.
- Boulanger, Yves, Marie-Sophie Ghuysen, Alain Nchimi, Michel Lewin, and Jamil Khamis. 2016. "Ultrasound Diagnosis and Follow-Up of Neonate Renal Candidiasis." *J. Belgian Soc. Radiol.* 100 (1):113-113. doi: 10.5334/jbr-btr.1059.
- Braun, B. R., W. S. Head, M. X. Wang, and A. D. Johnson. 2000. "Identification and characterization of *TUP1*-regulated genes in *Candida albicans*." *Genetics* 156 (1):31-44.
- Braun, B. R., D. Kadosh, and A. D. Johnson. 2001. "*NRG1*, a repressor of filamentous growth in *C. albicans*, is down-regulated during filament induction." *EMBO J.* 20 (17):4753-4761. doi: 10.1093/emboj/20.17.4753.
- Brien, Heath E., Jeri Lynn Parrent, Jason A. Jackson, Jean-Marc Moncalvo, and Rytas Vilgalys. 2005. "Fungal Community Analysis by Large-Scale Sequencing of Environmental Samples." *Applied and Environmental Microbiology* 71 (9):5544. doi: 10.1128/AEM.71.9.5544-5550.2005.
- Brock, Matthias. 2009. "Fungal metabolism in host niches." *Curr. Opin. Microbiol.* 12 (4):371-376. doi: 10.1016/j.mib.2009.05.004.
- Brown, Alistair J. P., Gordon D. Brown, Mihai G. Netea, and Neil A. R. Gow. 2014. "Metabolism impacts upon *Candida* immunogenicity and pathogenicity at multiple levels." *Trends Microbiol.* 22 (11):614-622. doi: 10.1016/j.tim.2014.07.001.
- Brown, G. D., D. W. Denning, N. A. Gow, S. M. Levitz, M. G. Netea, and T. C. White. 2012. "Hidden killers: human fungal infections." *Sci. Transl. Med.* 4 (165):165rv13. doi: 10.1126/scitranslmed.3004404.
- Brown, Gordon D. 2011. "Innate antifungal immunity: the key role of phagocytes." *Annu. Rev. Immunol.* 29:1-21. doi: 10.1146/annurev-immunol-030409-101229.
- Brusselsaers, Nele, Stijn Blot, and Dirk Vogelaers. 2011. "Deep-seated *Candida* infections in the intensive care unit." *Neth. J. Crit. Care.* 15 (4):183 - 189.
- Bülow, Roman David, and Peter Boor. 2019. "Extracellular Matrix in Kidney Fibrosis: More Than Just a Scaffold." *J. Histochem. Cytochem.* 67 (9):643-661. doi: 10.1369/0022155419849388.
- Byrnes, Edmond J., 3rd, Karen H. Bartlett, John R. Perfect, and Joseph Heitman. 2011. "*Cryptococcus gattii*: an emerging fungal pathogen infecting humans and animals." *Microbes Infect.* 13 (11):895-907. doi: 10.1016/j.micinf.2011.05.009.
- Calderone, Richard A., and Cornelius J. Clancy. 2012. *Candida and Candidiasis, Second Edition*: American Society of Microbiology.
- Carlisle, Patricia L., Mohua Banerjee, Anna Lazzell, Carlos Monteagudo, José L. López-Ribot, and David Kadosh. 2009. "Expression levels of a filament-specific transcriptional regulator are sufficient to determine *Candida albicans* morphology and virulence." *Proceedings of the National Academy of Sciences of the United States of America* 106 (2):599-604. doi: 10.1073/pnas.0804061106.
- Carlisle, Patricia L., and David Kadosh. 2010. "*Candida albicans* Ume6, a filament-specific transcriptional regulator, directs hyphal growth via a pathway involving Hgc1 cyclin-related protein." *Eukaryot. Cell* 9 (9):1320-1328. doi: 10.1128/EC.00046-10.
- Casadevall, A. 2017. "Don't Forget the Fungi When Considering Global Catastrophic Biorisks." *Health Secur.* 15 (4):341-342. doi: 10.1089/hs.2017.0048.

- Casadevall, A., and L. A. Pirofski. 1999. "Host-pathogen interactions: redefining the basic concepts of virulence and pathogenicity." *Infect. Immun.* 67 (8):3703-3713. doi: 10.1128/IAI.67.8.3703-3713.1999.
- Cenci, Elio, Antonella Mencacci, Giuseppe Del Sero, Cristiana Fé d'Ostiani, Paolo Mosci, Angela Bacci, Claudia Montagnoli, Manfred Kopf, and Luigina Romani. 1998. "IFN- γ Is Required for IL-12 Responsiveness in Mice with *Candida albicans* Infection." *J. Immunol. Res.* 161 (7):3543-3550.
- Chaffin, W. LaJean. 2008. "Candida albicans cell wall proteins." *Microbiol. Mol. Biol. Rev.* 72 (3):495-544. doi: 10.1128/MMBR.00032-07.
- Chandra, J., D. M. Kuhn, P. K. Mukherjee, L. L. Hoyer, T. McCormick, and M. A. Ghannoum. 2001. "Biofilm formation by the fungal pathogen *Candida albicans*: development, architecture, and drug resistance." *J. Bacteriol.* 183 (18):5385-5394. doi: 10.1128/jb.183.18.5385-5394.2001.
- Chen, C. G., Y. L. Yang, H. H. Cheng, C. L. Su, S. F. Huang, C. T. Chen, Y. T. Liu, I. J. Su, and H. J. Lo. 2006. "Non-Lethal *Candida albicans* CPH1/CPH1 EFG1/EFG1 Transcription Factor Mutant Establishing Restricted Zone of Infection in a Mouse Model of Systemic Infection." *Int. J. Immunopathol. Pharmacol.* 19 (3):561-565. doi: 10.1177/039463200601900312.
- Chen, Hui, Xuedong Zhou, Biao Ren, and Lei Cheng. 2020. "The regulation of hyphae growth in *Candida albicans*." *Virulence* 11 (1):337-348. doi: 10.1080/21505594.2020.1748930.
- Cheng, S. C., L. A. Joosten, B. J. Kullberg, and M. G. Netea. 2012. "Interplay between *Candida albicans* and the mammalian innate host defense." *Infect. Immun.* 80 (4):1304-1313. doi: 10.1128/iai.06146-11.
- Childers, Delma S., Ingrida Raziunaite, Gabriela Mol Avelar, Joanna Mackie, Susan Budge, David Stead, Neil A. R. Gow, Megan D. Lenardon, Elizabeth R. Ballou, Donna M. MacCallum, and Alistair J. P. Brown. 2016. "The Rewiring of Ubiquitination Targets in a Pathogenic Yeast Promotes Metabolic Flexibility, Host Colonization and Virulence." *PLoS Pathog.* 12 (4):e1005566. doi: 10.1371/journal.ppat.1005566.
- Chin, Voon Kin, Tze Yan Lee, Basir Rusliza, and Pei Pei Chong. 2016. "Dissecting *Candida albicans* Infection from the Perspective of *C. albicans* Virulence and Omics Approaches on Host-Pathogen Interaction: A Review." *Int. J. Mol. Sci.* 17 (10):1643. doi: 10.3390/ijms17101643.
- Chowdhury, P., S. H. Sacks, and N. S. Sheerin. 2004. "Minireview: functions of the renal tract epithelium in coordinating the innate immune response to infection." *Kidney Int.* 66 (4):1334-1344. doi: 10.1111/j.1523-1755.2004.00896.x.
- Clancy, C. J., and M. H. Nguyen. 2013. "Finding the "missing 50%" of invasive candidiasis: how nonculture diagnostics will improve understanding of disease spectrum and transform patient care." *Clin. Infect. Dis.* 56 (9):1284-1292. doi: 10.1093/cid/cit006.
- Cleary, Ian A., Anna L. Lazzell, Carlos Monteagudo, Derek P. Thomas, and Stephen P. Saville. 2012. "BRG1 and NRG1 form a novel feedback circuit regulating *Candida albicans* hypha formation and virulence." *Mol. Microbiol.* 85 (3):557-573. doi: 10.1111/j.1365-2958.2012.08127.x.
- Cleary, Ian A., Sara M. Reinhard, Anna L. Lazzell, Carlos Monteagudo, Derek P. Thomas, Jose L. Lopez-Ribot, and Stephen P. Saville. 2016. "Examination of the pathogenic potential of *Candida albicans* filamentous cells in an animal model of haematogenously disseminated candidiasis." *FEMS Yeast Res.* 16 (2):1-10. doi: 10.1093/femsyr/fow011 %J FEMS Yeast Research.

- Cleary, Ian A., Sara M. Reinhard, C. Lindsay Miller, Craig Murdoch, Martin H. Thornhill, Anna L. Lazzell, Carlos Monteagudo, Derek P. Thomas, and Stephen P. Saville. 2011. "Candida albicans adhesin Als3p is dispensable for virulence in the mouse model of disseminated candidiasis." *Microbiology* 157 (6):1806-1815. doi: 10.1099/mic.0.046326-0.
- Cleary, Ian A., and Stephen P. Saville. 2010. "An analysis of the impact of *NRG1* overexpression on the *Candida albicans* response to specific environmental stimuli." *Mycopathologia* 170 (1):1-10. doi: 10.1007/s11046-010-9297-2.
- Clement, Cristina C., Aniuska Becerra, Liusong Yin, Valerio Zolla, Liling Huang, Simone Merlin, Antonia Follenzi, Scott A. Shaffer, Lawrence J. Stern, and Laura Santambrogio. 2016. "The Dendritic Cell Major Histocompatibility Complex II (MHC II) Peptidome Derives from a Variety of Processing Pathways and Includes Peptides with a Broad Spectrum of HLA-DM Sensitivity." *J. Biol. Chem.* 291 (11):5576-5595. doi: 10.1074/jbc.M115.655738.
- Cornely, Oliver A., Christopher Bangard, and Natalie I. Jaspers. 2015. "Hepatosplenic candidiasis." *Clin. Liver Dis.* 6 (2):47-50. doi: 10.1002/cld.491.
- Crawford, Aaron, and Duncan Wilson. 2015. "Essential metals at the host-pathogen interface: nutritional immunity and micronutrient assimilation by human fungal pathogens." *FEMS Yeast Res.* 15 (7):fov071. doi: 10.1093/femsyr/fov071.
- Dalle, Frederic, Betty Wächtler, Coralie L'Ollivier, Gudrun Holland, Norbert Bannert, Duncan Wilson, Catherine Labruère, Alain Bonnin, and Bernhard Hube. 2010. "Cellular interactions of *Candida albicans* with human oral epithelial cells and enterocytes." *Cell Microbiol.* 12 (2):248-271. doi: 10.1111/j.1462-5822.2009.01394.x.
- Das, I., P. Nightingale, M. Patel, and P. Jumaa. 2011. "Epidemiology, clinical characteristics, and outcome of candidemia: experience in a tertiary referral center in the UK." *Int. J. Infect. Dis.* 15 (11):e759-63. doi: 10.1016/j.ijid.2011.06.006.
- de Groot, Piet W. J., Oliver Bader, Albert D. de Boer, Michael Weig, and Neeraj Chauhan. 2013. "Adhesins in human fungal pathogens: glue with plenty of stick." *Eukaryot. Cell* 12 (4):470-481. doi: 10.1128/EC.00364-12.
- Delaloye, Julie, and Thierry Calandra. 2014. "Invasive candidiasis as a cause of sepsis in the critically ill patient." *Virulence* 5 (1):161-169. doi: 10.4161/viru.26187.
- Denning, D. W., M. Kneale, J. D. Sobel, and R. Rautemaa-Richardson. 2018. "Global burden of recurrent vulvovaginal candidiasis: a systematic review." *Lancet Infect. Dis.* 18 (11):e339-e347. doi: 10.1016/s1473-3099(18)30103-8.
- Desai, Jigar V. 2018. "Candida albicans Hyphae: From Growth Initiation to Invasion." *J. Fungi* 4 (1):10-19. doi: 10.3390/jof4010010.
- Di Carlo, Paola, Gaetano Di Vita, Giuliana Guadagnino, Gianfranco Cocorullo, Francesco D'Arpa, Giuseppe Salamone, Buscemi Salvatore, Gaspare Gulotta, and Daniela Cabibi. 2013. "Surgical pathology and the diagnosis of invasive visceral yeast infection: two case reports and literature review." *World J. Emerg. Surg.* 8 (1):38-38. doi: 10.1186/1749-7922-8-38.
- Doedt, Thomas, Shankarling Krishnamurthy, Dirk P. Bockmühl, Bernd Tebarth, Christian Stempel, Claire L. Russell, Alistair J. P. Brown, and Joachim F. Ernst. 2004. "APSES proteins regulate morphogenesis and metabolism in *Candida albicans*." *Mol. Biol. Cell* 15 (7):3167-3180. doi: 10.1091/mbc.e03-11-0782.
- Dolin, Hallie H., Thomas J. Papadimos, Xiaohuan Chen, and Zhixing K. Pan. 2019. "Characterization of Pathogenic Sepsis Etiologies and Patient Profiles: A Novel Approach to Triage and Treatment." *Microbiol. Insights* 12:1178636118825081-1178636118825081. doi: 10.1177/1178636118825081.
- Dong, C., and R. A. Flavell. 2000. "Cell fate decision: T-helper 1 and 2 subsets in immune responses." *Arthritis Res.* 2 (3):179-188. doi: 10.1186/ar85.

- Dong, Lixue, Zhigang Li, Nancy R. Leffler, Adam S. Asch, Jen-Tsan Chi, and Li V. Yang. 2013. "Acidosis activation of the proton-sensing GPR4 receptor stimulates vascular endothelial cell inflammatory responses revealed by transcriptome analysis." *PLoS One* 8 (4):e61991-e61991. doi: 10.1371/journal.pone.0061991.
- Dunker, Christine, Melanie Polke, Bianca Schulze-Richter, Katja Schubert, Sven Rudolphi, A. Elisabeth Gressler, Tony Pawlik, Juan P. Prada Salcedo, M. Joanna Niemiec, Silvia Slesiona-Künzel, Marc Swidergall, Ronny Martin, Thomas Dandekar, and Ilse D. Jacobsen. 2021. "Rapid proliferation due to better metabolic adaptation results in full virulence of a filament-deficient *Candida albicans* strain." *Nat. Commun.* 12 (1):3899-3899. doi: 10.1038/s41467-021-24095-8.
- Edelstein, Charles L. 2008. "Biomarkers of acute kidney injury." *Adv. Chronic Kidney Dis.* 15 (3):222-234. doi: 10.1053/j.ackd.2008.04.003.
- Ene, Iuliana V., Sascha Brunke, Alistair J. P. Brown, and Bernhard Hube. 2014. "Metabolism in Fungal Pathogenesis." *Cold Spring Harb. Perspect. Med.* 4 (12):a019695. doi: 10.1101/cshperspect.a019695
- Ernst, Joachim F. 2000. "Transcription factors in *Candida albicans* – environmental control of morphogenesis." *Microbiology* 146 (8):1763-1774. doi: 10.1099/00221287-146-8-1763.
- Essen, Lars-Oliver, Marian Samuel Vogt, and Hans-Ulrich Mösche. 2020. "Diversity of GPI-anchored fungal adhesins." *J. Biol. Chem.* 401 (12):1389-1405. doi: 10.1515/hsz-2020-0199.
- Eyerich, K., S. Foerster, S. Rombold, H. P. Seidl, H. Behrendt, H. Hofmann, J. Ring, and C. Traidl-Hoffmann. 2008. "Patients with chronic mucocutaneous candidiasis exhibit reduced production of Th17-associated cytokines IL-17 and IL-22." *J. Invest. Dermatol.* 128 (11):2640-2645. doi: 10.1038/jid.2008.139.
- Felk, Angelika, Marianne Kretschmar, Antje Albrecht, Martin Schaller, Sabine Beinhauer, Thomas Nichterlein, Dominique Sanglard, Hans C. Korting, Wilhelm Schäfer, and Bernhard Hube. 2002. "*Candida albicans* Hyphal Formation and the Expression of the Efg1-Regulated Proteinases Sap4 to Sap6 Are Required for the Invasion of Parenchymal Organs." *Infect. Immun.* 70 (7):3689-3700. doi: 10.1128/IAI.70.7.3689-3700.2002.
- Fidel, P. L., Jr. 2002. "Distinct Protective Host Defenses against oral and vaginal Candidiasis." *Med. Mycol.* 40 (4):359-375.
- Fidel, P. L., Jr. 2004. "History and new insights into host defense against vaginal candidiasis." *Trends Microbiol.* 12 (5):220-227. doi: 10.1016/j.tim.2004.03.006.
- Filler, S. G., J. N. Swerdloff, C. Hobbs, and P. M. Lucket. 1995. "Penetration and damage of endothelial cells by *Candida albicans*." *Infect. Immun.* 63 (3):976-983. doi: 10.1128/iai.63.3.976-983.1995.
- Frantz, Christian, Kathleen M. Stewart, and Valerie M. Weaver. 2010. "The extracellular matrix at a glance." *J. Cell. Sci.* 123 (Pt 24):4195-4200. doi: 10.1242/jcs.023820.
- Fulurija, Alma, Robert B. Ashman, and John M. Papadimitriou. 1996. "Neutrophil depletion increases susceptibility to systemic and vaginal candidiasis in mice, and reveals differences between brain and kidney in mechanisms of host resistance." *Microbiology* 142 (12):3487-3496. doi: 10.1099/13500872-142-12-3487.
- Garey, K. W., M. Rege, M. P. Pai, D. E. Mingo, K. J. Suda, R. S. Turpin, and D. T. Bearden. 2006. "Time to initiation of fluconazole therapy impacts mortality in patients with candidemia: a multi-institutional study." *Clin. Infect. Dis.* 43 (1):25-31. doi: 10.1086/504810.
- Gauthier, Gregory M. 2017. "Fungal Dimorphism and Virulence: Molecular Mechanisms for Temperature Adaptation, Immune Evasion, and In Vivo Survival." *Mediators Inflamm.* 2017:8491383-8491383. doi: 10.1155/2017/8491383.
- Gerwien, Franziska, Christine Dunker, Philipp Brandt, Enrico Garbe, Ilse D. Jacobsen, and Slavena Vylkova. 2020. "Clinical *Candida albicans* Vaginal Isolates and a Laboratory Strain Show Divergent Behaviors during Macrophage Interactions." *mSphere* 5 (4):e00393-20. doi: 10.1128/mSphere.00393-20.

- Ghosh, Suman, Dhammika H. M. L. P. Navarathna, David D. Roberts, Jake T. Cooper, Audrey L. Atkin, Thomas M. Petro, and Kenneth W. Nickerson. 2009. "Arginine-induced germ tube formation in *Candida albicans* is essential for escape from murine macrophage line RAW 264.7." *Infect. Immun.* 77 (4):1596-1605. doi: 10.1128/IAI.01452-08.
- Gilbert, Andrew S., Robert T. Wheeler, and Robin C. May. 2014. "Fungal Pathogens: Survival and Replication within Macrophages." *Cold Spring Harb. Perspect. Med.* 5 (7):a019661-a019661. doi: 10.1101/cshperspect.a019661.
- Girmenia, Corrado, Erica Finolezzi, Vincenzo Federico, Michelina Santopietro, and Salvatore Perrone. 2011. "Invasive *Candida* infections in patients with haematological malignancies and hematopoietic stem cell transplant recipients: current epidemiology and therapeutic options." *Mediterr. J. Hematol. Infect. Dis.* 3 (1):e2011013-e2011013. doi: 10.4084/MJHID.2011.013.
- Gostinčar, Cene, Janja Zajc, Metka Lenassi, Ana Plemenitaš, Sybren de Hoog, Abdullah M. S. Al-Hatmi, and Nina Gunde-Cimerman. 2018. "Fungi between extremotolerance and opportunistic pathogenicity on humans." *Fungal Divers.* 93 (1):195-213. doi: 10.1007/s13225-018-0414-8.
- Gow, N. A., and B. Hube. 2012. "Importance of the *Candida albicans* cell wall during commensalism and infection." *Curr. Opin. Microbiol.* 15 (4):406-412. doi: 10.1016/j.mib.2012.04.005.
- Greenfield, R. A. 1992. "Host defense system interactions with *Candida*." *J. Med. Vet. Mycol.* 30 (2):89-104. doi: 10.1080/02681219280000141.
- Grubb, Sarah E. W., Craig Murdoch, Peter E. Sudbery, Stephen P. Saville, Jose L. Lopez-Ribot, and Martin H. Thornhill. 2008. "*Candida albicans*-endothelial cell interactions: a key step in the pathogenesis of systemic candidiasis." *Infect. Immun.* 76 (10):4370-4377. doi: 10.1128/IAI.00332-08.
- Grubb, Sarah E. W., Craig Murdoch, Peter E. Sudbery, Stephen P. Saville, Jose L. Lopez-Ribot, and Martin H. Thornhill. 2009. "Adhesion of *Candida albicans* to endothelial cells under physiological conditions of flow." *Infect. Immun.* 77 (9):3872-3878. doi: 10.1128/IAI.00518-09.
- Gulati, Megha, and Clarissa J. Nobile. 2016. "*Candida albicans* biofilms: development, regulation, and molecular mechanisms." *Microbes Infect.* 18 (5):310-321. doi: 10.1016/j.micinf.2016.01.002.
- Gupta, Krishan. 2001. "Fungal infections and the kidney." *Indian J. Nephrol.* 11:147-154.
- Hall, Rebecca A., and Mairi C. Noverr. 2017. "Fungal interactions with the human host: exploring the spectrum of symbiosis." *Curr. Opin. Microbiol.* 40:58-64. doi: 10.1016/j.mib.2017.10.020.
- Han, Ting-Li, Richard D. Cannon, and Silas G. Villas-Bôas. 2012a. "The metabolic response of *Candida albicans* to farnesol under hyphae-inducing conditions." *FEMS Yeast Res.* 12 (8):879-889. doi: 10.1111/j.1567-1364.2012.00837.x.
- Han, Ting-li, Richard D. Cannon, and Silas G. Villas-Bôas. 2012b. "Metabolome analysis during the morphological transition of *Candida albicans*." *Metabolomics* 8 (6):1204-1217. doi: 10.1007/s11306-012-0416-6.
- Han, W. K., V. Bailly, R. Abichandani, R. Thadhani, and J. V. Bonventre. 2002. "Kidney Injury Molecule-1 (KIM-1): a novel biomarker for human renal proximal tubule injury." *Kidney Int.* 62 (1):237-244. doi: 10.1046/j.1523-1755.2002.00433.x.
- Han, Yongmoon, and Jim E. Cutler. 1997. "Assessment of a Mouse Model of Neutropenia and the Effect of an Anti-Candidiasis Monoclonal Antibody in These Animals." *J. Infect. Dis.* 175 (5):1169-1175. doi: 10.1086/516455.
- Hao, B., C. J. Clancy, S. Cheng, S. B. Raman, K. A. Iczkowski, and M. H. Nguyen. 2009. "*Candida albicans* RFX2 encodes a DNA binding protein involved in DNA damage responses, morphogenesis, and virulence." *Eukaryot. Cell* 8 (4):627-639. doi: 10.1128/ec.00246-08.

- Hargarten, Jessica C., Tyler C. Moore, Thomas M. Petro, Kenneth W. Nickerson, and Audrey L. Atkin. 2015. "Candida albicans Quorum Sensing Molecules Stimulate Mouse Macrophage Migration." *Infect. Immun.* 83 (10):3857-3864. doi: 10.1128/IAI.00886-15.
- Hisajima, Tatsuya, Naho Maruyama, Yuko Tanabe, Hiroko Ishibashi, Tsuyoshi Yamada, Koichi Makimura, Yayoi Nishiyama, Kengo Funakoshi, Haruyuki Oshima, and Shigeru Abe. 2008. "Protective effects of farnesol against oral candidiasis in mice." *Microbiol. Immunol.* 52 (7):327-333. doi: 10.1111/j.1348-0421.2008.00044.x.
- Hogan, Deborah A., and Fritz A. Muhlschlegel. 2011. "Candida albicans developmental regulation: adenyl cyclase as a coincidence detector of parallel signals." *Curr. Opin. Microbiol.* 14 (6):682-686. doi: 10.1016/j.mib.2011.09.014.
- Hoog, Gerrit S. de. 2000. *Atlas of clinical fungi*. Utrecht: Centraalbureau voor Schimmelcultures.
- Horn, David L., Dionissios Neofytos, Elias J. Anaissie, Jay A. Fishman, William J. Steinbach, Ali J. Olyaei, Kieren A. Marr, Michael A. Pfaller, Chi-Hsing Chang, and Karen M. Webster. 2009. "Epidemiology and Outcomes of Candidemia in 2019 Patients: Data from the Prospective Antifungal Therapy Alliance Registry." *Clin. Infect. Dis.* 48 (12):1695-1703. doi: 10.1086/599039.
- Hornby, J. M., E. C. Jensen, A. D. Lisec, J. J. Tasto, B. Jahnke, R. Shoemaker, P. Dussault, and K. W. Nickerson. 2001. "Quorum sensing in the dimorphic fungus *Candida albicans* is mediated by farnesol." *Appl. Environ. Microbiol.* 67 (7):2982-2992. doi: 10.1128/aem.67.7.2982-2992.2001.
- Hoyer, L. L. 2001. "The ALS gene family of *Candida albicans*." *Trends. Microbiol.* 9 (4):176-180. doi: 10.1016/s0966-842x(01)01984-9.
- Hoyer, L. L., T. L. Payne, M. Bell, A. M. Myers, and S. Scherer. 1998. "Candida albicans ALS3 and insights into the nature of the ALS gene family." *Curr. Genet.* 33 (6):451-459. doi: 10.1007/s002940050359.
- Hu, Shouci, Ren Tong, Yang Bo, Pei Ming, and Hongtao Yang. 2019. "Fungal peritonitis in peritoneal dialysis: 5-year review from a North China center." *Infection* 47 (1):35-43. doi: 10.1007/s15010-018-1204-7.
- Huang, Guanghua, Qian Huang, Yujia Wei, Yue Wang, and Han Du. 2019. "Multiple roles and diverse regulation of the Ras/cAMP/protein kinase A pathway in *Candida albicans*." *Mol. Microbiol.* 111 (1):6-16. doi: 10.1111/mmi.14148.
- Huang, W., L. Na, P. L. Fidel, and P. Schwarzenberger. 2004. "Requirement of interleukin-17A for systemic anti-*Candida albicans* host defense in mice." *J. Infect. Dis.* 190 (3):624-631. doi: 10.1086/422329.
- Huang, Xinhua, Xiaoqing Chen, Yongmin He, Xiaoyu Yu, Shanshan Li, Ning Gao, Lida Niu, Yinhe Mao, Yuanyuan Wang, Xianwei Wu, Wenjuan Wu, Jianhua Wu, Dongsheng Zhou, Xiangjiang Zhan, and Changbin Chen. 2017. "Mitochondrial complex I bridges a connection between regulation of carbon flexibility and gastrointestinal commensalism in the human fungal pathogen *Candida albicans*." *PLoS Pathog.* 13 (6):e1006414. doi: 10.1371/journal.ppat.1006414.
- Inglis, Diane O., and Gavin Sherlock. 2013. "Ras signaling gets fine-tuned: regulation of multiple pathogenic traits of *Candida albicans*." *Eukaryot. Cell* 12 (10):1316-1325. doi: 10.1128/EC.00094-13.
- Jacobsen, I. D., D. Wilson, B. Wächtler, S. Brunke, J. R. Naglik, and B. Hube. 2012. "Candida albicans dimorphism as a therapeutic target." *Expert Rev. Anti. Infect. Ther.* 10 (1):85-93. doi: 10.1586/eri.11.152.
- Jiang, Dianhua, Jiurong Liang, and Paul W. Noble. 2011. "Hyaluronan as an immune regulator in human diseases." *Physiol. Rev.* 91 (1):221-264. doi: 10.1152/physrev.00052.2009.

- Johnson, Melissa D., Theo S. Plantinga, Esther van de Vosse, Digna R. Velez Edwards, P. Brian Smith, Barbara D. Alexander, John C. Yang, Dennis Kremer, Gregory M. Laird, Marije Oosting, Leo A. B. Joosten, Jos W. M. van der Meer, Jaap T. van Dissel, Thomas J. Walsh, John R. Perfect, Bart-Jan Kullberg, William K. Scott, and Mihai G. Netea. 2012. "Cytokine gene polymorphisms and the outcome of invasive candidiasis: a prospective cohort study." *Clin. Infect. Dis.* 54 (4):502-510. doi: 10.1093/cid/cir827.
- Kadosh, David, and Jose L. Lopez-Ribot. 2013. "*Candida albicans*: Adapting to succeed." *Cell Host Microbe* 14 (5):483-485. doi: 10.1016/j.chom.2013.10.016.
- Kaur, Rupinder, Biao Ma, and Brendan P. Cormack. 2007. "A family of glycosylphosphatidylinositol-linked aspartyl proteases is required for virulence of *Candida glabrata*." *Proc. Natl. Acad. Sci. U.S.A.* 104 (18):7628-7633. doi: 10.1073/pnas.0611195104.
- Kebara, Bessie W., Melanie L. Langford, Dhammika H. M. L. P. Navarathna, Raluca Dumitru, Kenneth W. Nickerson, and Audrey L. Atkin. 2008. "*Candida albicans* Tup1 is involved in farnesol-mediated inhibition of filamentous-growth induction." *Eukaryot. Cell* 7 (6):980-987. doi: 10.1128/EC.00357-07.
- Klein, B. S., and B. Tebbets. 2007. "Dimorphism and virulence in fungi." *Curr. Opin. Microbiol.* 10 (4):314-319. doi: 10.1016/j.mib.2007.04.002.
- Koh, Andrew Y., Julia R. Köhler, Kathleen T. Coggshall, Nico Van Rooijen, and Gerald B. Pier. 2008. "Mucosal Damage and Neutropenia Are Required for *Candida albicans* Dissemination." *PLoS Pathog.* 4 (2):e35. doi: 10.1371/journal.ppat.0040035.
- Köhler, J. R., B. Hube, R. Puccia, A. Casadevall, and J. R. Perfect. 2017. "Fungi that Infect Humans." *Microbiol. Spectr.* 5 (3):813-843. doi: 10.1128/microbiolspec.FUNK-0014-2016.
- Kornitzer, Daniel. 2019. "Regulation of *Candida albicans* Hyphal Morphogenesis by Endogenous Signals." *J. Fungi (Basel)* 5 (1):21. doi: 10.3390/jof5010021.
- Kronstad, James W., Rodgoun Attarian, Brigitte Cadieux, Jaehyuk Choi, Cletus A. D'Souza, Emma J. Griffiths, Jennifer M. H. Geddes, Guanggan Hu, Won Hee Jung, Matthias Kretschmer, Sanjay Saikia, and Joyce Wang. 2011. "Expanding fungal pathogenesis: *Cryptococcus* breaks out of the opportunistic box." *Nat. Rev. Microbiol.* 9 (3):193-203. doi: 10.1038/nrmicro2522.
- Kruger, Philipp, Mona Saffarzadeh, Alexander N. R. Weber, Nikolaus Rieber, Markus Radsak, Horst von Bernuth, Charaf Benarafa, Dirk Roos, Julia Skokowa, and Dominik Hartl. 2015. "Neutrophils: Between host defence, immune modulation, and tissue injury." *PLOS Pathog.* 11 (3):e1004651-e1004651. doi: 10.1371/journal.ppat.1004651.
- Krysan, Damian J., Fayyaz S. Sutterwala, and Melanie Wellington. 2014. "Catching fire: *Candida albicans*, macrophages, and pyroptosis." *PLoS Pathog.* 10 (6):e1004139-e1004139. doi: 10.1371/journal.ppat.1004139.
- Kullberg, Bart Jan, and Maiken C. Arendrup. 2015. "Invasive Candidiasis." *N. Engl. J. Med.* 373 (15):1445-1456. doi: 10.1056/NEJMra1315399.
- Kumar, Vinod, Shih-Chin Cheng, Melissa D. Johnson, Sanne P. Smeeckens, Agnieszka Wojtowicz, Evangelos Giamarellos-Bourboulis, Juha Karjalainen, Lude Franke, Sebo Withoff, Theo S. Plantinga, Frank L. van de Veerdonk, Jos W. M. van der Meer, Leo A. B. Joosten, Harry Sokol, Hermann Bauer, Bernhard G. Herrmann, Pierre-Yves Bochud, Oscar Marchetti, John R. Perfect, Ramnik J. Xavier, Bart Jan Kullberg, Cisca Wijmenga, and Mihai G. Netea. 2014. "ImmunoChip SNP array identifies novel genetic variants conferring susceptibility to candidaemia." *Nat. Commun.* 5 (1):4675. doi: 10.1038/ncomms5675.
- Langford, M. L., A. L. Atkin, and K. W. Nickerson. 2009. "Cellular interactions of farnesol, a quorum-sensing molecule produced by *Candida albicans*." *Future Microbiol.* 4 (10):1353-1362. doi: 10.2217/fmb.09.98.
- Laughlin, Maren R. 2014. "Normal roles for dietary fructose in carbohydrate metabolism." *Nutrients* 6 (8):3117-3129. doi: 10.3390/nu6083117.
- Leonhardt, Ines, Steffi Spielberg, Michael Weber, Daniela Albrecht-Eckardt, Markus Bläss, Ralf Claus, Dagmar Barz, Kirstin Scherlach, Christian Hertweck, Jürgen Löffler, Kerstin Hünninger,

- and Oliver Kurzai. 2015. "The fungal quorum-sensing molecule farnesol activates innate immune cells but suppresses cellular adaptive immunity." *mBio* 6 (2):e00143-e00143. doi: 10.1128/mBio.00143-15.
- Lionakis, M. S., J. K. Lim, C. C. Lee, and P. M. Murphy. 2011. "Organ-specific innate immune responses in a mouse model of invasive candidiasis." *J. Innate Immun.* 3 (2):180-199. doi: 10.1159/000321157.
- Lionakis, Michail S., Brett G. Fischer, Jean K. Lim, Muthulekha Swamydas, Wuzhou Wan, Chyi-Chia Richard Lee, Jeffrey I. Cohen, Phillip Scheinberg, Ji-Liang Gao, and Philip M. Murphy. 2012. "Chemokine receptor Ccr1 drives neutrophil-mediated kidney immunopathology and mortality in invasive candidiasis." *PLoS Pathog.* 8 (8):e1002865-e1002865. doi: 10.1371/journal.ppat.1002865.
- Lo, Hsiu-Jung, Julia R. Köhler, Beth DiDomenico, David Loebenberg, Anthony Cacciapuoti, and Gerald R. Fink. 1997. "Nonfilamentous *C. albicans* Mutants Are Avirulent." *Cell* 90 (5):939-949. doi: 10.1016/S0092-8674(00)80358-X.
- Lorenz, M. C., and G. R. Fink. 2001. "The glyoxylate cycle is required for fungal virulence." *Nature* 412 (6842):83-86. doi: 10.1038/35083594.
- Lorenz, Michael C., Jennifer A. Bender, and Gerald R. Fink. 2004. "Transcriptional response of *Candida albicans* upon internalization by macrophages." *Eukaryot. Cell* 3 (5):1076-1087. doi: 10.1128/EC.3.5.1076-1087.2004.
- Lorenz, Michael C., and Gerald R. Fink. 2002. "Life and death in a macrophage: role of the glyoxylate cycle in virulence." *Eukaryot. Cell* 1 (5):657-662. doi: 10.1128/ec.1.5.657-662.2002.
- Lu, Yang, Chang Su, and Haoping Liu. 2012. "A GATA transcription factor recruits Hda1 in response to reduced Tor1 signaling to establish a hyphal chromatin state in *Candida albicans*." *PLoS Pathog.* 8 (4):e1002663-e1002663. doi: 10.1371/journal.ppat.1002663.
- Lu, Yang, Chang Su, and Haoping Liu. 2014. "*Candida albicans* hyphal initiation and elongation." *Trends Microbiol.* 22 (12):707-714. doi: 10.1016/j.tim.2014.09.001.
- MacCallum, D. M., and F. C. Odds. 2005. "Temporal events in the intravenous challenge model for experimental *Candida albicans* infections in female mice." *Mycoses* 48 (3):151-161. doi: 10.1111/j.1439-0507.2005.01121.x.
- MacCallum, Donna M. 2012. "Hosting infection: experimental models to assay *Candida* virulence." *Int. J. Microbiol.* 2012:363764-363764. doi: 10.1155/2012/363764.
- MacCallum, Donna M., and Frank C. Odds. 2004. "Need for early antifungal treatment confirmed in experimental disseminated *Candida albicans* infection." *Antimicrob. Agents Chemother.* 48 (12):4911-4914. doi: 10.1128/AAC.48.12.4911-4914.2004.
- Machata, Silke, Sravya Sreekantapuram, Kerstin Hünninger, Oliver Kurzai, Christine Dunker, Katja Schubert, Wibke Krüger, Bianca Schulze-Richter, Cornelia Speth, Günter Rambach, and Ilse D. Jacobsen. 2021. "Significant Differences in Host-Pathogen Interactions Between Murine and Human Whole Blood." *Front. Immunol.* 11:565869-565869. doi: 10.3389/fimmu.2020.565869.
- Mantovani, A., M. A. Cassatella, C. Costantini, and S. Jaillon. 2011. "Neutrophils in the activation and regulation of innate and adaptive immunity." *Nat. Rev. Immunol.* 11 (8):519-531. doi: 10.1038/nri3024.
- Martin, Ronny, Gary P. Moran, Ilse D. Jacobsen, Antje Heyken, Jenny Domey, Derek J. Sullivan, Oliver Kurzai, and Bernhard Hube. 2011. "The *Candida albicans*-Specific Gene *EED1* Encodes a Key Regulator of Hyphal Extension." *PLoS One* 6 (4):e18394. doi: 10.1371/journal.pone.0018394.
- Mayer, François L., Duncan Wilson, and Bernhard Hube. 2013. "*Candida albicans* pathogenicity mechanisms." *Virulence* 4 (2):119-128. doi: 10.4161/viru.22913.
- McKenzie, C. G., U. Koser, L. E. Lewis, J. M. Bain, H. M. Mora-Montes, R. N. Barker, N. A. Gow, and L. P. Erwig. 2010. "Contribution of *Candida albicans* cell wall components to recognition by

- and escape from murine macrophages." *Infect. Immun.* 78 (4):1650-1658. doi: 10.1128/iai.00001-10.
- Meis, J. F., and A. Chowdhary. 2018. "*Candida auris*: a global fungal public health threat." *Lancet Infect. Dis.* 18 (12):1298-1299. doi: 10.1016/s1473-3099(18)30609-1.
- Min, Kyunghun, Shamoon Naseem, and James B. Konopka. 2019. "*N*-Acetylglucosamine Regulates Morphogenesis and Virulence Pathways in Fungi." *J. Fungi* 6 (1):1-16. doi: 10.3390/jof6010008.
- Miramón, Pedro, Christine Dunker, Hanna Windecker, Iryna M. Bohovych, Alistair J. P. Brown, Oliver Kurzai, and Bernhard Hube. 2012. "Cellular responses of *Candida albicans* to phagocytosis and the extracellular activities of neutrophils are critical to counteract carbohydrate starvation, oxidative and nitrosative stress." *PLoS One* 7 (12):e52850-e52850. doi: 10.1371/journal.pone.0052850.
- Miramón, Pedro, Lydia Kasper, and Bernhard Hube. 2013. "Thriving within the host: *Candida* spp. interactions with phagocytic cells." *Med. Microbiol. Immunol.* 202 (3):183-195. doi: 10.1007/s00430-013-0288-z.
- Miramón, Pedro, and Michael C. Lorenz. 2017. "A feast for *Candida*: Metabolic plasticity confers an edge for virulence." *PLoS Pathog.* 13 (2):e1006144. doi: 10.1371/journal.ppat.1006144.
- Miranda, L. N., I. M. van der Heijden, S. F. Costa, A. P. I. Sousa, R. A. Sienra, S. Gobara, C. R. Santos, R. D. Lobo, V. P. Pessoa, Jr., and A. S. Levin. 2009. "*Candida* colonisation as a source for candidaemia." *J. Hosp. Infect.* 72 (1):9-16. doi: 10.1016/j.jhin.2009.02.009.
- Miyazaki, H., and M. Hirano. 1996. "Effective clinical use of cyclophosphamide in hematological malignancies." *Gan To Kagaku Ryoho* 23 (14):1891-1895.
- Moore, Nicholas J. E., Johnsey L. Leef, and Yijun Pang. 2003. "Systemic Candidiasis." *RadioGraphics* 23 (5):1287-1290. doi: 10.1148/rg.235025162.
- Moran, Gary, David Coleman, and Derek Sullivan. 2012. "An Introduction to the Medically Important *Candida* Species." In *Candida and Candidiasis, Second Edition*. American Society of Microbiology.
- Moyes, David L., Duncan Wilson, Jonathan P. Richardson, Selene Mogavero, Shirley X. Tang, Julia Wernecke, Sarah Höfs, Remi L. Gratacap, Jon Robbins, Manohursingh Runglall, Celia Murciano, Mariana Blagojevic, Selvam Thavaraj, Toni M. Förster, Betty Hebecker, Lydia Kasper, Gema Vizcay, Simona I. Iancu, Nessim Kichik, Antje Häder, Oliver Kurzai, Ting Luo, Thomas Krüger, Olaf Kniemeyer, Ernesto Cota, Oliver Bader, Robert T. Wheeler, Thomas Gutschmann, Bernhard Hube, and Julian R. Naglik. 2016. "Candidalysin is a fungal peptide toxin critical for mucosal infection." *Nature* 532 (7597):64-68. doi: 10.1038/nature17625.
- Mukaremera, Liliane, Keunsook K. Lee, Hector M. Mora-Montes, and Neil A. R. Gow. 2017. "*Candida albicans* Yeast, Pseudohyphal, and Hyphal Morphogenesis Differentially Affects Immune Recognition." *Front. Immunol.* 8:629-629. doi: 10.3389/fimmu.2017.00629.
- Munro, David A. D., Peter Hohenstein, and Jamie A. Davies. 2017. "Cycles of vascular plexus formation within the nephrogenic zone of the developing mouse kidney." *Sci. Rep.* 7 (1):3273-3273. doi: 10.1038/s41598-017-03808-4.
- Murad, A. M., P. Leng, M. Straffon, J. Wishart, S. Macaskill, D. MacCallum, N. Schnell, D. Talibi, D. Marechal, F. Tekaia, C. d'Enfert, C. Gaillardin, F. C. Odds, and A. J. Brown. 2001. "*NRG1* represses yeast-hypha morphogenesis and hypha-specific gene expression in *Candida albicans*." *EMBO J.* 20 (17):4742-4752. doi: 10.1093/emboj/20.17.4742.
- Naglik, J., A. Albrecht, O. Bader, and B. Hube. 2004. "*Candida albicans* proteinases and host/pathogen interactions." *Cell Microbiol.* 6 (10):915-926. doi: 10.1111/j.1462-5822.2004.00439.x.
- Naglik, Julian R., Stephen J. Challacombe, and Bernhard Hube. 2003. "*Candida albicans* secreted aspartyl proteinases in virulence and pathogenesis." *Microbiol. Mol. Biol. Rev.* 67 (3):400-428. doi: 10.1128/mubr.67.3.400-428.2003.

- Navarathna, Dhammika H. M. L. P., Jacob M. Hornby, Navasona Krishnan, Anne Parkhurst, Gerald E. Duhamel, and Kenneth W. Nickerson. 2007. "Effect of Farnesol on a Mouse Model of Systemic Candidiasis, Determined by Use of a *DPP3* Knockout Mutant of *Candida albicans*." *Infect. Immun.* 75 (4):1609-1618. doi: 10.1128/IAI.01182-06.
- Navarathna, Dhammika H. M. L. P., Kenneth W. Nickerson, Gerald E. Duhamel, Thomas R. Jerrels, and Thomas M. Petro. 2007. "Exogenous Farnesol Interferes with the Normal Progression of Cytokine Expression during Candidiasis in a Mouse Model." *Infect. Immun.* 75 (8):4006-4011. doi: 10.1128/IAI.00397-07.
- Netea, M. G., N. A. Gow, C. A. Munro, S. Bates, C. Collins, G. Ferwerda, R. P. Hobson, G. Bertram, H. B. Hughes, T. Jansen, L. Jacobs, E. T. Buurman, K. Gijzen, D. L. Williams, R. Torensma, A. McKinnon, D. M. MacCallum, F. C. Odds, J. W. Van der Meer, A. J. Brown, and B. J. Kullberg. 2006. "Immune sensing of *Candida albicans* requires cooperative recognition of mannans and glucans by lectin and Toll-like receptors." *J. Clin. Invest.* 116 (6):1642-1650. doi: 10.1172/jci27114.
- Nickerson, Kenneth W., Audrey L. Atkin, Jessica C. Hargarten, Ruvini Pathirana, and Sahar Hasim. 2012. "Thoughts on Quorum Sensing and Fungal Dimorphism."
- Nobile, Clarissa J., and Alexander D. Johnson. 2015. "*Candida albicans* Biofilms and Human Disease." *Annu. Rev. Microbiol.* 69:71-92. doi: 10.1146/annurev-micro-091014-104330.
- Nobile, Clarissa J., Jeniel E. Nett, David R. Andes, and Aaron P. Mitchell. 2006. "Function of *Candida albicans* adhesin Hwp1 in biofilm formation." *Eukaryot. Cell* 5 (10):1604-1610. doi: 10.1128/EC.00194-06.
- Noble, Suzanne M., Brittany A. Gianetti, and Jessica N. Witchley. 2017. "*Candida albicans* cell-type switching and functional plasticity in the mammalian host." *Nat. Rev. Microbiol.* 15 (2):96-108. doi: 10.1038/nrmicro.2016.157.
- Noble, Suzanne M., and Alexander D. Johnson. 2005. "Strains and strategies for large-scale gene deletion studies of the diploid human fungal pathogen *Candida albicans*." *Eukaryot. Cell* 4 (2):298-309. doi: 10.1128/EC.4.2.298-309.2005.
- Nucci, Marcio, and Elias Anaissie. 2001. "Revisiting the Source of Candidemia: Skin or Gut?" *Clin. Infect. Dis.* 33 (12):1959-1967. doi: 10.1086/323759.
- Odds, F. 1988. *Candida and candidosis*. London; Toronto: Bailliere Tindall.
- Owari, Mitsugu, Masafumi Wasa, Takaharu Oue, Satoko Nose, and Masahiro Fukuzawa. 2012. "Glutamine prevents intestinal mucosal injury induced by cyclophosphamide in rats." *Pediatr. Surg. Int.* 28 (3):299-303. doi: 10.1007/s00383-011-3023-0.
- Pankhurst, Caroline L. 2009. "Candidiasis (oropharyngeal)." *BMJ Clin. Evid.* 2009:1304.
- Pappas, P. G., M. S. Lionakis, M. C. Arendrup, L. Ostrosky-Zeichner, and B. J. Kullberg. 2018. "Invasive candidiasis." *Nat. Rev. Dis. Primers* 4:18026. doi: 10.1038/nrdp.2018.26.
- Park, H., C. L. Myers, D. C. Sheppard, Q. T. Phan, A. A. Sanchez, E. Edwards J, and S. G. Filler. 2005. "Role of the fungal Ras-protein kinase A pathway in governing epithelial cell interactions during oropharyngeal candidiasis." *Cell. Microbiol.* 7 (4):499-510. doi: 10.1111/j.1462-5822.2004.00476.x.
- Pasricha, Shivani, James I. MacRae, Hwa H. Chua, Jenny Chambers, Kylie J. Boyce, Malcolm J. McConville, and Alex Andrianopoulos. 2017. "Extensive Metabolic Remodeling Differentiates Non-pathogenic and Pathogenic Growth Forms of the Dimorphic Pathogen *Talaromyces marneffeii*." *Front. Cell. Infect. Microbiol.* 7 (368):1-12. doi: 10.3389/fcimb.2017.00368.
- Perlroth, Joshua, Bryan Choi, and Brad Spellberg. 2007. "Nosocomial fungal infections: epidemiology, diagnosis, and treatment." *Med. Mycol.* 45 (4):321-346. doi: 10.1080/13693780701218689.
- Perše, Martina, and Željka Večerić-Haler. 2018. "Cisplatin-Induced Rodent Model of Kidney Injury: Characteristics and Challenges." *Biomed Res. Int.* 2018:1462802-1462802. doi: 10.1155/2018/1462802.

- Peters, Brian M., Glen E. Palmer, Andrea K. Nash, Elizabeth A. Lilly, Paul L. Fidel, Jr., and Mairi C. Noverr. 2014. "Fungal morphogenetic pathways are required for the hallmark inflammatory response during *Candida albicans* vaginitis." *Infect. Immun.* 82 (2):532-543. doi: 10.1128/IAI.01417-13.
- Pfaller, M. A. 1996. "Nosocomial candidiasis: emerging species, reservoirs, and modes of transmission." *Clin. Infect. Dis.* 22 Suppl 2:S89-94. doi: 10.1093/clinids/22.supplement_2.s89.
- Pfaller, M. A., and D. J. Diekema. 2004. "Rare and emerging opportunistic fungal pathogens: concern for resistance beyond *Candida albicans* and *Aspergillus fumigatus*." *J. Clin. Microbiol.* 42 (10):4419-4431. doi: 10.1128/JCM.42.10.4419-4431.2004.
- Pfaller, M. A., D. J. Diekema, D. L. Gibbs, V. A. Newell, D. Ellis, V. Tullio, A. Rodloff, W. Fu, T. A. Ling, and Group Global Antifungal Surveillance. 2010. "Results from the ARTEMIS DISK Global Antifungal Surveillance Study, 1997 to 2007: a 10.5-year analysis of susceptibilities of *Candida* Species to fluconazole and voriconazole as determined by CLSI standardized disk diffusion." *J. Clin. Microbiol.* 48 (4):1366-1377. doi: 10.1128/JCM.02117-09.
- Phan, Quynh T., Carter L. Myers, Yue Fu, Donald C. Sheppard, Michael R. Yeaman, William H. Welch, Ashraf S. Ibrahim, John E. Edwards, Jr., and Scott G. Filler. 2007. "Als3 Is a *Candida albicans* Invasin That Binds to Cadherins and Induces Endocytosis by Host Cells." *PLoS Biol.* 5 (3):e64. doi: 10.1371/journal.pbio.0050064.
- Polke, Melanie. 2017. "The role of the *Candida albicans* *EED1* in quorum sensing, morphogenesis and virulence." [Dissertation]. Jena: Friedrich Schiller University, 2017.
- Polke, Melanie, Marcel Sprenger, Kirstin Scherlach, María Cristina Albán-Proañó, Ronny Martin, Christian Hertweck, Bernhard Hube, and Ilse D. Jacobsen. 2017. "A functional link between hyphal maintenance and quorum sensing in *Candida albicans*." *Mol. Microbiol.* 103 (4):595-617. doi: 10.1111/mmi.13526.
- Pongpom, Monsicha, Pramote Vanittanakom, Panjaphorn Nimmanee, Chester R. Cooper, Jr., and Nongnuch Vanittanakom. 2017. "Adaptation to macrophage killing by *Talaromyces marneffei*." *Future Sci. OA* 3 (3):FSO215-FSO215. doi: 10.4155/foa-2017-0032.
- Prasad, N., and A. Gupta. 2005. "Fungal peritonitis in peritoneal dialysis patients." *Perit. Dial. Int.* 25 (3):207-222. doi: 10.1177/089686080502500302.
- Qian, Q, M A Jutila, N Van Rooijen, and J E Cutler. 1994. "Elimination of mouse splenic macrophages correlates with increased susceptibility to experimental disseminated candidiasis." *J. Immunol.* 152 (10):5000-5008.
- Rai, Laxmi Shanker, Rima Singha, Priya Brahma, and Kaustuv Sanyal. 2018. "Epigenetic determinants of phenotypic plasticity in *Candida albicans*." *Fungal Biol. Rev.* 32 (1):10-19. doi: 10.1016/j.fbr.2017.07.002.
- Rai, Maruti Nandan, Sriram Balusu, Neelima Gorityala, Lakshmi Dandu, and Rupinder Kaur. 2012. "Functional genomic analysis of *Candida glabrata*-macrophage interaction: role of chromatin remodeling in virulence." *PLoS Pathog.* 8 (8):e1002863-e1002863. doi: 10.1371/journal.ppat.1002863.
- Ramírez, Melissa A., and Michael C. Lorenz. 2007. "Mutations in alternative carbon utilization pathways in *Candida albicans* attenuate virulence and confer pleiotropic phenotypes." *Eukaryot. Cell* 6 (2):280-290. doi: 10.1128/EC.00372-06.
- Richardson, Jonathan P., and David L. Moyes. 2015. "Adaptive immune responses to *Candida albicans* infection." *Virulence* 6 (4):327-337. doi: 10.1080/21505594.2015.1004977.

- Richardson, Jonathan P., Hubertine M. E. Willems, David L. Moyes, Saeed Shoaie, Katherine S. Barker, Shir Lynn Tan, Glen E. Palmer, Bernhard Hube, Julian R. Naglik, and Brian M. Peters. 2018. "Candidalysin Drives Epithelial Signaling, Neutrophil Recruitment, and Immunopathology at the Vaginal Mucosa." *Infect. Immun.* 86 (2):e00645-17. doi: 10.1128/IAI.00645-17.
- Ruhela, Deepa, Mohan Kamthan, Paramita Saha, Subeer S. Majumdar, Kasturi Datta, Malik Zainul Abdin, and Asis Datta. 2015. "In vivo role of *Candida albicans* β -hexosaminidase (*HEX1*) in carbon scavenging." *MicrobiologyOpen* 4 (5):730-742. doi: 10.1002/mbo3.274.
- Sabbisetti, V. S., K. Ito, C. Wang, L. Yang, S. C. Mefferd, and J. V. Bonventre. 2013a. "Novel assays for detection of urinary KIM-1 in mouse models of kidney injury." *Toxicol. Sci.* 131 (1):13-25. doi: 10.1093/toxsci/kfs268.
- Sabbisetti, Venkata S., Kazumi Ito, Chang Wang, Li Yang, Stephen C. Mefferd, and Joseph V. Bonventre. 2013b. "Novel assays for detection of urinary KIM-1 in mouse models of kidney injury." *Toxicological sciences : an official journal of the Society of Toxicology* 131 (1):13-25. doi: 10.1093/toxsci/kfs268.
- Samaranayake, L. P. 1992. "Oral mycoses in HIV infection." *Oral Surg. Oral Med. Oral Pathol.* 73 (2):171-180. doi: 10.1016/0030-4220(92)90191-r.
- Samaranayake, L. P., and P. Holmstrup. 1989. "Oral candidiasis and human immunodeficiency virus infection." *J. Oral Pathol. Med.* 18 (10):554-564. doi: 10.1111/j.1600-0714.1989.tb01552.x.
- Sandai, Doblin, Zhikang Yin, Laura Selway, David Stead, Janet Walker, Michelle D. Leach, Iryna Bohovych, Iuliana V. Ene, Stavroula Kastora, Susan Budge, Carol A. Munro, Frank C. Odds, Neil A. R. Gow, and Alistair J. P. Brown. 2012. "The evolutionary rewiring of ubiquitination targets has reprogrammed the regulation of carbon assimilation in the pathogenic yeast *Candida albicans*." *mBio* 3 (6):e00495-12. doi: 10.1128/mBio.00495-12.
- Satchell, Simon C., and Filip Braet. 2009. "Glomerular endothelial cell fenestrations: an integral component of the glomerular filtration barrier." *Am. J. Physiol. Renal Physiol.* 296 (5):F947-F956. doi: 10.1152/ajprenal.90601.2008.
- Saville, Stephen P., Anna L. Lazzell, Alexander P. Bryant, Angelika Fretzen, Alex Monreal, Erik O. Solberg, Carlos Monteagudo, Jose L. Lopez-Ribot, and G. Todd Milne. 2006. "Inhibition of filamentation can be used to treat disseminated candidiasis." *Antimicrob. Agents Chemother.* 50 (10):3312-3316. doi: 10.1128/AAC.00628-06.
- Saville, Stephen P., Anna L. Lazzell, Ashok K. Chaturvedi, Carlos Monteagudo, and Jose L. Lopez-Ribot. 2008. "Use of a genetically engineered strain to evaluate the pathogenic potential of yeast cell and filamentous forms during *Candida albicans* systemic infection in immunodeficient mice." *Infect. Immun.* 76 (1):97-102. doi: 10.1128/IAI.00982-07.
- Saville, Stephen P., Anna L. Lazzell, Carlos Monteagudo, and Jose L. Lopez-Ribot. 2003. "Engineered control of cell morphology in vivo reveals distinct roles for yeast and filamentous forms of *Candida albicans* during infection." *Eukaryot. Cell* 2 (5):1053-1060. doi: 10.1128/EC.2.5.1053-1060.2003.
- Schild, Lydia, Antje Heyken, Piet W. J. de Groot, Ekkehard Hiller, Marlen Mock, Chris de Koster, Uwe Horn, Steffen Rupp, and Bernhard Hube. 2011. "Proteolytic Cleavage of Covalently Linked Cell Wall Proteins by *Candida albicans* Sap9 and Sap10." *Eukaryot. Cell* 10 (1):98-109. doi: 10.1128/EC.00210-10.
- Seider, K., S. Brunke, L. Schild, N. Jablonowski, D. Wilson, O. Majer, D. Barz, A. Haas, K. Kuchler, M. Schaller, and B. Hube. 2011. "The facultative intracellular pathogen *Candida glabrata* subverts macrophage cytokine production and phagolysosome maturation." *J. Immunol.* 187 (6):3072-3086. doi: 10.4049/jimmunol.1003730.
- Shapiro-Ilan, David I., James R. Fuxa, Lawrence A. Lacey, David W. Onstad, and Harry K. Kaya. 2005. "Definitions of pathogenicity and virulence in invertebrate pathology." *J. Invertebr. Pathol.* 88 (1):1-7. doi: 10.1016/j.jip.2004.10.003.

- Shapiro, Rebecca S., Nicole Robbins, and Leah E. Cowen. 2011. "Regulatory Circuitry Governing Fungal Development, Drug Resistance, and Disease." *Microbiol. Mol. Biol. Rev.* 75 (2):213-267. doi: 10.1128/MMBR.00045-10.
- Sil, A., and A. Andrianopoulos. 2014. "Thermally Dimorphic Human Fungal Pathogens-Polyphyletic Pathogens with a Convergent Pathogenicity Trait." *Cold Spring Harb. Perspect. Med.* 5 (8):a019794. doi: 10.1101/cshperspect.a019794.
- Singer, Mervyn, Clifford S. Deutschman, Christopher Warren Seymour, Manu Shankar-Hari, Djillali Annane, Michael Bauer, Rinaldo Bellomo, Gordon R. Bernard, Jean-Daniel Chiche, Craig M. Coopersmith, Richard S. Hotchkiss, Mitchell M. Levy, John C. Marshall, Greg S. Martin, Steven M. Opal, Gordon D. Rubenfeld, Tom van der Poll, Jean-Louis Vincent, and Derek C. Angus. 2016. "The Third International Consensus Definitions for Sepsis and Septic Shock (Sepsis-3)." *JAMA* 315 (8):801-810. doi: 10.1001/jama.2016.0287.
- Singh, Praveen, Sharmistha Ghosh, and Asis Datta. 2001. "Attenuation of Virulence and Changes in Morphology in *Candida albicans* by Disruption of the *N*-Acetylglucosamine Catabolic Pathway." *Infect. Immun.* 69 (12):7898-7903. doi: 10.1128/IAI.69.12.7898-7903.2001.
- Smith, Reuben L., Maarten R. Soeters, Rob C. I. Wüst, and Riekelt H. Houtkooper. 2018. "Metabolic Flexibility as an Adaptation to Energy Resources and Requirements in Health and Disease." *Endocr. Rev.* 39 (4):489-517. doi: 10.1210/er.2017-00211.
- Sobel, Jack D., Sabastian Faro, Rex W. Force, Betsy Foxman, William J. Ledger, Paul R. Nyirjesy, Barbara D. Reed, and Paul R. Summers. 1998. "Vulvovaginal candidiasis: Epidemiologic, diagnostic, and therapeutic considerations." *Am. J. Obstet. Gynecol.* 178 (2):203-211. doi: 10.1016/S0002-9378(98)80001-X.
- Sohn, K., C. Urban, H. Brunner, and S. Rupp. 2003. "*EFG1* is a major regulator of cell wall dynamics in *Candida albicans* as revealed by DNA microarrays." *Mol. Microbiol.* 47 (1):89-102. doi: 10.1046/j.1365-2958.2003.03300.x.
- Soll, D. R. 2004. "Mating-type locus homozygosity, phenotypic switching and mating: a unique sequence of dependencies in *Candida albicans*." *Bioessays* 26 (1):10-20. doi: 10.1002/bies.10379.
- Spellberg, Brad, Ashraf S. Ibrahim, John E. Edwards, Jr., and Scott G. Filler. 2005. "Mice with Disseminated Candidiasis Die of Progressive Sepsis." *J. Infect. Dis.* 192 (2):336-343. doi: 10.1086/430952.
- Staab, J. F., S. D. Bradway, P. L. Fidel, and P. Sundstrom. 1999. "Adhesive and mammalian transglutaminase substrate properties of *Candida albicans* Hwp1." *Science* 283 (5407):1535-1538. doi: 10.1126/science.283.5407.1535.
- Staab, J. F., K. Datta, and P. Rhee. 2013. "Niche-specific requirement for hyphal wall protein 1 in virulence of *Candida albicans*." *PLoS One* 8 (11):e80842. doi: 10.1371/journal.pone.0080842.
- Staib, Peter, Ulrich Lermann, Julia Blass-Warmuth, Björn Degel, Reinhard Würzner, Michel Monod, Tanja Schirmeister, and Joachim Morschhäuser. 2008. "Tetracycline-inducible expression of individual secreted aspartic proteases in *Candida albicans* allows isoenzyme-specific inhibitor screening." *Antimicrob. Agents Chemother.* 52 (1):146-156. doi: 10.1128/AAC.01072-07.
- Staib, Peter, and Joachim Morschhäuser. 2007. "Chlamyospore formation in *Candida albicans* and *Candida dubliniensis*— an enigmatic developmental programme." *Mycoses* 50 (1):1-12. doi: 10.1111/j.1439-0507.2006.01308.x.
- Steinman, Ralph M. 2006. "Linking Innate to Adaptive Immunity through Dendritic Cells." In *Innate Immunity to Pulmonary Infection*, 101-113.
- Stepchenkova, E. I., A. A. Shiriaeva, and Y. I. Pavlov. 2018. "Deletion of the *DEF1* gene does not confer UV-immutability but frequently leads to self-diploidization in yeast *Saccharomyces cerevisiae*." *DNA repair* 70:49-54. doi: 10.1016/j.dnarep.2018.08.026.

- Sudbery, P., N. Gow, and J. Berman. 2004. "The distinct morphogenic states of *Candida albicans*." *Trends Microbiol.* 12 (7):317-324. doi: 10.1016/j.tim.2004.05.008.
- Sudbery, Peter E. 2011. "Growth of *Candida albicans* hyphae." *Nat. Rev. Microbiol.* 9 (10):737-748. doi: 10.1038/nrmicro2636.
- Sun, Donglei, Peng Sun, Hongmei Li, Mingshun Zhang, Gongguan Liu, Ashley B. Strickland, Yanli Chen, Yong Fu, Juan Xu, Mohammed Yosri, Yuchen Nan, Hong Zhou, Xiquan Zhang, and Meiqing Shi. 2019. "Fungal dissemination is limited by liver macrophage filtration of the blood." *Nat. Commun.* 10 (1):4566-4566. doi: 10.1038/s41467-019-12381-5.
- Sun, Jianing N., Norma V. Solis, Quynh T. Phan, Jashanjot S. Bajwa, Helena Kashleva, Angela Thompson, Yaoping Liu, Anna Dongari-Bagtzoglou, Mira Edgerton, and Scott G. Filler. 2010. "Host cell invasion and virulence mediated by *Candida albicans* Ssa1." *PLoS Pathog.* 6 (11):e1001181-e1001181. doi: 10.1371/journal.ppat.1001181.
- Swidergall, Marc, and Scott G. Filler. 2017. "Oropharyngeal Candidiasis: Fungal Invasion and Epithelial Cell Responses." *PLoS Pathog.* 13 (1):e1006056. doi: 10.1371/journal.ppat.1006056.
- Swidergall, Marc, Mina Khalaji, Norma V. Solis, David L. Moyes, Rebecca A. Drummond, Bernhard Hube, Michail S. Lionakis, Craig Murdoch, Scott G. Filler, and Julian R. Naglik. 2019. "Candidalysin Is Required for Neutrophil Recruitment and Virulence During Systemic *Candida albicans* Infection." *J. Infect. Dis.* 220:1477-1488. doi: 10.1093/infdis/jiz322.
- Tanaka, M., W. M. Clouston, and W. Herr. 1994. "The Oct-2 glutamine-rich and proline-rich activation domains can synergize with each other or duplicates of themselves to activate transcription." *Mol. Cell. Biol.* 14 (9):6046-6055. doi: 10.1128/mcb.14.9.6046-6055.1994.
- Tao, L., H. Du, G. Guan, Y. Dai, C. J. Nobile, W. Liang, C. Cao, Q. Zhang, J. Zhong, and G. Huang. 2014. "Discovery of a "White-Gray-Opaque" Tristable Phenotypic Switching System in *Candida albicans*: Roles of Non-genetic Diversity in Host Adaptation." *PLoS Biol.* 12 (4):e1001830. doi: 10.1371/journal.pbio.1001830.
- Taschdjian, Claire L., James J. Burchall, and Philip J. Kozinn. 1960. "Rapid Identification of *Candida albicans* by Filamentation on Serum and Serum Substitutes." *JAMA Pediatr.* 99 (2):212-215. doi: 10.1001/archpedi.1960.02070030214011.
- Thompson, Delma S., Patricia L. Carlisle, and David Kadosh. 2011. "Coevolution of morphology and virulence in *Candida* species." *Eukaryotic Cell* 10 (9):1173-1182. doi: 10.1128/EC.05085-11.
- Tucey, Timothy M., Jiyoti Verma, Paul F. Harrison, Sarah L. Snelgrove, Tricia L. Lo, Allison K. Scherer, Adele A. Barugahare, David R. Powell, Robert T. Wheeler, Michael J. Hickey, Traude H. Beilharz, Thomas Naderer, and Ana Traven. 2018. "Glucose Homeostasis Is Important for Immune Cell Viability during *Candida* Challenge and Host Survival of Systemic Fungal Infection." *Cell Metab.* 27 (5):988-1006.e7. doi: 10.1016/j.cmet.2018.03.019.
- Uppuluri, Priya, Ashok K. Chaturvedi, Anand Srinivasan, Mohua Banerjee, Anand K. Ramasubramaniam, Julia R. Köhler, David Kadosh, and Jose L. Lopez-Ribot. 2010. "Dispersion as an important step in the *Candida albicans* biofilm developmental cycle." *PLoS Pathog.* 6 (3):e1000828-e1000828. doi: 10.1371/journal.ppat.1000828.
- Urban, C. F., U. Reichard, V. Brinkmann, and A. Zychlinsky. 2006. "Neutrophil extracellular traps capture and kill *Candida albicans* yeast and hyphal forms." *Cell. Microbiol.* 8 (4):668-676. doi: 10.1111/j.1462-5822.2005.00659.x.
- van de Veerdonk, Frank L., and Mihai G. Netea. 2010. "T-cell Subsets and Antifungal Host Defenses." *Curr. Fungal Infect. Rep.* 4 (4):238-243. doi: 10.1007/s12281-010-0034-6.
- Van Ende, Mieke, Stefanie Wijnants, and Patrick Van Dijck. 2019. "Sugar Sensing and Signaling in *Candida albicans* and *Candida glabrata*." *Front. Microbiol.* 10:99. doi: 10.3389/fmicb.2019.00099.
- Vautier, Simon, Rebecca A. Drummond, Kong Chen, Graeme I. Murray, David Kadosh, Alistair J. P. Brown, Neil A. R. Gow, Donna M. MacCallum, Jay K. Kolls, and Gordon D. Brown. 2015. "*Candida albicans* colonization and dissemination from the murine gastrointestinal tract:

- the influence of morphology and Th17 immunity." *Cell. Microbiol.* 17 (4):445-450. doi: 10.1111/cmi.12388.
- Vazquez, Jose A. 2000. "Therapeutic Options for the Management of Oropharyngeal and Esophageal Candidiasis in HIV/AIDS Patients." *HIV Clin. Trials* 1 (1):47-59. doi: 10.1310/T7A7-1E63-2KA0-JKWD.
- Verstrepen, K. J., and F. M. Klis. 2006. "Flocculation, adhesion and biofilm formation in yeasts." *Mol. Microbiol.* 60 (1):5-15. doi: 10.1111/j.1365-2958.2006.05072.x.
- Vesely, Elisa M., Robert B. Williams, James B. Konopka, and Michael C. Lorenz. 2017. "N-Acetylglucosamine Metabolism Promotes Survival of *Candida albicans* in the Phagosome." *mSphere* 2 (5):e00357-17. doi: 10.1128/mSphere.00357-17.
- Vylkova, Slavena, and Michael C. Lorenz. 2014. "Modulation of Phagosomal pH by *Candida albicans* Promotes Hyphal Morphogenesis and Requires Stp2p, a Regulator of Amino Acid Transport." *PLoS Pathog.* 10 (3):e1003995. doi: 10.1371/journal.ppat.1003995.
- Wächtler, Betty, Duncan Wilson, Katja Haedicke, Frederic Dalle, and Bernhard Hube. 2011. "From Attachment to Damage: Defined Genes of *Candida albicans* Mediate Adhesion, Invasion and Damage during Interaction with Oral Epithelial Cells." *PLoS One* 6 (2):e17046. doi: 10.1371/journal.pone.0017046.
- Wall, Gina, Daniel Montelongo-Jauregui, Bruna Vidal Bonifacio, Jose L. Lopez-Ribot, and Priya Uppuluri. 2019. "*Candida albicans* biofilm growth and dispersal: contributions to pathogenesis." *Curr. Opin. Microbiol.* 52:1-6. doi: 10.1016/j.mib.2019.04.001.
- Walsh, Thomas J., and Dennis M. Dixon. 1996. *Medical Microbiology. 4th edition. Chapter 75, Spectrum of Mycoses*: University of Texas Medical Branch at Galveston.
- Wartenberg, Anja, Jörg Linde, Ronny Martin, Maria Schreiner, Fabian Horn, Ilse D. Jacobsen, Sabrina Jenull, Thomas Wolf, Karl Kuchler, Reinhard Guthke, Oliver Kurzai, Anja Forche, Christophe d'Enfert, Sascha Brunke, and Bernhard Hube. 2014. "Microevolution of *Candida albicans* in Macrophages Restores Filamentation in a Nonfilamentous Mutant." *PLoS Genet.* 10 (12):e1004824. doi: 10.1371/journal.pgen.1004824.
- Weitzman, I., and R. C. Summerbell. 1995. "The dermatophytes." *Clin. Microbiol. Rev.* 8 (2):240-259. doi: 10.1128/CMR.8.2.240.
- Wellington, Melanie, Kristy Koselny, and Damian J. Krysan. 2012. "*Candida albicans* morphogenesis is not required for macrophage interleukin 1 β production." *mBio* 4 (1):e00433. doi: 10.1128/mBio.00433-12.
- Wellington, Melanie, Kristy Koselny, Fayyaz S. Sutterwala, and Damian J. Krysan. 2014. "*Candida albicans* triggers NLRP3-mediated pyroptosis in macrophages." *Eukaryot. Cell* 13 (2):329-340. doi: 10.1128/EC.00336-13.
- Westwater, Caroline, Edward Balish, and David A. Schofield. 2005. "*Candida albicans*-conditioned medium protects yeast cells from oxidative stress: a possible link between quorum sensing and oxidative stress resistance." *Eukaryot. Cell* 4 (10):1654-1661. doi: 10.1128/EC.4.10.1654-1661.2005.
- White, Theodore C., Keisha Findley, Thomas L. Dawson, Jr., Annika Scheynius, Teun Boekhout, Christina A. Cuomo, Jun Xu, and Charles W. Saunders. 2014. "Fungi on the skin: dermatophytes and *Malassezia*." *Cold Spring Harb. Perspect. Med.* 4 (8):a019802. doi: 10.1101/cshperspect.a019802.
- Whiteway, Malcolm, and Catherine Bachewich. 2007. "Morphogenesis in *Candida albicans*." *Annu. Rev. Microbiol.* 61:529-553. doi: 10.1146/annurev.micro.61.080706.093341.

- Wiesmann, F., J. Ruff, K. H. Hiller, E. Rommel, A. Haase, and S. Neubauer. 2000. "Developmental changes of cardiac function and mass assessed with MRI in neonatal, juvenile, and adult mice." *Am. J. Physiol. Heart Circ. Physiol.* 278 (2):H652-H657. doi: 10.1152/ajpheart.2000.278.2.H652.
- Willems, H. M. E., S. S. Ahmed, J. Liu, Z. Xu, and B. M. Peters. 2020. "Vulvovaginal Candidiasis: A Current Understanding and Burning Questions." *J. Fungi* 6 (1):27. doi: 10.3390/jof6010027.
- Williams, Robert B., and Michael C. Lorenz. 2020. "Multiple Alternative Carbon Pathways Combine To Promote *Candida albicans* Stress Resistance, Immune Interactions, and Virulence." *mBio* 11 (1):e03070-19. doi: 10.1128/mBio.03070-19.
- Wilson, Duncan, and Bernhard Hube. 2010. "Hgc1 mediates dynamic *Candida albicans*-endothelium adhesion events during circulation." *Eukaryot. Cell* 9 (2):278-287. doi: 10.1128/EC.00307-09.
- Wilson, Duncan, Julian R. Naglik, and Bernhard Hube. 2016. "The Missing Link between *Candida albicans* Hyphal Morphogenesis and Host Cell Damage." *PLoS Pathog.* 12 (10):e1005867-e1005867. doi: 10.1371/journal.ppat.1005867.
- Witchley, J. N., P. Penumetcha, N. V. Abon, C. A. Woolford, A. P. Mitchell, and S. M. Noble. 2019. "*Candida albicans* Morphogenesis Programs Control the Balance between Gut Commensalism and Invasive Infection." *Cell Host Microbe* 25 (3):432-443.e6. doi: 10.1016/j.chom.2019.02.008.
- Wittig, Franziska. 2016. "Secondary *Candida albicans* yeast cells differ from their primary counterparts in cell surface and host cell interaction." [Master thesis]. Jena: Friedrich Schiller University, 2016.
- Xiao, Hua, and Kuan-Teh Jeang. 1998. "Glutamine-rich Domains Activate Transcription in Yeast *Saccharomyces cerevisiae*." *J. Biol. Chem.* 273 (36):22873-22876. doi: 10.1074/jbc.273.36.22873.
- Xie, Jing, Li Tao, Clarissa J. Nobile, Yaojun Tong, Guobo Guan, Yuan Sun, Chengjun Cao, Aaron D. Hernday, Alexander D. Johnson, Lixin Zhang, Feng-Yan Bai, and Guanghua Huang. 2013. "White-Opaque Switching in Natural MTL α Isolates of *Candida albicans*: Evolutionary Implications for Roles in Host Adaptation, Pathogenesis, and Sex." *PLoS Biol.* 11 (3):e1001525. doi: 10.1371/journal.pbio.1001525.
- Xin, Hong, Farhan Mohiuddin, Jensen Tran, Abby Adams, and Karen Eberle. 2019. "Experimental Mouse Models of Disseminated *Candida auris* Infection." *mSphere* 4 (5):e00339-19. doi: 10.1128/mSphere.00339-19.
- Yan, Lei, Chunhui Yang, and Jianguo Tang. 2013. "Disruption of the intestinal mucosal barrier in *Candida albicans* infections." *Microbiol. Res.* 168 (7):389-395. doi: 10.1016/j.micres.2013.02.008.
- Yang, J., K. X. Liu, J. M. Qu, and X. D. Wang. 2013. "The changes induced by cyclophosphamide in intestinal barrier and microflora in mice." *Eur. J. Pharmacol.* 714 (1-3):120-124. doi: 10.1016/j.ejphar.2013.06.006.
- Yang, Weiming, Lei Yan, Chunrong Wu, Xiangwang Zhao, and Jianguo Tang. 2014. "Fungal invasion of epithelial cells." *Microbiol. Res.* 169 (11):803-810. doi: 10.1016/j.micres.2014.02.013.
- Yapar, Nur. 2014. "Epidemiology and risk factors for invasive candidiasis." *Ther. Clin. Risk Manag.* 10:95-105. doi: 10.2147/TCRM.S40160.
- Zakikhany, Katherina, Julian R. Naglik, Andrea Schmidt-Westhausen, Gudrun Holland, Martin Schaller, and Bernhard Hube. 2007. "*In vivo* transcript profiling of *Candida albicans* identifies a gene essential for interepithelial dissemination." *Cell. Microbiol.* 9 (12):2938-2954. doi: 10.1111/j.1462-5822.2007.01009.x.
- Zawrotniak, Marcin, Karolina Wojtalik, and Maria Rapala-Kozik. 2019. "Farnesol, a Quorum-Sensing Molecule of *Candida albicans* Triggers the Release of Neutrophil Extracellular Traps." *Cells* 8 (12):1611. doi: 10.3390/cells8121611.

- Zeidler, U., T. Lettner, C. Lassnig, M. Müller, R. Lajko, H. Hintner, M. Breitenbach, and A. Bito. 2009. "UME6 is a crucial downstream target of other transcriptional regulators of true hyphal development in *Candida albicans*." *FEMS Yeast Res.* 9 (1):126-142. doi: 10.1111/j.1567-1364.2008.00459.x.
- Zeuch, Henriette. 2019. "Charakterisierung der *C. albicans eed1Δ/Δ* Mutante in Interaktion mit murinen Makrophagen und Neutrophilen und Untersuchung des Einflusses von Farnesol auf den Metabolismus des Wildtyps ":[Bachelor thesis]. Jena: Friedrich Schiller University, 2019.
- Zhao, X., S. H. Oh, G. Cheng, C. B. Green, J. A. Nuessen, K. Yeater, R. P. Leng, A. J. P. Brown, and L. L. Hoyer. 2004. "ALS3 and ALS8 represent a single locus that encodes a *Candida albicans* adhesin; functional comparisons between Als3p and Als1p." *Microbiology* 150 (7):2415-2428. doi: 10.1099/mic.0.26943-0.
- Zheng, Xinde, Yanming Wang, and Yue Wang. 2004. "Hgc1, a novel hypha-specific G1 cyclin-related protein regulates *Candida albicans* hyphal morphogenesis." *EMBO J.* 23 (8):1845-1856. doi: 10.1038/sj.emboj.7600195.
- Zhu, Weidong, and Scott G. Filler. 2010. "Interactions of *Candida albicans* with epithelial cells." 12 (3):273-282. doi: 10.1111/j.1462-5822.2009.01412.x.

7. Appendix

7.1. Abbreviations

AIDS	acquired immunodeficiency syndrome
ALS	agglutinin-like sequence
ALT	alanine aminotransaminase
BMDM	bone marrow-derived macrophage
BSA	bovine serum albumin
C.	<i>Candida</i>
CAA	casamino acid
cAMP	3',5'-cyclic adenosine monophosphate
CFU	colony forming units
CO ₂	carbon dioxide
DCs	dendritic cells
DNA	deoxyribonucleic acid
ELISA	enzyme-linked immunosorbent assay
FOH	<i>E,E</i> -farnesol
GI	gastrointestinal
GlcNAc	N-acetyl-glucosamine
GPI	glycosyl-phosphatidyl-inositol
GUT cells	gastrointestinal-induced transition cells
HAG	hypha-associated gene
HIV	human immunodeficiency virus
HK	heat-killed
i.p.	latin: intra peritoneal
i.v.	latin: intra venous
ICU	intensive care unit
ID	infectious dose
IFN- γ	interferon- γ
IL	interleukin
LDH	lactate dehydrogenase
MHC II	major histocompatibility complex class II molecules
MOI	multiplicity of infection

MR	mannose receptor
NGAL	neutrophil gelatinase-associated lipocalin
O ₂	oxygen
OD	optical density
OPC	oropharyngeal candidiasis
p.i.	post infection
PAMPs	pathogen-associated molecular patterns
PBS	phosphate buffered saline
pH	latin: potential hydrogenii
PKA	protein kinase A
PRRs	pattern recognition receptors
RHE	reconstituted human oral epithelium
RNA	ribonucleic acid
<i>S.</i>	<i>Saccharomyces</i>
Saps	secreted aspartyl proteases
SD	synthetic minimal media
SNP	single-nucleotide polymorphism
sTREM-1	soluble triggering receptor expressed on myeloid cells
Th cells	T-helper cells
TLR	Toll-like receptor
Treg	regulatory T cells
USA	united states of america
VVC	vulvovaginal candidiasis
WT	wild type
YPD	yeast peptone dextrose

7.2. Additional methods

MPO ELISA

Myeloperoxidase MPO ELISA (Hycultec) was performed from supernatants of murine kidney homogenates according to manufacturer's instructions.

7.3 Curriculum vitae

7.4. Candidate's contributions to original publications

Manuscript I

Gerwien *et al.* (2020) mSphere

Own contribution

Christine Dunker planned and performed flow cytometry experiments to analyze exposure of PAMPs on the surface of *C. albicans*. She analyzed and interpreted the results, created the flow cytometry related figures and revised the manuscript.

Manuscript II

Machata *et al.* (2021), Front. Immunol.

Own contribution

Christine Dunker was involved in the isolation of murine neutrophils from bone marrow and performed *C. albicans* survival experiments in whole murine blood in the absence and presence of ketamine/xylazine, analyzed the respective results and created the figure. Christine Dunker provided mouse blood from systemically infected mice. She contributed in drafting and revising the manuscript.

Manuscript III

Dunker *et al.* (2021), Nat. Commun.

Own contribution

Christine Dunker planned, performed, evaluated and interpreted the following experiments: Murine systemic and intraperitoneal infection models, quantification of serum and urinary markers, histological analysis, isolation of immune cells from tissue, fungal interaction with immune cells, flow cytometry, analysis of flow cytometry, quantification of cytokines from tissue homogenates, growth curves, RNA isolation for RNAseq. Christine Dunker generated the majority of the figures, wrote the manuscript and was responsible for the revision.

7.5. Publications

- 2021** Dunker, C., Polke, M., Schulze-Richter, B., Schubert, K., Pawlik, T., Niemiec, M.J., Slesiona-Künzel, S., Swidergall, M., Martin, R., Jacobsen, I.D. (2021). Rapid proliferation due to better metabolic adaptation results in full virulence of a filament-deficient *Candida albicans* strain. *Nature Communications*, 12(1), 3899. <https://doi.org/10.1038/s41467-021-24095-8>
- 2021** Machata, S., Sreekantapuram, S., Hünninger, K., Kurzai, O., Dunker, C., Schubert, K., Krüger, W., Schulze-Richter, B., Speth, C., Rambach, G., & Jacobsen, I. D. (2021). Significant Differences in Host-Pathogen Interactions Between Murine and Human Whole Blood. *Frontiers in immunology*, 11, 565869. <https://doi.org/10.3389/fimmu.2020.565869>
- 2020** Gerwien, F., Dunker, C., Brandt, P., Garbe, E., Jacobsen, I. D., & Vylkova, S. (2020). Clinical *Candida albicans* Vaginal Isolates and a Laboratory Strain Show Divergent Behaviors during Macrophage Interactions. *mSphere*, 5(4), e00393-20. <https://doi.org/10.1128/mSphere.00393-20>
- 2018** Irmischer, S., Döring, N., Halder, L. D., Jo, E., Kopka, I., Dunker, C., Jacobsen, I. D., Luo, S., Slevogt, H., Lorkowski, S., Beyersdorf, N., Zipfel, P. F., & Skerka, C. (2018). Kallikrein Cleaves C3 and Activates Complement. *Journal of innate immunity*, 10(2), 94–105. <https://doi.org/10.1159/000484257>
- 2014** Miramón, P., Dunker, C., Kasper, L., Jacobsen, I.D., Barz, D., Kurzai, O., & Hube, B. (2014) A family of glutathione peroxidases contributes to oxidative stress resistance in *Candida albicans*. *Medical Mycology*, 52(3), 223-239. <https://doi.org/10.1093/mmy/myt021>
- 2012** Miramón, P., Dunker, C., Windecker, H., Bohovych, I. M., Brown, A. J., Kurzai, O., & Hube, B. (2012). Cellular responses of *Candida albicans* to phagocytosis and the extracellular activities of neutrophils are critical to counteract carbohydrate starvation, oxidative and nitrosative stress. *PLoS one*, 7(12), e52850. <https://doi.org/10.1371/journal.pone.0052850>

7.6. Talks and Posters

7.6.1. Talks

- 05/2016 Joint Meeting 2016 ILRS & GRK, Wittenberg, Germany. Title: Systemic inflammation precedes renal damage in mice systemically infected with *Candida albicans*
- 10/2015 ILRS Seminar, Jena, Germany. Title: Investigating the role of fungal morphology in the pathogenicity of *Candida albicans* infections
- 09/2015 67th Annual meeting of the German Society for Hygiene and Microbiology, Münster, Germany. Title: Investigating the role of fungal morphology in the pathogenicity of *Candida albicans* infections
- 05/2014 7th ILRS Symposium, Jena, Germany. Title: The role of filamentation in the pathogenesis of candidiasis
- 02/2014 Statusworkshop DGHM, Fachgruppe Eukaryontische Krankheitserreger, Göttingen, Germany. Title: The role of filamentation in the pathogenesis of candidiasis
- 02/2013 Statusworkshop DGHM, Fachgruppe Eukaryontische Krankheitserreger, Hannover, Germany. Title: A family of glutathione peroxidases are required for resistance to oxidative stress in the fungal pathogen *Candida albicans*

7.6.2. Posters

- 04/2016 13th ASM conference on *Candida* and candidiasis. Seattle, USA. Title: Systemic inflammation precedes renal damage in mice systemically infected with *C. albicans*
- 09/2015 Joined Event: 49th Scientific Meeting of the German-speaking mycological Society (DMyG) and the 1st International Symposium of the CRC/Transregio FungiNet, Jena, Germany. Title: Investigating the role of fungal morphology in the pathogenicity of *Candida albicans* infections
- 05/2015 ILRS Symposium, Jena, Germany Investigating the role of fungal morphology in the pathogenicity of *Candida albicans* infections
- 09/2014 48th Scientific Meeting of the German-speaking mycological Society (DMyG), Salzburg, Austria. Title: The role of filamentation in the pathogenesis of candidiasis
- 09/2013 Weimar Sepsis Update 2013, Weimar, Germany. Title: Glutathione peroxidases are required for the resistance to oxidative stress in *C. albicans*
- 09/2012 64th Annual meeting of the German Society for Hygiene and Microbiology (DGHM), Hamburg, Germany. Title: Glutathione peroxidases are required for normal resistance to oxidative stress in the fungal pathogen *Candida albicans*

7.7. Additional trainings and activities

Supervision

04/2021 – present	Bachelor thesis Julia Schumann
2019	Bachelor thesis Henriette Zeuch
2016	Master thesis Franziska Wittig
2015	Bachelor thesis Hanna Büttner
2014	Bachelor thesis Philipp Brumhard

Public relation activities

Since 2015	Team captain of the HKI dragon boat team
2014	Organization of the “Forsche Schüler Tag” at the HKI in Jena
2013	Contribution to the “Long Night of Science” at the HKI in Jena

Courses

05/2021	„Versuchstierkundlicher Kurs für Durchführende im Tierversuch“ (FELASA B equivalent)
08/2016	Biostatistics course
08/2016	LaTeX course
09/2013	„Übungskurs zum Erlernen tierexperimenteller Methoden für Maus und Ratte“

Grants

2012	Travel grant of the DGHM
------	--------------------------

7.8. Danksagung

Zuallererst möchte mich bei Prof. Ilse Jacobsen für die Möglichkeit bedanken, meine Dissertation in ihrer Forschungsgruppe durchführen zu können. Sie hat mich stets unterstützt und gefördert, war immer offen für Diskussionen und ansprechbar bei Problemen. Zudem möchte ich mich bei ihr für das mir entgegengebrachte Vertrauen bedanken. Ihr gilt auch mein Dank für die tatkräftige Unterstützung bei den Mausexperimenten, inklusive des Übernehmens von Nachtschichten.

Ein weiterer Dank gebührt meinem Zweitbetreuer Prof. Bernhard Hube, in dessen Abteilung ich die Ehre hatte, meine Diplomarbeit schreiben zu dürfen. Was ich in dieser Zeit gelernt habe, bildete die Grundlage für diese Doktorarbeit.

Ein großes Dankeschön geht auch an all meine jetzigen sowie ehemaligen Kollegen und Freunde aus der MI, der MPM und der ASP, mit denen ich in den vergangenen Jahren zusammengearbeitet habe. Vor allem möchte ich mich bei Melanie Polke bedanken. Zusammen haben wir uns bemüht, das Rätsel um *EED1* zu lösen. Und obwohl es uns nur zum Teil gelang und wir mitunter etwas frustriert waren, so hatten wir doch eine schöne Zeit. Weiterhin möchte ich mich bei all meinen über die Jahre wechselnden zahlreichen Büro-Kollegen bedanken, vor allem bei Katja und Bianca, Silke, Tony, Steffi, Nicole, Franzi und Silvia. Ihr alle seid der Grund gewesen, warum ich jeden Tag fröhlich und beschwingt auf Arbeit gekommen bin. Ohne die Hilfe meiner Kollegen wären vor allem die Tierversuche in der Form und Qualität, wie wir sie durchgeführt haben, nicht möglich gewesen. Danken möchte ich auch Katja, Birgit, Stephie und Nadja, die mich nach Kräften technisch unterstützt haben. Ihr alle habt dafür gesorgt, dass lange Tage nicht noch länger wurden. Dafür bin ich euch sehr verbunden.

Schließlich gebührt ein großer Dank meiner Familie, die für mich in allen Lebenslagen immer da war. Wir haben nicht nur die schönen Momente zusammen genossen, sondern auch schwere Zeiten zusammen durchgestanden, wofür ich unendlich dankbar bin. Ich danke vor allem meinem Partner, meinen Eltern sowie meinen Schwiegereltern dafür, dass sie mir den Rücken in stressigen Zeiten freigehalten und stets Verständnis aufgebracht haben, wenn die Tage lang wurden oder Wochenendarbeit zum Wohle der Versuchstiere notwendig war. Dank gebührt auch unserem kleinen Sonnenschein Karl, der hilft die Welt wieder aus Kinderaugen zu sehen und verdeutlicht, worauf es im Leben wirklich ankommt. Zu guter Letzt bedanke ich mich bei Arthi für die zahlreichen Hundespaziergänge, die stets geholfen haben, den Kopf wieder frei zu bekommen. Ohne Euch alle wäre das alles nicht möglich gewesen!

7.9. Selbstständigkeitserklärung

Hiermit erkläre ich, dass ich die vorliegende Arbeit selbst verfasst habe und keine anderen als die angegebenen Quellen und Hilfsmittel verwendet habe. Mir ist die geltende Promotionsordnung der Fakultät für Biowissenschaften der Friedrich-Schiller-Universität Jena bekannt. Personen, die mich bei den Experimenten, der Datenanalyse und der Verfassung der Manuskripte unterstützt haben, sind als Ko-Autoren auf den entsprechenden Manuskripten verzeichnet. Personen die mich bei der Verfassung der Dissertation unterstützt haben, sind in der Danksagung der Dissertation vermerkt. Die Hilfe eines Promotionsberaters wurde nicht in Anspruch genommen. Es haben Dritte weder unmittelbar noch mittelbar geldwerte Leistungen für Arbeiten erhalten, die im Zusammenhang mit dem Inhalt der vorgelegten Dissertation stehen. Die vorliegende Arbeit wurde in gleicher oder ähnlicher Form noch bei keiner anderen Hochschule als Dissertation eingereicht und auch nicht als Prüfungsarbeit für eine staatliche oder andere wissenschaftliche Prüfung verwendet.

Jena, den 27.08.2021

Christine Dunker